The distribution and feeding ecology of temperate marine sponges through shallow and mesophotic habitats

Benjamin John Harris

A thesis submitted to the Victoria University of Wellington

in fulfilment of the requirements for the degree of

Doctor of Philosophy

Victoria University of Wellington

2022

This thesis was conducted under the supervision of

Professor James J. Bell

(Primary Supervisor)

&

Professor Simon K. Davy

(Co-supervisor)

Victoria University of Wellington

Wellington, New Zealand

“Quit, don't quit. Noodles, don't noodles. You are too concerned with what was and what will be.”

Master Oogway, Zhao Dynasty

Abstract

Coastal benthic communities represent one of the most biodiverse ecosystems in the marine environment and perform numerous important ecological functions, including the cycling of carbon and other nutrients in the water column. However, the benthic communities of temperate ecosystems are far less studied than their tropical counterparts, especially beyond the top 30 m of water into the so-called temperate mesophotic zone (30 – 150 m), which remains largely unexplored globally. The lack of information regarding the structure and subsequent ecological functions of benthic communities in both shallow and temperate mesophotic ecosystems (TMEs) is likely to be imposing critical limits on our understanding of how temperate coastal ecosystems function generally, and the ecological services they provide. Marine sponges are often one of the most abundant organisms occurring in shallow temperate benthic habitats, and are likely to be performing important ecological functions, including transferring carbon from the water column to the benthos via their feeding activities. However, despite their high abundance, temperate marine sponges remain generally overlooked, where almost nothing is known about their distributions and potential ecological importance in both infralittoral and mesophotic habitats. The overall aim of this thesis was to address this knowledge gap by describing how sponges are distributed through the infralittoral and mesophotic zones of rocky reefs in New Zealand, and assessing the role of trophic relationships between sponges and microbial food sources in determining sponge distribution, population dynamics, and carbon retention in these habitats.

In Chapter 2 I addressed a key knowledge gap of how the composition and abundance of benthic communities (including sponges) change from the infralittoral zone to the almost entirely unexplored mesophotic zone at selected sites in New Zealand. I describe quantitative changes in the benthic community composition of rocky reefs from 5 to 120 m at six

locations across New Zealand, including the Fiordland Marine Area and the Poor Knights Marine Reserve. Benthic community data were analysed from videos and photographs collected using SCUBA (30 m) and a remotely operated vehicle (ROV) (>30 m). I found significant changes in community composition with depth at all locations, suggesting that temperate mesophotic ecosystems (TMEs) provide habitats different from those in shallower water. I found that regardless of the significant changes in sponge abundance with depth, TME benthic communities were consistently dominated by sponges. I show that the morphological composition of these sponge assemblages changes with depth at all locations. I created a sponge assemblage complexity metric to describe how changes in sponge morphologies with depth have potentially important ramifications in relation to the provisioning of habitat complexity. The implications of changes in sponge abundance and complexity through TMEs in relation to sponge trophodynamics is investigated in the following chapter.

The significant variation in both sponge abundance and the presence of free-substrate space were left unexplained in Chapter 2, where no correlations with multiple environmental variables could be found. In Chapter 3 I suggest that food availability is the most likely driver of these patterns. Here, I first describe the composition and distribution of the food pool within the size range potentially available to sponges, from the surface down to 120 m. I collected water samples from the Poor Knights and four sites in Fiordland from the innermost to the outermost locations of Doubtful Sound to accommodate the strong environmental gradient found in this region. Using flow cytometry, I identified and quantified the microbial community components available to sponges within the particulate organic carbon (POC) pool and show how the abundance of these components changes significantly with depth and across locations. I also show how dissolved organic carbon (DOC), as another potential resource to sponges, changes significantly along these same depth gradients. Using a

combination of cell sorting and scanning electron microscopy, I confirmed specific previously identified microbial populations, and corrected a previous misclassification of a cell population now reclassified as picoeukaryotes. I found strong positive correlations between sponge distributions and food availability when data from all Fiordland sites was combined, and some smaller-scale patterns at the Poor Knights. These observations provide fundamental ecological information about the composition and distribution of resources at the foundation of marine trophic structures in New Zealand's infralittoral and mesophotic habitats, and how the distribution of temperate sponges maybe determined by bottom-up effects.

In Chapter 4, I address the substantial knowledge gaps that remain in the potential dietary range and feeding preferences of temperate sponges, and how this might determine their population dynamics. I determined the diets of seven common sponge species occurring on shallow temperate reefs at three sites in New Zealand *in situ*. I assessed the potential for active food selection and interspecific differences in food preference to support resource partitioning and trophic plasticity. For the first time on shallow temperate reefs outside of the Mediterranean, I measured the uptake of multiple pelagic microbial communities as identified in the previous chapter, as well as DOC. Sponges showed active selection for different POC groups as well as between POC and DOC, although only two species (*P. penicillus* and *Polymastia* sp.) showed significant DOC retention. I found that retention efficiencies of specific POC groups were consistently high in all species that fed exclusively on POC. However, the consumption of DOC by only *P. penicillus* and *Polymastia* sp. coincided with lower retention efficiencies of POC groups and was entirely responsible for inter-specific differences in food selectivity and therefore resource-partitioning. Correlations between DOC availability and DOC consumption, and DOC selectivity indicate trophic plasticity in the study species. The results from this chapter suggest that sponges can 'switch' between food

types based on relative food availability as an active rather than passive response. I found limited evidence for niche partitioning within the POC food pool, but propose that trophic plasticity, generalist feeding strategies, and DOC consumption might help explain the high abundance of sponges relative to other benthic invertebrate groups in resource-poor environments.

The quantification of carbon retained by sponge assemblages is of considerable importance to our understanding of the ecological dynamics of benthic habitats generally. In Chapter 5, I combine multiple components from my previous research to estimate the potential range in quantity of carbon sponges are retaining at the assemblage scale as a result of their feeding activity on New Zealand reefs in the infralittoral and mesophotic zone. I determined the pumping volumes of five particularly common sponge species occurring on the Wellington South Coast *in situ* using SCUBA. I assessed potential correlations between multiple sponge biometrics (mass / number of oscula / size of oscula / total oscula area / pumping velocity) and pumping volume, to determine the most accurate and efficient way to standardize and extrapolate pumping volumes to entire assemblages. I found total oscula area (OSA) to be the best predictor of sponge pumping volume, and that the ratio of total oscula area to sponge size (~ 6%) to increase allometrically with sponge size, without any inter-specific variation. I used a range of potential OSA-specific pumping volume estimates, in combination with a range of POC retention efficiency estimates of different pelagic microbial groups, (determined in Chapter 4), to determine the range of total carbon mass retained by sponges. I then extrapolated this information to entire sponge assemblages at the Poor Knights Marine Reserve and in Doubtful Sound using sponge distribution information from the infralittoral and mesophotic zones of these regions (determined in Chapter 2). This study confirms the efficacy of applying OSA-specific pumping volumes to population scales, and demonstrates the significant contribution sponges make to the transfer of carbon (> 100% of available

carbon in the benthic boundary layer *per* hour) to the benthos through the infralittoral and mesophotic zone of New Zealand reefs.

The dominance of temperate sponges throughout both shallow and mesophotic zones and the large proportion of available carbon they transfer from the water column to the benthos is likely to have substantial ecological implications. This includes the regulation of the availability of microbial communities which are fundamental to other important ecological processes, such as primary production, and the microbial loop. Furthermore, while numerous factors are likely to determine the presence and proliferation of sponges in temperate environments (e.g. habitat availability, resource competition, environmental variables), the quantity of carbon accumulated by heterotrophic sponges fundamentally dictates the production potential of sponge assemblage biomass itself (as well as all other energetic outputs), and therefore forms the foundation on which all other ecological functions performed by sponges rely. The information provided by this thesis suggests that as the most dominant benthic organism throughout both infralittoral and mesophotic habitats, these ecological functions (most notably, the substantial pelagic-benthos carbon transfer) are likely to be of particularly high importance, especially in deeper habitats where the wider benthic community (and their associated ecological functions) becomes increasingly depauperate relative to sponges. As such, sponges are likely to be one of the most important functional components of temperate coastal ecosystems, where their consideration across the full habitat ranges available to them, from infralittoral to mesophotic zones, is essential in developing a holistic understanding of coastal temperate ecosystem dynamics generally.

Acknowledgements

I would firstly like to thank the George Mason Charitable Trust for funding this project, and George Mason personally for his assistance and support.

My sincere gratitude goes to my supervisor Prof James Bell and to my co-supervisor Prof Simon Davy for their continuous support and guidance over the course of this project. James has facilitated me in my PhD from start to finish, as well as providing me with many amazing opportunities in other research areas, for which I am extremely grateful. I would also like to thank James for his personal encouragement to persevere during challenging times. My appreciation goes to Simon for his invaluable insight and perspective and who has also provided much personal encouragement and support.

My gratitude goes to the Department of Conservation for their provision of permits and for funding much of my fieldwork. Thanks to the crew of the DoC vessel 'Southern Winds', and especially to Richard Kinsey, Chris Pascoe, Ross Funnell, and Chloe Corne for their help with fieldwork in Fiordland. I would also like to thank the crew of the DoC vessel 'Orca', Callum Lilley and Wayne Beggs, who also provided help in the field in Taranaki. I would like to acknowledge Dive Tutukaka, who provided logistical support for work at the Poor Knights.

My appreciation goes to NIWA Hamilton and specifically Mike Crump, for providing technical support for water sample analyses. My gratitude goes to the Hugh Green Cytometry Centre who provided essential technical support and resources. My special thanks go to Dr Kylie Price, who patiently guided me through techniques in flow cytometry which were a major component of this thesis. Kylie's professional insight has been an invaluable contribution to my work, as has her personal encouragement and support. I would also like to

express my thanks to Dr Nicole Poulton for generously providing valuable advice for flow cytometry analysis and interpretations.

My sincere thanks go to Snout for his encouragement and enthusiasm in facilitating my fieldwork, improving my diving skills over the course of my time at VUCEL, and for the best Friday morning tea! Thanks to all the VUW spongers for their friendship and help, especially Sandeep, Rama, Nora, Valerio, Francesca, Meg, and Albi. I would also like to thank Maggie and Bobby from the Davy lab for their friendship, and especially Bobby for helping me with my diving fieldwork in Wellington.

My deepest personal gratitude goes most of all to Jordan for sticking by me throughout my PhD and for her love and patience; I could not have done this without her. Thanks to Tom for keeping me in check and reminding me of my intellectual inferiority on daily basis due to his relentless academic success. Thanks to Chris, Nicky, and Lucy for their kindness and friendship. I would also like to express my deep thanks to Dez Lando, Stu, Rivkah, and Maya for their amazing friendship, coffee chats, and for helping me keep perspective. My gratitude also goes to Holly for her unwavering passion for the ocean, freezing morning swims, and coffee chats, without which the final months of my PhD would have been much more difficult.

Finally I would like to express my thanks to my mother Sarah, and my father John for their unwavering patience, kindness, and support, as well as to Sophie, David, Florence, and to Tilly who I can’t wait to meet.

Publications

Chapter 2 of this thesis is based on a manuscript published in *Marine Ecology Progress Series*

Chapter 2:

Publication: Benjamin Harris, Simon K. Davy, and James J. Bell (2021). Benthic community composition of temperate mesophotic ecosystems (TMEs) in New Zealand: sponge domination and contribution to habitat complexity. *Marine Ecology Progress Series, 671*, 21-43. https://doi.org/10.3354/meps13758

Conceptualization and Methodology: Benjamin Harris under the guidance of Prof. James J. Bell and Prof. Simon K. Davy.

Data collection: Benjamin Harris under the guidance of Prof. James J. Bell

Analysis: Benjamin Harris

Writing and editing: Benjamin Harris and edited by Prof. James J. Bell, Prof. Simon K. Davy

Table of Contents

List of Figures **16**

List of Tables **21**

Chapter 1 ..... **24**

General introduction **24**

1.1 Coastal benthic ecosystems **25**

1.2 Mesophotic ecosystems **25**

1.3 Marine Sponges **27**

1.4 The functional roles of sponges **28**

1.5 Sponge feeding ecology **30**

1.5.1 Particulate organic carbon **30**

1.5.2 Dissolved organic carbon **31**

1.6 Sponge feeding and population dynamics **33**

1.7 Improved access opportunities in mesophotic ecosystems **34**

1.8 Summary **35**

1.9 Aims and objectives **36**

Chapter 2 ..... **38**

Benthic community composition of temperate mesophotic ecosystems (TMEs) in New Zealand: sponge domination and contribution to habitat complexity **38**

Abstract **39**

2.1 Introduction **40**

2.2 Materials and Methods **44**

2.2.1 Study sites **44**

2.2.1.1 Fiordland National Park **44**

2.2.1.2 South Taranaki Bight: Patea **45**

2.2.1.4 Poor Knights Marine Reserve **47**

2.2.2 Benthic video collection **48**

2.2.3 CTD deployment **49**

2.2.4 Video analysis **50**

2.2.5 Data analysis **52**

2.3 Results **53**

2.3.1 Benthic community composition **53**

2.3.4 Sponge assemblage contribution to habitat complexity **64**

2.4 Discussion **69**

2.4.1 TME benthic community patterns 70
2.4.2 Sponge assemblage patterns 73
2.4.3 Sponge morphology and contribution to habitat complexity 75
2.4.4 Mesophotic TME surrogates 77
Chapter 3 79
Microbial community composition and distribution: a potential driver of sponge abundance through the infralittoral and mesophotic zone 79
***Abstract*..... 80**
3.2 Methods 86
3.2.1 Study Sites 86
3.2.3 ROV video sampling and analysis 88
3.2.4 POC analysis: Flow cytometry 89
3.2.6 Dissolved organic carbon analysis 92
3.2.7 Data analysis 92
3.3.1 Microbial community composition and SEM interpretations 93
3.3.4 DOC distribution 96
3.3.5 Distribution of specific POC components 101
3.3.6 Sponge – microbial abundance correlations 109
3.4 Discussion 109
3.4.1 Microbial population identification: SEM observations 110
3.4.2 Microbial group distributions 112
3.4.3 DOC distributions 113
3.4.4 Sponge-food correlations and implications 114
Chapter 4 117
Food selectivity and limitation as potential drivers of resource partitioning in temperate sponge assemblages 117
***Abstract*..... 118**
4.1 Introduction 119
4.2 Methods 123
4.2.1 Study Sites 123

4.2.2 Sponge-feeding assessments 126

4.2.3 Study species 126

4.2.4 *In situ* sampling 127

4.2.5 Flow Cytometry POC analysis 129

4.2.6 Dissolved organic carbon analysis 130

4.2.7 Data analysis 130

4.3 Results 134

4.3.1 Food retention 134

4.3.2 Food selection 138

4.3.4 Resource partitioning 141

4.3.5 Retention efficiency 142

4.3.6 Food availability / selectivity and retention efficiency 145

4.4.1 Ambient food availability and particle classifications 149

4.4.2 Sponge diet preference 151

4.4.3 Mechanisms and drivers of food selection 153

4.4.4 Resource partitioning 154

4.4.5 DOC retention, resource partitioning and ecological implications 155

Chapter 5 157

The contribution of sponge assemblages to pelagic-benthic transfer of carbon in the infralittoral and mesophotic zone 157

***Abstract*..... 158**

5.1 Introduction 159

5.2 Methods 163

5.2.1 Study Sites 163

5.2.2 Habitat assessments 164

5.2.3 Determining sponge abundance 166

5.2.4 Sponge food (POC) sampling and analysis 167

5.2.5 Flow cytometry 168

5.2.6 Particle retention efficiency 169

5.2.7 Sponge pumping volume 170

5.2.8 SPV – sponge morphological/physiological traits correlations 171

5.2.9 Regional-scale carbon flux calculations 171

5.2.10 Assumptions / limitations 174

5.3 Results 175

5.3.1 Sponge pumping metrics 175

5.3.2 Habitat and total food availability 176

5.3.3 Regional scale pumping rates and carbon transfer 177

5.4 Discussion 186

5.4.1 Extrapolating to assemblage scale pumping volumes 187

5.4.2 Assemblage scale carbon retention estimates 189

5.4.3 Broader ecological implications 192

Chapter 6 195

General discussion 195

6.1 Summary of key findings 196

6.2 Temperate mesophotic ecosystems and sponges 198

6.3 Sponge feeding: sponge population dynamics 200

6.4 Sponge feeding: wider ecological implications 202

6.5 Limitations and future directions 205

References 208

Appendices 243

Appendix A 244

Appendix B 277

Appendix C 290

Appendix D 306

List of Figures

Fig. 2.1 Survey locations at (A) the Poor Knights, (B) Parininihi Marine Reserve, (C) South Taranaki Bight, and (D) Fiordland Marine Area (FMA). Orange and green circles in the FMA represent survey locations in 2018 and 2019, respectively. Blue shaded regions show the locations of Marine Reserves. The yellow 'lightning bolt' symbol in (D) indicates the location of freshwater input from Manapouri hydroelectric power station.

Fig. 2.2 (Two pages)Abundance (as % coverage) of the 6 most abundant benthic groups at (A) Poor Knights, (B) inner, (C) mid, and outer (D) Fiordland, and (E) Patea and Parininihi at 25 m only. Algal groups have been separated to maintain meaningful visualisation of invertebrate groups due to large differences in abundance values. Values are means ± SE. CCA: crustose coralline algae.

Fig. 2.3 Canonical analysis of principal coordinates (CAP) ordination of sampled benthic community composition at all survey locations across all depths with groups factored as location (A). Groups were then factored as depth at (B) the Poor Knights, (C) inner Fiordland, (D) mid Fiordland, and (E) outer Fiordland. Analysis is based on a Bray-Curtis similarity matrix of percentage cover data. Clusters are based on resemblance levels at 10% (green), 20% (blue), and 30% (turquoise).

Fig. 2.4 Canonical analysis of principal coordinates (CAP) ordination of sponge assemblage morphological composition at all survey locations across all depths with groups factored as location (A). Groups were then factored as depth at (B) the Poor Knights, (C) inner Fiordland, (D) mid Fiordland, and (E) outer Fiordland. Analysis is based on a Bray-Curtis similarity matrix of percentage cover data. Clusters are based on resemblance levels at 10% (green), 20% (blue), and 30% (turquoise).

Fig. 2.5 Sponge assemblage morphological complexity scores at 10 m depth increments at Poor Knights, inner, mid, and outer Fiordland, Patea, and Parininihi. Assemblage complexity scores equal the sum of the complexity score assigned to each morphological type of sponge (ranging from 1−5, Table A2.2) multiplied by the abundance of each morphology in a quadrat. Figure shows mean of quadrat scores + SE.

Fig. 2.6 Total sponge cover as binned into high, medium, and low complexity at 10 m depth increments at Poor Knights, inner, mid, and outer Fiordland, Patea, and Parininihi

Fig. 2.7 Relative abundance (of sponge assemblage) of low, medium, and high complexity sponge morphologies over 10 m depth increments at Poor knights, inner, mid, and outer Fiordland, Patea, and Parininihi

Fig. 3.1 Survey locations at the Poor Knights (top) and Doubtful Sound (bottom) in 2019. Blue shaded regions show the locations of marine reserves.

Fig. 3.2 SEM images of *Midiscus* spp. (A) and Pennales spp. (B) and unidentified globular (C) and oblong (D) cells representing 'picoeukaryote' population originally distinguished and gated during flow cytometry analyses as *Prochlorococcus.*

Fig. 3.3 SEM images of *Synechococcus* sp. group (A) and individual cell (B) found within sorted population group P3 (see Fig. B3.4) representing the '*Synechococcu*s sp.' population, originally distinguished and gated during flow cytometry analyses.

Fig. 3.4 SEM images of 'heterotrophic bacteria' group (A) and an individual cell (B) found within the sorted population group P3 (see Fig. B3.4) representing the 'heterotrophic bacteria' population originally distinguished and gated during flow cytometry analyses.

Fig. 3.5 Concentration (cells ml^{-1}) of total nucleic-acid positive cells (A), heterotrophic bacteria (B), picoeukaryotes (C), and *Synechococcus* sp. (D) from the surface down to 80 m

at Poor Knights and Fiordland Site 1, and from the surface down to 120 m at Fiordland Sites 2 - 4. Error bars are mean ± SE.

Fig. 3.6 Dissolved organic carbon (DOC) concentrations (μmol/L) from the surface down to 80 m at the Poor Knights and Fiordland Site 1, and down to 120 m at Fiordland Sites 2 & 3. Error bars are mean ± SE.

Fig. 3.7 Linear regression relationship between total ambient cells (cells L^{-1}) and sponge abundance (% cover) at 0, 10, 30, 50, and 80 m at the Poor Knights Marine Reserve. Vertical bars are sponge abundances ± SE, horizontal bars are DOC concentrations ± SE.

Fig. 3.8 Linear regression relationship between DOC concentration (μm L^{-1}) and sponge abundance (% cover) across four Fiordland sites (A) at 10 , 30 , 50, 80, and 120 m (0 m excluded, see discussion) and the Poor Knights (B) at 0, 10, 30, 50, and 80 m. Vertical bars are sponge abundances ± SE, horizontal bars are DOC concentrations ± SE.

Fig. 3.9 Linear regression relationships of total nucleic-acid positive counts, heterotrophic bacteria, picoeukaryotes and *Synechococcus* sp. (ml^{-1} for all cell groups) with sponge abundance (% cover) across four Fiordland sites. Abundances of both sponges and cell groups were collected at distinct depth categories of 0, 10 , 30 , 50, 80, and 120 m. Here, 10 – 120 m is shown for total nucleic-acid positive counts and heterotrophic bacteria while 30 – 120 m is shown for picoeukaryotes and *Synechococcus* sp. (see Discussion). Vertical bars are sponge abundances ± SE, horizontal bars are cell abundance ± SE.

Fig. 4.1 Map showing sampling sites at Parininihi Marine Reserve (A) and Wellington Harbour (B1) and Breaker Bay (B2). Blue boxes show the borders of Parininihi Marine Reserve (A) Taputeranga Marine Reserve (B).

Fig. 4.2 Example of gating strategy of isolated populations of three main food groups between inhalant and exhalent water (sample is from *Tethya* sp.). Dot plots show how the

coordinates of applied population gates are exactly replicated from the ambient/inhalant sample to the exhalent sample for each sponge-replicate sample pair.

Fig. 4.3 Cell counts (*per* ml) of ambient and exhalent water from 5 replicates of 7 study species. Counts are *per* oscula and do not consider number of oscula *per* specimen or pumping rate.

Fig. 4.4 DOC concentrations in ambient and exhalent water from five replicates of 7 study species.

Fig. 4.5 Retention efficiency (expressed as %) of three POC food groups removed by 5 replicates of 7 sponge species (error bars are +/- SE).

Fig. 4.6 Mean filtration selectivity (± SE) by seven common sponge species of *Synechococcus* sp., picoeukaryotes, heterotrophic bacteria and DOC as estimated by the electivity index (ϵ_i), where 0 represents no preference, +1 represents high positive preference and -1 high negative preference for the different food types (Chesson, 1983).

Fig. 4.7 Retention efficiency (expressed as %) of DOC removed by five replicates of seven sponge species (error bars are +/- SE)

Fig. 4.8 Logarithmic relationship between sponge-food retention efficiency and ambient food availability of 3 POC groups (*Synechococcus* sp., picoeukaryotes and heterotrophic bacteria)

Fig. 4.9 Logarithmic relationship between sponge-food selectivity (α) and ambient food availability of 3 POC groups (*Synechococcus* sp., picoeukaryotes and heterotrophic bacteria) and DOC across seven sponge species. See Table C4.7 for regression coefficients for fitted lines and *per*-species relationships.

Fig. 5.1 ROV locations in 2018 and ROV and water sample locations at Doubtful Sound in 2019. See Chapter 1 for full map, including Poor Knights locations.

Fig. 5.2 Estimated water volumes of the inner, mid, and outer regions of Doubtful Sound.

Fig. 5.3 Linear regression relationships (±CI) between the OSA (mm^2) and sponge pumping volumes (ml min^{-1}) of *Dysidea* sp. *Clathrina sp. Suberites* sp. *Tedania* sp. and *Tethya* sp. (A), and all the square-root data of species combined (±CI) (B). See Table 5.1 for R^2 coefficients.

Fig. 5.4 Linear regression relationship between 2D total sponge area (cm^2) and total oscula area (cm^2) of 5 sponge species. See Table 5.1 for R^2 coefficients for individual species.

List of Tables

Table 3.1 PERMANOVA results showing the effect of depth (0 m, 10 m, 30 m, 50 m, 80 m, 120 m), location and the interaction between depth and location on the relative abundance of microbial community components (four groups) and on DOC concentration.

Table 3.2 PERMANOVA results showing the site differences of the effect of depth (levels: 0 m, 10 m, 30 m, 50 m, 80 m, 120 m) on the concentration of three different cell groups, total nucleic acid positive events (three groups combined plus unidentified populations) and DOC. DOC concentrations were not determined at Site 4.

Table 3.3 PERMANOVA results showing the effect of depth (0 m, 10 m, 30 m, 50 m, 80 m, 120 m) on the concentration of three different cell groups, total nucleic acid positive events (3 groups combined plus unidentified populations) and DOC. DOC concentrations were not determined at Site 4.

Table 3.4 PERMANOVA results showing the effect of depth (0 m, 10 m, 30 m, 50 m, 80 m, 120 m) on the abundance of four POC groups DOC concentrations at the Poor Knights, Fiordland combined, and four individual Fiordland sites.

Table 3.5 Linear regression results showing correlations between sponge assemblage abundance and the abundance of four POC groups and DOC concentrations at the Poor Knights, Fiordland across full depth profiles.

Table 4.1 PERMANOVA results for differences in cells counts in ambient/inhalant and sponge exhalent water samples for 3 POC groups, total POC, and DOC from 7 sponge species

Table 4.2 PERMANOVA results for Manly-Chesson's alpha index (α) scores for 7 species whereby significant results indicate food selectivity within 3 POC groups (top) and within 3

POC groups and DOC (bottom

Table 4.3 PERMANOVA pairwise tests of Manly-Chesson's alpha index (α) scores of 3 POC food groups by 5 sponge species and 3 POC groups with DOC for 2 sponge species

Table 4.4 Variation in food retention efficiency according to species and food groups and a two-way interaction between food group and species from PERMANOVA tests. POC groups only (left). POC groups and DOC included (right

Table 4.5 Pairwise differences in retention efficiency of four food groups across seven sponge species

Table 4.6 Pairwise differences in retention efficiency of three POC food groups for seven individual sponge specie

Table 5.1 Linear regression tests between multiple morphological traits and pumping rate equation components to determine the best predictor of overall sponge pumping volume

Table 5.2 Average OSA (cm^2), corresponding pumping volume based on predicted y-values from linear regression coefficients of average OSC, and OSC standardized to 1 cm^2 (see Table 5.1 & Fig. 5.3). Error values for OSC pumping volume are the standard error of the estimate in regression formulas. Assemblage range is the assemblage mean ± the standard error of the estimate.

Table 5.3 Descriptions of morphological traits and allometric scaling relationships between OSC and sponge area (2d cm^2 area).

Table 5.4 Estimated volume of water (m^3), sponge habitat (m^2), sponge cover ± SE, and range of sponge assemblage pumping volume ($m^3\ min^{-1}$) (see methods and Table 5.3) within the inner, mid, outer, and total region of Doubtful Sound and the Poor Knights. Water volume at the Poor Knights is the estimate of the benthic layer (see methods).

Table 5.5 Estimates of cell counts (individual cells) and equivalent carbon Kg *per* m^3 and *per* region water volume (Table 5.4) of heterotrophic bacteria, picoeukaryotes, *Synechococcus* sp., and all cells combined, at the inner, mid, and outer regions of Doubtful Sound, as well as the entirety of Doubtful Sound and the Poor Knights. Water volume estimates at the Poor Knights include the benthic layer only (see methods)

Table 5.6 Estimates of carbon (Kg C) in the form of heterotrophic bacteria, picoeukaryotes, and *Synechococcu*s sp., cells as well as all POC groups combined, pumped through full sponge assemblages *per* minute at the inner, mid, and outer regions of Doubtful Sound, as well as the entirety of Doubtful Sound and the Poor Knights. The percentage of the full POC pool being pumped *per* 24 h is also reported. Value ranges are based on the SE range from the mean pumping volume of five species (Table 5.2). The SE range of ambient availability of each POC group occurring in each region is not considered

Table 5.7 Estimates of carbon (Kg C) in the form of heterotrophic bacteria, picoeukaryotes, and *Synechococcu*s sp. cells, as well as all POC groups combined, retained by full sponge assemblages *per* 24 h period at the inner, mid, and outer regions of Doubtful Sound, as well as the entirety of Doubtful Sound and the Poor Knights. The percentage of the total carbon retained of the full POC pool *per* 24 h is also reported. Average retention efficiency of heterotrophic bacteria, picoeukaryotes, and *Synechococcus* sp. cells across seven species was 58 ± 8, 81 ± 6, and 71 ± 9 respectively (see Chapter 4). The low and high values range reported are the mean retention efficiency ± SE and mean pumping volume ± SE.

Chapter 1
General introduction

1.1 Coastal benthic ecosystems

Coastal b enthic ecosystems are among the most diverse and productive on earth (Poore and Wilson, 1993), representing a key component of global marine ecological functions, including climate regulation, nutrient cycling, and primary productivity (Falkowski, 1998). Benthic communities are primarily composed of diverse invertebrate fauna (Bolam et al. 2002) that contribute to these large-scale ecological functions by regulating the transfer, sequestration, and cycling of carbon and other nutrients between the substrate and the overlying water column (Kristensen, 1984; Kristensen & Blackburn, 1987; Snelgrove, 1999; Austen et al. 2002; Covich et al. 2004). Despite their recognised importance to ecological functioning on a global scale, most of our understanding of benthic communities and their associated ecological functions comes largely from shallow coastal habitats, which have received a high level of ecological research effort generally. However, the exploration and subsequent understanding of coastal benthic communities immediately beyond these shallow habitats, into so-called mesophotic ecosystems, is much more limited (Baker et al. 2016; Turner et al. 2017; 2019). Given the substantial benthic habitat that mesophotic ecosystems provide, their omission from marine ecological investigations imposes significant restrictions to the holistic understanding of coastal marine ecosystems, and the subsequent application of appropriate management strategies (Turner et al. 2019).

1.2 Mesophotic ecosystems

The definition of mesophotic ecosystems remains ambiguous, with researchers often providing their own criteria (Hinderstein et al. 2010; Kahng et al. 2010), leading to possible confusion (Cerrano et al. 2019). Recently, Cerrano et al. (2019) attempted to resolve this confusion by providing a definition based on location-specific light attenuation, where the mesophotic zone receives approximately 1% of the surface irradiance. However, while this

metric accounts for significant differences in light availability across locations, it is still subject to temporal/seasonal variability. Instead, mesophotic ecosystems can be most simply defined as benthic habitats occurring between ~30 and 150 m (Turner et al. 2019). Most of the limited research effort and understanding of mesophotic ecosystems is derived from tropical environments, known as mesophotic coral ecosystems (MCEs), although their potential ecological importance has only been discussed relatively recently (Lesser et al. 2009; Kahng et al. 2014; Cerrano et al. 2019). Most studies have been purely descriptive, while process-oriented, ecological-based studies are scarce (Lesser et al. 2009). In reviewing numerous descriptions of MCE benthic communities globally, Kahng et al. (2010) provided some insight into how these habitats support benthic communities that are distinct from those occurring in shallow water, and as such, are likely to be performing different ecological functions. It has been suggested that MCEs might serve as a potential refuge for shallow species during short-term disturbances, such as storm surges (e.g. Harmelin-Vivien, 1994) or acute pollution events (e.g. van Dam et al. 2011), as well as long-term environmental stressors, such as ocean warming (e.g. De'ath et al. 2012) and acidification (e.g. Hughes et al. 2017). This concept has been termed; the deep reef refuge hypothesis (DRRH), and highlights the potential importance of mesophotic ecosystems as anthropogenic pressures increase. However, it has also been suggested that multiple anthropogenic stressors threaten mesophotic ecosystems themselves (Rocha et al. 2018; Bell et al. *in review*), further emphasising the need to determine the contributions of mesophotic benthic communities to broader ecosystem dynamics and functions.

Benthic communities in temperate mesophotic zones (TMEs) have only very recently been formally recognised, are far less explored, and are poorly understood compared to their tropical counterparts, (Cerrano et al. 2019; Turner et al. 2019). Some recent reviews of studies of benthic communities in TMEs are available (Cerrano et al. 2019; Chimienti et al.

2019; de Oliveira-Soares et al. 2020), but these are all restricted to studies within the Mediterranean. This reflects the disproportionate research effort on TMEs in this bioregion generally (e.g. Cerrano et al. 2010; Bo et al. 2011; Bianchelli et al. 2013; Di Camillo et al. 2013; Chimienti et al. 2018; Idan et al. 2018) where TMEs in other regions have been largely overlooked (Bell et al. *in review*) (but see Keesing et al. 2012; James et al 2017).

Light attenuation is the primary environmental driver characterising the ecology of mesophotic zones in both temperate and tropical environments (Cerrano et al. 2019). Reduced light availability leads to the decline, and eventually, the exclusion of algae and other photosynthetic benthic organisms (Lesser et al. 2009), generating changes in the competitive pressure on the benthic community (Cárdenas et al. 2012; 2016). This might be especially pronounced in TMEs where the reduction in light availability and subsequent reduction in macroalgal abundance is expected to decline more quickly with depth, than for corals in MCEs with deeper light penetration. The ecological dynamics of TMEs are therefore likely to be heavily determined by the relative abundance and composition of the benthic invertebrate community, including bryozoans, ascidians, polychaetes, cnidarians, and sponges.

1.3 Marine Sponges

Marine sponges (Porifera) are one of the most ancient extant animal phyla (Müller, 2003), possibly pre-dating the Cambrian explosion by > 50Ma (Turner, 2021) but see (Muscente et al. 2015). 90% of the approximately 8,500 confirmed species (Van Soest et al. 2012) belong to the class Demospongiae, with the remaining species belonging to the classes Calcarea, Hexactinellida, and Homoscleromorpha (Hooper et al., 2002). Although, an additional 2,500 unconfirmed species across these classes have also been identified (Van Soest et al. 2012). Lacking internal organs, sponges consist of three layers of cells. Flattened pinacocyte cells

form the outermost layer of the sponge known as the pinacoderm. In Hexactinellida, Homoscleromorpha, and Demospongiae silica spicules (and/or spongin), form a skeletal matrix under the pinacoderm known as the mesohyl (Bergquist, 2001), while spicules formed of calcium carbonate define the class Calcarea (Hartman, 1964). The choanoderm forms the innermost sponge layer, consisting of choanocytes cells. These cells use flagella to maintain a unidirectional flow of water through a complex internal canal system, generating an internal pump. Oxygen, carbon, and other nutrients in the ambient water are drawn into the sponge through small holes in the pinacoderm known as the ostia, pumped through the internal canal system, and utilized by the sponge in metabolic activity and the production of detrital matter, mucus, gametes and sponge tissue. Their simple physiology is likely to be a key attribute that has allowed sponges to be the one of the most ubiquitous animal phyla in our oceans (Zhang & Pratt, 1994).

1.4 The functional roles of sponges

Due to the significant knowledge gap of mesophotic ecosystems generally, sponges in mesophotic habitats are poorly understood, especially in TMEs which remain widely unexplored. However, the distribution, abundance, and ecological functions of sponges have been well documented in shallow, accessible areas (<30 m) in temperate (e.g. Roberts et al. 2006; Bell, 2007), tropical (e.g. Diaz & Rützler, 2001; Lesser & Slattery, 2013) and polar (McClintock et al. 2005) environments, where they are among the most abundant benthic invertebrates occurring on rocky-reef habitats (Bell & Barnes, 2000; Schlacher et al. 2007). These studies of shallow sponge assemblages suggest they are particularly important components of benthic communities due to the wide range of ecological functions they perform (see Bell et al. 2008). For example, sponges can be important providers of micro-habitat for dense and diverse microbial communities that are phenotypically distinct from those occurring in the surrounding water column (Wulff, 2006; Taylor et al. 2007; Webster &

Taylor, 2012). Sponges can also provide direct habitat for a wide range of other invertebrates (see Klitgaard, 1995; Ribeiro et al. 2003), some of which live on the surface, such as small crustaceans, while others are considered as endofauna, living inside the sponge itself (Saffo, 1992). Sponge assemblages can also provide habitat complexity for the wider benthic community (Maldonado et al. 2012) as reef building organisms (Miller et al. 2012; Knudby et al. 2013) where high local biodiversity has been attributed to sponge grounds (Klitgaard & Tendal, 2004; Murillo et al. 2012; Hawkes et al. 2019), which can act as fish nurseries (Klitgaard, 1995; Freese & Wing, 2003). Despite the development of structural (Hill et al. 2005; Brunner et al. 2009) and biochemical (Pawlik et al. 1995) defence strategies, sponge tissue can provide a resource for both generalist predatory fish species (Wulff, 1994) as well as specialist spongivorous species, such as hawksbill turtles (*Eretmochelys imbricata*) (Meyland, 1988). Sponges are also effective spatial competitors (Bell & Barnes, 2003; Wulff, 2006), and can therefore restrict the distribution and abundance of other benthic community organisms, such as corals *via* overgrowth of damaged or stressed individuals (Rützler, 2002), or *via* allelochemically mediated interactions, causing necrosis of coral tissue (de Voogd et al. 2004).

The most significant ecological functions performed by sponges are those directly associated with their suspension feeding activity, including bentho-pelagic coupling (Perea-Blázquez et al. 2012), the mediation of primary production by controlling nutrient availability (Bell, 2008; Maldonado et al. 2012; Murillo et al. 2012; Kutti et al. 2013), and converting dissolved organic carbon (DOC) which is generally inaccessible to the wider ecological community, into available particulate organic carbon (POC) *via* the sponge loop (de Goeij et al. 2013; Rix et al. 2016) (see section 1.5.2 below).

1.5 Sponge feeding ecology

1.5.1 Particulate organic carbon

As suspension feeders, sponges have developed mechanisms for capturing microbial components (< 5 µm) of the POC pool (Gili and Coma, 1998). The entire body plan of a sponge is specialized for this process (Riisgård et al. 1993), where large volumes of water are pumped through choanocyte chambers (2−12 ml water cm^{-3} min^{-1}) (Reiswig, 1974; 1981; Pile, 1997; Gili & Coma, 1998) to capture enough food to sustain base-metabolic requirements, reproduction, and growth. Compared to other suspension feeders, sponges can exhibit very large individual body volumes (e.g. *Xestospongia* spp.; 116,721 ± 29,275 cm^3 (Mcgrath et al. 2018)), high pumping rates (> 35 ml min^{-1} cm^{-3} sponge (Weisz et al. 2008)), and high retention efficiencies (up to 99%) of planktonic cell groups (Pile et al. 1997; McMurray et al. 2018). The feeding activity of sponges is therefore considered to be of particular ecological importance. The microbial components of the POC pool observed to be retained by sponges includes cyanobacteria (notably *Synechococcus* sp. and *Prochlorococcus*), heterotrophic bacteria, and autotrophic picoeukaryotes (Yahel et al. 2006; Hadas et al. 2009). The microbial community is a key component of fundamental marine ecological functions, contributing to an estimated 25% of global marine primary production (Flombaum et al. 2013), and in combination with heterotrophic bacteria, and the microbial loop, they form the foundation of marine food webs (Azam et al. 1983; Whitman et al. 1998). Changes in the availability of these microbial groups in the water column by sponge feeding activity (Perea-Blázquez et al. 2012; Valentine et al. 2019), is therefore expected to be of considerable ecological importance, and is a necessary consideration in developing a holistic understanding of the ecological dynamics of benthic habitats generally. This is especially important where sponges occur in high abundance.

1.5.2 Dissolved organic carbon

While POC has been shown to be a key component of the sponge diet, more than 90% of the total organic carbon (TOC) pool small enough to enter through the sponge ostia consists of DOC (Pawlik et al. 2018). DOC is operationally defined as any organic carbon that passes through a GF/F filter (retention rating < 0.7µm) (Hansell & Carlson 2014). This represents the largest exchangeable carbon reservoir in the marine environment (Druffel et al. 1992; Hansell & Carlson, 2014) and consists of a broad range of components derived from numerous potential sources. These include small remnants of phagocytized microbial cells, exudates from photosynthetic bacteria (Thornton, 2014), macrophytes (Brylinsky, 1977) and corals (Crossland, 1987; Haas et al. 2011), as well as allochthonous terrestrial sources delivered *via* estuaries and streams (Raymond & Spencer, 2015). DOC normally needs to be recycled *via* the microbial loop (Azam et al. 1983) before it can be utilized by the wider ecological community. However, it is now apparent that some sponges can bypass the microbial loop by retaining and metabolizing DOC directly (de Goeij, 2008; 2013; Rix, 2016; 2017). A review by de Goeij et al. (2017) found that for a total of 20 sponge species for which DOC retention has been assessed (at the time of publication), 17 species showed significant DOC uptake. However, only three of the 20 species assessed were temperate species (*Dysidea avara*, *Agelas oroides,* and *Chondrosia reniformis*), all of which were examined in the Spanish Mediterranean (Ribes et al. 1999; 2012). A limited number of studies assessing the feeding behaviour of deep-water sponges, have considered DOC as part of the potential sponge diet, but with mixed outcomes. Yahel et al. (2007) and Kahn et al. (2015) showed no uptake of DOC by two hexactinellid species in a deep Norwegian fjord and by *Aphrocallistes vastus* in the North East Pacific. However, Bart et al. (2020) showed that DOC represents > 90% of the total carbon removal of sponges occurring on a deep-water reef in the North Atlantic. This confirms that sponges outside of tropical environments are capable

of significant DOC retention. However, to date, no studies have confirmed sponge-DOC uptake in true temperate environments outside of the Mediterranean, or outside of deep-water habitats in either the mesophotic or infralittoral zone. I suggest this is due to the research bias towards sponges occurring in resource limited environments (e.g. de Goeij et al. 2008; 2013; Pawlik & McMurray, 2020; Bart et al. 2020; 2021), rather than indicative of a lack of DOC retention and utilization by temperate sponges generally. While the consideration of DOC retention by sponges might help resolve observations of apparent resource deficits (as has been demonstrated in early sponge-DOC interaction studies (de Goeij, 2013)), this does not mean DOC retention is necessarily exclusive to sponges occurring in these environments. As such, sponges in temperate habitats require substantially more attention to establish the potentially wide spectrum of their feeding behaviour, and subsequent contributions to carbon-benthic transfer and the sponge loop, as well as the implications for the population dynamics of sponges themselves.

The sponge-loop has been described as analogous to the microbial loop, where sponges recycle DOC previously inaccessible to the wider ecological community by retaining DOC, converting it into detritus, mucus or sponge biomass, and then passing it onto other organisms as POC via detrital or predatory pathways (McMurray et al. 2018; Pawlik & McMurray, 2020). In combination with the microbial-loop, the sponge-loop provides a solution as to how diverse and abundant ecological communities can thrive in the oligotrophic habitats of tropical marine environments. However, it is likely that this would also have considerable ecological significance in temperate environments, especially during periods of low productivity, or in deeper habitats, such as TMEs with lower availability of autotrophic POC components than their shallow counterparts. Recent evidence for a cold-water deep-sea sponge loop in the North Atlantic (Bart et al. 2020), and the limited literature describing the

feeding ecology of temperate marine sponges also supports this suggestion indirectly (see below).

1.6 Sponge feeding and population dynamics

Perea-Blázquez et al. (2013) showed significant seasonal fluctuations in food availability in shallow temperate sponge assemblages in New Zealand, and Perea-Blázquez (2012) showed linear increases in total POC retention with increases in ambient food availability. Furthermore, Perea-Blázquez et al. (2011) showed that sponge assemblages in the same region exhibit resource partitioning within the POC pool. The combination of these observations suggests that sponges in temperate environments might be subject to food limitation. If food limitation is occurring in these sponge assemblages, then the ability to retain and utilize DOC would be an evolutionarily advantageous trait. The potential role of food limitation and bottom-up effects in determining sponge assemblage distributions has been one of the most contentious debates in sponge ecological science to date (see Pawlik et al. 2018). Trussell et al. (2006) initially asserted that the abundance of tropical sponges is being driven by bottom-up effects. This was derived from observed relationships between POC concentrations and depth, sponge abundance, and size, combined with a lack of evidence of top down effects reported in an early study by Randall & Hartman (1968). However, Pawlik et al. (2013) showed experimentally, that top-down control of sponge predators had a significant impact on sponge growth but found no evidence for food limitation. Lesser & Slattery (2013) responded with further correlative evidence linking depth-dependent food availability with sponge abundance, but this was disputed by Pawlik et al. (2015) who found no evidence of food limitation in a review of the literature, and noted that the omission of DOC considerations by Lesser & Slattery (2015) undermines their conclusions. The debate surrounding the relative importance of top-down vs. bottom-effects on sponge assemblage abundance and distribution remains unresolved, and is likely to

continue, but this has been entirely set in tropical environments. The role of food availability in structuring temperate sponge assemblages however, has not been tested explicitly, where only inferences from sponge feeding behaviour have been made (Perea-blasquez et al. 2012). In temperate, shallow infralittoral zones, sponge abundance and their subsequent ecological functions are likely to be most heavily determined by other factors besides predation or food limitation, namely, spatial competition with other benthic organisms (e.g. turfing algae, Cárdenas et al. 2012). Therefore, explanations from other factors have not necessarily required consideration. However, below the infralittoral zone, spatial competition with algae and other organisms is likely to diminish where explanations of observable patterns in sponge assemblage distributions (if any) would require the consideration of other environmental and biotic drivers. Given the lower abundance of sponge predators in temperate environments compared to tropical environments (Wulff, 2006), I suggest one of the most likely of these drivers would be food availability. However, to assess the role of food limitation on sponge distributions in TMEs as well as the contribution of these sponges to the transfer of carbon to the benthos, the full spectrum of food available to sponges must be considered, including the potential of DOC consumption, as suggested by Pawlik et al. (2015).

1.7 Improved access opportunities in mesophotic ecosystems

The limited research effort afforded to both MCEs and TMEs compared to shallow habitats is predominantly due to the practical difficulties of first-person access. Most of the mesophotic zone occurs beyond the limits of recreational SCUBA (40 m), where diving activities involving closed circuit rebreathers (CCR), or open circuit systems utilizing Trimix configurations, require substantially greater expertise, training, and is more costly. Furthermore, observation time is limited due to decompression considerations, which may reduce the spatial coverage of sampling and replication (Lam et al. 2006). In the past, the use of remotely operated vehicles (ROVs) in mesophotic zones has often been prohibitively

expensive, where the use of Class III ROVs which require substantial deployment infrastructure and multiple professional operators, has led to projects prioritising exploration into bathyal and even abyssal zones, capitalising on extreme pressure ratings in areas truly inaccessible to first-person exploration (Danovaro et al. 2014). However, in recent years, robotics technology has advanced considerably, with class I ROVs becoming smaller, cheaper, and capable of a wider range of tasks, providing more opportunities for researchers to investigate previously overlooked mesophotic habitats. As such, both MCEs and TMEs are beginning to receive greater research attention, but significant gaps remain in our scientific understanding, limiting our ability to make scientifically based decisions for the conservation and management of these ecosystems (Turner et al. 2019).

1.8 Summary

Following the European Coral Reef Symposium (ECRS; Oxford, UK, 14 December 2017), Turner et al. (2019) produced multiple key research questions that they claim, if answered, would substantially increase our understanding of the ecological functioning of TMEs. Within the research theme: "Ecological Processes" they asked: "What are the population and community structure and dynamics of mesophotic species, and to what extent do benthic species contribute to the three-dimensional structure of MEs?" Recognising the ecological importance of tropical sponges in shallow environments, but the substantial knowledge gap of temperate sponge distributions and their ecological functions in both shallow and mesophotic environments, this thesis attempts to provide some answers to this question, using the distribution and feeding dynamics of marine sponges specifically.

In summary, marine sponges are abundant and widespread components of shallow benthic communities and have been shown to perform important ecological functions through suspension feeding activity on microbial communities as well as DOC. However, much of

our understanding of sponge ecological dynamics is from tropical environments whereas temperate sponges have been less investigated. Moreover, almost nothing is known about how sponges are distributed and function in TMEs outside of the Mediterranean. This thesis therefore aimed to address this significant knowledge gap, as outlined below.

1.9 Aims and objectives

Chapter 2 *Benthic community composition of temperate mesophotic ecosystems (TMEs) in New Zealand: sponge domination and contribution to habitat complexity*

Aims and objectives:

1) Describe how benthic community structure changes from shallow water to the mesophotic zone (5−120 m) on New Zealand rocky reefs. 2) Characterize sponge abundance and morphological complexity across these zones allowing an assessment of their contribution to TME habitat complexity.

Chapter 3 *Sponge food pool composition and distributions: a potential driver of sponge assemblage abundance through the infralittoral and mesophotic zone in New Zealand*

Aims and objectives:

1) Identify the microbial community components (POC) within the size range available to temperate New Zealand sponges using a combination of flow cytometry and scanning electron microscopy (SEM). 2) Determine changes in abundance of POC components and DOC concentrations from 0 – 120 m on temperate New Zealand rocky reef habitats. 3) Test correlations between sponge food pool components and sponge abundance to assess the potential role of bottom-up effects on temperate sponge distributions.

Chapter 4 *Importance of food selectivity and limitation as drivers of resource partitioning in temperate sponge assemblages*

Aims and objectives:

1) Determine the full natural diet and food preferences (food-group selectivity) of six common demosponge species and one common calcareous sponge species *in situ,* on temperate New Zealand reefs. 2) To identify any inter-specific differences in selectivity of POC groups, as well as between POC and DOC food sources as a potential mechanism supporting resource partitioning. 3) Describe the relationship between the ambient availability, food selectivity and retention efficiency of different food-groups by these same sponge species, to assess the role of food availability in feeding behaviour and the potential for food limitation.

Chapter 5 *The contribution of sponge assemblages to pelagic-benthic transfer of carbon in the infralittoral and mesophotic zones of New Zealand reefs*

Aims and objectives:

1) Investigate the relationships between sponge morphological and physiological traits and sponge pumping volume, to establish a standardized metric for pumping volume. 2) Extrapolate a standardized metric of sponge pumping volume determined in Aim 1 to assemblage-scale percentage cover data at Doubtful Sound and the Poor Knights Islands. 3) Determine total sponge habitat availability and food availability at these same locations. 4) Estimate the total and proportional exchange of POC from the water column to the benthos by sponges through a combination of habitat availability data, sponge distribution data (Chapter 2), food availability and food retention efficiency information (Chapters 3 & 4), and assemblage pumping information calculated in Aim 2.

Chapter 2

Benthic community composition of temperate mesophotic ecosystems (TMEs) in New Zealand: sponge domination and contribution to habitat complexity

Abstract

Temperate mesophotic ecosystems (TMEs) typically occur between 30 and 150 m depth and support rich benthic communities. However, despite their widespread distribution and ecological importance, TMEs are one of the most poorly studied marine ecosystems globally. I measured changes in the benthic community composition of rocky reefs through the infralittoral and mesophotic zone from 5 to 120 m at 6 locations across New Zealand (the Poor Knights Islands, the inner, mid-, and outer regions of the Fiordland Marine Area (FMA), and the North and South Taranaki Bights) which were considered as potential shallow-water TME surrogates due to these sites having environmental conditions and biological communities similar to deeper-water communities. Benthic community data were analysed from videos and photographs collected using SCUBA (<30 m) and a remotely operated vehicle (ROV) (>30 m). I found significant changes in community composition with depth at all locations, suggesting that TMEs provide habitats different from those in shallower water. I consistently found that TME benthic communities were dominated by sponges, but their abundance varied significantly with depth at 3 out of 4 locations, while the morphological composition of these assemblages changed with depth at all locations. Given their particularly high abundance and morphological complexity, I suggest that sponge assemblages make an important contribution to habitat complexity in benthic TME communities.

2.1 Introduction

Determining the drivers of biodiversity patterns and understanding how different organisms contribute to ecosystem functioning is critical for the implementation of effective biodiversity monitoring and conservation management strategies (Balmford & Gaston, 1999; Costello et al. 2010). However, this first requires the distribution and abundance of organisms to be determined, which poses many practical challenges for marine species compared to terrestrial species. As a result, significant gaps persist in our understanding of many marine ecosystems (Costello et al. 2010), which limits our ability to make effective management decisions (Van Jaarsveld et al. 1998). Coastal benthic marine ecosystems are among the most bio-diverse and productive on Earth (Poore & Wilson, 1993). These ecosystems occur in a broad range of geophysical spaces and environmental conditions (Covich et al. 2004), where particularly active hydrological regimes play an important role in ecosystem dynamics (Austen et al. 2002). Intertidal and shallow coastal benthic communities have received a high level of research effort compared to deeper water, so-called mesophotic habitats, which generally occur deeper than 30 m, approaching the limits of recreational SCUBA (Kahng et al. 2010). First-person access to these environments requires substantially greater expertise, training, and is more costly. Furthermore, observation time is limited due to decompression considerations, which may reduce the spatial coverage of sampling and replication (Lam et al. 2006). While the use of re motely operated vehicles (ROVs) in these zones is possible, in the past this has often been prohibitively expensive.

Past research of mesophotic ecosystems has predominantly focused on tropical mesophotic coral ecosystems (MCEs) (e.g. Lesser et al. 2009; Kahng et al. 2014), with comparable ecosystems from temperate environments having been only recently formally recognised (Cerrano et al. 2019; Turner et al. 2019). The definition of MCEs remains ambiguous, with researchers often providing their own criteria, but generally, this zone extends from

approximately the edge of recreational SCUBA limits at 40 m, where zooxanthellate corals decline (Hinderstein et al. 2010), down to 150 m, where light availability becomes significantly reduced (<1% of the surface light). Studies of equivalent depth zones in temperate mesophotic ecosystems (TMEs) are far fewer (see James et al. 2017; Cerrano et al. 2019).

Furthermore, no studies have considered the transition of entire benthic communities through the complete infralittoral (here classified as 5−30 m) and mesophotic (30− 150 m) range (5−150 m) (Cerrano et al. 2019). This research gap is likely due to the practical obstacles of working below recreational SCUBA limits, with projects employing large ROVs and autonomous underwater vehicles (AUVs) instead prioritising exploration far into the bathyal or even abyssal zones, capitalising on extreme pressure ratings in areas truly inaccessible to first-person exploration (Danovaro et al. 2014). However, in recent years, robotics technology has advanced considerably, with ROVs becoming smaller and cheaper, providing more opportunities for researchers to investigate previously overlooked TMEs. Low-cost ROVs are capable of generating species distribution and abundance data of comparable quality to those gathered using SCUBA (Boavida et al. 2016), but from deeper depths. The reduction in light availability is the primary environmental driver characterising the ecology of mesophotic zones in both temperate and tropical climates. It generates declines in, and eventually, the exclusion of algae and other photosynthetic organisms (Lesser et al. 2009), changing competitive pressures on benthic fauna. The ecological dynamics of the mesophotic zone, therefore, appear to be increasingly determined by the community composition and relative abundance of the benthic invertebrate fauna and the functions they perform, including sponges, bryozoans, ascidians, hard corals, and soft corals. Marine sponges (Porifera) are among the most abundant sessile benthic invertebrates in shallow rocky-reef environments (Bell & Barnes, 2000; Schlacher et al. 2007), frequently occurring on hard

substrate across all global marine bioregions (van Soest et al. 2012). These suspension feeders perform a wide range of important ecological functions including moving substantial amounts of carbon (and other nutrients) from the water column to the benthos, substrate stabilisation and bio-erosion, acting as strong spatial competitors, and providing 3-dimensional habitat (Bell, 2008). The distribution abundance and ecological functions of sponges have been well documented in shallow, accessible areas (<30 m) in temperate (e.g. Roberts et al. 2006; Bell, 2007), tropical (e.g. Diaz & Rützler, 2001; Lesser & Slattery, 2013) and polar (McClintock et al. 2005) environments, but again, assemblages in the mesophotic zone are less understood, especially in temperate regions. Although sponges are effective spatial competitors (Bell & Barnes, 2003), they are expected to increase in abundance with depth, as has been demonstrated in tropical regions (Lesser & Slattery, 2018) as light penetration declines through the infralittoral zone and their competition with algae reduces (Cárdenas et al. 2012), although generalisations of these patterns require caution (see Scott & Pawlik, 2019). As a result, the functions that sponges perform may play an increasingly important role with increasing depth into the mesophotic zone. A particularly important function that sponges perform in temperate regions is the creation of habitat complexity for the wider benthic community, as temperate environments generally lack the complex habitat structures provided by reef-building corals that characterize tropical reefs (Graham & Nash, 2013). Furthermore, the transition from the infralittoral to the mesophotic zone in temperate regions sees a significant decline and the eventual exclusion of light-dependent habitat-forming organisms, such as canopy-forming macroalgae species and branching forms of crustose coralline algae. Therefore, the relative importance of habitat complexity provided by sponges is likely to be increasingly important with depth, regardless of whether sponges show significant increases in abundance. The habitat complexity provided by sponge assemblages can increase the abundance and biodiversity of associated organisms (Maldonado et al. 2017,

Folkers & Rombouts, 2020) in numerous ways, including providing refugia for prey organisms (Ryer et al. 2004), hunting habitat for predators (Miller et al. 2012), and direct sponge habitat for obligate sponge dwellers (Henkel & Pawlik, 2005). Three-dimensional morphologically complex sponge assemblages are also likely to alter local hydrodynamics by reducing surface boundary layers and providing greater environmental heterogeneity (Beazley et al. 2013). Quantifying changes in sponge cover and complexity with changes in benthic community composition through the infralittoral and mesophotic zones is therefore an essential component in understanding the overall ecological dynamics and functions of coastal benthic communities. Despite a particularly high abundance and diversity of sponges in New Zealand (Downey et al. 2012), less research effort has been afforded to this South Pacific region compared to other temperate areas (Bell et al. 2020). Furthermore, the mesophotic zones where sponges are potentially most abundant and functionally significant as provisioners of habitat complexity have been largely overlooked (but see taxonomy assessments of specimens found at 190 m by Kelly & Rowden, 2019). Here I focus on the full transitional depth range from the infralittoral to the mesophotic zone across multiple sites in New Zealand, within the same depths considered to be mesophotic on tropical coral reefs (30−150 m). I propose that mesophotic habitats in temperate regions are location-specific due to highly dynamic coastal environments, where in some circumstances, TME-like communities may occur in much shallower water than MCEs due to particularly low light penetration. Therefore, I also considered some shallow benthic habitats without depth profiles (<30 m) in the Taranaki region of New Zealand's North Island, which have been previously considered to be more characteristic of deeper water reefs (Battershill & Page, 1996). Here, particularly high turbidity reduces light availability, potentially reducing the persistence of algal species. Algae are generally highly abundant in the shallow (<20 m) coastal areas of New Zealand reefs and often compete effectively with the wider benthic community for

habitat space (Choat & Schiel, 1982). A reduction in algal abundance due to low light availability could facilitate the proliferation of invertebrates, such as those sponges that would normally be found in deeper habitats. Comparing these low light shallow habitats with deeper water mesophotic zones may help elucidate the mechanisms driving the benthic community composition and distribution of TMEs in temperate ecosystems. If these shallow-water sites resemble deeper water TME communities, then they might act as models for future TME studies, as they are much easier to access.

The aims of this study were to: (1) describe how benthic community structure changes from shallow water to the mesophotic zone (5−120 m) on New Zealand rocky reefs; and (2) characterize sponge abundance and morphological complexity across these zones allowing an assessment of their contribution to TME habitat complexity.

2.2 Materials and Methods

2.2.1 Study sites

Four geographic regions were chosen to represent a wide range of potential shallow water (<30 m) and deeper water mesophotic habitats (30−150 m), in New Zealand: Fiordland National Park, South Taranaki Bight, North Taranaki at Parininihi Marine Reserve, and Poor Knights Marine Reserve (Fig. 2.1). Surveys took place between 2018 and 2019 (Table A2.1). Unlike Fiordland and the Poor Knights, the chosen Taranaki locations do not exhibit large vertical depth profiles. However, these shallow horizontal reefs (see 2.2.1.2 – 3) have been posited as potential shallow water mesophotic surrogates and are included in this study to investigate this suggestion further.

2.2.1.1 Fiordland National Park

The Fiordland Marine Area (FMA) is in the southwest of New Zealand's South Island (Fig. 2.1D) and covers 928 000 ha that includes the waters of 14 fiords with 10 marine reserves (Ministry for the Environment, 2014). Surveys took place over 2 years in February 2018 and 2019 at 28 and 4 sites, respectively (Table A2.1). Sites surveyed in both years were categorised into inner, mid, and outer regions, according to their relative distance to the open ocean. The mid-region (8.1−12.5 km from the open ocean) contained more sites than the inner (16.9−20.2 km) and outer (0.8−6.8 km) regions, as weather conditions restricted accessibility at outer sites and fewer deep-water vertical walls were available at inner sites. Fiord systems are characterised by submerged vertical walls that provide a habitat for diverse biological communities that are usually very different from those communities found on the adjacent open coast (Howe et al. 2010). The high annual rainfall (>6400 mm) and rapid runoff from the steep topography in the FMA, results in a tannin-rich freshwater surface layer 1− 4 m deep that is maintained throughout the year creating strong depth gradients in salinity and temperature (Goodwin & Cornelisen, 2012). This phenomenon is particularly apparent in the inner-most reaches of each fiord, where the exchange of water from the open ocean is most limited. This is artificially accentuated at Deep Cove at the inner reaches of Doubtful Sound, where freshwater arrives via a hydroelectric power station from Lake Manapouri, 10 km to the northeast. It is likely that the high-level input of freshwater strongly influences patterns of community composition and abundance (Howe et al. 2010), but still very little is known about the benthic community in this region.

2.2.1.2 South Taranaki Bight: Patea

Sampling in South Taranaki took place at 3 sites separated by no more than 500 m in June 2018 (Fig. 2.1C). The area consists of a large shallow bay (< 50 m deep) that extends south and east from the south coast of Taranaki on New Zealand's North Island. The surveyed reef is situated approximately 11 km offshore from the mouth of the Patea River, consisting of

broken boulders and rocky ledges ranging from 15 to 30 m deep. The extensive shallow areas are mainly soft sediment habitats and experience regular high energy swells that generate high turbidity and relatively low visibility. Periodic large inputs of turbid freshwater from the Patea River (ln-source data available at >110 m3 s^{-1}, March 2018) may also contribute to this effect.

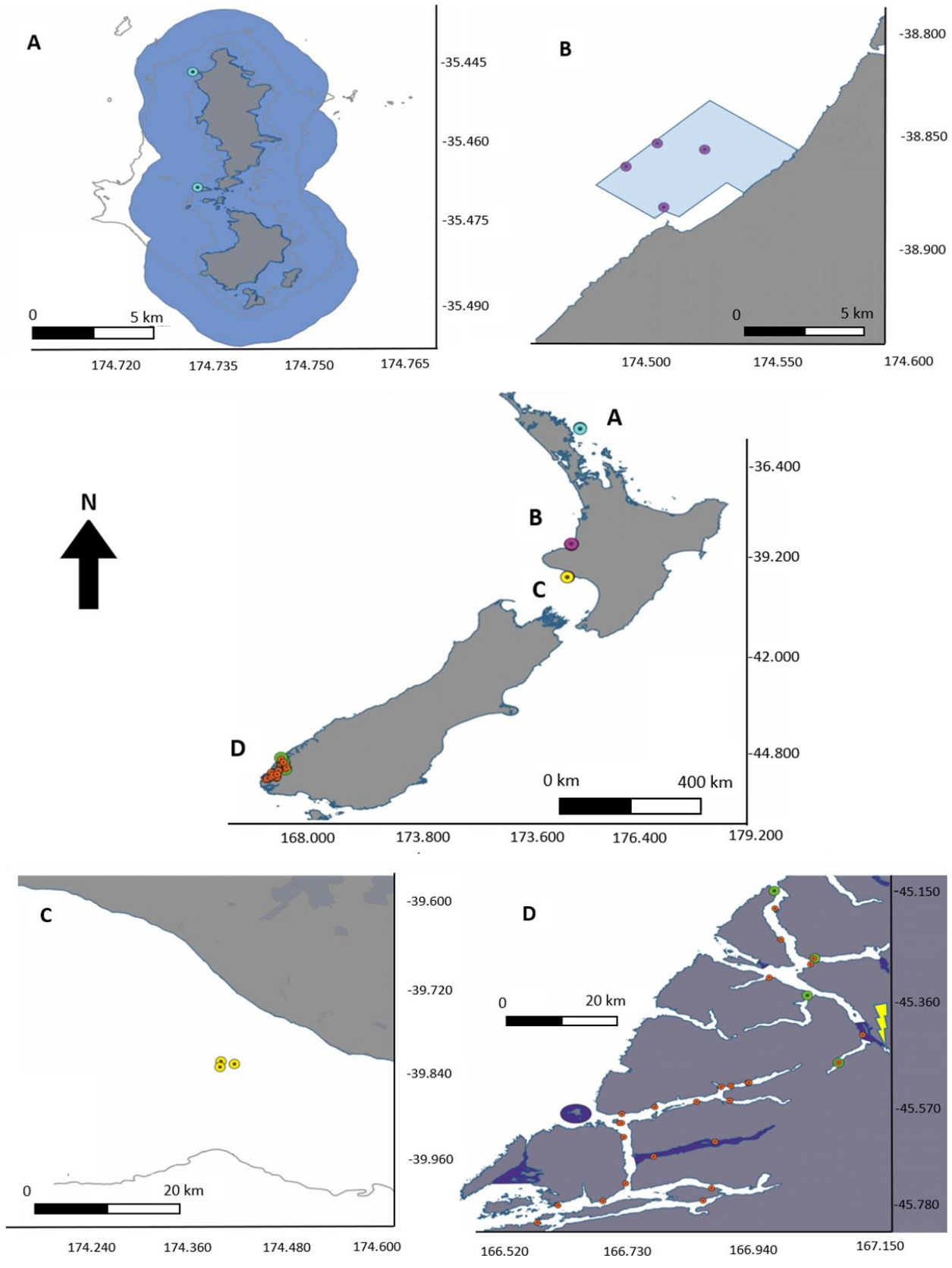

Fig. 2.1 Survey locations at (A) the Poor Knights, (B) Parininihi Marine Reserve, (C) South Taranaki Bight, and (D) Fiordland Marine Area (FMA). Orange and green circles in the FMA represent survey locations in 2018 and 2019, respectively. Blue shaded regions show the locations of Marine Reserves. The yellow 'lightning bolt' symbol in (D) indicates the location of freshwater input from Manapouri hydroelectric power station.

2.2.1.3 North Taranaki Bight (Parininihi Marine Reserve)

Fieldwork in North Taranaki took place at 4 locations separated by a maximum of 3 km in March 2019 (Fig. 2.1B). The Pariokariwa reef at Parininihi Marine Reserve extends 5 km northeast from the 'White Cliffs' in the southwest corner of the North Taranaki bight. The reef consists of rocky boulders and ledges ranging from approximately 10 to 25 m deep. This area receives frequent, high energy swells generating high turbidity. The reserve has been an area of scientific interest since Battershill & Page (1996) described a particularly dense and di verse sponge assemblage thought to be more normally associated with deeper waters.

2.2.1.4 Poor Knights Marine Reserve

Fieldwork at the Poor Knights Marine Reserve took place in March 2018 and December 2019 at 2 sites (Fig. 2.1A). Sites were chosen according to the largest depth profiles available (maximum of 85 m). The reserve covers an area of 15 km^2 and is situated 22 km offshore east of Matapouri on the northeast coast of New Zealand's North Island. Consisting of 2 main islands, vertical walls descend to an observed maximum of approximately 85 m before reaching a sandy bottom with intermittent boulder complexes. The area is exposed to strong currents and oceanic water, with deep light penetration and low turbidity, which supports abundant and diverse pelagic, coastal, and benthic communities. This includes very diverse and abundant sponge assemblages with over 140 species being recorded (see Kelly & Sim-

Smith, 2009), with many species in shallow water, thought to be facilitated by the shade provided by a macroalgal canopy (Battershill & Page, 1996).

2.2.2 Benthic video collection

The ROV 'SAL', Model DG2 (Deep Trekker Inc.) with an internal and external mounted GoPro 4 silver camera (set at 60 fps at 1080p resolution) and an internal (4k) camera mounted on an independent remotely controlled swivel was deployed at all locations. Studies using AUVs and ROVs for quantitative assessments of benthic communities have been criticised for overlooking potential parallax error (e.g. Rivero Calle, 2010 as discussed in Lesser & Slattery, 2019). This issue is less problematic when employing a randomized point-count approach for percentage cover analysis of images whereby the whole area is not used (Scott et al. 2019). However, I set the internal camera to linear mode and kept the camera angled perpendicular to the substrate to minimize parallax error as far as possible.

ROV deployment protocol varied slightly according to each location. At Fiordland and the Poor Knights, the ROV was driven vertically downwards from the vessel and then towards the wall once the estimated maximum depth of the wall had been reached. Approaching the wall from the deepest possible depth reduced the likelihood of entanglement with features on the wall itself. The ROV was driven along the wall on a horizontal transect for approximately 10 min. Lasers were used on the ROV to determine distance from the wall (1 m) producing frame grabs of similar scales. A precise scale was not required for determining the abundance of benthic organisms using an area occupied approach. The ROV was then driven upwards 10 m and another transect completed. This process was repeated at 10 m depth increments until the shallowest transects at 30 m were completed at each site. The maximum depth reached was 120 m at Fiordland and 80 m at the Poor Knights. The ROV protocol for the south and north Taranaki locations was tailored for horizontal rather than vertical reef structures. The

ROV was driven vertically down from the vessel, set at an angle of approximately 85°, and then driven along a horizontal transect for approximately 10 min. Other benthic communities less than 30 m deep were sampled using SCUBA, whereby the same diver would swim horizontally along a wall at 3 transect depths of 25, 15, and 5 m, taking photographs (Nikon D800 with Ikelite Housing and YS50 TTL strobe) approximately every meter and 1 m from the substrate. Preliminary tests were undertaken to test the consistency between data derived from ROV deployments and SCUBA. I employed the same protocols as described above for both ROV deployments and SCUBA to assess the same designated area of substrate. I found no significant differences between data derived from ROV and SCUBA images of the same quadrats (Fig. A2.1).

2.2.3 CTD deployment

CTD model RBRconcerto/201801 was set to log temperature (°C), turbidity (NTU), salinity (PSU), chlorophyll a (mg l^{-1}), depth (m), and conductivity (SI) every second. Two replicate deployments were made at each site down to the deepest ROV transect. Descent rate was approximately 2 m s^{-1}, and the ascent rate was approximately 1 m s^{-1}. The CTD was deployed at all sites at all locations. CTD data were extracted using the RBR software. The use of CTD data allowed us to determine if any correlations existed between environmental variables and benthic community distributions. CTD data were averaged according to the same 10 m increments as categorized in the community distribution data to allow for statistical correlations. Extreme outliers in the CTD data only occurred for turbidity at the lowest 50 cm of each deployment due to disturbance of soft sediment when touching the seafloor; these obvious outliers were removed. As this study was undertaken across a relatively large geographic scale and with some temporal variability, the precise values of the environmental variables measured were not used for between-location comparisons.

2.2.4 Video analysis

Videos collected from ROV deployments were analysed using VLC media player; 10 frame grabs were extracted from each transect as replicates. The choice of frame grabs for analysis was dependent on the efficacy of each image. Frame grabs exhibiting the lowest occurrence of blurring and with the most perpendicular perspective of the substrate were prioritized. This ensured the greatest accuracy of the proceeding analyses and reduced potential selection bias toward images displaying specific community compositions or components. Coral point count (CPC) was used to estimate the percentage cover of (1) 9 benthic groups at the phylum level, namely Porifera, Bryozoa, Cnidaria, Ascidiacea, Annelida (only polychaetes observed), Echinodermata, Mollusca, Chordata, Brachiopoda; (2) 3 mixed levels of algae, namely crustose coralline algae (CCA), macroalgae, and branching coralline algae; and (3) 'unidentified' organisms that could not be confidently assigned to any of the predefined phyletic groups due to indistinguishable gross morphological traits or the obstruction of view due to overlapping organisms in the image. Bare substrate was included ensuring the total cover of each image quadrat equalled 100%. The 9 phyla described, covered every identifiable organism observed. A single analyst carried out all CPC image analyses to maintain quality control. All 9 phyla were included in statistical analyses. However, I only provide figures for the 6 overall most abundant groups (Fig. 2.2), as the abundance of the remaining groups was extremely low in most transects. A second database was created from CPC where the sponges were broken down into 10 morphological types based on, but not exclusive to, those categorized by Bell & Barnes (2001): encrusting, repent, digitate, massive, branching, flabellate, globular, tube, calcareous, and other. Calcareous was applied as a description specifically for the species *Leucettusa lancifera*, which was particularly common at Fiordland and morphologically distinct from the other categories. Repent refers to both cushion and repent forms as described by Bell & Barnes (2001), as these could not be easily

distinguished due to perpendicular ROV camera angles restricting perspectives required to differentiate them. ‘Other’ refers to any morphology that could not be assigned to any of the 9 specific categories. To determine the contribution of sponge assemblages to habitat complexity, all morphologies described above were binned into levels of high, medium, and low complexity (Table A2.2). The relative complexity levels were assigned based on the true surface area of different morphologies relative to their individual cover as observed in a 2-dimensional image (Fig. A2.2). Images were taken of upright specimens of each morphology, and surface area was determined using foil closely wrapped around the entire specimen. The 3 morphologies with the lowest ratios were categorized as low complexity, the next 4 morphologies that exhibited larger but similar ratios were categorized as medium complexity, and the 3 morphologies with the largest ratios were categorized as high complexity. These categories are qualitative and were designed to demonstrate the relative changes in the overall (% cover) and relative (% of sponge assemblage) contributions of different morphological complexities across different depths. Changes in the cover of each morphological group can be seen in Fig. A2.3. I also applied a full quadrat complexity score to sponge assemblages in each depth bin to assess the changes in the overall complexity of the sponge assemblage across depth. These scores were derived from the same image cover/surface area ratios as described above but were assigned a value of 1−5 in complexity (1 = lowest complexity, 5 = highest complexity; see Table A2.2). With a particularly low image cover/surface area ratio, encrusting forms were given a lower score (1) than the other low complexity forms (2), while branching forms were given a higher score (5) than the other high complexity forms (4) due to a particularly high ratio. The assigned scores were then multiplied by the abundance value (% cover) of each morphology in a quadrat to provide an overall complexity score in a quadrat that also considers the total cover of each morphology. Complexity values (1−5) were also qualitative and used to estimate relative (as opposed to actual) changes in sponge

provisioning to habitat complexity. CPC randomly allocates points over an image; the user then manually identifies the substrate or benthic taxa beneath each point. The software uses this input to estimate substrate composition across the entire frame-grab (percentage cover of each substrate/ benthos), exporting the information as a comma-separated values (CSV) database. A maximum of 100 points was sufficient to reach the plateau of the species accumulation curve (Fig. A2.4) for each location. These were generated from tests of randomised frame-grabs assigned with: 10, then 20, 60, 80, 100, 120, 140 points.

2.2.5 Data analysis

Data was analysed using Rstudio 3.5.1 and PRIMER V6 + PERMONOVA. Permutational multivariate analysis of variance (PERMANOVA) was used to determine the effect of fixed factors (i.e. depth) on multivariate data (i.e. community composition and sponge assemblage morphological composition) using a Bray-Curtis resemblance matrix. PERMANOVA in PRIMER was also used to determine any differences between depth categories of univariate (i.e. sponge cover) and multivariate data as post-hoc pairwise tests. Data were checked in Rstudio 3.5.1 for homoscedasticity and that assumptions of normality were met by observing standardized residuals plotted against theoretical quantiles (QQ plot), as well as residuals *vs*. fitted and leverage values. Data was log-transformed to improve normality and reduce heteroscedasticity where appropriate, although this is not an underlying assumption for permutational tests. Raw CTD environmental data were visualized as line graphs. SIMPER analysis was used to determine those groups most responsible for the differences between depths. Canonical analysis of principal coordinates (CAP) was used to visualise the variation in community data and sponge assemblage morphological composition based on depth, whereby the distances amongst centroids were calculated from a Bray-Curtis resemblance matrix. CAP analysis was chosen, as this method finds axes through the multivariate cloud of data points, which discriminate among a priori groups. Benthic group vectors from

multidimensional scaling (MDS) were then overlaid according to a Pearson's rank correlation threshold of 0.4 to visualise the most important community or sponge categories explaining these distribution patterns. Sponge complexity bins from the relative image cover/surface area ratios were analysed both as the percentage cover of the substrate and as a proportion of the total sponge assemblage cover. This took into consideration of how relative assemblage complexity changed with depth, while controlling for any changes in overall sponge cover.

2.3 Results

2.3.1 Benthic community composition

At the Poor Knights, overall community composition varied considerably with depth (Pseudo-$F_{8,133}$ = 7.675, $p < 0.001$) (Figs. 2.2A & 2.3), with significant differences between almost every 10 m increment (Table A2.3 for post-hoc t-test results and pattern exceptions). This was attributed to an overall significant decline in macroalgae and significant changes in ascidian and cnidarian cover with depth (Fig. 2.2A, Table A2.4). While sponges showed significant variation in their cover with depth, they were the most abundant benthic group at every depth, ranging from a low of 36.6% (±5 SE) cover at 30 m to 72.3% (±5.2 SE) at 70 m, compared with the next most overall abundant group (bryozoans), which ranged from a low of 6.2% (±1.2 SE) at 5 m to a high of 27.5% (±5.1 SE) cover at 25 m (Fig. 2.2A).

At the inner Fiordland sites community composition also changed significantly with depth (Pseudo-$F_{9,116}$ = 12.341, $p < 0.001$). Here, a particularly distinct community was found at 5 m (Fig. 2.3C) as a result of particularly high macroalgal cover and an absence of sponges and CCA (Fig. 2.2B). There were significant changes in community composition across the shallow depth range (15−30 m), resulting from further declines in macroalgae, a significant decline in CCA from a very high cover (89.3% ± 2.3 SE) at 15 m, and a corresponding increase in sponge cover (Fig. 2.2B, Table A2.5). Community composition was similar

within the 30−60 m depth range, but it was distinct from the shallower and deeper depths (Fig. 2.2B). The 30−60 m region was characterised by a relatively high abundance of polychaetes (ranging from 3.7% ± 1.1 to 5.9% ± 0.9 SE). Community composition changed again into a distinct deeper depth zone (70−100 m), characterised by a higher bryozoan cover and reduced sponge and polychaete cover. Limited change in community composition occurred within this depth zone (Table A2.5 & S6).

At the mid Fiordland sites, community composition changed significantly with depth (Pseudo-$F_{12,577}$ = 17.071, $p < 0.001$). The change down to 70 m (Figs. 2.2C & 2.3, Table A2.7) was primarily due to a reduction in CCA cover, where the shallowest depths (5−25 m) were characterised by high CCA cover (35.1% ± 3.6−24.7% ± 5 SE). The initial increase and then decline of sponges at this same depth was also responsible for the overall changes seen in community composition (Fig. 2.2C, Tables A2.7 & A2.8). However, the community then changed beyond 70 m and remained similar down to 120 m (Table A2.7). This deeper region was characterized by higher polychaete cover but lower ascidian, cnidarian, and sponge cover (Fig. 2.2C) compared to other shallower depths, and an absence of macroalgae. However, sponge cover remained high relative to other groups (ranging from 4.5% ± 1.5 to 12.1% ± 1.4 SE).

Outer Fiordland sites showed a significant (Pseudo $F_{12,293}$ = 6.821, $p < 0.001$) but less rapid change in community composition with depth than the mid Fiordland sites (Fig. 2.2D, Table A2.9). CCA showed a large decline from 5 to 30 m, while macroalgae also showed a major decline from 15 to 30 m (Fig. 2.2D) explaining community composition differences both within this region and between shallower and deeper depths. However, no significant changes in community structure were seen throughout the entire depth range of 60−120 m, with this zone being characterised by consistently high sponge cover and an absence of all algal groups (Fig. 2.2D, Tables A2.9 & A2.10). The significant difference in community composition

between shallow and deeper depths was attributed to the disappearance of algae. Sponges showed consistently higher cover relative to other groups, with the average similarity in community composition across the full depth range being most attributed to sponges, except for at 5 m (Fig. 2.2D, Table A2.10).

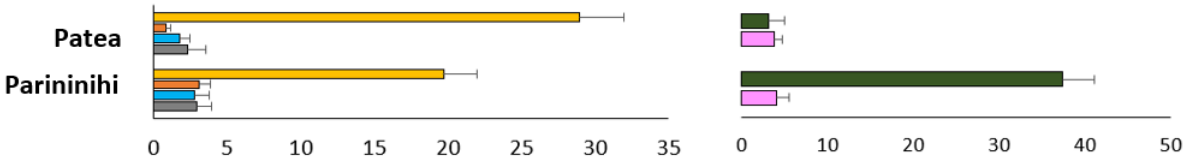
Patea
Parininihi
0 5 10 15 20 25 30 35
0 10 20 30 40 50

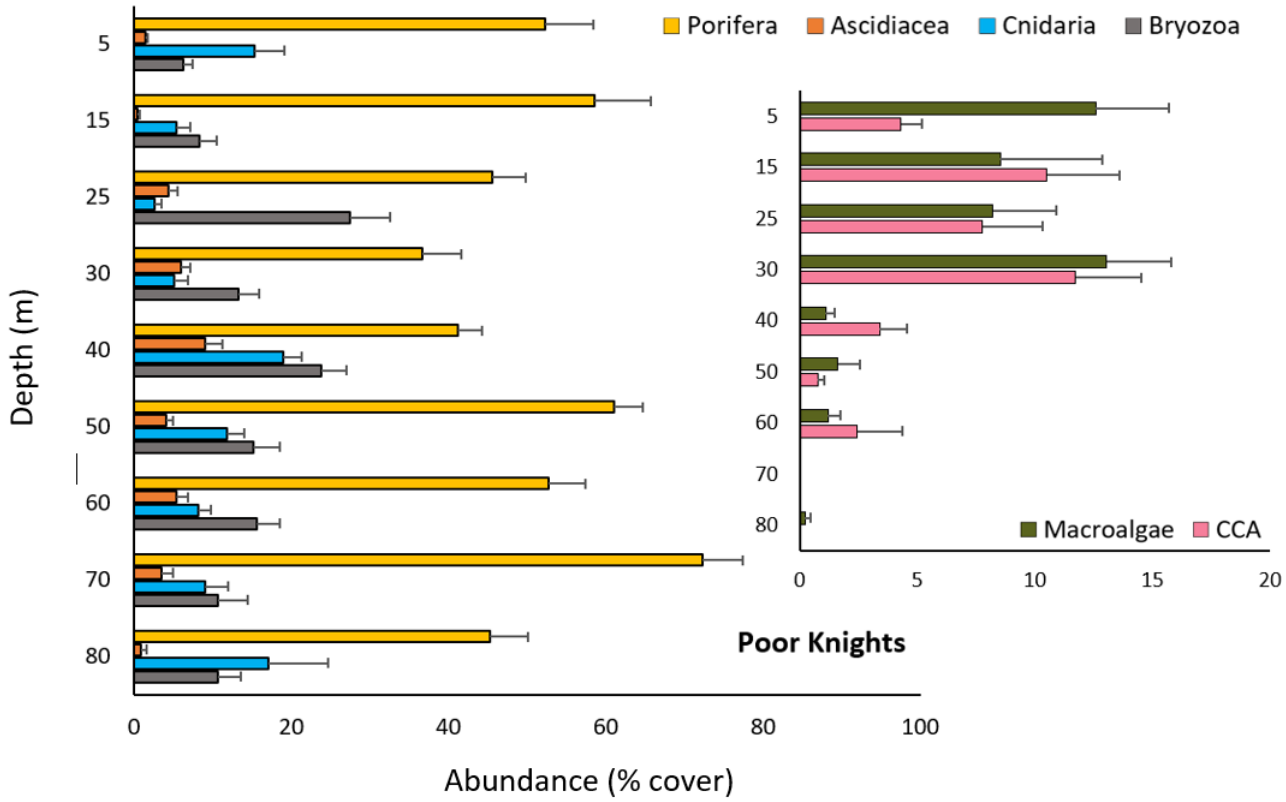
Porifera
Ascidiacea
Cnidaria
Bryozoa
Depth (m)
5 15 25 30 40 50 60 70 80
0 20 40 60 80 100
Poor Knights
Macroalgae
CCA
0 5 10 15 20
Abundance (% cover)

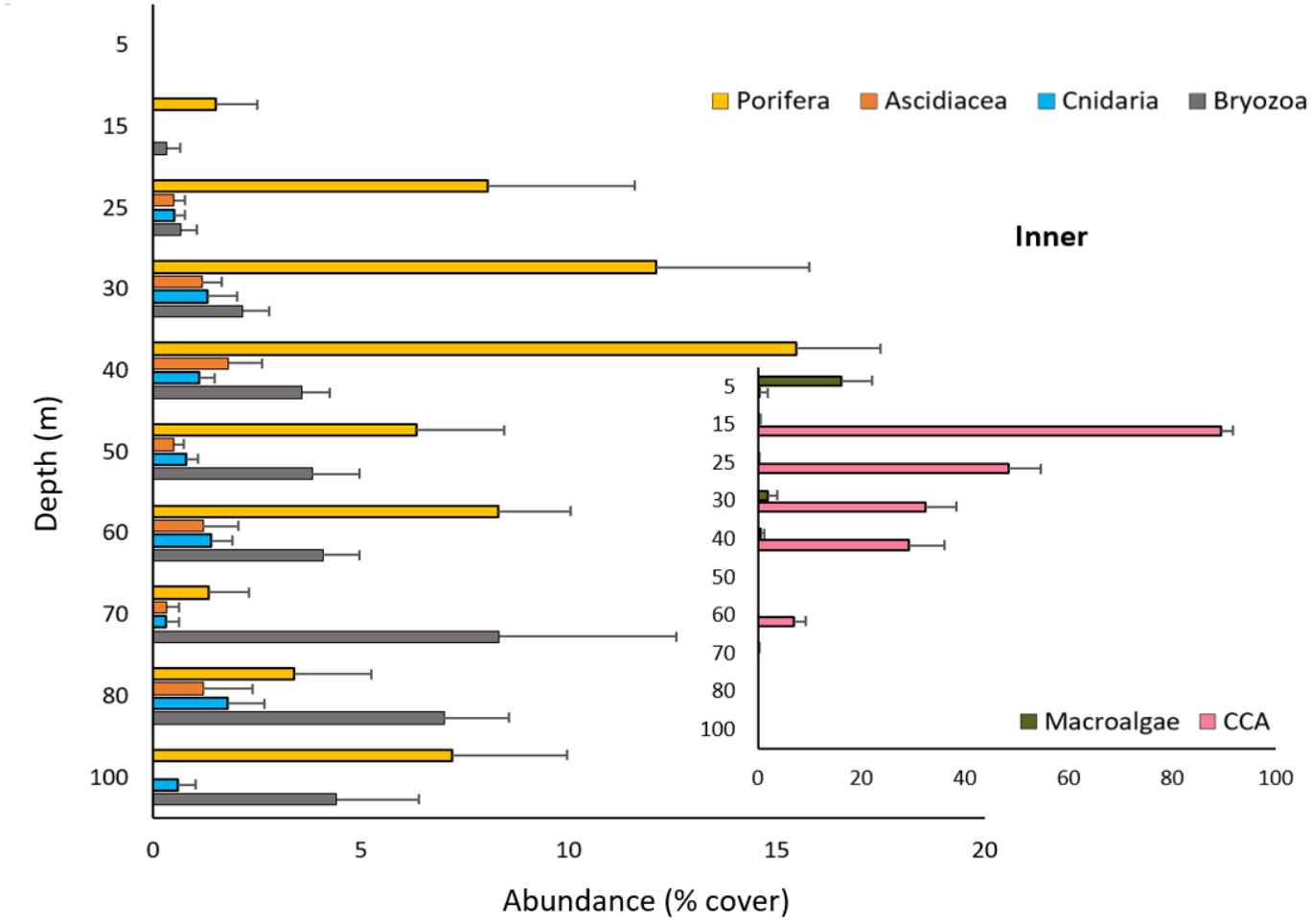
Porifera
Ascidiacea
Cnidaria
Bryozoa
Depth (m)
5 15 25 30 40 50 60 70 80 100
0 5 10 15 20
Inner
Macroalgae
CCA
0 20 40 60 80 100
Abundance (% cover)

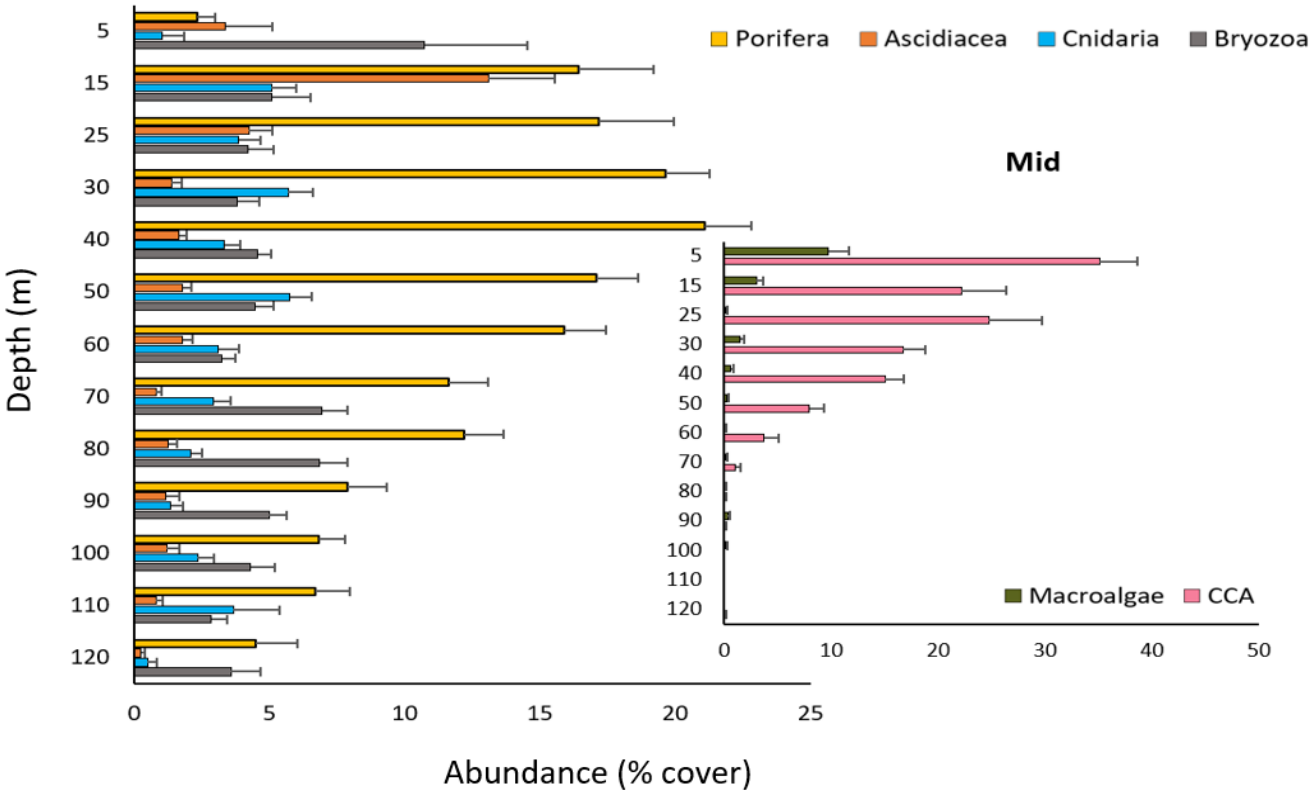

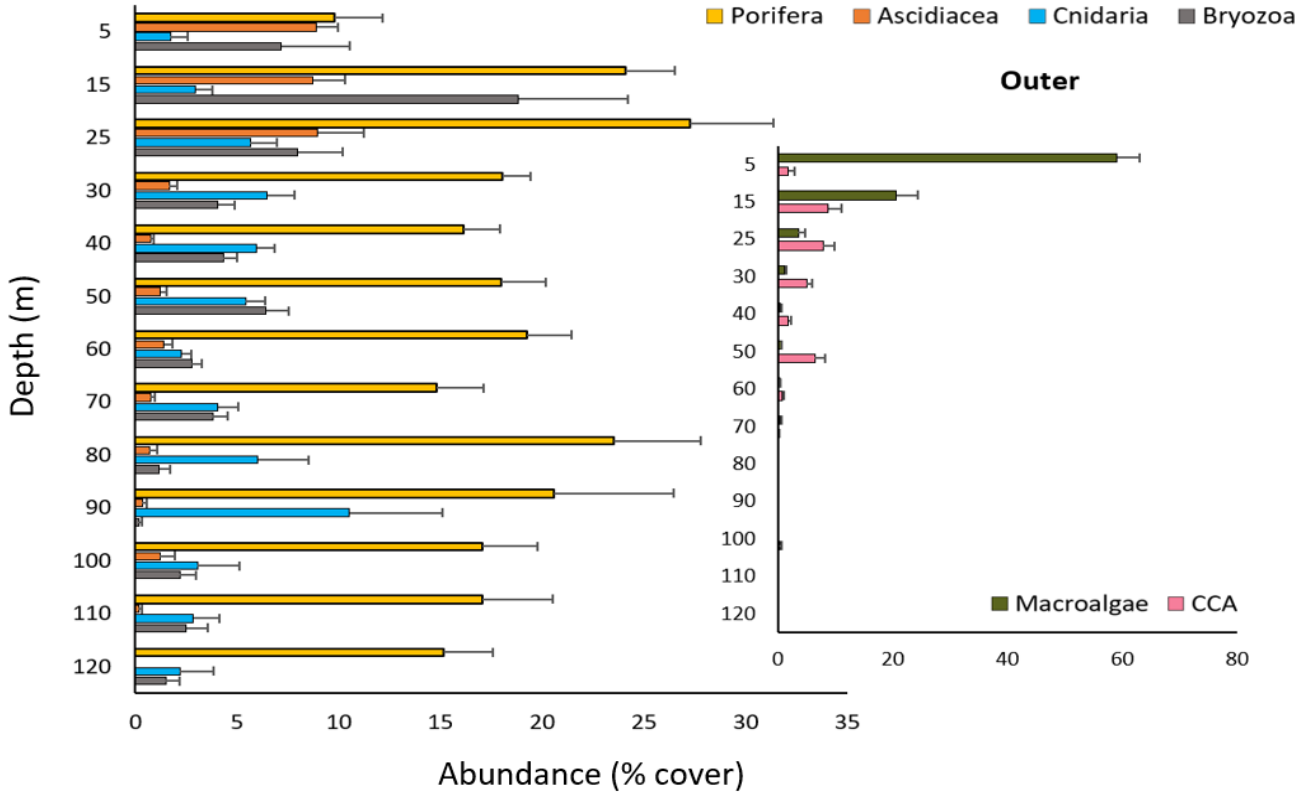

Fig. 2.2 (above and this page). Abundance (as % coverage) of the 6 most abundant benthic groups at Poor Knights, inner, mid, and outer Fiordland, aswell as Patea and Parininihi at 25 m only. Algal groups have been separated to maintain meaningful visualisation of invertebrate groups due to large differences in abundance values. Values are means ± SE. CCA: crustose coralline algae.

2.3.2 Changes in sponge cover with depth

Sponges were the most abundant invertebrate community group at all locations and were particularly abundant at the Poor Knights with a range of 36% (±5 SE) to 72% cover (±5.2 SE) (Fig. 2.2). Sponge cover was also significantly different between depths at Poor Knights ($F_{8,133} = 4.338$, $p < 0.001$, inner Fiordland ($F_{9,116} = 4.482$, $p < 0.0001$), mid Fiordland ($F_{12,577} = 11.01$, $p < 0.0001$), but not at outer Fiordland ($F_{12,293} = 1.476$, $p < 0.132$). At the Poor Knights sites, sponge cover was highly variable with the highest peak of cover occurring in the mesophotic zone. Sponge cover showed a significant decline from 15 m (58.5% ± 7.1 SE) to 30 m (36.6% ± 5) ($p < 0.05$) before significantly increasing again at 50 m (60.1% ± 4.7 SE) ($p < 0.001$), which was maintained down to 70 m (72.3% ± 5.2 SE) before a non-significant decrease at 80 m (45.3% ± 4.8 SE) (Fig. 2.2A). At the inner Fiordland sites, sponge cover increased from no cover at 5 m to a peak of 15.46% (±2 SE) cover at 40 m (Fig. 2.2B), which was significantly higher than all other depth bins (range of $p < 0.05$ to $p < 0.001$), except at 30 m. A significant decline occurred beyond 40 m, where cover remained below 10% at all remaining depths sampled (Fig. 2.2B). At the mid Fiordland sites, sponge cover was lowest at 5 m (2.4% ± 4.8 SE cover) and then increased rapidly between 5 and 15 m to 16.4% (±2.8 SE) ($p < 0.001$), reaching a peak at 40 m (21.1% ± 1.7 SE). Abundance then significantly declined from 40 down to 120 m ($p < 0.001$). After an initial significant increase between 5 and 15 m (from 9.8% ± 2.3 to 24.1% ± 2.4 SE) ($p < 0.001$) (Fig. 2.2D), the outer Fiordland sites showed no further significant change in sponge cover across depth categories. Sponge cover at Patea (25 m) was particularly high (30% ± 3 SE) and higher than macroalgae and CCA cover (3.1 ± 1.9 to 3.9% ± 0.8 SE, respectively). Parininihi had lower sponge cover (19.6% ± 2.3 SE) but with high corresponding macroalgae cover (37.4% ± 3.6 SE) (Fig. 2.2E).

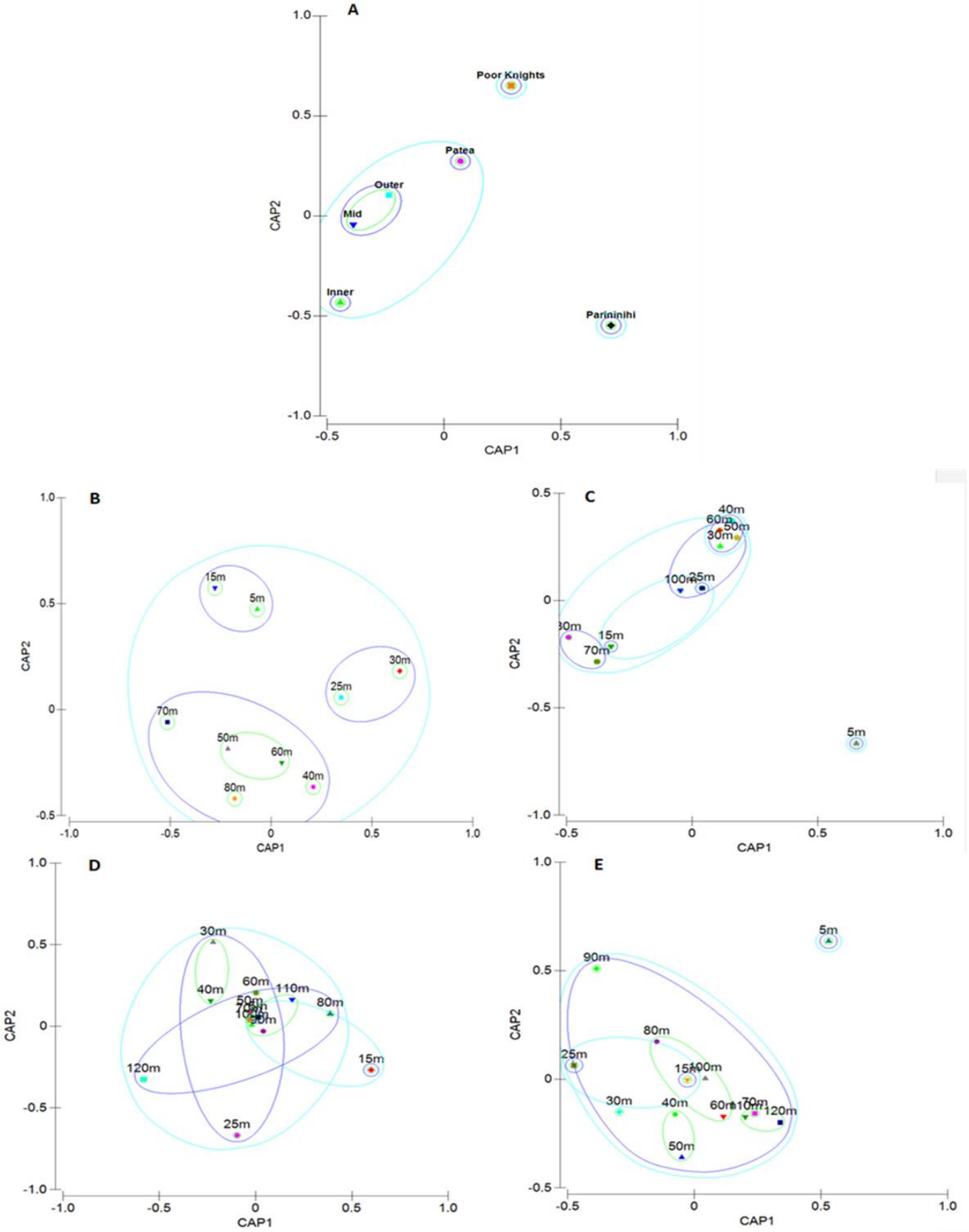

Fig. 2.3 Canonical analysis of principal coordinates (CAP) ordination of sampled benthic community composition at all survey locations across all depths with groups factored as location (A). Groups were then factored as depth at (B) the Poor Knights, (C) inner Fiordland, (D) mid Fiordland, and (E) outer Fiordland. Analysis is based on a Bray-Curtis

similarity matrix of percentage cover data. Clusters are based on resemblance levels at 10% (green), 20% (blue), and 30% (turquoise).

2.3.3 Sponge assemblage morphological composition

Sponge assemblage morphological composition was significantly different between depths at all locations with depth profiles: Poor Knights ($F_{8,133} = 5.65$, $p < 0.001$); inner Fiordland ($F_{9,116} = 4.53$, $p < 0.0001$); mid Fiordland ($F_{12,577} = 6.99$, $p < 0.0001$); and outer Fiordland ($F_{12,293} = 3.37$, $p < 0.001$), (Tables A.211–A.214). At the Poor Knights, encrusting sponges (low complexity, Table A2.2) were the most abundant morphologies at all depths except 80 m (Figs. 2.4B & S3A), where their cover declined significantly from a peak of 50.6% (±7.6 SE) at 15 m to 4.1% (±1.9 SE) at 80 m ($p < 0.001$). Here, branching and massive sponges became the most dominant forms (both > 9% total cover at 80 m) having both increased in cover significantly from where they first appeared at 15 m ($p < 0.01$) and 5 m ($p < 0.001$), respectively. Repent and flabellate forms also increased significantly at deeper depths from 3.9% (±0.9 SE) at 5 m to a peak of 17.3% (±2.9 SE) at 50 m ($p < 0.001$), and 0% at 5−15 m to a peak of 6.4% (±4.4 SE) at 80 m ($p < 0.001$), respectively (Fig. A2.3A).

Depth-related changes in the morphological composition of sponge assemblages at inner Fiordland sites were more difficult to elucidate given the low overall sponge cover (Figs. 2.2B & S3B). However, encrusting, globular, and repent sponges were the most abundant forms overall (Fig. A2.3B). These forms all increased in cover at mid-range depths, all peaking at 30 or 40 m (encrusting: 11.4% ± 2.1 SE; repent: 1.3% ± 0.5 SE; globular: 2.3% ± 0.5 SE) and then declining into the deeper depth zones where at 100 m repent forms disappeared entirely, and globular and encrusting forms dropped to 0.6% (±0.3 SE) and 3.6% (±1.4 SE), respectively (Fig. A2.3B). SIMPER analysis showed that similarities in assemblage morphological composition between depth bins were explained by the presence of encrusting morphologies due to their consistently high relative abundance. At the mid

Fiordland sites, each morphological type was represented across a wider depth range than at inner Fiordland sites (Fig. A2.3C). Overall, encrusting sponges were again the most dominant form at every depth (Fig. A2.3C). However, after peaking at 40 m (14.9% ± 1.4 SE), encrusting forms then declined significantly with increasing depth down to 120 m (2.1% ± 1.2 SE) ($p < 0.001$), (Fig. A2.3C). Globular forms followed a similar pattern to encrusting forms, peaking at 30 m (1.8% ± 0.3 SE) and then declining down to 120 m (0.3% ± 0.1 SE) ($p < 0.001$). Repent forms peaked at a shallower depth of 15 m (2.6% ± 0.9 SE), and then steadily declined, but non-significantly, with depth until 60 m (0.9% ± 0.2 SE) beyond which their cover changed very little with increasing depth. Massive forms showed no obvious pattern with depth. At both depth extremes, sponge assemblages were generally defined by lower cover of all morphologies (Fig. 2.2 & S3).

While most sponge morphologies were more abundant at every depth at the outer Fiordland sites than mid Fiordland sites, the relative abundance patterns were similar. However, encrusting sponges were an exception, where their cover did not change as much with depth as found at the mid Fiordland sites, only showing a non-significant drop in cover after 90 m, ranging from a low of 4.2% (±1.6 SE) to a high of 5.2% (±2 SE) cover (Fig. A2.3D). Repent sponges were the next most abundant form and followed a similar depth pattern to that at mid Fiordland sites, with a peak in cover at 15 and 25 m (7.5% ± 2.7 SE and 5.1% ± 0.5 SE, respectively). This was significantly higher than all other depths ($p < 0.001$) and steadily declined with depth (Fig. A2.3D) with the exception of a second smaller peak occurring at 120 m (4.3% ± 1.5 SE). As with the mid Fiordland sites, globular sponges peaked from 30−50 m (3.0% ± 0.4 to 2.2% ± 0.3 SE), but again, as with repent forms, a second peak in cover occurred at 120 m (4.3% ± 1.4 SE) (Fig. A2.3D). Massive forms showed no obvious pattern with depth except for a peak in cover between 80 and 110 m that was significantly higher than at all depths above 80 m and below 25 m ($p < 0.01$). A maximum cover of 4.5%

(±1.9 SE) was reached at 110 m before significantly reducing in abundance, declining to 0.2% (±0.2 SE) cover at 120 m ($p < 0.05$) (Fig. A2.3D).

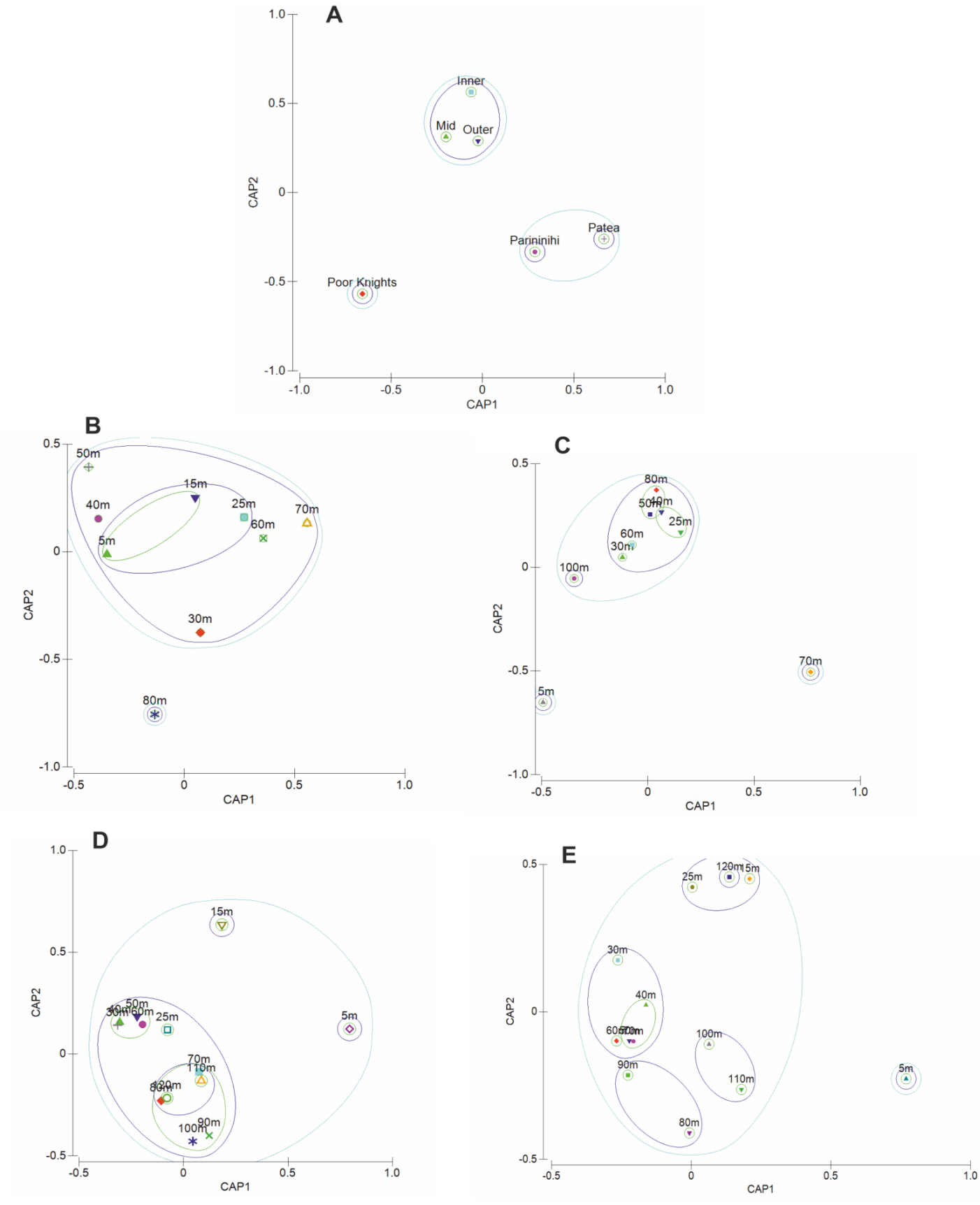

Fig. 2.4 Canonical analysis of principal coordinates (CAP) ordination of sponge assemblage morphological composition at all survey locations across all depths with groups factored as location (A). Groups were then factored as depth at (B) the Poor Knights, (C) inner Fiordland, (D) mid Fiordland, and (E) outer Fiordland. Analysis is based on a Bray-Curtis similarity matrix of percentage cover data. Clusters are based on resemblance levels at 10%

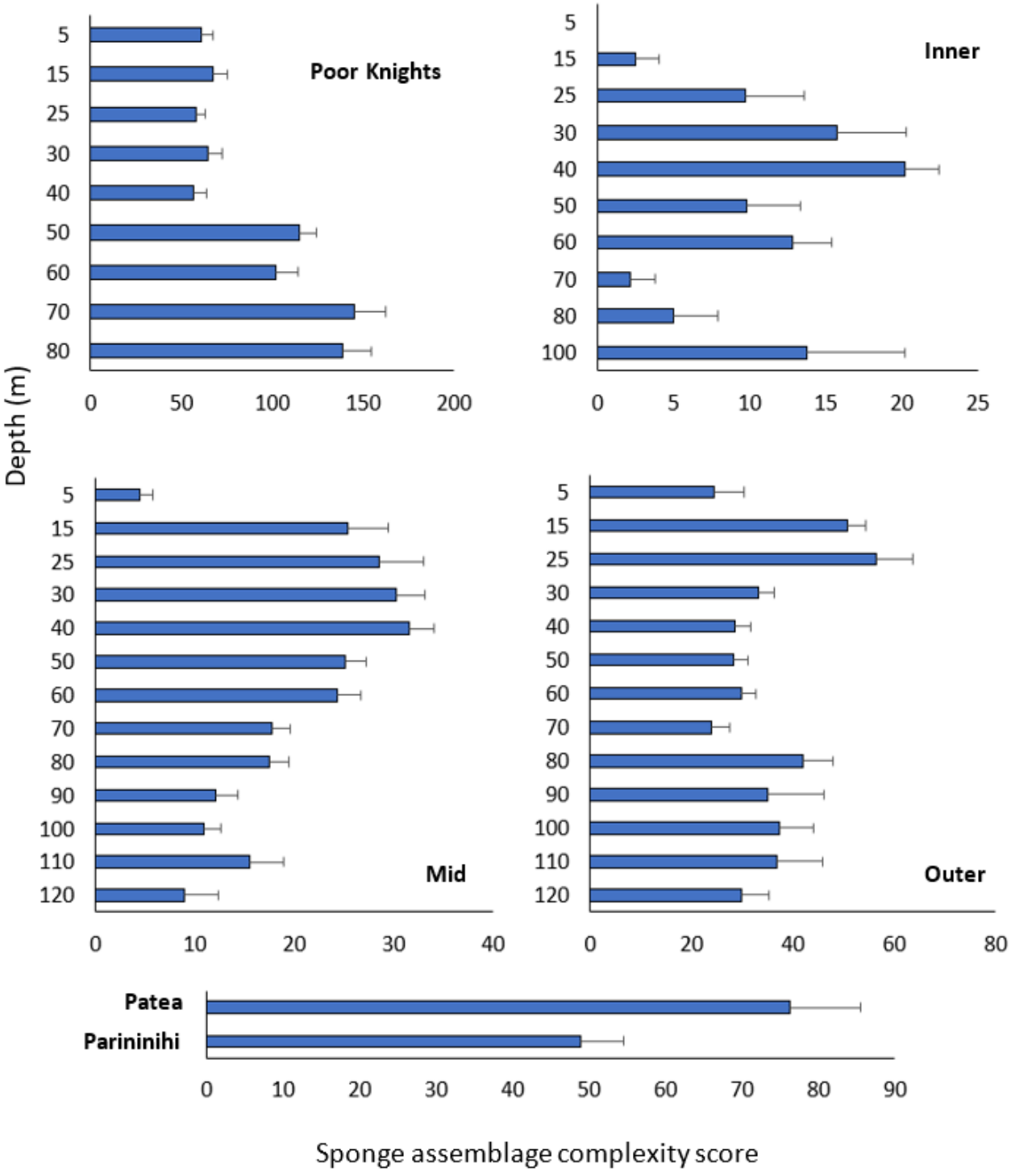

Fig. 2.5 Sponge assemblage morphological complexity scores at 10 m depth increments at Poor Knights, inner, mid, and outer Fiordland, Patea, and Parininihi. Assemblage complexity scores equal the sum of the complexity score assigned to each morphological type of sponge (ranging from 1−5, Table A2.2) multiplied by the abundance of each morphology in a quadrat. Sampling effort was homogenous across depth bins and sites. Figure shows mean of quadrat scores + SE.

2.3.4 Sponge assemblage contribution to habitat complexity

Sponge assemblage morphological complexity (as assemblage complexity score, see Table A2.2) changed significantly with depth at all locations (Fig. 2.5). Poor Knights ($F_{8,133} = 10.8$, $p < 0.0001$) showed a significant increase beyond 40 m ($F_{8,133} = 5.05$, $p < 0.0001$), while overall morphological complexity at inner Fiordland ($F_{9,116} = 4.02$, $p < 0.0001$) peaked at 30 and 40 m. At mid Fiordland ($F_{12,577} = 9.72$, $p < 0.0001$) overall morphological complexity also peaked at 40 m, but with a reduction in complexity beyond this depth. At outer Fiordland ($F_{12,293} = 2.79$, $p < 0.001$) overall sponge morphological complexity peaked at 15 m (Fig. 2.5). Low complexity morphologies were consistently the most abundant group followed by medium and high complexity forms throughout the infralittoral and upper mesophotic regions of all locations (Fig. 2.6). However, the deeper depths (>70 m) at all locations showed an increase in medium and high complexity forms compared to shallow regions in respect to actual cover (Fig. 2.6) and proportionally to the full sponge assemblage (Fig. 2.7). At the Poor Knights, low complexity forms initially declined significantly with depth ($p < 0.01$) from a peak at 15 m (57.9% ± 7 SE) (Fig. 2.6) representing 99.1% of the total sponge assemblage (Fig. 2.7), down to 28.1% (±3.2 SE) at 40 m. Cover of low complexity forms was variable below 40 m, but at 80 m there was significantly lower coverage (12.6% ± 3.1 SE) compared to all other depth bins (except for 30 m) ($p < 0.01$), representing only 27.9% of the total sponge assemblage. Medium and high complexity forms were generally more abundant

below 40 m. Medium complexity forms had significantly more coverage at 80 m (22.2% ± 6.8 SE) than all other depth bins ($p < 0.01$). High complexity forms peaked in coverage (13.7% ± 4.3 SE) at 70 m, which was significantly higher than all depth bins in the infralittoral zone (below 30 m) ($p < 0.05$) (Fig. 2.6). Medium and high complexity forms represented 49 and 23.1%, respectively, of the sponge assemblage at 80 m (Fig. 2.7). The relative increase of high complexity forms below 60 m was positively correlated with the overall in - crease in sponge cover ($F_{1,75} = 2.96$, $p < 0.01$). At inner Fiordland, medium complexity forms were most abundant at 100 m with 3% (±1.9 SE) total cover (Fig. 2.6), representing 41.7% of the total sponge assemblage (Fig. 2.7). High complexity forms only occurred at 60 m and at very low overall cover (0.2% ± 0.2 SE), representing only 2.6% of the total sponge assemblage. Low complexity forms were significantly more abundant than medium and high complexity forms at all depths ($p < 0.0001$) but dropped to a low of 58.3% of the total sponge assemblage cover at 100 m, indicating a relative increase in importance of medium complexity forms (Figs. 2.6 & 2.7). At mid Fiordland, high complexity forms were generally low in overall cover with a maximum of 1.3% (±0.5 SE) cover at 25 m (Fig. 2.6). However, high complexity forms became increasingly abundant relative to the overall sponge assemblage, reaching highest proportional cover (20.4%) at the deepest surveyed depth bin (120 m) (Fig. 2.7). Medium complexity forms showed a similar pattern, becoming more proportionally abundant below 80 m, reaching a high of 23.9% at 110 m (Fig. 2.7) but peaking in overall cover at 60 m (2.4% ± 0.7 SE) (Fig. 2.6). At outer Fiordland, the highest sponge cover recorded (27.3% ± 4.1 SE) at 25 m (Fig. 2.2) coincided with the greatest coverage of high complexity forms (2.6% ± 0.8 SE) (Fig. 2.6). This represented 9.4% of the sponge assemblage (the highest proportion of high complexity forms recorded at this location) (Fig. 2.7). The cover of medium complexity forms showed two peaks of high cover at 15 and 25 m (7% ± 2.1 and 7% ± 1.4 SE, respectively) and 100−110 m (7.2% ± 2 to 6.8%

± 2.1 SE, respectively) (Fig. 2.7). However, the assemblage-relative abundance of medium complexity forms significantly increased through the lower mesophotic region from 60 to 110 m (8.9 and 40.2%, respectively) ($p < 0.0001$) and correlated with overall sponge cover ($F_{1,165} = 2.35$, $p < 0.05$) with a significant assemblage-relative reduction in low complexity forms over the same depth range (84.2 to 56.7%) ($p < 0.01$) (Fig. 2.7). Patea showed the highest sponge assemblage complexity score of all locations at 25 m (Fig. 2.5) with an overall cover of 17.2% (±3.5 SE) of medium complexity forms (Fig. 2.6) representing 59.3% of the sponge assemblage (Fig. 2.7) and the only location to exceed the proportion of low complexity forms (9.8%) at this depth. Parininihi showed a lower overall sponge complexity than Patea (Fig. 2.5) coinciding with lower overall sponge cover (Fig. 2.2E). The lower overall complexity score is unsurprising, as the overall sponge complexity metric considers cover as well as morphological complexity scores. However, Parininihi showed the highest overall cover of high complexity forms (2.9% ± 0.6 SE) of all locations at 25 m (Fig. 2.6), which also represented the largest proportion of high complexity forms of any assemblage (14.7%) at 25 m across all locations (Fig. 2.7).

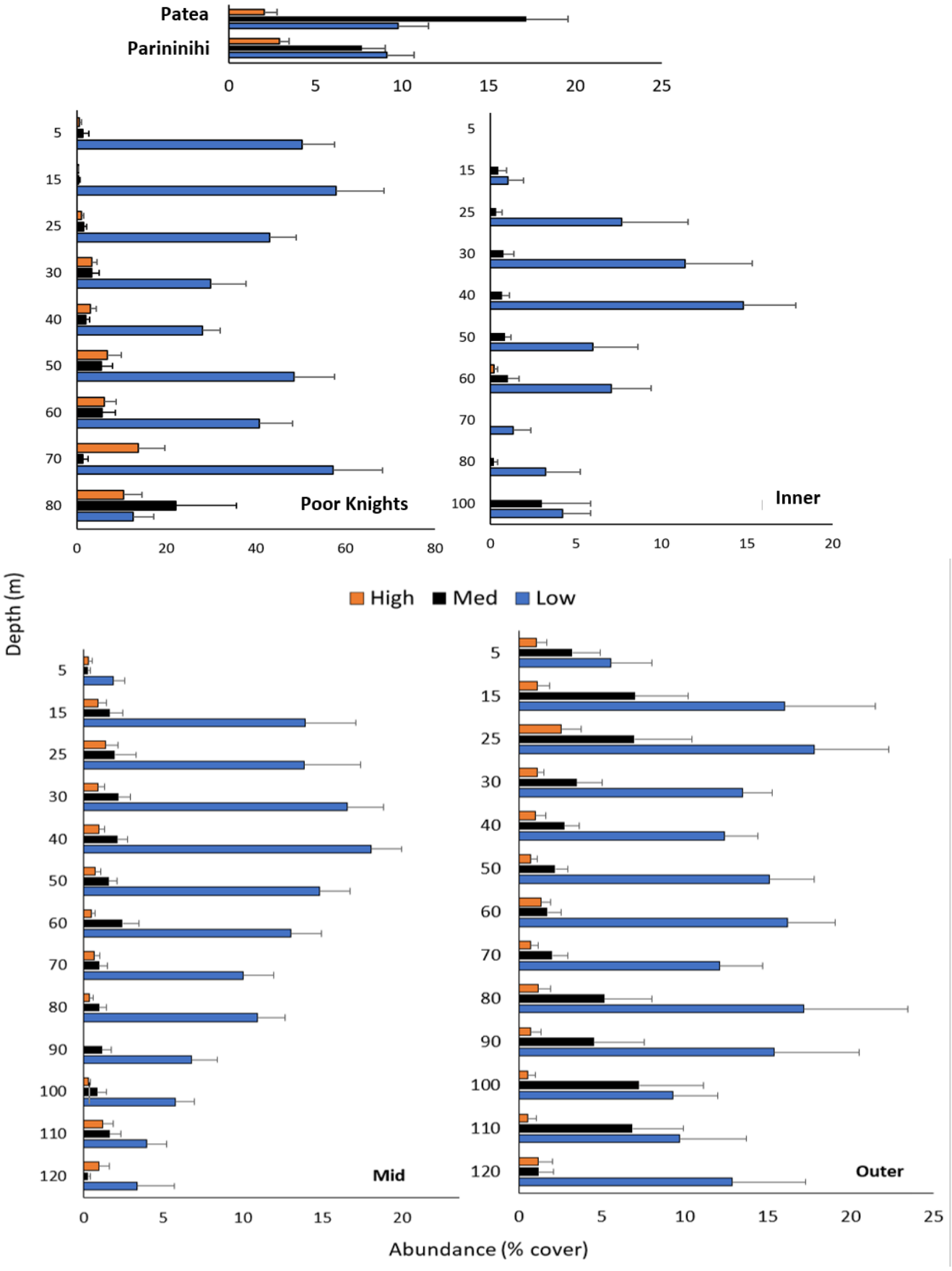

Fig. 2.6 Total sponge cover as binned into high, medium, and low complexity at 10 m depth increments at Poor Knights, inner, mid, and outer Fiordland, Patea, and Parininihi. Figure shows mean + SE.

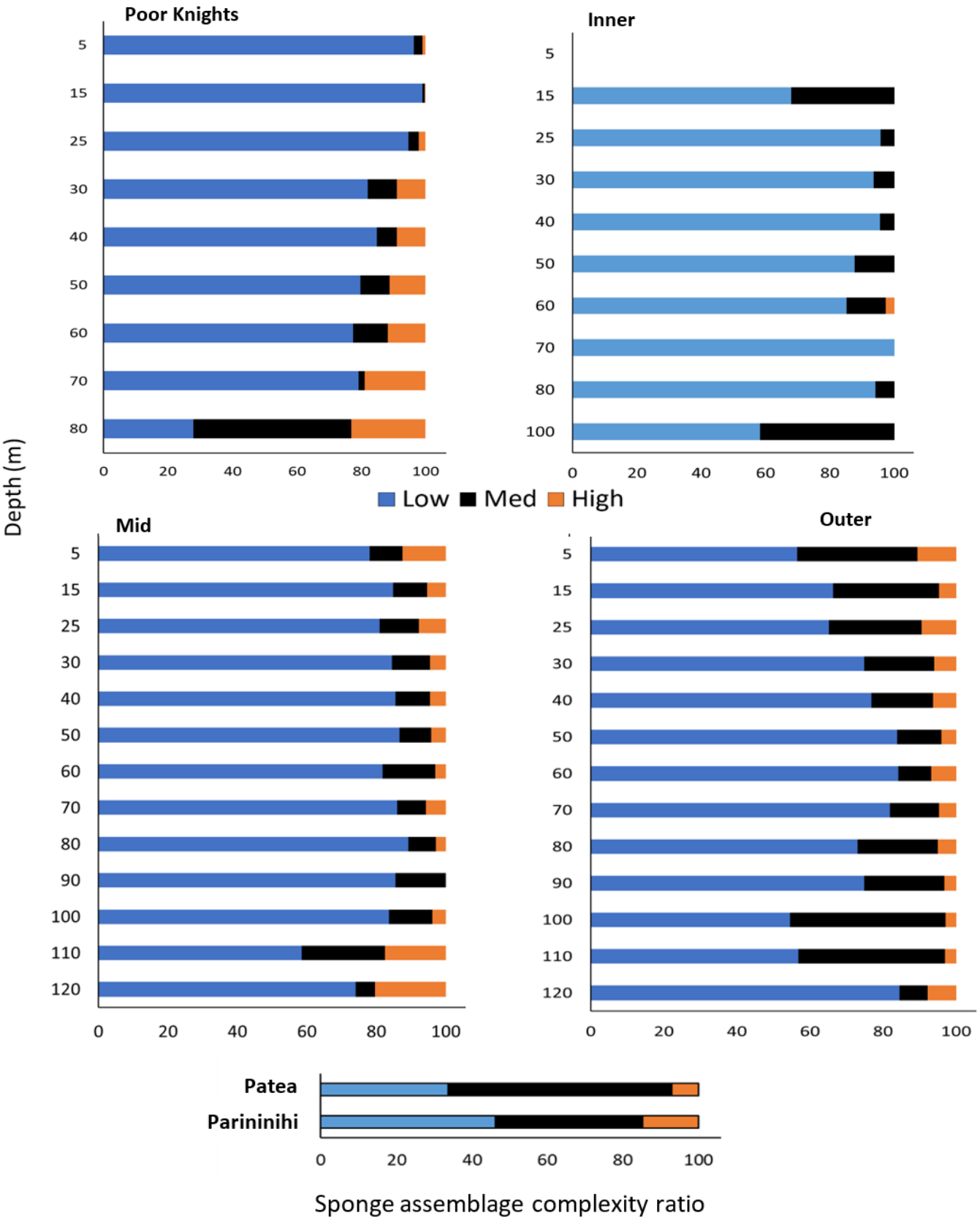

Fig. 2.7 Relative abundance (of sponge assemblage) of low, medium, and high complexity sponge morphologies over 10 m depth increments at Poor knights, inner, mid, and outer Fiordland, Patea, and Parininihi.

2.3.5 Environmental variables

Temperature declined with increasing depth at all locations but stabalized before reaching the depth limits of all sites (Fig. A2.5C). Chlorophyll a concentration also decreased with depth at all locations, dropping most rapidly with depth at inner Fiordland sites, while Poor Knights and outer Fiordland chlorophyll a showed little decline with depth (Fig. A2.5D). Salinity was lower in the first 20 m at inner Fiordland sites than all other locations but rapidly increased with depth, reaching similar concentrations to mid and outer Fiordland sites by 20 m (Fig. A2.5A). Poor Knights showed very little change in salinity with depth (Fig. S5A). Inner Fiordland sites and Poor Knights showed similar average turbidity values with no substantial change with depth (Fig. A2.5B). While turbidity decreased gradually with depth at mid Fiordland sites, it increased with depth at outer Fiordland sites (Fig. A2.5B). These environmental variables showed strong multi-collinearity with depth in linear models; beyond acceptable thresholds of variance inflation factors (>5 VIF). This restricts the evaluation of independent effects of specific environmental variables on community distributions without carrying out experimental tests.

2.4 Discussion

Very little is known about the community composition, abundance, and ecological significance of TMEs. Our study is the first to demonstrate how benthic community composition (at the phylum level) changes from the upper reaches of the infralittoral zone (> 5 m) through mesophotic depth ranges (down to 120 m) for TMEs in New Zealand. My results show that TMEs have abundant benthic communities with significantly different compositions to those occurring at shallow depths (Figs. 2.2 & 2.3, Tables A2.4− A.210) and are therefore likely to provide different ecological services and functions, compared to shallow water communities. However, this study also suggests that TME community compositions can vary significantly across relatively small geographical scales as sampling

location had a significant effect on the depth-related patterns of all TMEs sampled. This suggests that the environmental drivers that determine the benthic community distribution patterns of TMEs are not exclusively associated with depth. Our results also show how shallow-water reefs with reduced light availability are not necessarily appropriate surrogates for deeper water TMEs but instead harbour their own local communities. I also show the substantial contribution of sponges to TMEs relative to other benthic groups and their importance in providing habitat complexity especially in areas below 50 m.

2.4.1 TME benthic community patterns

The most abundant invertebrate phyla occurring across all TMEs were (in descending order) Porifera, Bryozoa, Ascidia, Cnidaria, and Annelida. While sponges were consistently among the most important organisms in characterising the benthic community throughout the infralittoral and mesophotic zone, the high variability in benthic community composition across the locations surveyed likely prevents generalised descriptions of the depth-related patterns of New Zealand TMEs being possible. Indeed, all locations had different depth-related community composition patterns. However, as expected, both macroalgae and CCA declined rapidly with depth and were generally absent below 60 m. As algae are important provisioners of habitat in shallow regions, the exclusion of algae from mesophotic zones is likely to increase the relative importance of sponges to habitat complexity.

At the Poor Knights, the decline in algal cover with increased depth is likely responsible for the increase in benthic animals into the upper mesophotic zone (40 m) as spatial competition between algae and the benthic invertebrate community is reduced. This has been shown in other temperate regions (e.g. Bell & Barnes, 2000; Cárdenas et al. 2012) and is perhaps similar to the relief of spatial competition from algae (Scott et al. 2019) and corals (see Lesser et al. 2018; Bell et al. 2019) in MCEs. However, this relationship is not necessarily

causal, as other abiotic factors, such as substratum inclination (Preciado & Maldonado, 2005), have been shown to have a more significant effect than algal presence on the abundance of benthic organisms in temperate environments. Furthermore, benthic invertebrate groups have also been shown to exhibit high abundance and diversity in conjunction with high algal abundances at shallow depths (e.g. Konar & Iken, 2005). Indeed, the possibility of the co-occurrence of high abundances of algae and sponges was supported by my observations from Parininihi Marine Reserve. It has also been suggested that canopy-forming algae (e.g. *Ecklonia radiata*) can facilitate the abundance and diversity of other benthic invertebrate groups (Cárdenas et al. 2016). These observations from other temperate regions indicate that the mechanisms driving benthic community diversity patterns in TMEs are likely to be context-specific whereby algal abundance may only be an important driver in some locations. This was also confirmed by my own observations of TMEs at inner Fiordland sites, where diversity increased with depth (down to 60 m), which cannot have been a consequence of relief from spatial competition with macroalgae, as algae were almost completely absent below 5 m. While spatial competition from algae might be important in MCEs and certain TMEs with high light availability, such as the Poor Knights, the ecological mechanisms driving the depth-related patterns in community composition and diversity in low light habitats with low algal abundances are likely to be very different.

The reduction in macroalgae with depth is one of the few taxon-specific patterns that occurred at all locations albeit at very different rates and with variable consequences for the wider benthic community. Importantly, the relationship between algae and the wider benthic community becomes more complex when considering that the relationship is two-way with potential negative feedback effects, as some benthic invertebrate groups can also directly determine the distribution and abundance of algae, for example via predation (Tuya et al. 2004). Furthermore, algae comprise an extremely broad group and individual species are

likely to respond differently to the abiotic and biotic factors occurring throughout TMEs depending on species-specific traits. For example, CCA persisted much deeper than other macroalgal species at all locations surveyed, and in some cases, continued far into the mesophotic zone (>60 m), with potentially limiting (Breitburg, 1984) and facilitative (Nelson, 2009) effects on the deeper community components of these TMEs. The only other taxon-specific depth pattern found at all locations was the higher cover of polychaetes (Annelida) at deeper depths (>60 m), where they occupied up to 6% of the substrate (at 60 m at inner Fiordland). Every organism counted in this category was either *Spirobranchus cariniferus* or *Galeolaria hystrix*, 2 species of filter feeding fan worms. These tube-building polychaetes are endemic to New Zealand and southern Australia. While both these species have been observed in the intertidal zone (Riedi & Smith, 2015), my results suggest an overwhelming preference for deeper environments, the reasons for which are not immediately obvious. However, at the Poor Knights, polychaetes were almost completely absent throughout the full depth range where other groups across the benthic invertebrate community (especially sponges) were particularly abundant. Inter-phyletic spatial competition might, therefore, be playing a significant role in the overall exclusion of this group in shallow waters (Bell & Barnes, 2003). Another explanation for the apparent absence of this phylum at the Poor Knights is that the species occurring here, and in the shallower depth zones of other locations are less conspicuous than the large and gregarious reef-building polychaetes found further south, and therefore, were missed during image analysis. This group might not be subject to the spatial competition imposed by other benthic groups and are instead directly utilizing the habitat that more spatially competitive organisms (such as sponges) provide.

2.4.2 Sponge assemblage patterns

I found that sponges were the most dominant benthic community group at every location, through the infralittoral and mesophotic zone reaching very high cover in some cases in the lower mesophotic zone (Fig. A2.6). For example, sponge cover exceeded 70% cover in the lower mesophotic regions of the Poor Knights (Fig. 2.2A), approaching some of the highest reported abundances in MCEs (Lesser & Slattery, 2018) and exceeding those reported for the shallow reefs of other temperate regions (e.g. Bell et al. 2020). The mesophotic-like reefs in Taranaki also exhibited high sponge cover relative to those reported on other temperate reefs within the same depth range (15− 25 m), particularly Patea, which had 30% total sponge cover; higher than reported for any other shallow temperate reefs outside of the Mediterranean (see Bell et al. 2020). The TMEs at all the other locations surveyed had mean sponge cover similar to those observed in temperate infralittoral zones (< 30 m) elsewhere in the world which range from 8 to 18% cover, with the exception of the particularly high abundances found in shallow waters of the Mediterranean (see Bell et al. 2020). However, quantitative information of sponge abundance in the mesophotic zones of other temperate regions is sparse and often derived from narrower depth ranges (e.g. Heyns et al. 2016 [45−75 m], Ferrari et al. 2018 [25−50 m], Idan et al. 2018 [95−120 m]) or is derived from a specimen count approach (number of specimens m−2) without specific depth considerations (e.g. Bo et al. 2012). I observed high sponge cover occurring beyond the infralittoral zones where sponges remained the dominant benthic invertebrate group throughout depth profiles at all sites. However, full depth profile patterns were highly variable. This high degree of variability does not support the sponge increase hypothesis as suggested by Lesser (2006), and Lesser & Slattery (2013), who observed increases in sponge abundance with depth in MCEs. My results are more reflective of those reported by Scott et al. (2019), who also demonstrated high variability in sponge abundance with depth and supported by a review of

the sponge increase hypothesis in Scott & Pawlik (2019), but again, this study was carried out in tropical environments with likely different ecological dynamics driving sponge distributions. It has been suggested that macroalgae are likely to have important contributions to sponge distributions either as facilitative (Cárdenas et al. 2016) or competitive (Easson et al. 2014) interactions. Indeed, I observed a negative correlation between macroalgae and sponge cover within the infralittoral zone, but this was only correlative, and relief from competition from macroalgae might not necessarily be the dominant driver of any observed increases in sponge abundance as demonstrated by Preciado & Maldonado (2005). Furthermore, spatial competition with macroalgae cannot explain the continued variation in sponge cover throughout the deeper regions of the TMEs observed where macroalgae are absent. The variation in sponge cover throughout TMEs is, therefore, likely to be in response to different drivers to those occurring at shallow depths. In particularly diverse and abundant TME benthic communities, this might include spatial competition with other benthic invertebrates rather than just algae, such as bryozoans (Russ, 1982) and ascidians (de Voogd et al. 2004; Chadwick & Morrow, 2011). In more depauperate TME benthic communities, where the substrate is more freely available, limiting factors to sponge distributions might include other ecological mechanisms, such as food availability. The effect of food limitation on the distribution of sponge assemblages remains a contentious topic in certain MCEs (e.g. Slattery & Lesser, 2015; Pawlik et al. 2018), but evidence from other regions supports the hypothesis that food availability could be an important factor in the ecological dynamics of sponges generally (Wooster et al. 2019). To my knowledge, no studies have investigated the role of food limitation on sponge assemblage distributions in TMEs, but given our understanding of sponge responses to temporal variability in food availability from shallow (Perea Blázquez et al. 2013) and abyssal (Kahn et al. 2012) temperate zones, investigations of

food limitation will be important for increasing our understanding of the mechanisms driving sponge assemblage distributions through TMEs.

2.4.3 Sponge morphology and contribution to habitat complexity

Different sponge morphologies can provide different ecosystem functions (Bell, 2008; Folkers & Rombouts, 2020), particularly the provision of habitat (Bell, 2008; Maldonado et al. 2017), which is likely to be particularly important in temperate ecosystems that lack 3D reef-building corals (Graham & Nash, 2013). For example, sponges have been shown to (1) provide important biogenic habitat structure for commercially important species (e.g. Miller et al. 2012); (2) form local biodiversity centres in deep-sea environments (e.g. Hogg et al. 2010); and (3) provide refuge from predation pressure for benthic invertebrates (Henkel & Pawlik, 2005) and fishes (Ryer et al. 2004). Furthermore, sponge morphology has been shown to be closely related to the abundance and diversity of their associated macrofauna (Gherardi et al. 2001). Changes in sponge morphological complexity with depth (as assemblage complexity scores, Table A2.2) were site specific (Fig. 2.5) and closely resembled sponge cover-depth patterns (Fig. 2.2). This was not unexpected due to the inclusion of sponge cover in the assemblage morphological complexity metric. However, categorizing sponge morphologies into high, medium, and low complexity bins revealed how levels of complexity changed with depth independent of overall sponge cover, both in terms of substrate cover (Fig. 2.6) and relative to the overall sponge assemblages (Fig. 2.7). While the specific details of depth patterns of sponge assemblage contributions to habitat complexity varied across TME locations, the overall pattern is one of increasing importance of medium and high complexity sponge assemblages with progression into the mesophotic zone. This has important ecological implications for TMEs harbouring high sponge abundances. The ecological functions of TMEs will involve different ecological community dynamics to shallow regions where the relative importance and contribution of sponges to

habitat complexity is less pronounced due to the higher relative abundance of other habitat-forming organisms, including macroalgae. Indeed, with the significant reduction in abundance of bryozoans, particularly low ascidian abundance, and the absence of macroalgae and CCA, the sponge assemblage in the lower mesophotic region of the Poor Knights appears to be the primary source of biotic habitat complexity in this ecosystem. A similar pattern was reflected at mid Fiordland sites albeit to a lesser extent, whereby the cover of medium and high complexity forms at mid Fiordland remained relatively stable with depth while low complexity forms declined significantly. This resulted in a much higher cover of high and medium complexity forms proportionally to the overall sponge assemblage in the lower mesophotic zones. Outer Fiordland sites showed a significant increase of total (Fig. 2.6) and proportional (Fig. 2.7) cover of medium complexity sponges between 100 and 110 m. Even in circumstances of low overall cover, again, sponges appear to be the primary source of habitat complexity in these TMEs. While the importance of the sponge assemblages to numerous ecological functions, including the provision of habitat complexity, have been discussed, the mechanisms generating these observed patterns observed remain unknown, whereby the environmental variables considered in this study do not show any obvious correlations with sponge distributions. Further study is required to consider a wider range of both abiotic and biotic variables to determine these drivers. Sponge assemblages have been observed to be most affected by substrate inclination relative to a number of quantified biotic and abiotic factors in a multivariate analysis by Preciado & Maldonado (2005). Although changing substrate complexity and inclination with depth were not quantified in this study, these factors provide a possible explanation for the total and proportional morphological complexity depth patterns of sponge communities that were observed in the deeper zones (>70 m) of the TMEs surveyed. The environmental variables that were measured in these zones were relatively stable at these deeper zones (Fig. A2.5) and, therefore, are unlikely to

be fully responsible for the observed changes in the morphological composition of the sponge community.

2.4.4 Mesophotic TME surrogates

Parininihi and Patea were only surveyed across a limited depth profile between 15 and 25 m, beyond which, rocky reef becomes homogeneous sandy habitat. However, these locations are known to have poor light penetration and visibility (Battershill & Page, 1996) and as such were chosen to determine if low-light shallow reefs can harbour benthic communities analogous to those found at deeper locations and potentially act as shallow surrogates for deeper TMEs more generally. My results suggest that this was not the case and that these reefs harbour different community compositions to those occurring in TMEs, but also from those occurring at the same depths in other locations in New Zealand. However, these reefs do appear to be more similar to deeper habitats in regard to their sponge assemblages and the particularly high morphological complexity of these assemblages. High and medium sponge morphologies were significantly more abundant at both Patea and Parininihi than in the infralittoral zones of the other locations surveyed. As such, while these shallow reefs may not be suitable direct surrogates for the wider benthic communities of TMEs, they provide valuable opportunities to develop our understanding of the ecological functions of sponge assemblages more typical of TMEs and are also likely to provide valuable insights into the driving mechanisms behind TME community compositions generally, since they experience limited light availability. Furthermore, it is likely that these shallow mesophotic-like ecosystems are common along the west coast of New Zealand and, therefore, require further investigation. My results suggest that TMEs can support abundant benthic communities distinct from those occurring at shallow depths in the infralittoral zone. However, depth-related patterns were very location specific, making it difficult to generalise between TMEs. More direct assessments of TME benthic communities at the species-level would help

elucidate any common benthic community patterns that might exist. However, one consistent characterisation of all the sites surveyed was the domination of sponges throughout TME depth profiles. Furthermore, as a consequence of their high cover relative to other phyla within the wider benthic community, and particularly high gross morphological variation, my results suggest that these sponge assemblages are providing important ecological functions through the provisioning of habitat complexity. This is especially important in the deeper regions of the TMEs studied, as other important habitat complexity provisioners such as macroalgae and branching forms of crustose coralline algae decline in the infralittoral and upper mesophotic zones. I suggest that TME research should prioritise multivariate analyses of the ecological drivers of TME community distributions, including abiotic drivers such as substrate inclination, habitat complexity and the direct quantification of light availability, and biotic considerations such as spatial competition, habitat provisioning, predation, anthropogenic disturbance, and food availability.

Chapter 3

Microbial community composition and distribution: a potential driver of sponge abundance through the infralittoral and mesophotic zone

Abstract

Sponges are consistently the most dominant benthic invertebrates occurring on rocky-reef habitats through the infralittoral and mesophotic zones in New Zealand. However, they exhibited significant variability through these depth profiles and did not necessarily occupy all available substrate space, despite being generally spatially competitive organisms. A lack of correlation between sponge distributions and multiple environmental variables revealed in the previous chapter leaves observations of unoccupied bare substrate, and sponge distribution patterns unexplained. Here I explored the hypothesis that food availability might be the most important driver of depth-related sponge distribution patterns. In this chapter, I described the composition and distribution of the sponge food pool (as multiple POC food groups and dissolved organic carbon (DOC)) through depth (0 -120 m) on rocky-reef habitats in New Zealand. Using a combination of flow cytometry and scanning electron microscopy (SEM) to identify and enumerate microbial groups, I corrected previous misclassifications of marine microbial compositions in New Zealand. I found strong positive correlations between sponge distribution and food availability when I combined data from all Fiordland sites, and some smaller-scale patterns at the Poor Knights, including significant increases in sponge assemblage morphological complexity coinciding with significant drops in food availability at the deepest observed depths. These observations provide important ecological information about the composition and distribution of resources at the foundation of marine trophic structures in infralittoral and mesophotic environments, and how sponges appear to be subject to bottom-up effects in these habitats.

3.1 Introduction

Marine microbial autotrophs contribute up to 25% of global marine primary production (Flombaum et al. 2013) and in combination with heterotrophic bacteria, form the foundation of marine food webs (Azam et al. 1983; Whitman et al. 1998). The organic carbon provided by microbial communities moves through complex food webs until ultimately, animals at the highest trophic levels are supported (Mostajir et al. 2015). However, some large benthic suspension feeders, such as marine sponges, can bypass complex trophic pathways and access resources at the base of marine food webs, forming close trophic interactions with microbial communities directly.

Sponges have developed mechanisms for efficiently capturing autotrophic and heterotrophic microbial constituents (< 5 µm) of the particulate organic carbon (POC) pool (Gili & Coma, 1998). The entire body plan of a sponge is specialized for this process (Riisgård et al. 1993), whereby large volumes of water are pumped through choanocyte chambers (2−12 ml water cm^{-3} min^{-1}) (Reiswig, 1974; 1981; Pile, 1997; Gili & Coma, 1998) to capture enough food to sustain base-metabolic requirements, reproduction, and growth. Sponges are also capable of consuming dissolved organic carbon (DOC), which is comprised of a wide range of components from numerous sources, including phagocytized cell remnants, exudates from photosynthetic bacteria (Thornton, 2014), macrophytes (Brylinsksy, 1977) and corals (Crossland, 1987; Haas et al. 2011), sponge detritus (de Goeij et al. 2013), and allochthonous material from terrestrial environments delivered *via* rivers and estuaries (Raymond & Spencer, 2015). However, the trophodynamics of sponge-DOC interactions is still poorly understood despite DOC representing over 90 % of the total carbon small enough to enter through the sponge ostia (Pawlik et al. 2018) and providing a primary food source for certain species (e.g. de Goeij et al. 2008; de Goeij et al. 2013; McMurray et al. 2018; Mueller et al. 2014). Most studies considering sponge-DOC interactions have been undertaken in tropical

environments (e.g. de Goeij et al. 2008; de Goeij et al. 2013; McMurray et al. 2018; Mueller et al. 2014), whereas temperate species have been almost entirely overlooked. However, a limited number of studies from the Mediterranean (Ribes et al. 1999; 2012), deep-sea (Bart et al. 2020), and shallow temperate habitats (Chapter 4), have indicated that sponges outside of tropical environments are also capable of consuming DOC, albeit with high variability (see review by de Goeij et al. 2017). DOC is therefore an essential consideration alongside POC components when assessing sponge trophodynamics in all environments (Pawlik et al 2015; Chapter 4).

Observations of sponge dominance in food-depleted environments, such as the deep-sea (Bart et al. 2020) and submarine caves (e.g. Bell, 2002), suggest that sponges might be less vulnerable to low food availability than other benthic suspension feeders. Observations of increased sponge abundance (McMurray et al. 2015) correlating with coral declines (Norstrom et al. 2009; Villamizar et al. 2013; de Bakker et al. 2017) in tropical habitats support this suggestion (albeit indirectly). In these earlier studies, spatial competition appears to be the primary limiting factor for sponge distributions rather than food availability. Two reviews of sponge-food limitation studies in the Caribbean (Pawlik et al. 2015; 2018) conclude that there is limited evidence for food limitation (or bottom-up effects) in this region, where turbulence, spatial competition, and predation (top-down effects) are considered to be the primary factors determining sponge assemblage structure and distribution. Conversely, other studies have shown positive correlations between food availability and sponge abundance along depth gradients, suggesting that bottom-up effects are likely to be playing a role in sponge distributions (e.g. Lesser, 2006; Trussell et al. 2006), but these results have been explicitly disputed (e.g. Scott & Pawlik, 2019). Regardless of the evidence for the role of bottom-up effects on sponge distributions, almost all studies have focused on tropical habitats and on specific physiological responses to food availability of

specific species (e.g. Wooster et al. 2019; Trussell et al. 2006). Conclusions drawn from gradients of depth and food from specific tropical regions such as the Caribbean (Pawlik et al. 2018), where much of this debate has been focused, are unlikely to be universal across tropical environments (Wilkinson & Cheshire, 1990; Pawlik et al. 2018), and highly unlikely to translate to temperate systems that have not been previously considered. While the debate regarding the role of bottom-up effects on sponges in tropical habitats is on-going (Lesser & Slattery, 2018; Pawlik et al. 2018), the role of bottom-up effects in temperate habitats might be particularly ecologically important, more pronounced, and subsequently, more easily elucidated for the following reasons:

1) Temperate benthic habitats might exhibit more freely-available substrate space into the mesophotic zone compared to tropical habitats, as competition for space with highly light-dependent macroalgae (Cárdenas et al. 2012) becomes rapidly and significantly reduced with depth (Krause-Jensen et al. 2007). Free-substrate space demands an ecological explanation given the high proliferation and abundance of temperate sponges in other areas with low algal cover (Bell, 2002; Maldonado et al. 2017). This also provides an opportunity to test the importance of food limitation on sponge distribution because the potential confounding factor of spatial competition has been reduced.

2) Predation (top-down effects) has been identified as one of the most important limiting mechanisms acting on sponges in tropical environments (Pawlik et al. 2015; 2018), but this is unlikely to translate to temperate habitats where large sponge predators are uncommon and less diverse (Wulff, 2006; Bell et al. 2020). The reasons for the disparity in the abundance and diversity of sponge predators between tropical and temperate environments remain unclear (Bell et al. 2020) but it means that bottom-up effects are more likely to be an important limiting mechanism where sponges do not occupy free-substrate space.

3) Phototrophy appears to be less common in temperate than tropical sponges (Wilkinson, 1987), although more investigations comparing tropical and temperate sponges are required (Lemloh, 2009). As such, temperate sponges might be particularly vulnerable to bottom-up effects, as energy requirements are predominantly met *via* suspension feeding while phototrophic activity is less important as a compensatory mechanism for low levels of water column-derived food. Furthermore, even where temperate sponges do exhibit high phototrophic capacity, this effect is likely to be accentuated with increased depth, where light penetration declines more rapidly than in tropical environments.

Increased food availability (specifically POC) with depth through the infralittoral and mesophotic zones on oligotrophic Caribbean tropical reefs has been observed (Pawlik et al. 2015, 2018), but this pattern is not necessarily reflected in highly dynamic, nutrient-rich, temperate coastal habitats. Here, significant seasonal and depth fluctuations in light availability, temperature, water column mixing, and nutrient availability are likely to generate significant variations in food availability through space (Zhang et al. 2018) and time (Ribes et al. 1999; Perea-Blázquez et al. 2013a). While some assessments of the sponge food pool in temperate environments have been made (e.g. Perea-Blázquez et al. 2010), they have been predominantly limited to the infralittoral zone, within SCUBA limits (< 30 m). Working exclusively in this depth range restricts our understanding of sponge food pool dynamics, as the abundance and composition of sponge assemblages are likely to change significantly in the circalittoral zone where spatial competition with macroalgae decreases (Easson et al. 2014) and free-substrate space increases (Chapter 2).

The accurate identification of microbial groups within the sponge food pool is an important prerequisite for understanding the role of bottom-up effects and sponge trophodynamics generally. This is because different microbial groups have varied nutritional value (Gantt et al. 2019), are likely to be distributed differently according to specific traits (i.e. heterotrophic

or autotrophic cells) and perhaps most importantly, some food groups are preferred by sponges over others, and these preferences appear to be species-specific (subsequently generating resource partitioning in multi-species assemblages) (see Yahel et al. 2006; Maldonado et al. 2010; Perea-Blázquez et al. 2013b).

Flow cytometry has been employed to identify and enumerate specific components of the POC pool available to sponges in tropical (Slattery & Lesser, 2018), sub-tropical (Yahel et al. 2006) and temperate environments (Perea-Blázquez et al. 2010), and with on-going technological developments (e.g. spectral cytometry), it is unlikely it has reached its full potential for ecological applications. Flow cytometry allows for the differentiation of cells based on size, complexity, and nucleic acid content (after nucleic-acid staining). However, used alone, this technique cannot reliably reveal the specific identity of the 'events' being quantified without pre-existing knowledge of the microbial composition expected in the assessed geographic region, and how distinguishable traits of specific populations translate into flow cytometry outputs. Extrapolating microbial identifications from flow cytometry analyses of samples from different environments can potentially lead to misclassifications of entire distinguishable groups. For example, one of the very few studies of sponge feeding and food distributions in New Zealand by Perea-Blázquez (2010), assigned *Prochlorococcus* to a distinct cell population exhibiting a "typical" *Prochlorococcus* fluorescent signature during flow cytometry analyses. However, this cyanobacterium is normally associated with tropical or subtropical marine environments (Flombaum et al. 2013) and is unlikely to occur in the high abundances reported from the region of the study. Employing a combination of flow cytometry and other cell identification techniques such as microscopy or genome sequencing is therefore a more reliable approach for the identification of microbial populations, especially when investigating previously understudied environments.

The previous chapter demonstrated how the abundance of sponge assemblages changed significantly through the infralittoral and mesophotic zones of New Zealand reefs from 0-150 m, but no environmental mechanisms explaining this variability were found (see Chapter 2 supplementary material). Furthermore, the observation of considerable free-substrate space below the infralittoral zone in some regions, and very high sponge abundance with limited free-substrate space in other regions (Fig. B3.1) requires an explanation besides spatial competition with algae or other benthic invertebrates. In recognition of optimal foraging theory and the lack of any apparent environmental mechanisms explaining observed sponge distributions, the current study hypothesizes that food availability is likely to be the predominant mechanism explaining the variability in sponge-depth distributions observed on temperate New Zealand reefs.

The aims of this study were therefore to: 1) Identify the microbial community components (POC) within the size range available to temperate New Zealand sponges using a combination of flow cytometry and scanning electron microscopy (SEM); 2) determine changes in abundance of POC components and DOC concentrations from 0 – 120 m on temperate New Zealand rocky reef habitats; and 3) test correlations between sponge food pool components and sponge abundance to assess the potential role of bottom-up effects on temperate sponge distributions.

3.2 Methods

3.2.1 Study Sites

Four and two sites in Doubtful Sound and the Poor Knights Marine Reserve respectively, were chosen for this study (Fig. 3.1). Fiordland sites were distributed along a gradient from the most inner areas of Doubtful Sound at Hall Arm to the most outward reach of Thompson Arm. See section 2.2.1.4 and 2.2.1.1 for detailed descriptions of study sites.

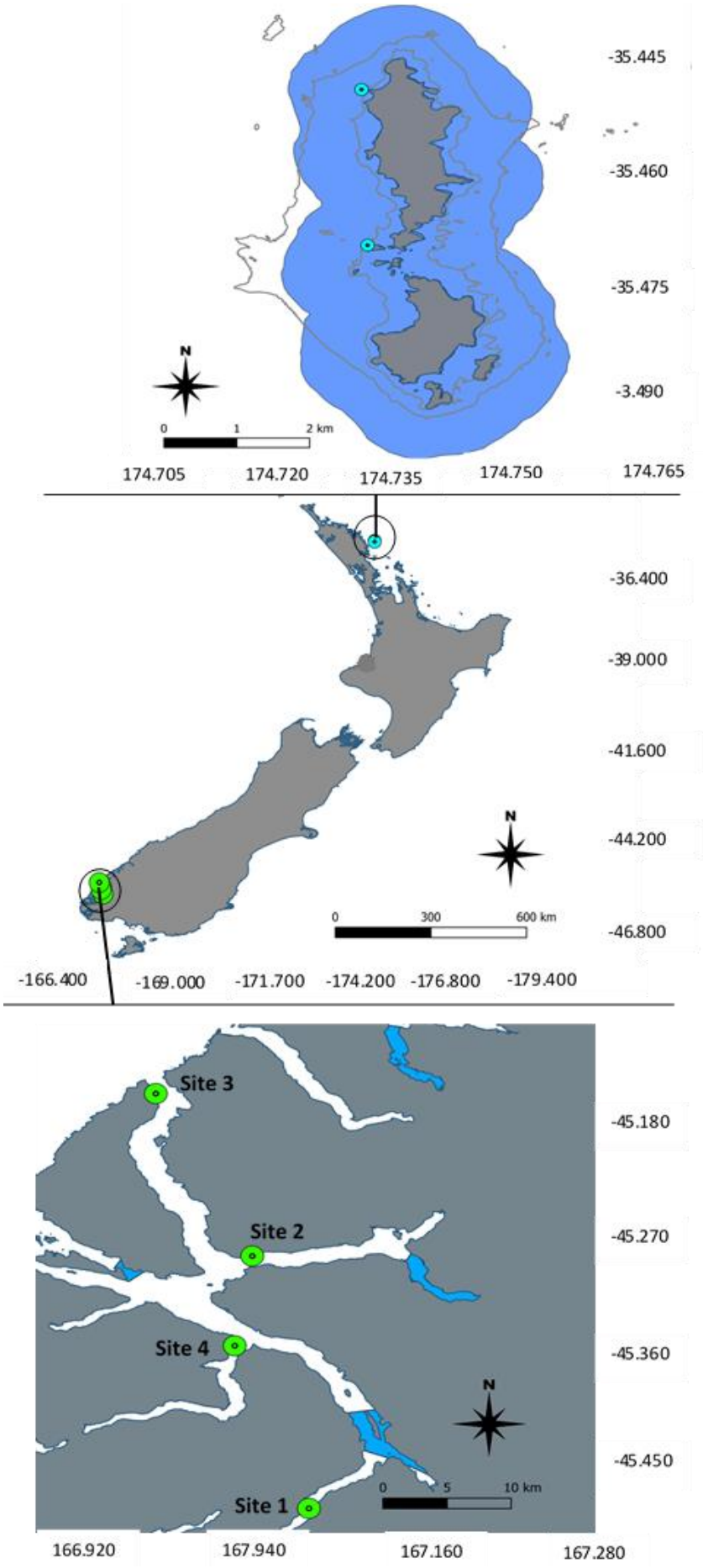

Fig. 3.1 Survey locations at the Poor Knights (top) and Doubtful Sound (bottom) in 2019. Blue shaded regions show the locations of marine reserves.

3.2.2 Microbial community sampling

Water samples from Fiordland sites were collected from the surface (0 – 5 m), then at 10 m, 30 m, 50 m, 80 m, and 120 m. Water samples from the Poor Knights were collected from the surface (0 – 5 m), then at 10 m, 30 m, 50 m, 80 m. All samples were collected using a 5-L NISKIN bottle (General Oceanics) assembled by the National Institute of Water and Atmosphere (NIWA). Upon retrieval, water was dispensed into 3 x 1.8 ml cryovials, fixed with EM grade 25% glutaraldehyde, snap-frozen in liquid nitrogen, and stored at -80°C for subsequent POC analyses using a combination of flow cytometry and SEM (see below). For the determination of DOC concentration, samples were dispensed into a sterile 50 ml syringe with a pre-combusted 13 mm 0.7 µm binder-free glass fibre filter fitted inside a 13 mm stainless steel filter holder (Pall®). Water passing through the filter was deposited into 40 ml pre-combusted EPA glass vials, fixed with EM grade hydrochloric acid (0.1% final concentration), and frozen at -20°C until analysis. Care was taken not to exceed the pressure capacity of the filter when delivering samples into vials.

3.2.3 ROV video sampling and analysis

For the full detailed description of the following protocol, see Chapter 2.2. Briefly, the ROV 'SAL', Model DG2 (Deep Trekker Inc.) with an internal and external mounted GoPro 4 silver camera (set at 60 fps at 1080p resolution) and an internal (4k) camera set to linear mode was deployed at each location (Fig. 5.1). The ROV was driven along vertical or near-vertical walls on a horizontal transect for approximately 10 min, producing frame grabs of similar scales. The ROV was then driven upwards for 10 m and another transect completed. This process was repeated at 10 m depth increments until the shallowest transect at 30 m was completed at each site. The maximum depth reached was 120 m at Fiordland and 80 m at the Poor Knights. Sponge assemblages less than 30 m deep were sampled using SCUBA,

whereby the same diver would swim horizontally along a wall at three transect depths of 25, 15, and 0 - 5 m, taking photographs (Nikon D800 with Ikelite Housing and YS50 TTL strobe) approximately every meter and 1 m from the substrate. No significant differences between data derived from ROV and SCUBA images of the same quadrats were found (see Chapter 2 & Fig. A2.1). Videos collected from ROV deployments were analysed using VLC Media Player; 10 frame grabs were extracted from each transect as replicates. The selection of frame grabs was determined by the availability of quality still images. Coral point count (CPC) was used to estimate the percentage cover of sponges

3.2.4 POC analysis: Flow cytometry

A BD LSRFortessa™ bench-top flow cytometer equipped with six lasers (20 mW 355 nm UV, 50 mW 405 nm Violet, 75 mW 445 nm Blue Violet, 100 mW 488 nm Blue, 150 mW 532 nm Green, and 40 mW 633 nm Red) was used to determine the abundance of different planktonic populations in water samples. The cytometer was calibrated using BD Cytometer Setup and Tracking Beads (Cat No. 641319). Polystyrene beads were used for particle size calibration: 3 μm Rainbow Beads (Spherotech, Cat No. RCP-30-20A) and ApogeeMix that range in size from 110 nm – 1300 nm (Apogee Flow Systems, Cat No. 1493). The nucleic-acid binding dye SYBR Green I (Invitrogen™) was excited by the 488 nm Blue laser and the emission was detected by the 515/20 nm bandpass filter off the Blue laser. SYBR Green I has a binding preference for dsDNA, though it also binds ssDNA and RNA with lower affinity. SYBR Green I ensured that the broadest spectrum of biological entities in the sample were captured, including viruses (Marie et al. 1999). A 1:40 000 SYBR Green I/sample ratio provided the best compromise between population discrimination and signal saturation and compensation issues (Figs. B3.2 & B3.3). An unstained subsample was run for every sampling depth (*per* location) to provide a gating control for stained samples. The cytometer

was set to a flow rate of 40 µm *per* min and run for 300 s for every sample, producing a consistent total analysed volume of 0.2 ml.

Flow cytometry data were analysed using the software package FlowJo V10.8.0. All nucleic-acid positive events (SYBR Green I positive) were discriminated and gated in the first instance using the signal area (A) from side scattered light (SSC-A, proportional to particle complexity) *vs.* the 515/20 detector off the blue laser (SYBR Green I). The nucleic acid positive events gate focuses on the events of interest, while excluding unwanted inorganic particles and instrument noise (Fig. B3.2 & B3.3). The population of nucleic acid positive events was then analysed further to distinguish populations of interest based on distinct fluorescence signatures. Distinct populations exhibiting bright orange fluorescence emission (excited by the Green laser and seen in the 575/25 detector) were considered *Synechococcus* sp. in the first instance in the accordance with the relevant literature (e.g. Perea-Blázquez et al. 2010). These cyanobacteria contain phycobiliproteins that emit orange fluorescence that can be detected separately from the red fluorescence emitted from their chlorophyll *a*. Populations emitting bright red fluorescence (excited by the Blue laser and seen in the 685/35 detector), denoting the presence of chlorophyll *a*, and with dim orange fluorescence were considered as *Prochlorococcus* in the first instance in line with the relevant literature (e.g. Perea-Blázquez et al. 2010). The distinct and dense population with minimal fluorescence properties was considered to be largely heterotrophic bacteria, which lack in chlorophyll. However, this abundant group represents a broad range of numerous types of small nucleic acid-positive entities, including viruses (Marie et al. 1999). However, this population was not mined further to discriminate any sub-populations separately at higher resolution, and the label 'heterotrophic bacteria' was retained to maintain consistency with the relevant literature. Specific gate locations were drawn separately for each sampled depth at each location but were kept consistent across replicates and pseudo-replicates. The movement of

gates was necessary due to variability and spread of fluorescent signatures across samples according to variations in depth and time of day. However, populations of interest remained distinguishable across samples and their fluorescent signatures remained within the expected regions for each of their assigned categories.

3.2.5 POC analysis: Scanning Electron Microscopy

Samples were gated on clearly defined populations occurring on cytograms as described above and then physically sorted and deposited onto 13 mm MCE filters (0.1 µm pore-size) using an BD Influx™ Cell Sorter. Filters were attached to a custom-made 1 mm gridded plastic platform with a low-vacuum hose attached underneath to generate suction through the filter to encourage particles to settle on the filter and to remove excess water. 10 000 cells were delivered onto separate filters from each population (Fig. B3.4). Filters were then submerged in Karnovsky's half K fixative (2 ml 25% glutaraldehyde; 2.5 ml distilled water; 7.5 ml 0.4 M sodium cacodylate; 3 ml 1.0 M sucrose) for 1 h in a well-plate. The fixative was then replaced with an EM buffer (7.5 ml 0.4 M sodium cacodylate; 3 ml 1 M sucrose; 9.5 ml distilled water) and left for 30 min. The buffer was then replaced with standard osmium fixative (2.5 ml 4% osmium; 5 ml 0.4 M sodium cacodylate; 2.5 ml distilled water) and left for 2 h. The filters were then placed into a custom-made stainless steel rack and dehydrated with a graded ethanol series of 30, 50, 70, 80, 90, 95, and 100% (x2), and then critical-point-dried, still in the holder, in a Baltec CPD-030 (Balzers, Liechtenstein) using ethanol as the exchange fluid (critical point temperature = 60 bar/Tc 241 °C), which is miscible with water. The dried filters were removed from the holder, secured onto stubs using carbon tape, sputter-coated with platinum (5 µm), and left in a vacuum drier until scanning election microscopy (SEM) examination. SEM was undertaken using a JEOL 6500F set to 10Kv and 4A to avoid the destruction of the sample and filter during high resolution examination. Images were analysed using ImageJ V1.8.0_172.

3.2.6 Dissolved organic carbon analysis

DOC concentration was determined using high temperature combustion catalytic oxidisation (Shimadzu Cooperation). After filtering through a glass fibre filter (see above), the remaining TOC (now operationally considered as 'dissolved components') in the sample was combusted by heating to 680 °C in an oxygen-rich environment. The carbon dioxide generated was detected using an infrared gas analyser (NDIR detection). The concentration of total carbon in the sample was obtained through a comparison with a calibration curve. The oxidized sample was sparged with nitrogen to isolate the inorganic carbon in the sample and again measured by NDIR. TOC (as DOC) concentration was then calculated by subtracting the inorganic carbon concentration from total carbon concentration. Determination of DOC concentration was conducted by the National Institute of Water and Atmospheric Science (NIWA, Hamilton, New Zealand).

3.2.7 Data analysis

A two-way PERMANOVA was used to determine any differences in the microbial community between depths and locations. Abundance data were square-root transformed and used to generate a Bray-Curtis similarity index for PERMANOVA tests. Pseudo replicates were used for *post hoc* pairwise tests only where main PERMANOVA tests yielded significant results from data of true replicates (triplicates).

Linear regression models were created in R to determine relationships between the abundance of microbial groups and sponge abundance through 0, 10, 30, 50, 80, and 120 m depth increments. Specific transformations of data were applied based on best linear model tests of assumptions of normality. Given the confounding effect of the freshwater layer on shallow cyanobacterial distributions, data from the top layer (0 m) were excluded from regression analyses (see methods) of correlations with cyanobacteria and sponge distributions at

Fiordland. The Poor Knights receives very little freshwater runoff and considerable water column mixing, so surface data of sponge and microbial populations were retained.

3.3 Results

3.3.1 Microbial community composition and SEM interpretations

Flow cytometry analyses revealed three distinct microbial sub-populations that were identified as heterotrophic bacteria (lacking in both chlorophyll and phycoerythrin), *Synechococcus* sp. (high in phycoerythrin and chlorophyll) and *Prochlorococcus* in the first instance in accordance with other studies of microbial community composition from similar locations (Perea-Blázquez et al. 2011; 2012; 2013). However, SEM images showed a diverse microbial community within the sorted populations previously categorized as *Prochlorococcus*, with a range of cell morphologies and cell sizes, most of which did not reflect those typical of *Prochlorococcus* (Fig. 3.2). The microbial populations gated on similar regions across all cytograms was therefore re-categorized as autotrophic picoeukaryotes, a diverse group of larger (ranging from ~ 0.2 – 4.5 µm) and more complex autotrophic eukaryotic cells than either the prokaryotic *Prochlorococcus* or *Synechococcus* sp. This was supported by FCS *vs.* SSC plots (Fig. B3.5), and by FCS *vs.* Red fluorescence (Comp_B_685/35) plots (Fig. B3.6), which showed distinctly higher nucleic-acid content and larger cell sizes than both *Prochlorococcus* and *Synechococcus* sp., respectively. The sorted group previously classified as *Synechococcus* sp. reflected the expected morphological traits from this cyanobacterium with high consistency in size and morphology across all collected cells (Fig. 3.3). However, SEM did not yield successful results for the group categorized as heterotrophic bacteria, where cells consistently collapsed during SEM protocol trials, and in some cases revealed unexpected and unusual results (Fig. 3.4). The artefacts seen in Fig. 3.4 were proposed as inorganic by-products created during filter preparation protocols in the first

instance, given the very structured patterns they formed (Fig. B3.7). However, mass spectrometry tests revealed these artefacts to consist of organic carbon and very small amounts of osmium as would be expected from natural cells after the SEM preparation protocol. These were therefore considered as true cells that exhibited catastrophic loss of morphological integrity, which had been organised into the observed patterns by an unknown and undesired process, most likely occurring during critical-point-drying.

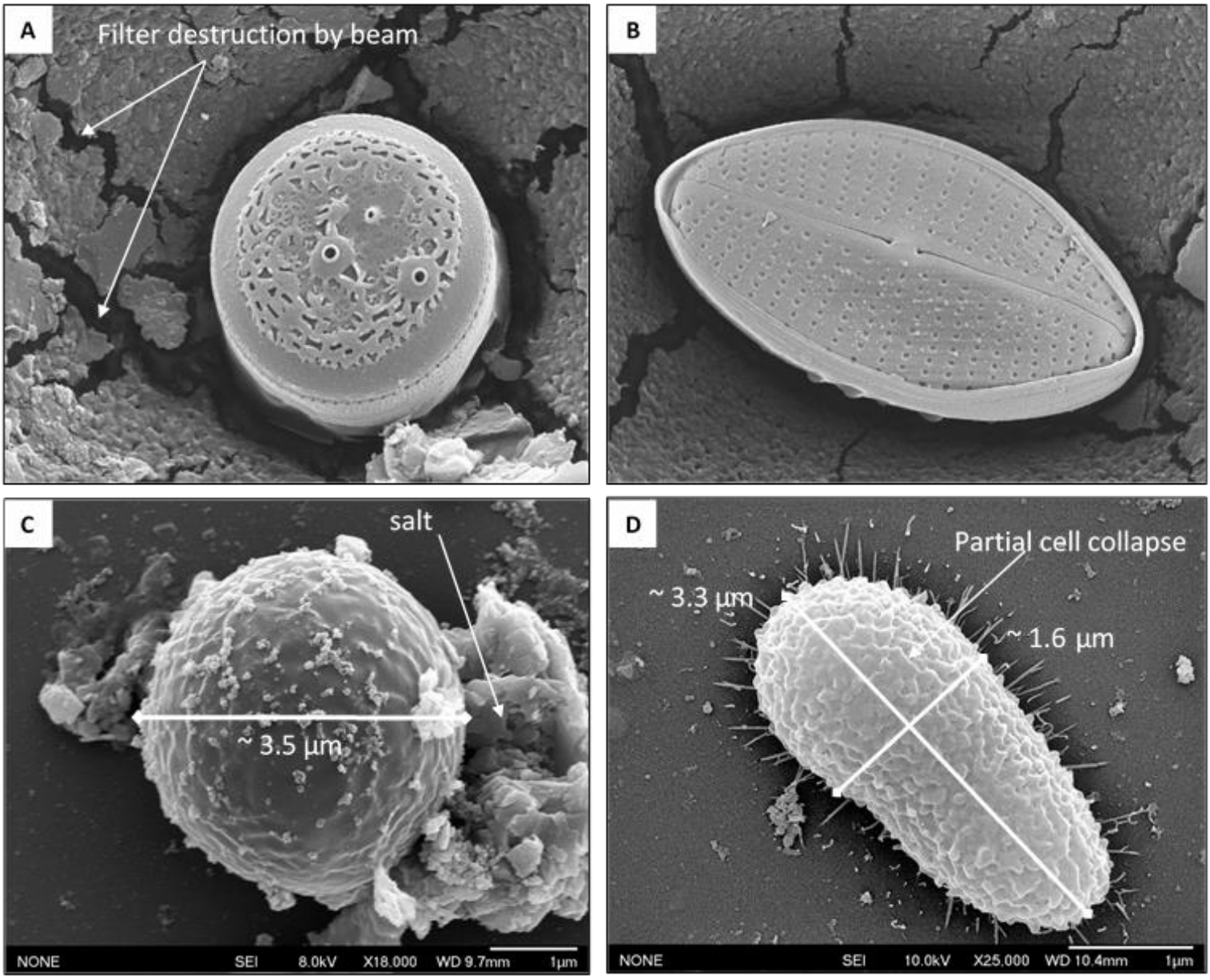

Fig. 3.2 SEM images of *Midiscus* spp. (A) and Pennales spp. (B) and unidentified globular (C) and oblong (D) cells representing 'picoeukaryote' population originally distinguished and gated during flow cytometry analyses as *Prochlorococcus.*

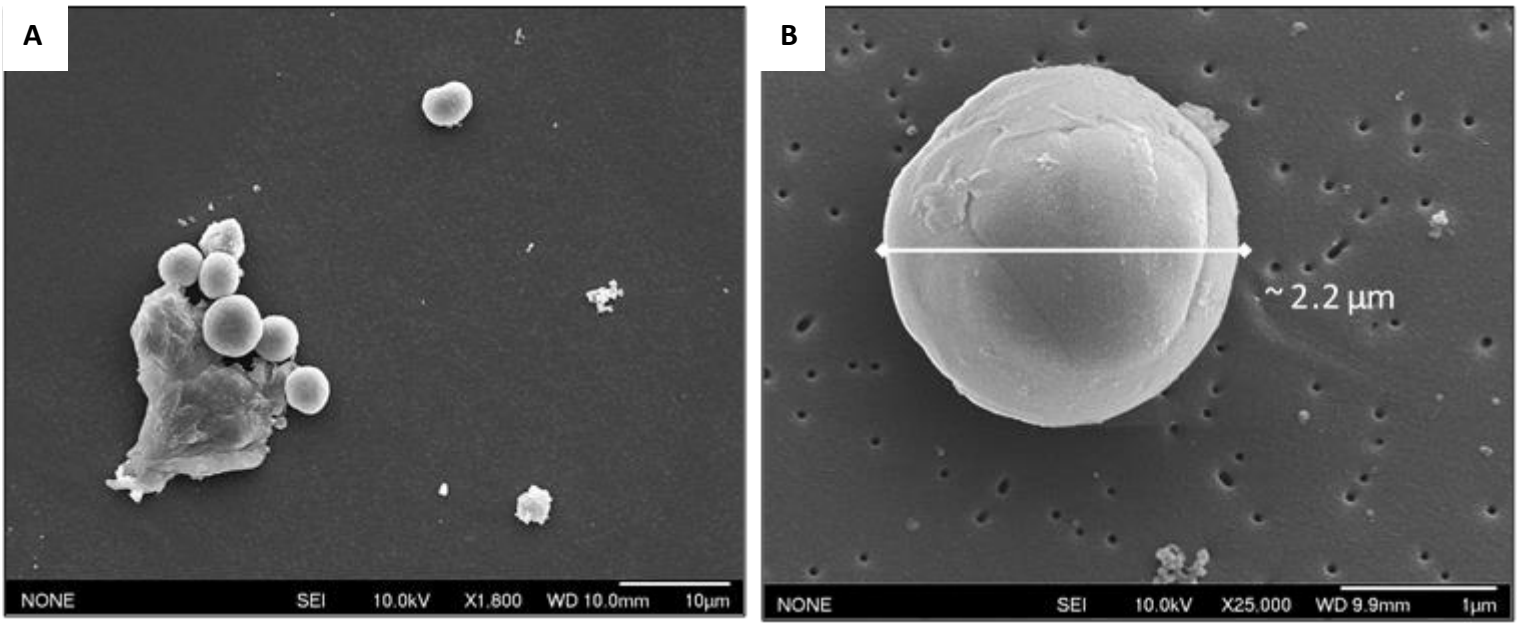

Fig. 3.3 SEM images of *Synechococcus* sp. group (A) and individual cell (B) found within sorted population group P3 (see Fig. B3.4) representing the '*Synechococcu*s sp.' population, originally distinguished and gated during flow cytometry analyses.

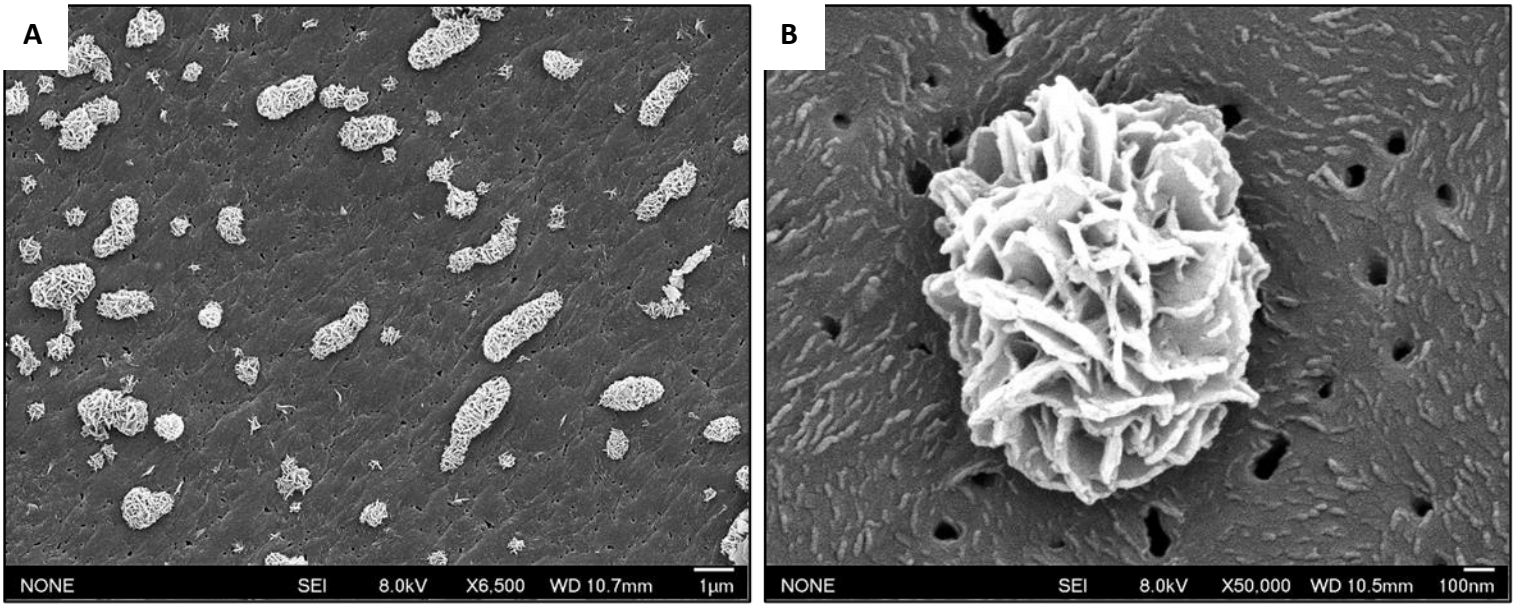

Fig. 3.4 SEM images of 'heterotrophic bacteria' group (A) and an individual cell (B) found within the sorted population group P3 (see Fig. B3.4) representing the 'heterotrophic bacteria' population originally distinguished and gated during flow cytometry analyses.

3.3.3 Total microbial community distribution

PERMANOVA tests showed a significant difference in the overall microbial community composition (POC as total nucleic-acid positive counts, heterotrophic bacteria, picoeukaryotes and *Synechococcus* sp.) of full depth profiles (all depths included in the test) between locations (four Fiordland sites and the Poor Knights) (Table 3.1 & Fig. 3.5). POC composition was also significantly different across depth categories when all locations were included in PERMANOVA tests (Table 3.1). Furthermore, an interactive effect of depth and location on POC composition was found, where the effect of depth was significantly different between locations (Table 3.1). *Post hoc* pairwise tests showed significant differences in full-depth profile microbial community composition between all locations, except for Fiordland sites 3 and 4 ($t = 1.595$, $p = 0.113$) (Table 3.2). Due to a significant interaction effect of location and depth on POC composition, and the pairwise differences between almost all locations (Table 3.2), sites were analysed independently to determine specific depth differences. Poor Knights ($F_{4,13} = 2.169$, $p = 0.09$) showed no significant difference in overall POC composition with depth, however, POC was significantly different according to depth at all Fiordland sites (Table 3.3 & Fig. 3.5) when considered independently.

3.3.4 DOC distribution

PERMANOVA tests showed that full-depth profile DOC concentrations were significantly different across locations (four Fiordland sites and the Poor Knights) (Table 3.1). However, DOC concentrations also varied significantly with depth when all locations were included (Table 3.1) and PERMANOVA tests showed an interactive effect of depth and location,

where the significant effect of depth was significantly different between locations (Table 3.1). *Post hoc* pairwise tests showed that the difference in DOC concentration according to location was reflected in all paired sites except for between Site 1 and Site 3 (Table 3.2). Significant site-specific depth differences in DOC concentration were seen at all sites, including the Poor Knights (Table 3.3 & Fig. 3.6).

Table 3.1 PERMANOVA results showing the effect of depth (0 m, 10 m, 30 m, 50 m, 80 m, 120 m), location and the interaction between depth and location on the relative abundance of microbial community components (four groups) and on DOC concentration.

Factor	**Microbial community (POC)**			**DOC**		
	Pseudo-F	**p-value**	**df**	**Pseudo-F**	**p-value**	**df**
Location	53.976	< 0.001	4,47	136.07	< 0.001	3,47
Depth	24.387	< 0.001	5,47	25.523	< 0.001	5,47
Depth*Location	6.556	< 0.001	18,47	20.848	< 0.001	13,47

Table 3.2 PERMANOVA results showing the site differences of the effect of depth (levels: 0 m, 10 m, 30 m, 50 m, 80 m, 120 m) on the concentration of three different cell groups, total nucleic acid positive events (three groups combined plus unidentified populations) and DOC. DOC concentrations were not determined at Site 4.

Location pair	**Microbial community (POC)**		**DOC**	
	t	P	t	P
Poor Knights – Site 1	12.207	< 0.001	17.678	< 0.001
Poor Knights – Site 2	8.528	< 0.001	26.412	< 0.001
Poor Knights – Site 3	2.445	< 0.001	12.312	< 0.001
Poor Knights – Site 4	4.422	< 0.001	-	-
Site 1 – Site 2	2.258	0.024	7.005	< 0.001
Site 1 – Site 3	9.101	< 0.001	0.872	0.4
Site 1 – Site 4	14.117	< 0.001	-	-
Site 2 – Site 3	7.638	< 0.001	2.745	< 0.012
Site 2 – Site 4	8.540	< 0.001	-	-
Site 3 – Site 4	1.595	0.113	-	-

Table 3.3 PERMANOVA results showing the effect of depth (0 m, 10 m, 30 m, 50 m, 80 m, 120 m) on the concentration of three different cell groups, total nucleic acid positive events (3 groups combined plus unidentified populations) and DOC. DOC concentrations were not determined at Site 4.

Location	**Microbial community (POC)**		**DOC**		
	F	p	F	p	df
Poor Knights	2.169	0.09	58.986	< 0.001	4,17
Site 1	16.108	< 0.001	58.07	< 0.001	4,14
Site 2	6.470	0.003	62.079	< 0.001	5,17
Site 3	11.483	< 0.001	3.389	0.025	5,17
Site 4	45.517	< 0.001	-	- -	-

Table 3.4 PERMANOVA results showing the effect of depth (0 m, 10 m, 30 m, 50 m, 80 m, 120 m) on the abundance of four POC groups DOC concentrations at the Poor Knights, Fiordland combined, and four individual Fiordland sites.

Location	**Nucleic-acid events**		**Heterotrophic bacteria**		**Picoeukaryotes**		***Synechococcus* sp.**		**DOC**	
	F	p	F	p	F	p	F	p	F	p
Poor Knights	1.307	0.293	0.272	0.936	25.038	< 0.001	65.422	0.001	58.986	< 0.001
Fiordland	5.946	<0.001	2.693	0.025	12.652	< 0.001	8.317	< 0.001	4.918	0.002
Site 1	10.078	0.004	11.586	0.003	36.186	< 0.001	48.918	< 0.001	58.070	< 0.001
Site 2	5.640	0.008	0.729	0.601	25.652	< 0.001	24.519	< 0.001	62.079	< 0.001
Site 3	9.786	<0.001	3.206	0.022	72.892	< 0.001	27.32	< 0.001	3.389	< 0.025
Site 4	38.879	<0.001	2.478	0.092	63.336	< 0.001	94.21	< 0.001	-	-

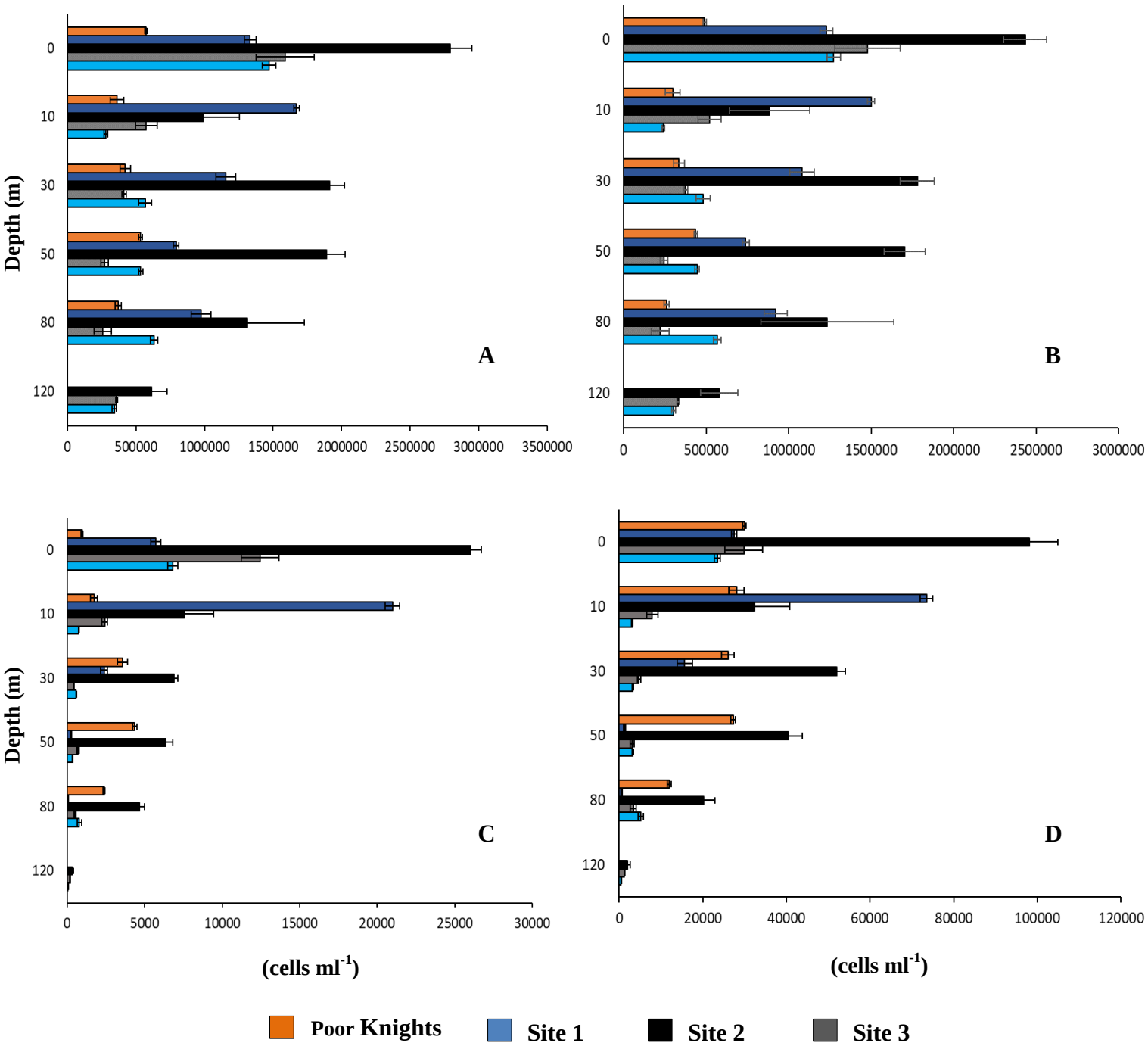

Fig. 3.5 Concentration (cells/ml^{-1}) of total nucleic-acid positive cells (A), heterotrophic bacteria (B), picoeukaryotes (C), and *Synechococcus* sp. (D) from the surface down to 80 m at Poor Knights and Fiordland Site 1, and from the surface down to 120 m at Fiordland Sites 2 - 4. Error bars are mean ± SE.

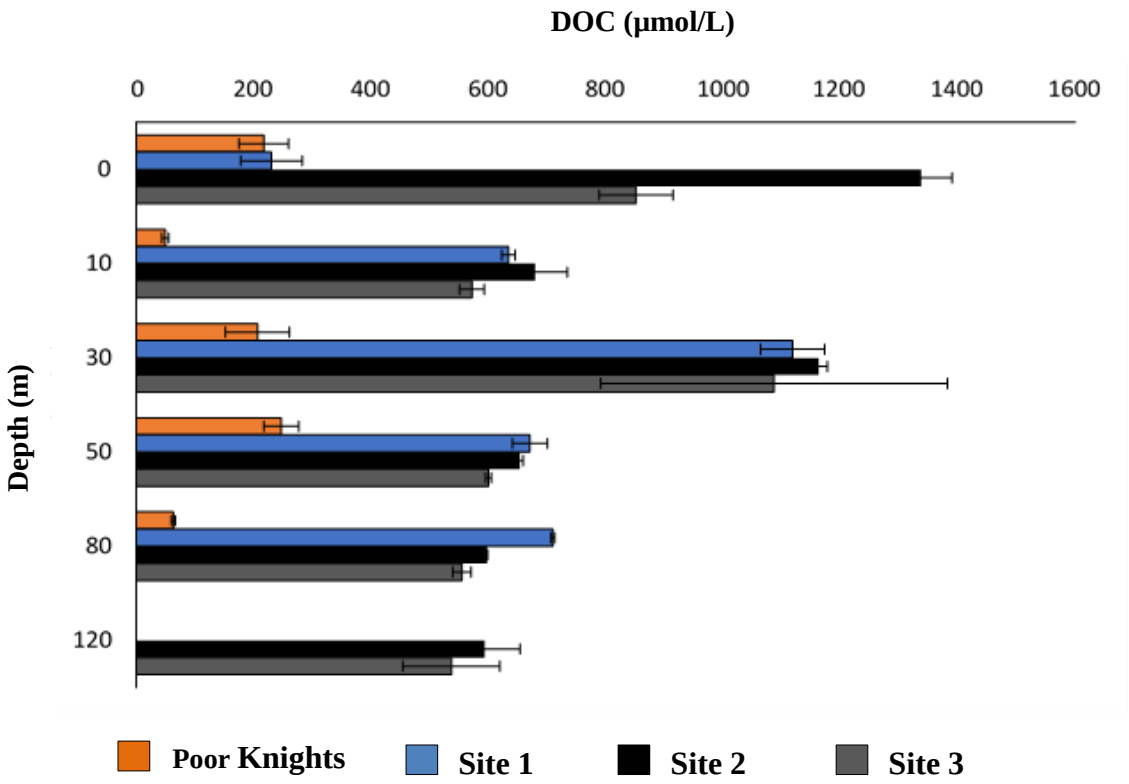

Fig. 3.6 Dissolved organic carbon (DOC) concentrations (µmol/L) from the surface down to 80 m at the Poor Knights and Fiordland Site 1, and down to 120 m at Fiordland Sites 2 & 3. Error bars are mean ± SE.

3.3.5 Distribution of specific POC components

The group categorized as heterotrophic bacteria was significantly more abundant than both picoeukaryotes ($t = 8.07$, $p < 0.001$) and *Synechococcus* sp. ($t = 7.62$, $p < 0.001$) when depth categories were combined at the Poor Knights. *Synechococcus* sp. was significantly more abundant than picoeukaryotes over this same depth profile ($t = 14.56$ $p < 0.001$). Heterotrophic bacteria were also significantly more abundant at Fiordland Site 1 (picoeukaryotes: $t = 14.13$, $p < 0.001$; *Synechococcus* sp.: $t = 13.84$, $p < 0.001$), with significantly higher abundance of *Synechococcus* sp. than picoeukaryotes ($t = 2.42$, $p < 0.02$). The same observation of higher abundance of heterotrophic bacteria was found at Fiordland

Site 2 (picoeukaryotes: $t = 6.79$, $p < 0.001$; *Synechococcus* sp.: $t = 6.63$, $p < 0.001$) also with higher abundance of *Synechococcus* sp. than picoeukaryotes ($t = 4.08$ $p < 0.001$); Site 3 (heterotrophic bac. > picoeukaryotes: $t = 4.31$, $p < 0.001$; heterotrophic bac. > *Synechococcus* sp.: $t = 4.24$, $p < 0.001$), with more *Synechococcus* sp. than picoeukaryotes ($t = 2.26$ $p < 0.02$); and Site 4 (heterotrophic bac. > picoeukaryotes: $t = 6.61$, $p < 0.001$; heterotrophic bac. > *Synechococcus* sp.: $t = 6.55$, $p < 0.001$), with higher abundance of *Synechococcus* sp. than picoeukaryotes ($t = 2.55$ $p < 0.01$).

The abundance of total nucleic-acid positive events did not significantly change with depth at the Poor Knights (Table 3.4 & Fig. 3.5). This was explained by no change in the abundance of heterotrophic bacteria with depth since they were the most abundant microbial group, while the abundance of both picoeukaryotes and *Synechococcus* sp. significantly changed with depth. Picoeukaryotes showed significant pairwise difference between depths (Table B3.1), with no distinct pattern through the depth profile and a significant drop in abundance beyond 50 m ($t = 13.51$, $p < 0.001$) (Fig. 3.5 & Table 3.4). *Synechococcus* sp., however, showed little change between depth increments down to 50 m (Table B3.1), where abundance dropped significantly from to 50 to 80 m ($t = 18.22$, $p < 0.001$), and was found at significantly lower abundance than at all other depths (Table B3.1).

The abundance of total nucleic-acid positive particles changed significantly with depth when all Fiordland sites were combined, and at all Fiordland sites individually (Table 3.4), but with site specific variability (Fig. 3.5). No discernible pattern was found at Site 1, with significant differences in abundance between all depth increments except for between 30 and 80 m (Table B3.2). This was mirrored by the distribution of heterotrophic bacteria, which is unsurprising given the high proportion of DNA events being represented by this group. However, a distinct depth pattern in *Synechococcus* sp. abundance was observed, with a significant increase in abundance from 0 to 10 m ($t = 30.97$, $p < 0.001$) and subsequent

significant drops in abundance between every depth increment from 10 to 120 m (Table B3.2). Picoeukaryotes also increased significantly in abundance from 0 to 10 m ($t = 25.58$, $p < 0.001$) and significantly decreased sequentially with depth increments beyond 10 m (Table B3.2).

At Site 2, a significantly higher abundance of DNA was found at 0 m than at all other depths (Table B3.3). Abundance of DNA peaked again between 30 – 50 m before significantly dropping from 50 to 80 m ($t = 2.31$, $p = 0.03$), down to a similar abundance to that found at 10 m. Heterotrophic bacteria were also most abundant at 0 m and exhibited a similar pattern to DNA except for no significant variability in adjacent depth increments 50 and 80 m ($t = 1.67$, $p = 0.11$). Both picoeukaryotes and *Synechococcus* sp. were also significantly more abundant at the surface (0 m) (Table B3.3). Both microbial groups significantly dropped in abundance from 0 to 10 m ($t = 8.32$, $p < 0.001$; $t = 15.26$, $p < 0.001$, for picoeukaryotes and *Synechococcus* sp. respectively). Picoeukaryote abundance did not significantly differ between 10 m and any other depth increment down to 80 m, but this is most likely due to high variability at 10 m (Fig. 3.5). After 80 m, abundance of picoeukaryotes dropped significantly (80 – 120 m: $t = 3.11$, $p < 0.01$) to the lowest abundance across the full depth profile (Table B3.3). *Synechococcus* sp. showed a second peak in abundance at 50 m, after which it significantly dropped in abundance between 50, 80 and 120 m (Table B3.3).

Site 3 also showed the highest abundances of DNA at 0 m (Fig. 3.5 & Table B3.4). Beyond 10 m, the abundance of DNA was significantly different between all pairwise depth comparisons except for between 50 and 80 m ($t = 0.79$, $p < 0.43$), but it did not show any distinct patterns across the full depth-profile. As the main constituent of total DNA events, heterotrophic bacteria followed the same depth profile. Picoeukaryotes were significantly more abundant at 0 m than at all other depths, and were significantly less abundant at 120 m (Table B3.4), following a clear pattern of sequential reduction in abundance with depth

except for between 50 and 80 m where it did not change ($t = 0.79$, $p = 0.43$). *Synechococcus* sp. followed a similar pattern albeit less extreme, showing a continued reduction in abundance with depth but no significant reductions between 10 – 30m (m ($t = 0.79$, $p = 0.43$), and 50 – 80 m ($t = 0.087$, $p = 0.93$).

Site 4 also showed a peak in DNA abundance at 0 m, where it was significantly higher than at all other depths. However, after an initial significant drop from the surface to the lowest abundance at 10 m ($t = 27.21$, $p < 0.001$), DNA abundance significantly increased again from 10 – 30 m ($t = 6.79$, $p < 0.001$), where it did not change significantly until 80 m. Abundance dropped significantly again from 80 m down to 120 m ($t = 9.17$, $p < 0.001$) (Fig. 3.5 & Tables A.25). As with the other sites, heterotrophic bacterial distribution mirrored the pattern described above for DNA. Picoeukaryotes were again significantly more abundant at 0 m than at all other depths, and significantly less abundant at 120 m (Table B3.5). This significant reduction in abundance with depth occurred sequentially, except at 80 m where a small increase in abundance was seen before becoming extremely depauperate at 120 m (< 50 cells/ml). *Synechococcus* sp. was significantly more abundant at the than all other depths. After a significant reduction in abundance from 0 to 10 m ($t = 37.53$, $p < 0.001$), the abundance of *Synechococcus* sp. remained stable until a significant reduction from 50 – 80 m ($t = 2.83$, $p < 0.01$) and 80 – 120 m ($t = 11.38$, $p < 0.001$).

Table 3.5 Linear regression results showing correlations between sponge assemblage abundance and the abundance of four POC groups and DOC concentrations at the Poor Knights, Fiordland across full depth profiles.

Location	**Nucleic-acid events**			**Heterotrophic bacteria**			**Picoeukaryotes**			***Synechococcus* sp.**			**DOC**		
	R^2	F	p	R^2	F	p	R^2	F	p	R^2	F	P	R^2	F	p
Poor Knights	0.03	0.1	0.78	0.00	0.01	0.92	0.01	0.04	0.85	0.03	0.10	0.77	0.03	0.10	0.77
Fiordland	0.06	0.27	0.63	0.06	0.25	0.64	0.23	1.23	0.33	0.10	0.46	0.55	0.18	0.89	0.40
							Excluding 0 – 10 m								
Poor Knights	0.13	0.30	0.64	0.08	0.18	0.72	0.01	0.01	0.92	0.03	0.05	0.84	0.03	0.06	0.82
Fiordland	**0.94**	**32.44**	**0.03***	**0.93**	**27.84**	**0.03***	**0.88**	**14.42**	**0.06***	**0.92**	**21.63**	**0.04***	0.58	2.77	0.24

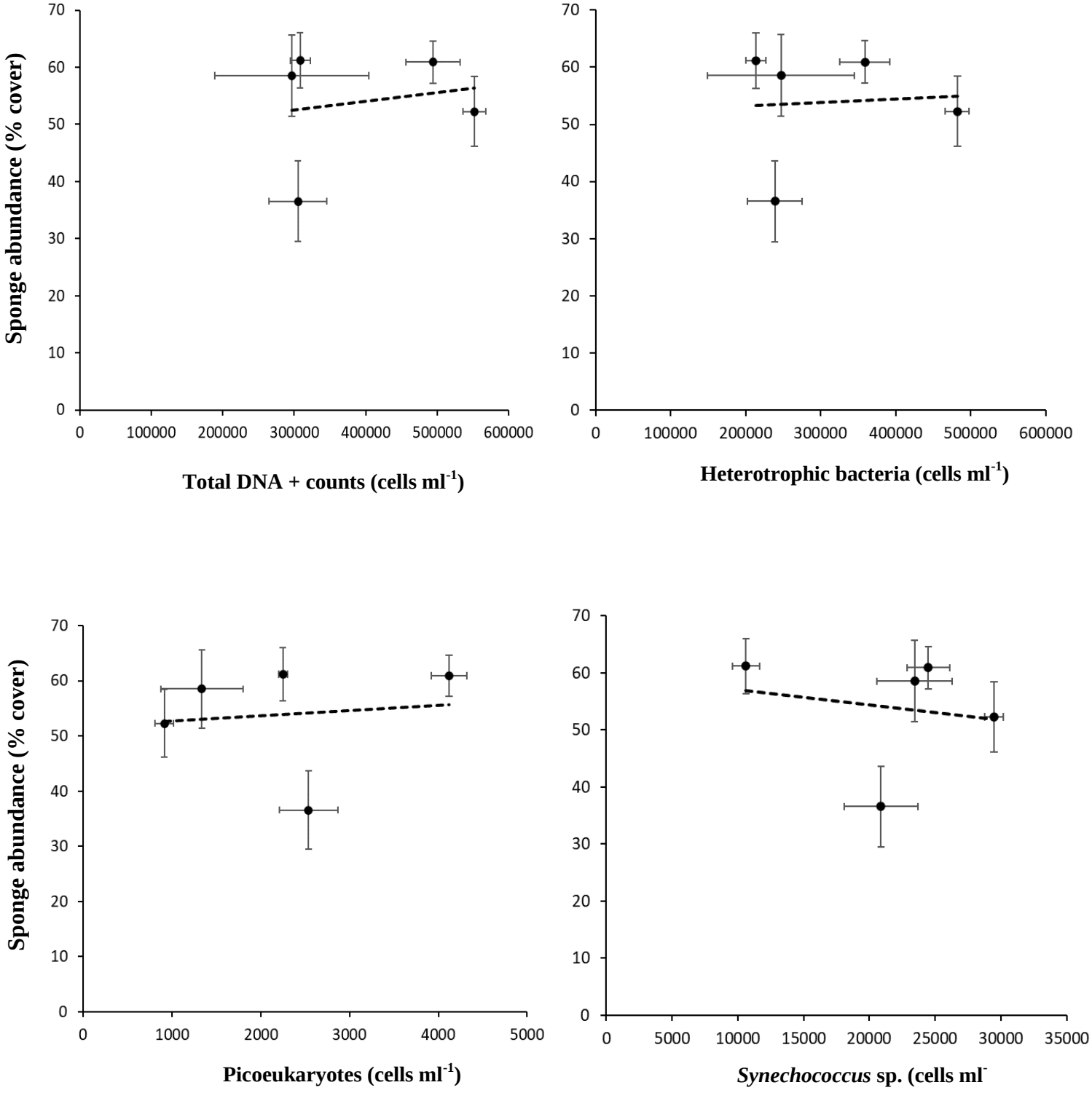

Fig. 3.7 Linear regression relationship between total ambient cells (cells L^{-1}) and sponge abundance (% cover) at 0, 10, 30, 50, and 80 m at the Poor Knights Marine Reserve. Vertical bars are sponge abundances ± SE. Horizontal bars are DOC concentrations ± SE.

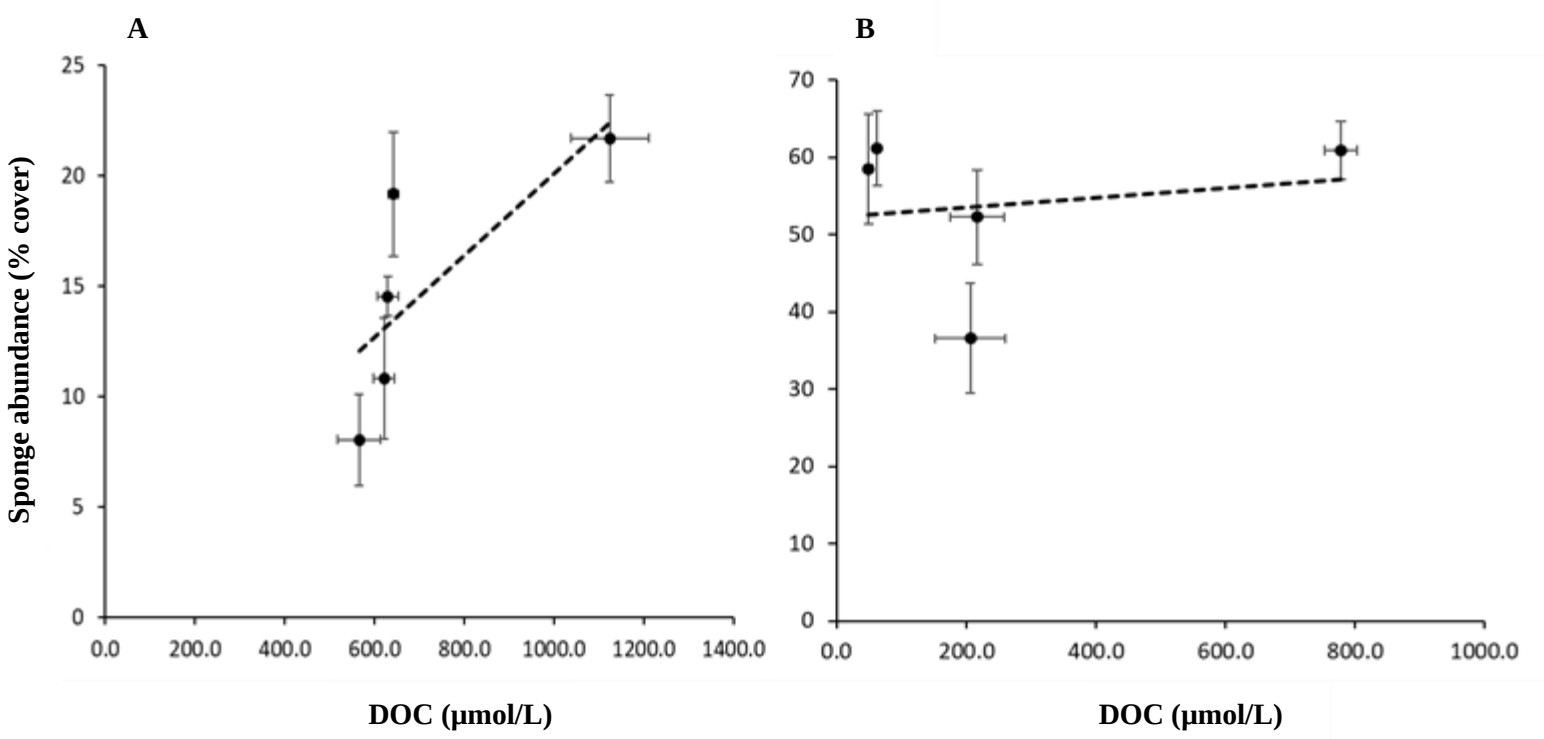

Fig. 3.8 Linear regression relationship between DOC concentration (µm/L) and sponge abundance (% cover) across four Fiordland sites (A) at 10 , 30 , 50, 80, and 120 m (0 m excluded, see discussion) and the Poor Knights (B) at 0, 10, 30, 50, and 80 m. Vertical bars are sponge abundances ± SE, horizontal bars are DOC concentrations ± SE.

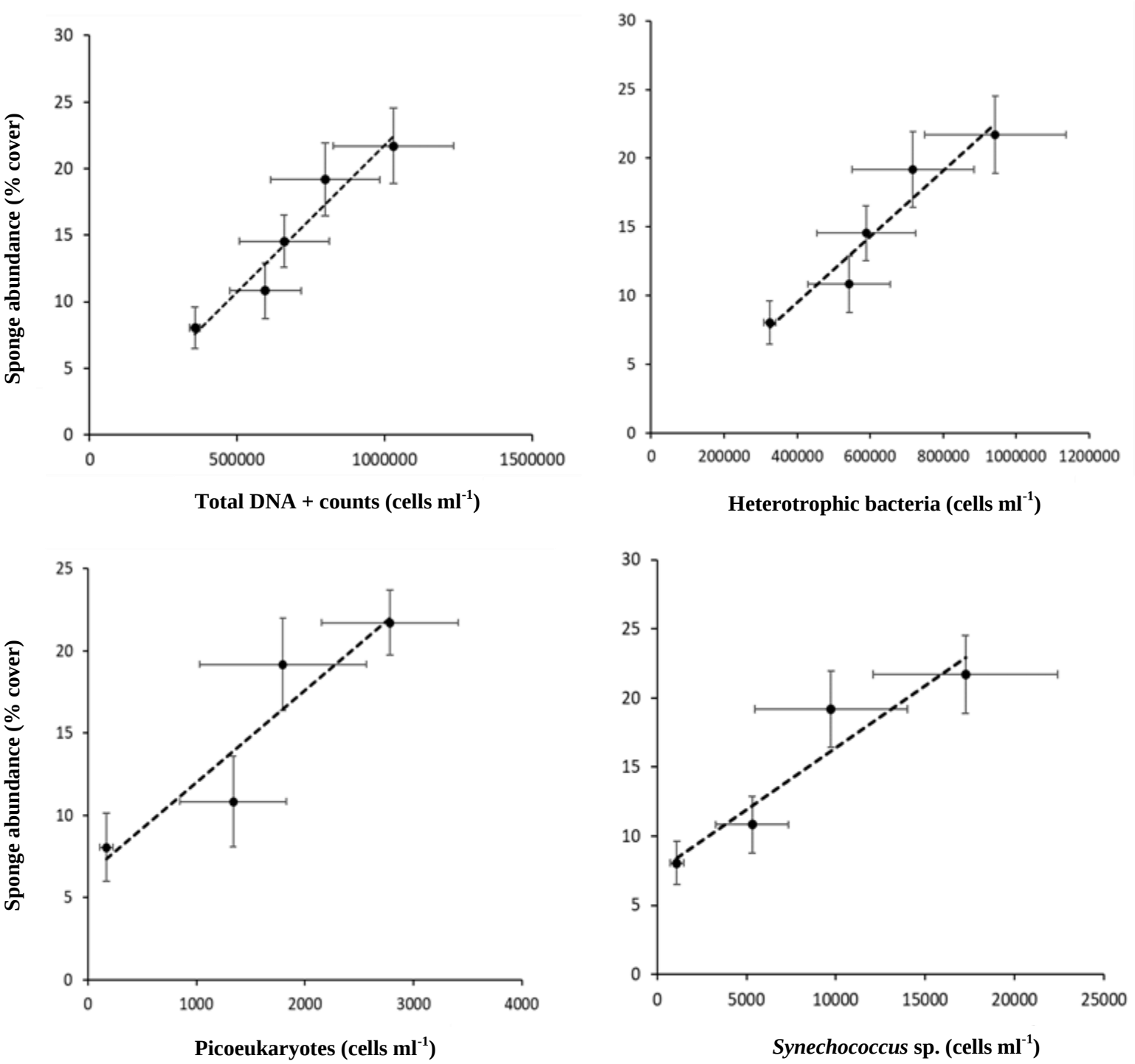

Fig. 3.9 Linear regression relationships of total nucleic-acid positive counts, heterotrophic bacteria, picoeukaryotes and *Synechococcus* sp. (ml^{-1} for all cell groups) with sponge abundance (% cover) across four Fiordland sites. Abundances of both sponges and cell groups were collected at distinct depth categories: 0, 10, 30, 50, 80, and 120 m. Here, 10 – 120 m is shown for total nucleic-acid positive counts and heterotrophic bacteria while 30 – 120 m is shown for picoeukaryotes and *Synechococcus* sp. (see Discussion). Vertical bars are sponge abundances ± SE, horizontal bars are cell abundance ± SE.

3.3.6 Sponge – microbial abundance correlations

No correlation was found between sponge abundance and the abundance of any individual microbial group, total nucleic acid events (Fig. 3.7) or DOC (Fig. 3.8) concentration at the Poor Knights over the full depth profile (Table 3.5) or when surface abundance data were excluded (see Methods and Discussion) from regression analyses (Table 3.5). Furthermore, no correlations were observed between sponge and microbial distributions at any individual Fiordland site except for Site 2, which showed positive correlations between the abundance of sponges and all microbial groups when 0 -10 m were removed from the analyses (Table B3.6). However, a strong positive correlation was seen between sponge abundance and all individual microbial groups below 10 m when all Fiordland sites were combined (Fig. 3.9 & Table 3.5). DOC showed no correlation with sponge abundance at any individual site or when all Fiordland sites were combined (Fig. 3.8 & Table 3.5).

3.4 Discussion

Marine sponges are consistently the most dominant benthic invertebrates occurring on rocky-reef habitats through infralittoral and mesophotic zones in New Zealand (Chapter 2). However, sponge assemblages exhibit significant variability in abundance through these depth profiles. Furthermore, New Zealand reefs exhibit significant unoccupied substrate in some regions, especially below the infralittoral zone (Fig. B3.1), indicating that one or more limiting factors besides spatial competition are restricting the proliferation of sponges in these habitats. The previous chapter revealed a lack of correlation between sponge distribution and multiple environmental variables (including temperature, salinity, chlorophyll-*a*, turbidity, dissolved oxygen) leaving the presence of unoccupied substrate, and sponge distribution patterns unexplained. In the current study, I suggested reasons for why food availability might be the most likely predominant driver/limiting factor of the sponge distributions

observed. I tested this suggestion by assessing correlations between sponge abundance and the availability of multiple microbial groups within the size range available to sponges (< 5 µm), as well as DOC.

For the first time, this study describes the composition and distribution of the sponge food pool (as multiple POC food groups and DOC) through extended depth ranges (0-120 m) of rocky-reef habitats in New Zealand, along which sponges have been observed to dominate the benthic community. Using a combination of flow cytometry and SEM to identify and enumerate microbial groups, I corrected previous misclassifications of microbial compositions in New Zealand waters. I found strong positive correlations between sponge distribution and food availability when I combined data from all Fiordland sites, suggesting that these sponge assemblages are subject to bottom-up effects. I found no correlations between food and sponge distributions at the Poor Knights but did observe some interesting smaller-scale patterns requiring further investigation.

These observations provide important ecological information about the composition and distribution of resources at the foundation of marine food webs in New Zealand's infralittoral and mesophotic habitats. They also provide an essential starting point from which the mechanisms driving spatial and temporal changes in temperate marine sponge assemblages, and the important ecological functions they provide, can be determined.

3.4.1 Microbial population identification: SEM observations

Testing assumptions of flow cytometry interpretations using SEM proved to be an important component of this study, the outcomes of which suggest that similar procedures would be a valuable component of future investigations that choose to employ flow cytometry to enumerate microbial populations in unexplored environments. SEM analyses showed the populations originally assumed as *Prochlorococcus* by Perea-Blázquez et al. (2011) to be a

much more heterogeneous and complex group of larger cells referred to as autotrophic picoeukaryotes. This broad category of photosynthetic eukaryotic cells, ranging from 0.8 - 3 µm in size (Schmidt, 2019), more closely reflects observations from sponge-related studies assessing temperate rather than tropical microbial community compositions, as would be expected (e.g. Morganti et al. 2016). This re-classification has important ecological ramifications, as this group exhibits traits that are very different to *Prochlorococcu*s. The most obvious differences are the complex internal structures (nucleus and organelles) that fundamentally differentiate eukaryotes and bacteria, but also different physiological traits that determine their spatial-temporal distributions and ecological functions (Schmidt, 2019). Although less abundant than cyanobacterial groups such as *Prochlorococcus* and *Synechococcus* sp., picoeukaryotes have been shown to match these cyanobacteria in terms of primary production of marine biomass (Worden et al. 2004). This reclassification also has important ramifications for our understanding of sponge trophodynamics, where the consumption of picoeukaryotes by sponges is very likely to represent different values of total carbon retention and exchange, compared to *Prochlorococcus* (Perea-Blázquez et al. 2013b) Furthermore, if picoeukaryotes were to be retained by sponges at high efficiencies, this would imply a significantly more diverse diet than previously proposed specifically in New Zealand sponges (i.e. those proposed by Perea-Blázquez et al. 2011; 2012).

Dividing the heterotrophic bacterial population into multiple size categories before running flow cytometry and SEM analysis would provide further valuable insights into the composition of this group, as it likely contains a wide variety of cell types that were not discriminated effectively at high resolution in this study. SEM analyses of this group were problematic and yielded unsatisfactory results. While this study was able to correct the previous categorization of *Prochlorococcus,* and tentatively confirm the composition of the *Synechococcus* sp. population successfully, the additional application of genome sequencing

would benefit future studies by providing a powerful analytical toolbox for identification of marine microbial communities.

3.4.2 Microbial group distributions

As an offshore group of small islands, The Poor Knights Marine Reserve is immediately exposed to pelagic waters in all directions, and therefore, likely undergoes considerable water-column turnover it. Furthermore, this area is characterized by particularly high light penetration for a temperate marine environment. Both factors might explain the observed lack of change in the microbial community composition with depth. Significant mixing of the water column would likely contribute to the vertical homogenization of the microbial community through depth profiles, while significant light penetration facilitates the proliferation of autotrophic microbes at deeper depths (Partensky & Vaulot, 1999). However, significant changes in the abundance of autotrophic groups (*Synechococcus* sp. and picoeukaryotes) were seen when considered individually.

The surface freshwater layer at Fiordland likely plays an important role in the shallow distributions of the microbial community. The higher abundance of total nucleic acid events observed at the surface might be due to the large input of terrestrially sourced microbial organisms lacking in chlorophyll-*a* which were not discriminated from the total nucleic acid population. The presence of distinct and novel microbial populations in these surface water samples supports the suggestion of terrestrially derived microbial entities occurring in high abundance in this region. This proposed effect of the freshwater layer is further supported by the unusual picoeukaryote and *Synechococcus* sp. distribution patterns observed at Site 1 (Hall Arm), which also exhibits the most prominent freshwater layer of all sites (Howe et al. 2010). This is due to its proximity to the outflow of freshwater from Lake Manapouri *via* the Manapouri hydroelectric power station, while undergoing minimal flushing from the open

ocean. Here, both picoeukaryotes and *Synechococcus* sp. were particularly limited at 0 m, where they would normally be expected to be in highest abundance, as exhibited at the other Fiordland sites. Both groups increased significantly in abundance from 0 to 10 m below the freshwater layer. *Synechococcus* sp. and most likely, the majority of the picoeukaryotes observed, are exclusively marine organisms and sensitive to salinity thresholds (Schmidt, 2019), below which they cannot persist and proliferate, as observed at Hall Arm.

3.4.3 DOC distributions

DOC concentrations were significantly higher at all Fiordland sites and across all depths than those observed at the Poor Knights (except for 0 m at Site 1). Some of these DOC concentrations exceeded the highest values (>700 μmol C L^{-1}) reported by Barrón & Duarte (2015) of 3510 estimates of DOC concentrations from coastal regions globally. For example, all Fiordland sites exhibited mean DOC values >1000 μmol C L^{-1} at the 30 m depth band. The consistency of this peak occurring at 30 m at all Fiordland sites does not have an immediately obvious explanation. However, the primary source and composition of DOC maybe very heterogeneous, even within single samples (Lee et al. 2004). Determining these origins and compositions would help elucidate the mechanisms behind this pattern. This is beyond the scope of this study, but is an ecologically important consideration, as the specific source and composition of DOC is likely to have a significant effect on the ability of marine organisms, including both the microbial community and sponges, to utilize, fix, and recycle this resource (Lee et al. 2004; Mentges et al. 2019). The Poor Knights demonstrated DOC values within the ranges expected from an open-ocean environment (Barrón & Duarte 2015). Again, while no patterns were observed, assessing the origins and composition of the DOC sampled at the Poor Knights at higher resolution might reveal more distinct patterns in its distribution, as well as potential correlations with distribution patterns of benthic community components. Some of these organisms might be net producers such as macroalgae (Watanabe

et al. 2020) and corals (Naumann et al. 2010), or net consumers of this resource such as sponges (Mueller et al. 2014).

3.4.4 Sponge-food correlations and implications

Initial observations of sponge and total microbial community abundances from the Poor Knights were surprising given the extremely high abundance of sponges throughout full depth profiles (significantly higher than those across the same depth gradients at all Fiordland sites), while the abundances of the overall microbial community was significantly lower than those found at any Fiordland sites at all depths. This suggests that the availability of heterotrophic microbial groups specifically can be dismissed as a determining mechanism of the sponge assemblage distributions observed. However, this does not necessarily refute the hypothesis of bottom-up effects on these sponge assemblages, as the literature regarding temperate sponge food preferences (albeit limited) consistently reports lower retention efficiency of heterotrophic bacteria and preference for autotrophic groups (see Chapter 4). Furthermore, when assessing the microbial community in more detail, the abundance of specifically autotrophic groups was higher at the Poor Knights than those at Fiordland (except for anomalies at Fiordland Site 2) beyond 30 m, potentially facilitating the continued high abundance of sponges into the mesophotic zone of the Poor Knights. While autotrophic microbial groups also did not correlate with sponge distributions over the full depth gradient, a significant decline in both *Synechococcus* sp. and picoeukaryotes coincided with a significant drop in sponge abundance at 80 m and a significant increase in sponge morphological complexity. Assessing a larger depth profile, or multiple sites exhibiting the same depth profiles in the same environment (which continue to exhibit correlations between autotrophic microbe availability and sponge assemblage abundance and morphological complexity), would provide more robust evidence for bottom-up effects. However, the significant increase in assemblage complexity coinciding with the significant reduction in

autotrophic microbe availability is what would be expected if bottom-up effects were occurring. Sponge morphologies exhibiting higher surface area and subsequently greater particle capture efficiency would be beneficial and selected for in areas of low resource availability. This is supported by numerous observations of high complexity sponge forms occurring in food limited environments, such as mesophotic and abyssal zones generally (Hogg et al. 2010; Beazley et al. 2013; Bart et al. 2020). The reduction in potentially damaging wave action to fragile three-dimensional morphologies (Palumbi, 1986; George et al. 2018) at deeper depths might also facilitate a broader range of more complex morphologies. Furthermore, a higher proportion of three-dimensional complex morphologies might be the result of the selection of these forms in environments with high sedimentation rates, such as deep mesophotic habitats. Here, more complex morphologies are more resilient to sedimentation than encrusting and massive morphologies (Bell et al. 2015). However, the Poor Knights did not exhibit any significant increases in turbidity at the deepest reaches of the reef and wave action is unlikely to be a significant factor beyond 30 m where fragile fan gorgonians and black corals occur in high abundance. This suggests that an increase in food particle capture efficiency is likely to be playing the most significant role in this change in morphological composition of the sponge assemblage.

The strong positive correlation between food availability of all food groups at Fiordland supports the hypothesis that bottom-up effects are driving temperate sponge distributions. Furthermore, numerous other potential drivers of sponge distributions identified in other studies, such as substrate type (Hunting et al. 2013; Duckworth, 2015) and inclination (Preciado & Maldonado, 2005), wave action (George et al. 2018), turbidity (Scheffers et al. 2010), intra-phyletic (Cárdenas et al. 2012) and inter-phyletic (Rützler, 1970) spatial competition, and predation (Pawlik et al. 2013; 2018) are unlikely to have significant effects on the specific assemblages assessed in this study for the following reasons: 1) Substrate type

and inclination were consistent through the depth profiles observed (80 – 90 degrees); 2) Significant free substrate space was observed beneath the infralittoral zone, undermining the suggestion of spatial competition; 3) Wave action is extremely minimal inside the protection of Fiordland arms; and 4) While sponge predation has been observed to some extent in temperate environments (e.g. Maschette et al. 2020), it is likely to be very limited (if it occurs at all) on Fiordland reefs. Top-down pressure from sponge predators is thought to decline significantly at high latitudes (Wulff, 2006) following long-established observations of broad-scale ecological trends, and no observations of sponge predation have been reported in southern New Zealand. This strongly undermines the potential role of top-down effects.

Considering the significant variability of food availability, the correlation of this variability with sponge distributions, the lack of environmental drivers, and the unlikely contribution of other biotic mechanisms (predation, spatial competition etc), food availability appears to be the most likely driver of the patterns observed in Fiordland, and the abundance and morphological composition of sponge assemblages in the deepest regions of the Poor Knights. However, this conclusion is based on correlative information. To explicitly test and confirm this conclusion with greater confidence requires the application of an experimental design, preferably *in situ*. Although a particularly difficult task given the dynamic nature of the habitat and ecological interaction in question, this would provide robust evidence that bottom-up effects are the predominant driver of temperate sponge distributions. Furthermore, quantifying the specific diet preferences of the most abundant sponge species occurring in these regions would provide essential information to further elucidate the trophodynamics and population dynamics of temperate sponge assemblages in New Zealand.

Chapter 4

Food selectivity and limitation as potential drivers of resource partitioning in temperate sponge assemblages

Abstract

Sponge feeding activity is ecologically important due to the transfer of organic carbon from the water column to the benthos, where it can then be recycled back to the water column through numerous pathways. These interactions are also likely to determine the abundance, distribution, and composition of sponge assemblages themselves. Despite this, substantial gaps remain in our understanding of the trophodynamics of temperate sponges, including their potential dietary range and feeding preferences. This study examines the *in situ* diets of seven common sponge species occurring on shallow temperate reefs at three sites in New Zealand. I assessed the potential for active food selection and interspecific differences in food preference to support resource partitioning and trophic plasticity. I measured sponge particulate organic carbon (POC) and dissolved organic carbon (DOC) uptake. Sponges showed active selection between POC groups as well as between POC and DOC, although only two species (*P. penicillus* and *Polymastia* sp.) showed significant DOC consumption. I found that retention efficiencies of specific POC groups were consistently high in all species that fed exclusively on POC. However, the consumption of DOC by only *P. penicillus* and *Polymastia* sp. coincided with lower retention efficiencies of POC groups and was entirely responsible for inter-specific differences in food selectivity and therefore resource-partitioning. Correlations between DOC availability and DOC consumption and DOC selectivity indicate trophic plasticity in the study species, which suggests that sponges can 'switch' between food types based on relative food availability as an active rather than passive response. I found limited evidence for niche partitioning within the POC food pool, but propose that trophic plasticity, generalist feeding strategies, and DOC consumption might help explain the high abundance of specific sponges relative to other benthic invertebrate groups in resource-poor environments.

4.1 Introduction

The exchange of organic matter between the water column and the benthos plays a key role in the trophodynamics of marine ecosystems, and is likely to be an important driver in determining the structure and distribution of benthic communities (Cattaneo-Vietti et al. 1999). Benthic communities themselves are central to this process, performing important functional roles at the base of marine food webs by regulating water column chemistry and recycling carbon via suspension feeding on plankton, detritus, and other organic matter.

Marine sponges are often one of the most abundant benthic groups occurring on (but not limited to) rocky-reef habitats (Fromont & Garson, 1999; Bell & Barnes, 2000; Schlacher et al. 2007) in tropical, polar, and temperate environments, and from intertidal to abyssal zones (Bell et al. 2020). Compared with other suspension feeders, sponges can exhibit very large individual body volumes (e.g. *Xestospongia* spp.; 116,721 ± 29,275 cm^3 (Mcgrath et al. 2018)), high pumping rates (> 35 ml min^{-1} cm^{-3} sponge (Weisz et al. 2008)), and high retention efficiencies (up to 99%) of planktonic cell groups (Pile et al. 1997; McMurray et al. 2018). Therefore, feeding activity of sponges is of high ecological importance; contributing to the movement of organic carbon from the water column to the benthos and transforming organic carbon into sponge biomass or detritus to be recycled back into the benthic community (de Goeij et al. 2013). The inextricable trophic link between sponges and the water column is also likely to act as a driver of the distribution and abundance of sponge assemblages themselves, as a result of bottom-up effects (Lesser & Slattery, 2013; but see Pawlik et al. (2013)). The extent of bottom-effects depends largely on the susceptibility of sponges to food-limitation (food availability not meeting metabolic, growth, and reproductive demands), and is likely to be habitat, species, and season dependent (Pawlik et al. 2018). Bottom-up effects also have broader implications for the wider benthic community, as sponge assemblages perform other important ecological functions aside from those directly

associated with feeding (Bell, 2008), including habitat provisioning (Maldonado et al. 2017), spatial competition (López-Victoria et al. 2006), and substrate erosion (Schönberg et al. 2017) and consolidation (Schönberg, 2016).

Most sponge feeding studies have been conducted in tropical environments and have considered a range of food types from the particulate organic carbon (POC) pool. The POC food pool available to sponges includes cyanobacteria (notably *Synechococcus* and *Prochlorococcus*), heterotrophic bacterioplankton, and autotrophic picoeukaryotes (Yahel et al. 2006; Hadas et al. 2009). However, the relative abundance of these groups exhibits significant spatial and temporal variation (Flombaum et al. 2013). Contrary to early assumptions (see Pile et al. 1996; Ribes et al. 1999), particle selectivity has been indicated in multiple studies (Hanson et al. 2009; Topçu et al. 2010; Perea-Blázquez, 2011), as has inter-specific variation in preference for different POC groups, implying resource partitioning within multi-species assemblages (e.g. Perea-Blázquez et al. 2011). Sponge-food selectivity has been determined based on cell type and size (Yahel et al. 2006), but the relative ambient availability of different food groups has also been shown to be an important mechanism in determining feeding behaviour (Duckworth & Battershill, 2001). Considering POC availability in relation to feeding behaviour means that particle retention efficiency, as well true feeding preferences (controlling for food availability), can be calculated. Subsequently, inferences about possible food limitation and resource partitioning can be determined.

While POC has been shown to be a key component of the sponge diet, it represents only a small proportion of total organic carbon (TOC) in the marine environment, with over 90% of the TOC pool small enough to enter through the sponge ostia consisting of dissolved rather than particulate organic carbon (DOC) (Pawlik et al. 2018). Marine DOC consists of a broad range of components from several sources, including phagocytized cell remnants and exudate from photosynthetic bacteria (Thornton, 2014), macrophytes (Brylinsky, 1977) and corals

(Crossland 1987; Haas et al. 2011), as well as allochthonous terrestrial sources (Raymond & Spencer, 2015). DOC is operationally defined as any organic carbon that will pass through a GF/F filter (retention rating < 0.7µm) (Hansell & Carlson, 2014), which represents the largest exchangeable carbon reservoir in the marine environment (Druffel et al. 1992; Hansell & Carlson, 2014), but normally requires recycling by the microbial community before it is made available to the wider ecological community via the microbial loop (Azam et al. 1983). Despite studies showing preferential feeding on specific POC groups by sponges (Maldonado et al. 2012), it is now apparent that some sponges can bypass the microbial loop by retaining and metabolizing DOC themselves (de Goeij, 2008; 2013; Rix, 2016; 2017).

Despite the ubiquity of DOC throughout the world's oceans, and increasing evidence of sponge-DOC utilization as a common phenomenon, our understanding of sponge-DOC interactions is derived almost exclusively from tropical environments (McMurray et al. 2018; Mueller et al. 2014; Rix et al. 2016; 2017; de Goeij, 2017), while temperate regions have been overlooked. A review by de Goeij et al. (2017) found a total of 20 sponge species for which DOC retention has been assessed (at the time of publication), 17 of which showed DOC uptake. However, only three of the 20 species assessed were temperate species (*Dysidea avara*, *Agelas oroides,* and *Chondrosia reniformis*), all of which were examined in the Spanish Mediterranean (Ribes et al. 1999; 2012), a warm temperate environment. A limited number of studies assessing the feeding behaviour of deep-water sponges have considered DOC as part of the potential diet with mixed outcomes. Yahel et al. (2007) and Kahn et al. (2015) showed no uptake of DOC by two hexactinellid species in a deep Norwegian fjord and by *Aphrocallistes vastus* in the North East Pacific. However, Bart et al. (2020) showed that DOC represents > 90% of the total carbon removal of sponges occurring on a deep-water reef in the North Atlantic. However, given the broad taxonomic range of the

sponge phylum (> 8500 species), inter-specific differences in feeding behaviour may have evolved from resource competition pressures and geographical variation in food availability.

Low resource availability in tropical (Hatcher, 1990) and deep-sea cold water environments might be an important mechanism explaining the high DOC retention rates by some sponges observed in these habitats. Here, high trophic plasticity and alternative resource accumulation strategies could evolve if low resource availability imposes sufficient evolutionary pressure to do so. The observed persistence of sponges in particularly resource-limited environments explains the research bias towards DOC-sponge interactions in tropical habitats. However, the same resource limitation pressures might also apply to temperate sponges, especially during significant seasonal reductions in productivity and POC availability (Evans & Parslow, 1985) or in deeper temperate mesophotic ecosystems (TMEs) where food might be more limited still, due to reduced photosynthetically active radiation. Multi-species assemblages of temperate sponges occurring even in highly-productive infralittoral habitats have been shown to exhibit resource partitioning of the available POC pool (Perea-Blázquez, 2013). This might be a response to the limited availability of specific components of the POC pool in which case, the ability to utilize DOC would be advantageous. High retention efficiencies of specific POC food pool components (Perea-Blázquez et al. 2012) support this suggestion, indicating that food-saturation levels of specific POC components are not being reached.

There are broader ecological ramifications if DOC is consumed by temperate sponges, most notably because of its role in the sponge-loop (de Goej et al. 2013). The sponge-loop has been described as analogous to the microbial loop, where sponges recycle DOC previously inaccessible to the wider ecological community, converting it into POC in the form of detritus and potentially sponge biomass (McMurray et al. 2018; Pawlik & McMurray, 2020). The sponge-loop, in combination with the microbial-loop, provides a solution as to how

diverse and abundant ecological communities can thrive in otherwise oligotrophic habitats of tropical marine environments. However, it is likely that this would also have considerable ecological significance in temperate environments, especially during periods of low productivity or in deeper habitats, such as TMEs with markedly lower POC availability than their shallow counterparts. Recent evidence for a cold-water deep-sea sponge loop in the North Atlantic supports this suggestion (Bart et al. 2020).

Investigating the potential food-pool available to temperate sponges (DOC and POC components) is therefore essential to our understanding of how multi-species assemblages co-exist at high densities on temperate rocky reefs through resource partitioning, the role of bottom-up effects in the interaction between sponges and food availability, and the broader importance of sponge trophodynamics in temperate environments. The aims of this study are: 1) to determine the full natural diet and food preferences (food-group selectivity) of six common demosponge species and one common calcareous sponge species *in situ,* on temperate New Zealand reefs; 2) to identify any inter-specific differences in selectivity of POC groups, as well as between POC and DOC food sources as a potential mechanism supporting resource partitioning; and 3) describe the relationship between the ambient availability, food selectivity and retention efficiency of different food-groups by these same sponge species, to assess the role of food availability in feeding behaviour and the potential for food limitation.

4.2 Methods

4.2.1 Study Sites

Sampling was undertaken using SCUBA at Parininihi Marine Reserve (PMR) on the North Taranaki Bight (Fig. 4.1B) in January 2020, and in Wellington Harbour and Breaker Bay on the Wellington South Coast (WSC), (Fig. 4.1A) from May to July 2020. PMR is

characterised by a morphologically diverse and abundant sponge assemblage (Chapter 2) occurring on horizontal reef platforms from 15 - 25 m with low light availability, and as a result, has been previously considered as a potential shallow water surrogate for mesophotic depths (30 -150 m) (Chapter 2; Battershill 1996). Breaker Bay is characterised by rocky reef habitat with vertical crevices and gullies harbouring a diverse and abundant sponge assemblage consisting of numerous common species found in similar habitats across New Zealand (Berman & Bell, 2010; 2016). The WSC is a highly dynamic environment with multiple large current systems, causing fluctuations in water temperature, strong winds, and frequent high energy swells. Wellington Harbour is characterized by fine, soft-sediment substrate with a rocky reef perimeter down to approximately 5 m. Wellington Harbour is subject to more stable environmental conditions than the adjacent southerly facing coast. This habitat is characterized by low light availability, low abundance of algae, and a high abundance of a limited number of sponge species, (predominantly *Suberites* sp.) occurring on the reef/sediment line on dispersed rocky cobble.

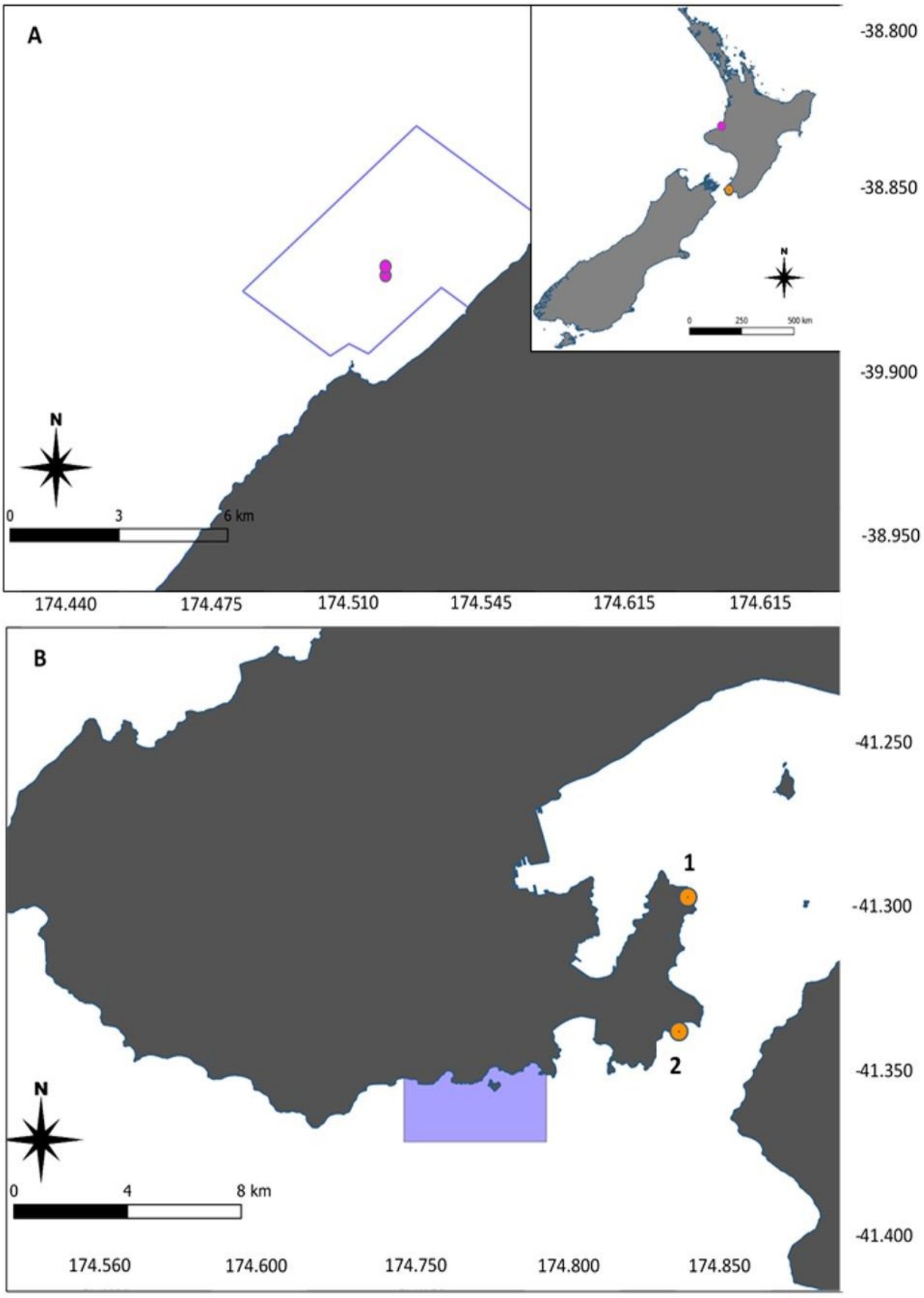

Fig. 4.1 Map showing sampling sites at Parininihi Marine Reserve (A) and Wellington Harbour (B1) and Breaker Bay (B2). Blue boxes show the borders of Parininihi Marine Reserve (A) Taputeranga Marine Reserve (B).

4.2.2 Sponge-feeding assessments

Sponge feeding dynamics were determined based on differences in exhalent/inhalant cell concentrations from a single osculum of each specimen. Early determinations of the sponge diet were undertaken under laboratory conditions where the natural variability in food-pool composition is difficult to replicate and natural sponge feeding behaviour cannot be assured (Diaz & Ward, 1997). Other studies carried out *in situ* have commonly used chambers with multiple inherent issues, including the disturbance of ambient current for pumping activities, sample contamination from pinacocyte cell loss from the sponge-dermal layers, disturbance/stress through the displacement of the specimen, and over-time reduction in oxygen availability. All these factors have the potential to significantly disrupt feeding activity or bias results. Here, a modified *in situ* inhalant/exhalent approach (Yahel et al. 2005) was employed to: avoid direct disturbance to the specimen; ensure natural pumping rates were not interrupted; and reduce the likelihood of sample contamination from sponge exudates (see Parker, 1914; Jørgensen, 1955; Reiswig, 1974; Yahel et al. 2005; Hadas et al. 2008). This is especially important for DOC analysis, as it is highly sensitive, and DOC contaminants cannot be easily distinguished from target DOC and subsequently controlled for (see below for controlling for potential sponge cell/microbiome contaminants in POC analysis).

4.2.3 Study species

Polymastia penicillus and a second *Polymastia* sp. were chosen for feeding assessments at PMR. Both species are common across New Zealand's North Island, including deeper regions of the WSC (> 20 m) (personal observations), but occur in shallower water at PMR, making *in situ* assessments easier. The demosponges *Dysidea* sp., *Tethya* sp., and *Tedania* sp., and the calcareous sponge *Clathrina* sp. were chosen for feeding assessments at Breaker

Bay. All species are highly abundant in this region and common in similar habitats across New Zealand (Berman & Bell. 2010). *Suberites* sp. were assessed in Wellington Harbour. The species used all have large oscula compared to many others found in shallow temperate environments (other morphologies more common in TMEs and numerous tropical sponges often exhibit significantly larger oscula), facilitating the sampling protocol described below.

4.2.4 *In situ* sampling

Five specimens of each species were chosen based on sponge size where mid-size-range was preferred (approximately 4 - 5 cm diameter for *Suberites* sp. and approximately 25 - 50 cm for other species), except for *Tethya* sp. where the largest specimens were preferred, as the maximum size limit appears to be significantly less than for other assessed species (< 7 cm diameter). Specimens were also chosen based on the orientation of the sponge on the substrate, for the stable application of the sampling apparatus and easy access to the sponge oscula. Individuals with larger oscula (minimum > 1 cm diameter) were prioritised, to increase the accessibility of sampling apparatus and reduce the risk of disturbance and sample contamination via apparatus-sponge contact. Sampling was carried out based on a modified technique described by Morganti et al. (2016). Fluorescein food-dye was injected at the base of the sponge using a 50 ml syringe and observed as it was exhaled from the sponge osculum, to confirm pumping as an indicator of on-going suspension feeding. Food-dye exhalent speed was also filmed to ascertain pumping rates, for the determination of the appropriate rate of sample extraction (see below). After all observable dye had been exhaled from the sponge, two PEEK tubes (25 μm IDM) (IDEX) connected to a flexible tripod were placed 2 cm from the sponge for the sampling of inhalant water and 2 mm inside the most easily accessible exhalent sponge aperture for the sampling of exhalent water. Syringe needles (OD = 0.69 mm) connected to the distal ends of the PEEK tubes were then inserted into two pre-combusted, evacuated EPA 60 ml glass vials with silicone septa caps, and fitted inside a

weighted vial holder allowing for the simultaneous collection of ambient (inhalant) and exhalent water. Needles were checked for sample flow, and the time was noted. Extraction rate was targeted to < 1 % of the sponge pumping rate to prevent contamination of the exhalent sample from ambient water. Sampling rate can be pre-determined using the following equation (derived from the Hagen-Poiseuille equation):

$$F = \frac{\Delta P * \pi * r}{s * K * L * V}$$

Where F is flow, ΔP = differential pressure (bar), r = inlet tubing internal radius (cm), K (Kelvin function) = 2.417 x 10^{-9} (sec^{-2}), L = tube length (cm), V = water viscosity (g cm^{-1} sec^{-1}).

Preliminary field tests showed the extraction rate to be inconsistent despite all controllable factors in the equation remaining constant. These inconsistencies are expected to be due to the high variability in water turbidity occurring in dynamic natural marine environments, which affect the efficiency of laminar flow inside the PEEK tubing. Therefore, while this equation was useful for constructing the sampling system assembly to make extraction rates conservatively slow, the actual extraction rate was calculated post-sampling as the volume of water collected over time. All true extraction rates remained < 5% of the average *per* osculum pumping rate of each species. Samples for POC analysis were dispensed into 5 ml cryovials from the EPA vials immediately on the surface, fixed with EM grade 25% glutaraldehyde (0.1% concentration), snap-frozen in liquid nitrogen, and stored at -80^{o}C until analysis. Samples for determination of DOC concentration were filtered through a pre-combusted 13 mm binder-free G/F filter (PALL 66251) fitted inside a 13 mm stainless steel Swinney filter holder (PALL 4042), into a new pre-combusted 40 ml EPA glass vial, fixed with EM grade hydrochloric acid (0.1% final concentration), and frozen at – 20^{o}C until DOC analysis.

Sponges were photographed for determination of osculum number and size and removed from the substrate while ensuring that no tissue was left attached the substrate. Specimens were then dried for 48 h at 70 ℃, weighed, and then ashed in a muffle furnace for 8 h at 500 ℃ to determine ash-free dry weight (ASFDW = dry weight – ashed remains).

4.2.5 Flow Cytometry POC analysis

A BD LSRFortessa™ bench-top flow cytometer equipped with 6 lasers (20 mW 355 nm UV, 50 mW 405 nm Violet, 75 mW 445 nm Blue Violet, 100 mW 488 nm Blue, 150 mW 532 nm Green, and 40 mW 633 nm Red) was used to determine the abundance of different planktonic populations in ambient and exhalent water samples. The cytometer was calibrated using BD Cytometer Setup and Tracking Beads (Cat No. 641319). Polystyrene beads were used for particle size calibration: 3µm Rainbow Beads (Spherotech, Cat No. RCP-30-20A) and ApogeeMix which range in size from 110nm – 1300nm (Apogee Flow Systems, Cat No. 1493). The nucleic-acid binding dye SYBR Green I was excited by the 488 nm Blue laser and the emission was detected by the 515/20nm bandpass filter off the Blue laser. SYBR Green I has a binding preference for dsDNA, it also binds ssDNA and RNA with lower affinity. SYBR Green I use ensured the broadest spectrum of biological entities in the sample were captured, including viruses (Marie et al. 1999). A 1:40 000 SYBR Green I/sample ratio provided the best compromise between population discrimination and signal saturation and compensation issues (see Chapter 3). An unstained subsample was run for each sampling period (*per* dive) to provide a gating control for stained samples. The cytometer was set to a flow rate of 40 µm *per* min and run for 300 s for every sample, producing a consistent total analysed volume of 0.2 ml.

4.2.6 Dissolved organic carbon analysis

DOC concentration was determined using high temperature combustion catalytic oxidisation (Shimadzu Cooperation). After filtering through a glass fibre filter (see above), the remaining TOC (now operationally considered as dissolved components) in the sample was combusted by heating to 680 °C in an oxygen-rich environment. The carbon dioxide generated was detected using an infrared gas analyser (NDIR detection). The concentration of total carbon in the sample was obtained through a comparison with a calibration curve formula. The oxidized sample was sparged with nitrogen to isolate the inorganic carbon in the sample and again measured by NDIR. TOC (as DOC) concentration was then calculated by subtracting the inorganic carbon concentration from total carbon concentration. Determination of DOC concentration was conducted by the National Institute of Water and Atmospheric Science (NIWA, Hamilton, New Zealand).

4.2.7 Data analysis

Flow cytometry data was analysed using the software package FlowJo V10.8.0. All nucleic-acid positive events (SYBR Green I positive) were discriminated and gated in the first instance using the signal area (A) from Side Scattered lighted (SSC-A, proportional to particle complexity) *vs*. the 515/20 detector off the blue laser (SYBR Green I). The nucleic acid positive events gate focuses on the events of interest, while excluding unwanted inorganic particles and instrument noise (Figs. B3.3 & B3.4). The population of nucleic acid positive events was then analysed further to distinguish populations of interest based on distinct fluorescent signatures. Distinct populations exhibiting bright orange fluorescence emission (excited by the Green laser and seen in the 575/25 detector) were considered *Synechococcus* sp. (Fig. 4.2). These cyanobacteria contain phycobiliproteins that emit orange fluorescence that can be detected separately from the red fluorescence emitted from their

chlorophyll *a*. Populations emitting bright red fluorescence (excited by the Blue laser and seen in the 685/35 detector), denote the presence of chlorophyll *a,* and with dim orange fluorescence were labelled as picoeukaryotes, as a broad taxonomic group of photosynthetic eukaryotes less than 5 µm in diameter. The distinct and dense population with minimal fluorescence properties were considered heterotrophic bacteria lacking in chlorophyll (Fig. 4.2). This abundant group represents a broad range of numerous types of small nucleic acid-positive entities such as viruses that are represented alongside heterotrophic bacteria (Marie et al. 1999). SYBR Green I is able to more broadly label nucleic acid species compared to other dyes applied in similar studies (e.g. Hoechst 33342). Despite this group likely including other species besides bacteria, the label 'heterotrophic bacteria' was retained for consistency with the relevant literature. This population was not mined further to discriminate any sub-populations separately at higher resolution, but it was considered essential to the aims of this study to include all possible potential sponge-food particles. Specific gate locations were drawn separately for different specimens as appropriate due to small amounts of variability and spread of fluorescent signatures across replicates, most likely due to small variations in depth and the time of day. However, gates for inhalant and exhalent sample pairs of single specimens were copied across from the inhalant to exhalent plots, to ensure that differences in the number of cells of each population (cell retention) were derived from a consistent region (Fig. 4.2) for intra-sample comparisons. A small number of specimens exhibited an increase in a specific cell population in exhalent samples with very low phycobiliprotein and chlorophyll *a* content but was distinguishable from the heterotrophic bacteria population (Fig. C4.1). These were considered sponge-derived cells being shed naturally via the exhalent stream, as they were not present or significantly lower in corresponding ambient/inhalant samples and it was ensured that the PEEK tubing never contacted the sponge tissue. They

were therefore gated as a separate entity and omitted from total POC and heterotrophic bacteria retention counts as appropriate (Fig. C4.1).

PERMANOVA was used in PRIMER V6 to determine differences between log-transformed inhalant and exhalent cell counts, to determine any significant retention of each food group.

Food selectivity was quantified using the Manley-Chesson's selectivity index, which is not sensitive to changes in food availability unless the behaviour of the animal itself changes. The evaluation of particle selectivity (food preference) was determined in R using the package 'selectpref', applying Chesson's selectivity index (α) (case 1 in Chesson, 1983):

$$\hat{\alpha} = F_i \left(\sum_{i=1}^{m} Fi \right) - 1$$

Chesson's index is an indicator of relative prey preference rather than a measure of diet proportion, which accounts for variability in food availability that can fluctuate significantly over small spatial scales. For visual display of food preference, an electivity index, ranging from -1 to + 1, was applied to Chesson's index scores. 0 represents no preference, +1 represents highest possible positive preference and – 1 represents the highest possible negative preference. This was calculated as:

$$\epsilon_i = \frac{m\alpha_i - 1}{(m-2)\alpha_i + 1}$$

Chesson's index scores were calculated according to a total of four food groups (three POC groups and DOC) for *Polymastia penicillus* and *Polymastia* sp., which showed significant DOC retention (see results), while only POC food groups (3 groups) were used for the

remaining species, which showed no significant DOC retention. PERMANOVA in PRIMER V6 was used to determine differences in Chesson's index scores for each food group, to determine food selectivity within each species.

A two-way PERMANOVA was used to determine any differences in Chesson's index scores (selectivity) between species as a measure of resource partitioning. The ratio of cells retained relative to the ambient cell availability (inhalant count) was used to determine food retention efficiency (as %) ((Ambient – Exhalent / Ambient)100). Selectivity and efficiency data were square-root transformed and used to generate a Bray-Curtis similarity index for PERMANOVA tests. Determination of retention efficiency is subject to the relative availability of food groups and, as such, has different ecological implications to significant interspecific differences in Chesson's index scores (food selectivity).

Linear regression models were created in R to determine relationships between ambient food availability and food retention efficiencies and Chesson's index scores. Specific transformations of data were applied based on best linear model tests of assumptions of normality. A limited number of replicates of two species yielded net gains in total POC counts and therefore negative retention efficiency values that were to cancelled-out to zero.

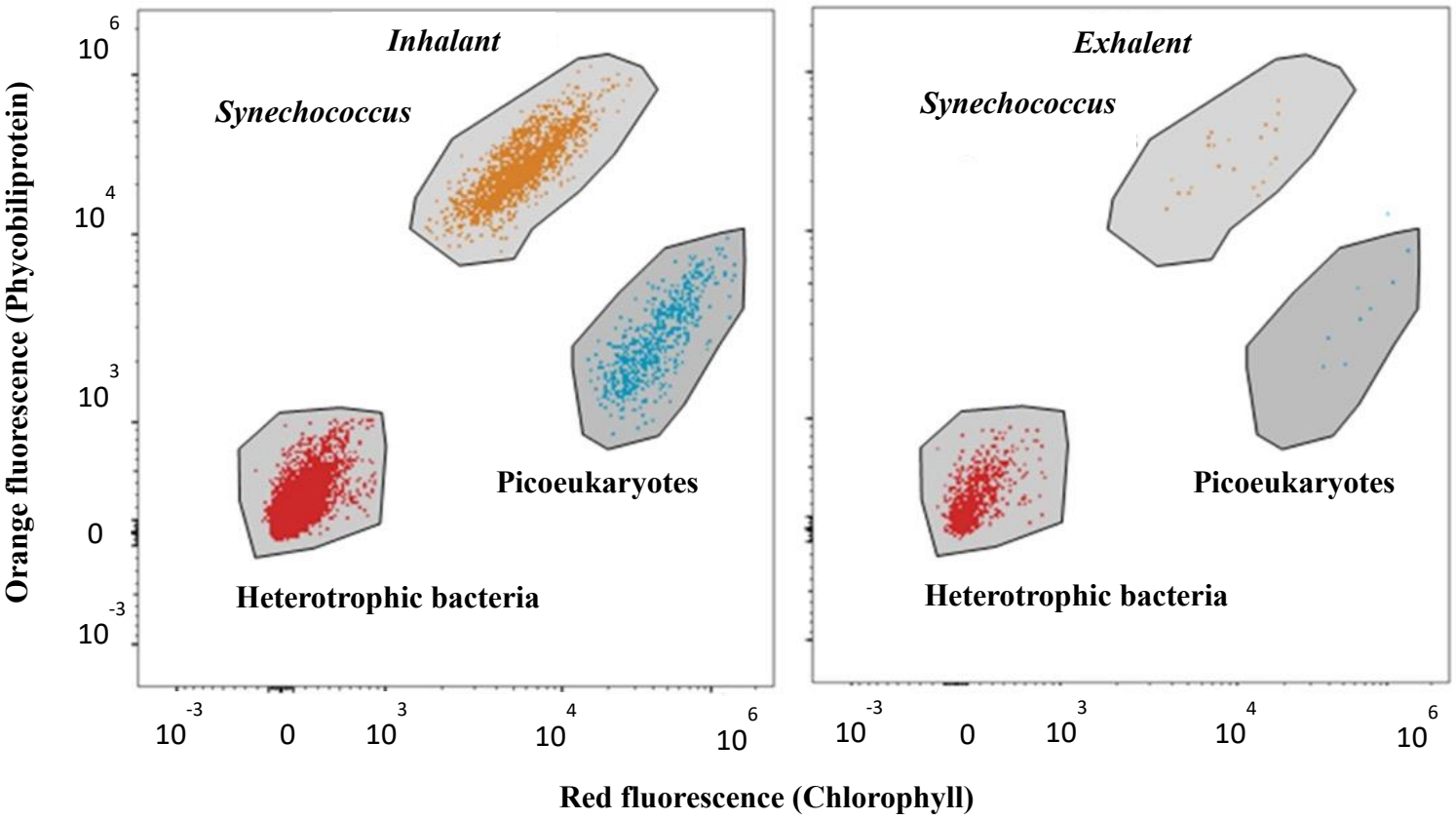

Fig. 4.2 Example of gating strategy of isolated populations of three main food groups between inhalant and exhalent water (sample is from *Tethya* sp.). Dot plots show how the coordinates of applied population gates are exactly replicated from the ambient/inhalant sample to the exhalent sample for each sponge-replicate sample pair. Shaded regions show the gate borders drawn around isolated populations.

4.3 Results

4.3.1 Food retention

PERMANOVA tests showed significantly lower concentrations of cells in the exhalent water compared to the inhalant water for at least one POC group for all but one sponge species, indicating feeding on suspended POC (Fig. 4.3 & Table 4.1). *Polymastia* sp. did not exhibit any significant difference between inhalant and exhalent samples for any POC group or total

POC (all POC groups combined) (Fig. 4.3 & Table 4.1). No significant differences in DOC concentration were observed in exhalent water compared to ambient water for any species sampled on the WSC (Fig. 4.4 & Table 4.1). In some cases, *Tedania* sp. and *Suberites* sp. had a higher exhalent DOC concentration than ambient concentration, though there was high variability and no significant net DOC production overall (Fig. 4.4 & Table 4.1). However, *Polymastia penicillus* and *Polymastia* sp. at PMR had significantly lower DOC concentrations in their exhalent *versus* ambient water, indicating feeding on DOC by these two species (Fig. 4.4 & Table 4.1). The significant retention of DOC by the two *Polymastia* species coincided with a lack of retention of POC, with *Polymastia* sp. not showing any significant retention of any POC group, and *Polymastia penicillus* showing no significant retention of *Synechococcus* sp. (Table 4.1) and a significantly lower retention efficiency of total POC than all other sponge species (Table C4.1 & Fig. 4.5). *Tedania* sp. was an exception, showing significant retention of picoeukaryotes only (Table 4.1 & Fig. 4.3).

Table 4.1 PERMANOVA results for differences in cells counts in ambient/inhalant and sponge exhalent water samples for 3 POC groups, total POC, and DOC from 7 sponge species.

	POC		DOC		
Species	**F-statistic**	**p-value**	**F-statistic**	**p-value**	**Df**
Tethya sp.	26.50	< 0.01*	0.7384	0.52	1,8
Tedania sp.	1.344	0.299	0.1217	0.861	1,8
Suberites sp.	78.58	< 0.01*	0.0157	0.978	1,8
P. penicillus	6.19	< 0.05*	21.936	< 0.01*	1,8
Polymastia sp.	0.94	0.321	1.621	< 0.05*	1,8
Dysidea sp.	5.1	0.05*	1.182	0.283	1,8
Clathrina sp.	7.02	0.029*	3.036	0.143	1,8

	Synechococcus		**Picoeukaryotes**		**Heterotrophic bacteria**		
Species	**F-statistic**	**p-value**	**F-statistic**	**p-value**	**F-statistic**	**p-value**	**Df**
Tethya sp.	42.173	< 0.01*	33.224	< 0.01*	32.724	< 0.01*	1,8
Tedania sp.	1.537	0.334	6.852	< 0.05*	3.123	0.136	1,8
Suberites sp.	7.638	< 0.05*	9.995	< 0.01*	67.092	< 0.01*	1,8
P. penicillus	4.678	0.064	8.021	< 0.05*	5.585	< 0.05*	1,8
Polymastia sp.	1.016	0.457	2.528	0.153	0.998	0.206	1,8
Dysidea sp.	19.719	< 0.01*	20.668	< 0.01*	15.626	< 0.01*	1,8
Clathrina sp.	7.666	< 0.05*	12.645	< 0.05*	7.111	< 0.05*	1,8

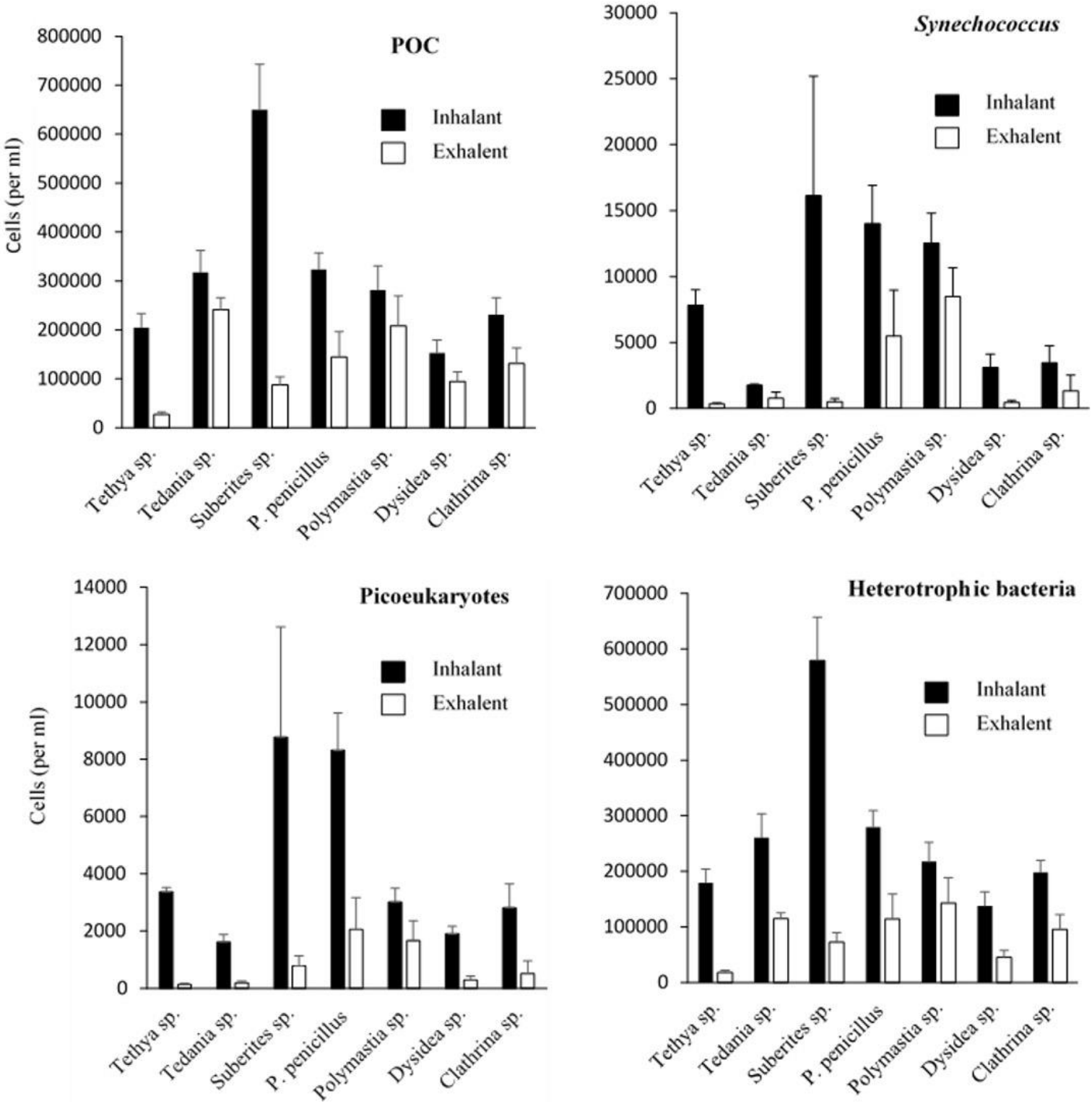

Fig. 4.3 Cell counts (*per* ml) of ambient and exhalent water from 5 replicates of 7 study species. Counts are *per* oscula and do not consider number of oscula *per* specimen or pumping rate. Error bars are mean +SE.

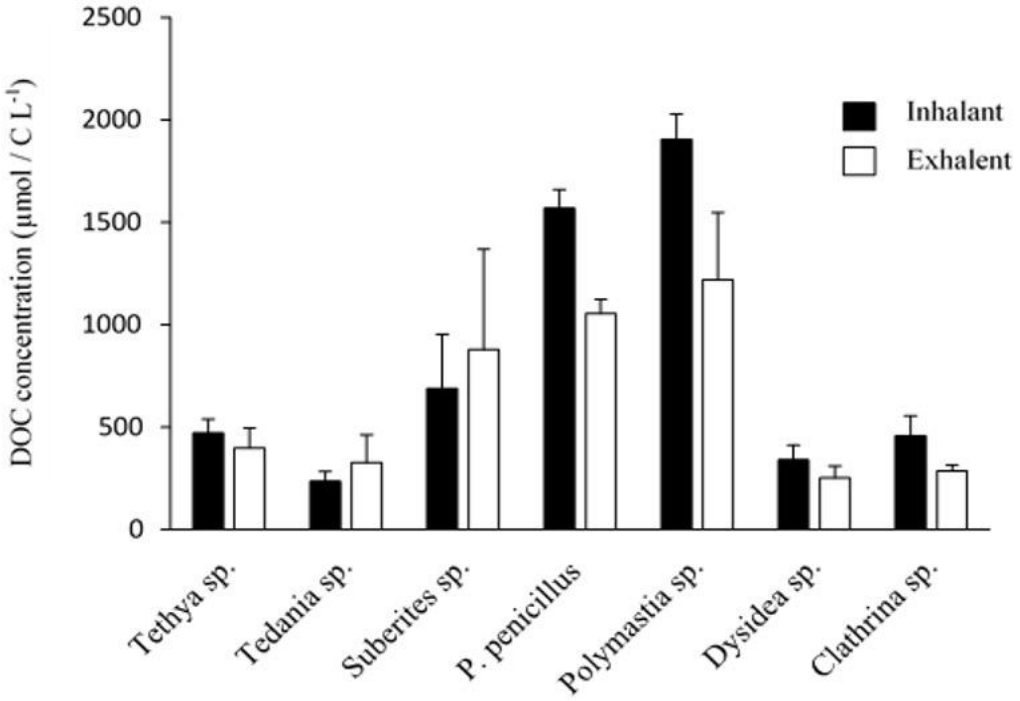

Fig. 4.4 DOC concentrations in ambient and exhalent water from five replicates of 7 study species. Error bars are mean +SE.

4.3.2 Food selection

PERMANOVA tests showed a significant effect of food-group on Chesson's index scores when all species were considered ($F_{3,92} = 3.221$, $p < 0.01$), implying food selectivity within the sponges (Fig. 4.6). All sponge species exhibited selective feeding except for *Tedania* sp. and *Polymastia* sp., as determined by significant differences between Chesson index scores between food groups (Table 4.2 & Fig. 4.6). *Tethya* sp., *Dysidea* sp. and *Clathrina* sp. showed no preference between picoeukaryotes and *Synechococcus* sp., but exhibited preference for these food groups over heterotrophic bacteria (Table 4.3). *Suberites* sp. showed a distinct preference for *Synechococcus* sp. over all other food groups (Table 4.3). *Polymastia penicillus* showed preference for picoeukaryotes over DOC but did not show any distinct preference for the other food groups.

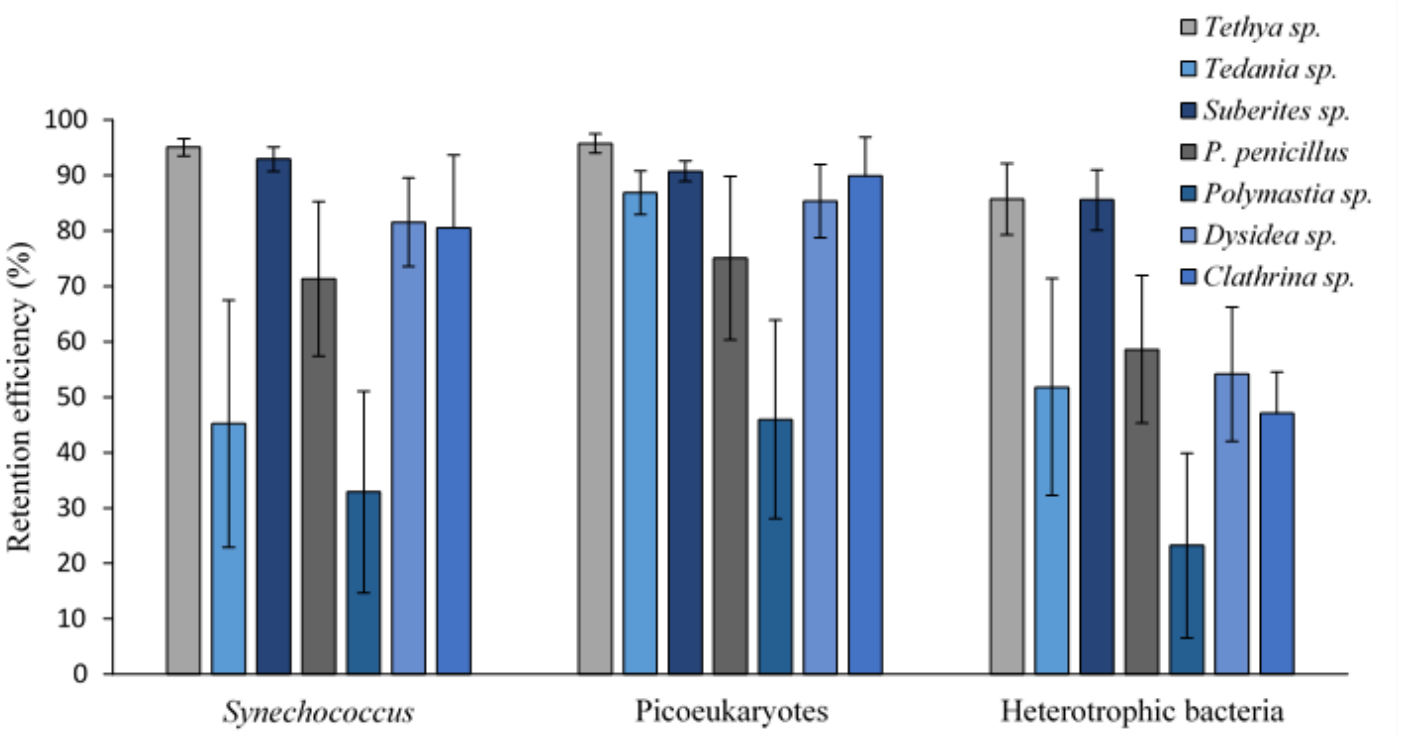

Fig. 4.5 Retention efficiency (expressed as %) of three POC food groups removed by 5 replicates of 7 sponge species (error bars are +/- SE).

Table 4.2 PERMANOVA results for Manly-Chesson's alpha index (α) scores for 7 species whereby significant results indicate food selectivity within 3 POC groups (top) and within 3 POC groups and DOC (bottom).

Species	F-statistic	df	p-value
***Tethya* sp.**	3.167	2,12	0.0146*
***Tedania* sp.**	0.583	2,12	0.46
***Suberites* sp.**	3.142	2,12	0.036*
***Dysidea* sp.**	2.229	2,12	0.012*
***Clathrina* sp.**	12.705	2,12	0.003*
	POC groups and DOC		
Polymastia Penicillus	3.781	3,16	> 0.030*
***Polymastia* sp.**	1.362	3,16	0.263

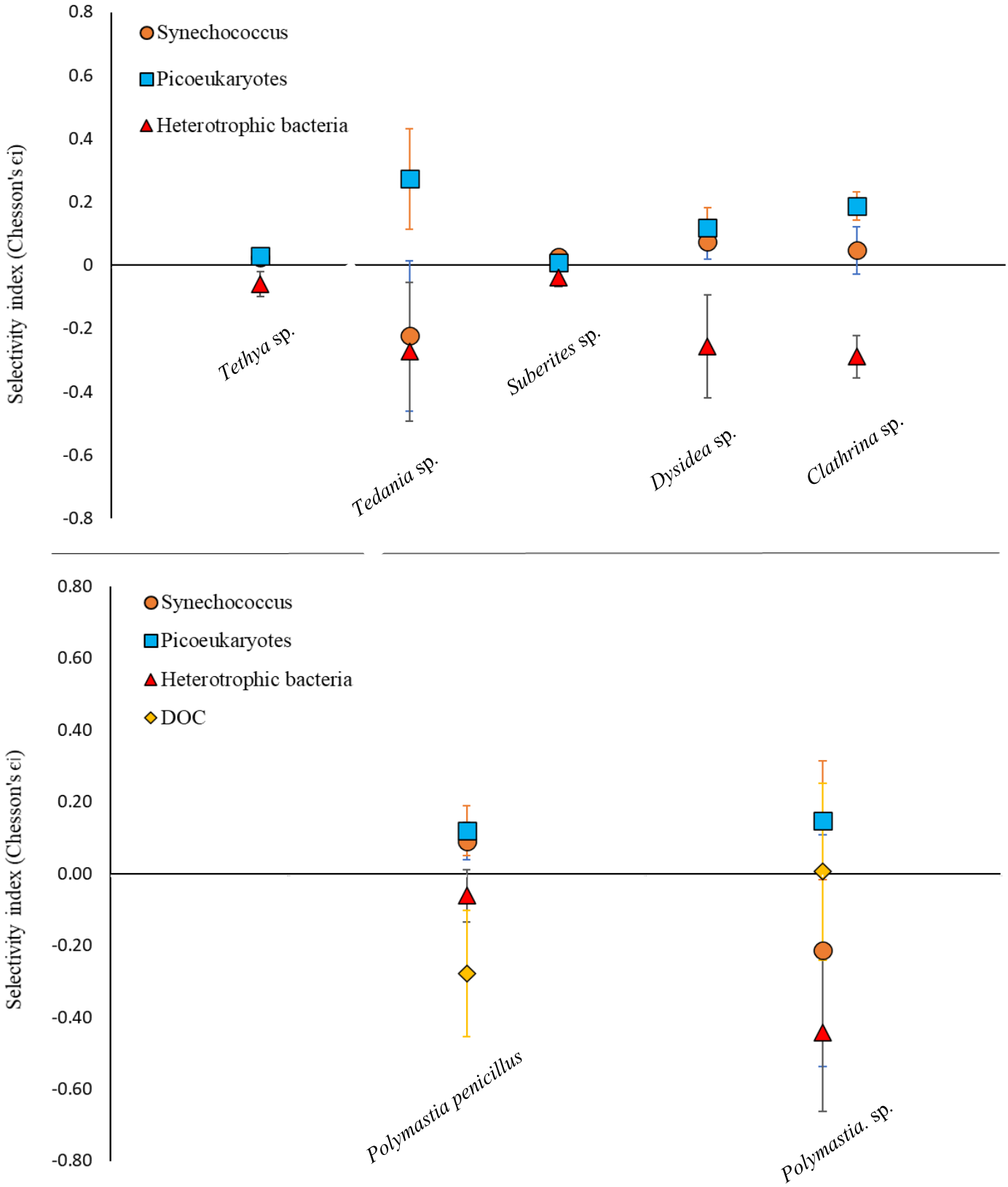

Fig. 4.6 Mean filtration selectivity (± SE) by seven common sponge species of *Synechococcus* sp., picoeukaryotes, heterotrophic bacteria and DOC as estimated by the electivity index (ϵ_i), where 0 represents no preference, +1 represents high positive preference and -1 high negative preference for the different food types (Chesson, 1983).

Table 4.3 PERMANOVA pairwise tests of Manly-Chesson's alpha index (α) scores of 3 POC food groups by 5 sponge species and 3 POC groups with DOC for 2 sponge species. DOC-POC T-values were not calculated for species not exhibiting significant DOC retention.

Species	**Syne – Pico**		**Syne – Het**		**Pico - Het**		**Syne -DOC**		**Pico – DOC**		**Het - DOC**	
	T-value	**p-value**	**T-value**	**p-value**	**T-value**	**p-value**	**T-value**	**p-value**	**T-value**	**p-value**	**T-value**	**p-value**
Tethya sp.	0.200	0.829	1.929	0.009*	1.899	0.036*						
Tedania sp.	1.047	0.273	0.005	0.856	1.086	0.113						
Suberites sp.	0.888	0.394	2.178	0.015*	1.585	0.117						
Dysidea sp.	0.514	0.631	1.461	0.039*	1.567	0.041*						
Clathrina sp.	1.561	0.131	3.075	0.033*	4.983	0.007*						
P. penicillius	0.319	0.7	1.634	0.131	1.725	0.133	2.267	0.051	2.325	0.047*	1.446	0.178
Polymastia sp.	1.558	0.328	0.741	0.550	1.201	0.146	1.482	0.292	0.608	0.636	0.959	0.473

4.3.4 Resource partitioning

PERMANOVA tests showed a significant effect of species on Chesson's index scores, indicating inter-specific resource partitioning within the sponges (Psuedo-$F_{6,108}$ = 2.357, p < 0.01). However, *post hoc* pairwise tests revealed that this was largely explained by the feeding behaviour of *Polymastia penicillus* (which exhibited significant DOC retention), while the remaining species showed no significant pairwise differences in Chesson's index scores (Table C4.2). To test if this was a result of DOC consumption specifically, DOC was removed from the Chesson's index formulae for the two *Polymastia* species. In this case, a significant effect of species was also seen on Chesson's index score (Psuedo-$F_{6,98}$ = 2.335, p = 0.012), but *post hoc* testing showed this to be entirely explained by *Polymastia* sp. which showed a significant difference in Chesson scores compared to all other species (Table C4.3) due the lack of retention of any POC groups (Table 4.1). Both *Polymastia* species feeding on

DOC where therefore excluded from the PERMANOVA test. In this subsequent analysis, there was no effect of species on Chesson's index score and no differences between any paired species were apparent (Table C4.4) ($F_{4,70} = 1.783$, $p < 0.111$).

4.3.5 Retention efficiency

PERMANOVA tests showed that food-group had a significant effect on food retention efficiency when all species were considered, both for when DOC was included ($F_{3,112} = 12.474$, $p < 0.001$) and excluded ($F_{2,84} = 3.513$, $p < 0.02$) from the food-group factor (Table 4.5). Pairwise tests for all sponge species combined showed significantly greater retention efficiency of picoeukaryotes than all other food groups (Table 4.5). Both *Synechococcus* sp. and heterotrophic bacteria were retained with similar efficiency, and with significantly higher efficiency than DOC (Table 4.5). This is unsurprising, as only *Polymastia penicillus* and *Polymastia* sp. showed significant DOC retention (Fig. 4.3) and, even then, at relatively low efficiency (33.89 % ± 4.8 and 33. 70 % ± 15.9 respectively) when compared to POC retention by other POC feeding species (Fig. 4.5 and Fig. 4.7). *Tethya* sp. and *Suberites* sp. retained POC with significantly greater efficiency (83.6 % ± 6.1 SE and 84.2 % ± 5.5 SE, respectively) than all other species (Fig. 4.5 & Table C4.1 for *post hoc* species comparisons). This can be explained by *Tethya* sp. and *Suberites* sp. having a significantly higher retention efficiency of heterotrophic bacteria (85.7 % ± 6.4 SE and 85.6 % ± 5.4 SE, respectively) than all other species that consumed this same food group (Fig. 4.5 & Table C4.1). Despite this, only *Clathrina* sp. and *Dysidea* sp. exhibited significantly lower retention efficiency of heterotrophic bacteria than picoeukaryotes ($t = 3.618$, $p = 0.012$ and $t = 1.454$, $p = 0.03$ respectively). All other sponge species showed no significant difference in retention efficiency between the various POC groups (Table 4.6). Retention efficiency of *Synechococcus* sp. exceeded 95% for specific individuals of all sponge species, though with extremely high variability within certain species (e.g. *Polymastia* sp. 0 – 99 %). The retention

efficiency of picoeukaryotes was consistently high (75 – 96%) with the only significant pairwise difference found for *Tethya* sp. and *Polymastia* sp. (Table C4.1). This was expected, as *Polymastia* sp. was the only species that did not exhibit any significant uptake of picoeukaryotes, while *Tethya* sp. exhibited a consistently high retention efficiency of picoeukaryotes across replicates (89 – 99 %).

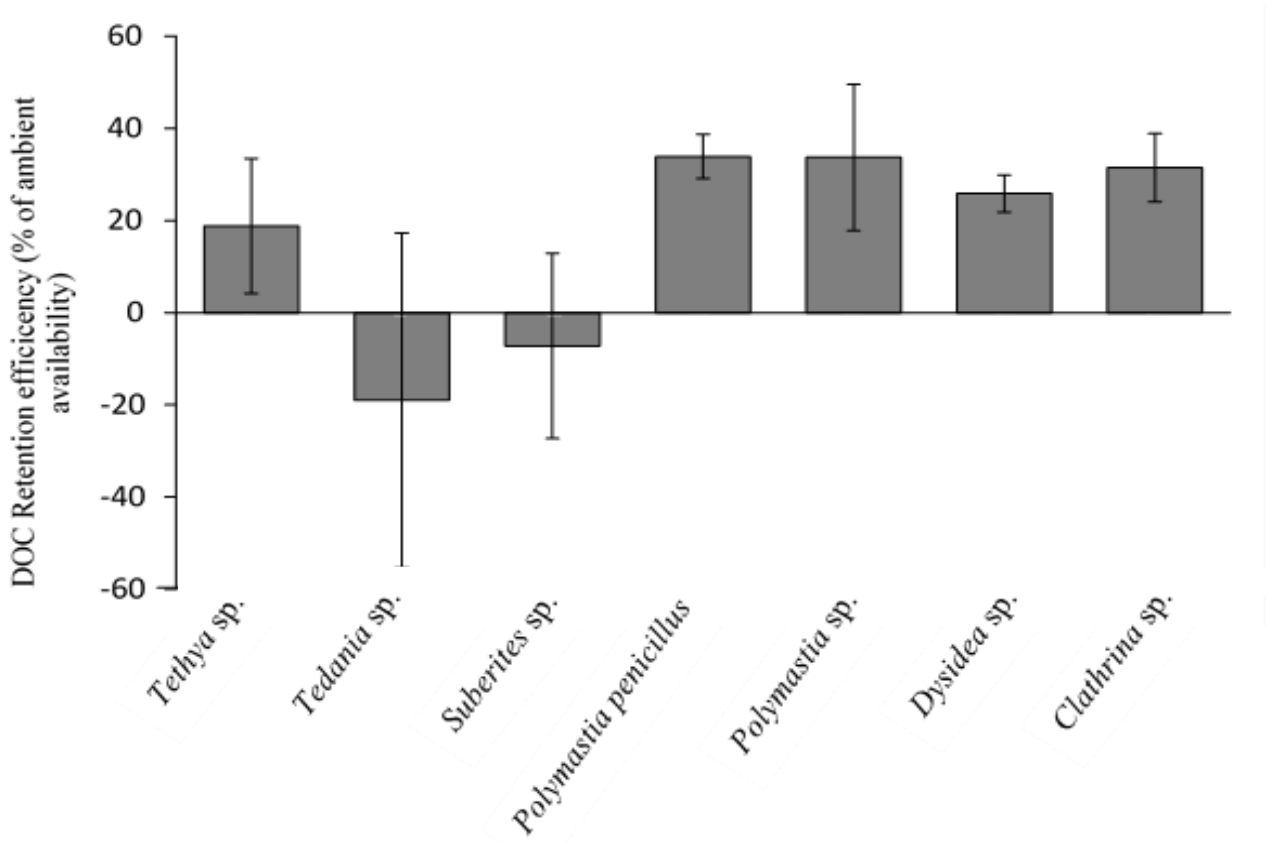

Fig. 4.7 Retention efficiency (expressed as %) of DOC removed by five replicates of seven sponge species (error bars are +/- SE)

Table 4.4 Variation in food retention efficiency according to species and food groups and a two-way interaction between food group and species from PERMANOVA tests. POC groups only (left). POC groups and DOC included (right).

Source of variation	**POC**			**POC with DOC**		
	df	**F-value**	**p-value**	**df**	**F-value**	**p-value**
Species	6,84	5.800	< 0.002*	6,112	4.448	< 0.0001*
Food group	2, 84	3.513	< 0.02*	3, 112	12.474	< 0.0001*
Species*Food group	12, 84	0.870	0.227	18, 112	1.743	< 0.022*

Table 4.5 Pairwise differences in retention efficiency of four food groups across seven sponge species.

Pairwise food group	**t-value**	**p-value**
Synechococcus sp. - Picoeukaryotes	1.994	0.037*
Synechococcus sp. - Heterotrophic bacteria	1.057	0.302
Synechococcus sp. – DOC	3.817	< 0.0001*
Picoeukaryotes - Heterotrophic bacteria	2.726	< 0.001*
Picoeukaryotes – DOC	6.479	< 0.0001*
Heterotrophic bacteria - DOC	3.216	< 0.001*

Table 4.6 Pairwise differences in retention efficiency of three POC food groups for seven individual sponge species

Species	**Syne – Pico**		**Syne – Het**		**Pico - Het**	
	t-value	**p-value**	**t-value**	**p-value**	**t-value**	**p-value**
Tethya sp.	0.275	0.838	1.357	0.124	1.430	0.123
Tedania sp.	1.755	0.164	0.511	0.828	1.359	0.122
Suberites sp.	0.750	0.48	1.210	0.254	0.908	0.565
Polymastia. p.	0.115	0.793	0.544	0.537	0.633	0.502
Polymastia sp.	1.211	0.36	0.452	0.745	1.343	0.173
Dysidea sp.	0.375	0.624	1.318	0.086	1.454	0.029*
Clathrina sp.	0.717	0.565	1.782	0.113	3.168	0.012*

4.3.6 Food availability / selectivity and retention efficiency

Heterotrophic bacteria were consistently the most abundant POC food group available for all sponges examined (> 200,000 cells/ml) followed by *Synechococcus* sp. (1000 – 25,000 cells/ml) and picoeukaryotes (1000 – 12,000 cells/ml). Ambient DOC concentrations at PMR were significantly higher than on the WSC, which corresponded with a significantly greater retention efficiency of DOC by sponges at PMR (*Polymastia penicillus* and *Polymastia* sp.) compared to species on the WSC, which did not show significant DOC retention. However, DOC availability was positively correlated with DOC retention when assessed across all sponge species ($R^2 = 0.47$, $F_{1,33} = 29.09$, $p = < 0.001$) but not with DOC retention efficiency ($R^2 < 0.05$, $F_{1,33} = 1.90$, $p = 0.178$) (Fig. 4.8 & Table C4.6). When considered independently from the other species, the two DOC-feeding *Polymastia* species did not show any significant relationship between DOC availability and retention efficiency ($R^2 < 0.005$, $F_{1,8} < 0.004$, $p = 0.995$). However, DOC availability was significantly positively correlated with DOC

selectivity overall ($R^2 = 0.21$, $F_{1,33} = 8.64$, $p = < 0.01$) (Fig. 4.9 & Table C4.7). The ambient availability of all individual POC groups was also positively correlated with POC retention when considered across all sponge species (picoeukaryotes - $R^2 = 0.60$, $F_{1,33} = 50.2$, $p < 0.001$); (*Synechococcus* sp. - $R^2 = 0.46$, $F_{1,33} = 27.92$, $p < 0.001$); (heterotrophic bacteria - $R^2 = <0.49$, $F_{1,33} = 31.88$, $p < 0.001$). Ambient availability of heterotrophic bacteria also showed a significant positive correlation with retention efficiency ($R^2 = 0.20$, $F_{1,33} = 8.1$, $p < 0.01$) (Fig. 4.8 & Table C4.6). However, no relationship between the ambient availability and selectivity of heterotrophic bacteria ($R^2 = 0.04$, $F_{1,33} = 1.38$, $p < 0.25$) was observed (Fig. 4.9 & Table C4.7). This was also the case for picoeukaryotes ($R^2 = 0.07$, $F_{1,33} = 0.22$, $p < 0.64$), while a weak negative correlation between the ambient availability and selectivity of *Synechococcus* sp. was seen ($R^2 = 0.16$, $F_{1,33} = 6.263$, $p < 0.01$). However, removing outliers showing zero retention of *Synechococcus* sp. (produced by the lack of POC uptake by *Polymastia* sp.) removed this effect ($R^2 = 0.01$, $F_{1,33} = 0.33$, $p < 0.57$) (Fig. 4.9 & Table C4.7). (See Tables A2.8 – A2.14 for breakdown by species).

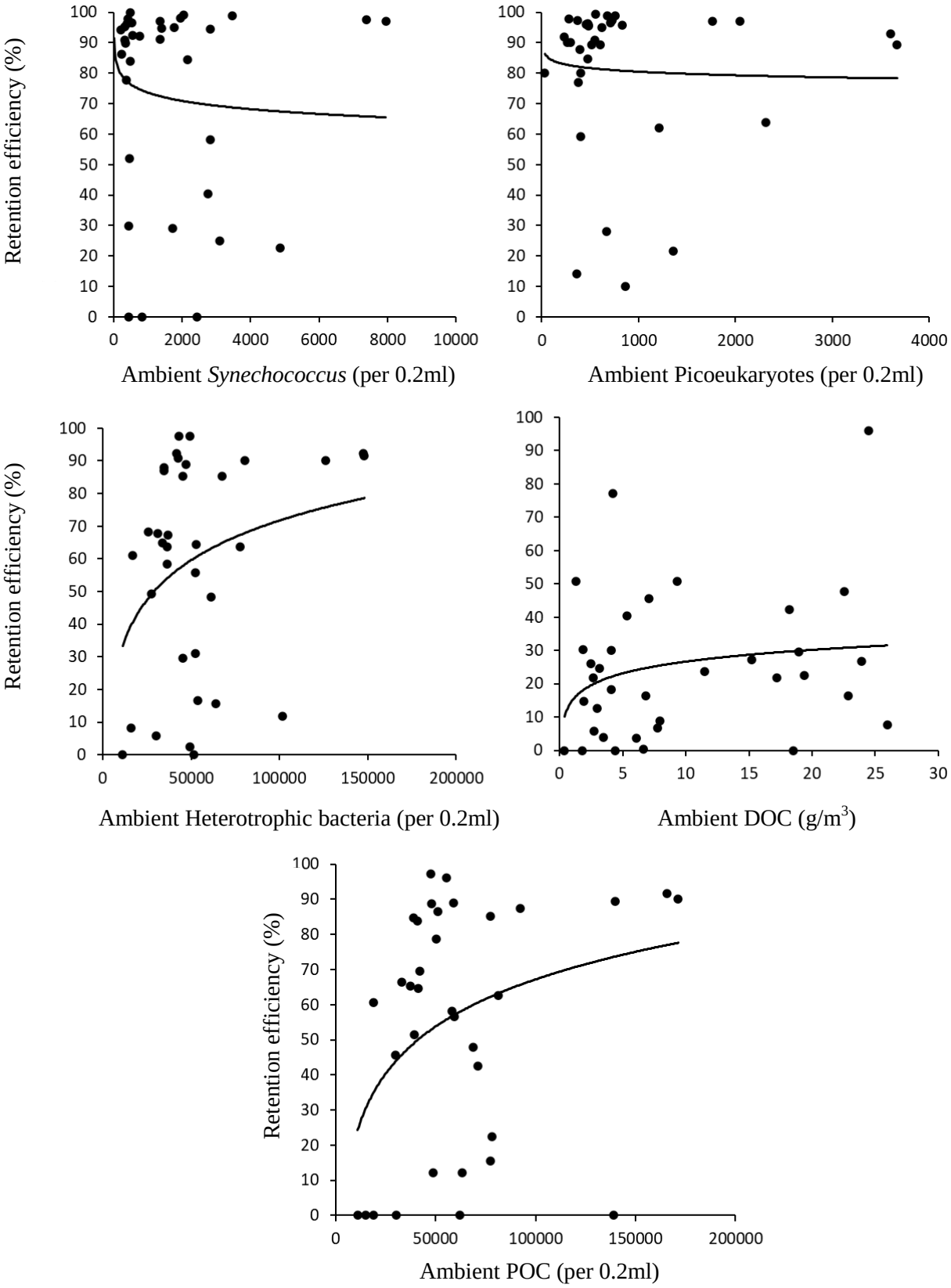

Fig. 4.8 Logarithmic relationship between sponge-food retention efficiency and ambient food availability of 3 POC groups (*Synechococcus* sp., picoeukaryotes, and heterotrophic bacteria).

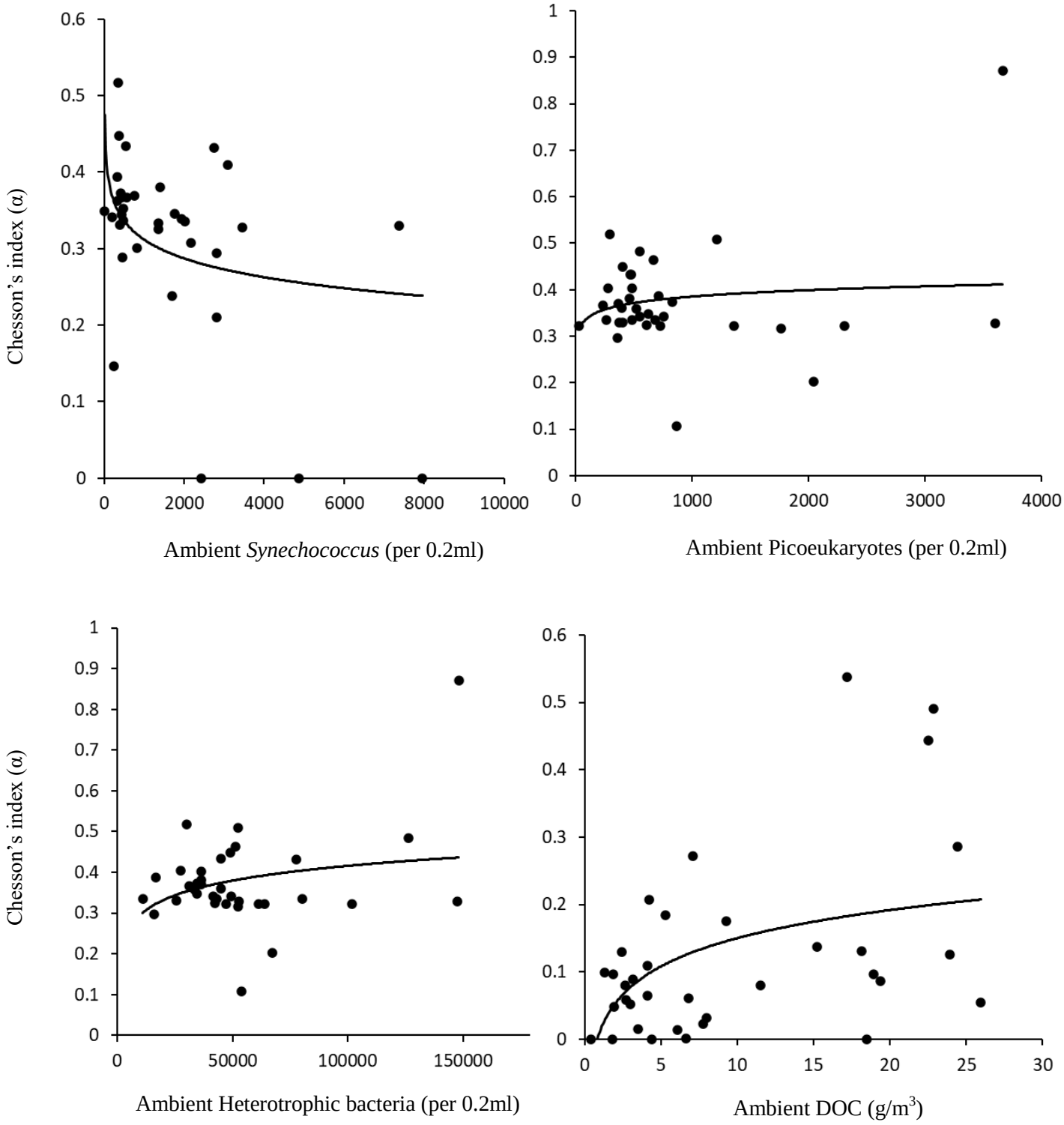

Fig. 4.9 Logarithmic relationship between sponge-food selectivity (α) and ambient food availability of 3 POC groups (*Synechococcus* sp., picoeukaryotes and heterotrophic bacteria) and DOC across seven sponge species. See Table C4.7 for regression coefficients for fitted lines and *per*-species relationships.

4.4 Discussion

Despite the importance of sponge-water column interactions significant gaps remain in our understanding of the trophodynamics of temperate sponges. This includes their potential dietary range and feeding preferences. Importantly, this is the first study outside of the Mediterranean to consider both POC and DOC as potential components of temperate sponge diets, despite the ubiquity of DOC, and evidence of significant DOC retention from tropical and deep-sea environments. My results show that selectivity of POC as well as between POC and DOC-based resources is common, but the consumption of DOC by some species is what generates inter-specific differences in food selectivity and therefore resource-partitioning. Resource-partitioning within the POC pool was not found, suggesting the consumption of DOC specifically to be an important mechanism facilitating abundant multi-species sponge assemblages on temperate reefs. The correlation between DOC availability and DOC consumption and selectivity might indicate trophic plasticity in certain sponge species, allowing them to actively switch between food types based on relative food availability Trophic plasticity and generalist feeding strategies might help explain the high abundance of specific sponge species relative to other benthic invertebrate groups in resource-poor environments. However, the observation of high retention efficiency of POC suggests that, even in resource-rich environments, some sponge species might be food-limited depending on their specific food preferences.

4.4.1 Ambient food availability and particle classifications

The consistently higher abundance of ambient heterotrophic bacteria relative to other food groups is consistent with other sponge feeding studies from a variety of environments (e.g. McMurray, 2016; Yahel, 2006; Hanson et al. 2009), but this has been demonstrated to be highly seasonal in some cases. For example, Topçu et al. (2010) found extremely low

heterotrophic bacterial populations abundances in the Mediterranean, while in summer these bacteria were the most abundant food group. This is in contrast with the findings of the present study, where heterotrophic bacteria numerically dominated the ambient microbial communities in both summer (PMR) and winter (WSC) samples. This provides a specific example of a wider potential issue of including Mediterranean habitats under the category of 'temperate' marine environments generally, as is common in earlier studies (e.g. Ribes et al. 1999) as there are likely to be important environmental differences.

The higher concentrations of ambient *Synechococcus* sp. than picoeukaryotes in this study appear to contradict the limited observations from similar locations. Perea-Blázquez et al. (2012; 2013) found consistently higher abundances of *Prochlorococcus* than *Synechococcus* sp. on the WSC over multiple years. However, this is more likely due to misidentification and methodological differences rather than true ecological differences. The application of SYBR Green I is more effective than the nucleic acid dyes used by Perea-Blázquez et al. (2012) in capturing a wider range of nucleic acid-positive events (Marie et al. 1997). The broader capture of events might not necessarily occur proportionally across distinct populations which would partly explain this discrepancy. The suggestion of misidentification refers to the classification of specific populations on flow cytometry plots as *Prochlorococcus*, which are more likely to be picoeukaryotes. *Prochlorococcus* is highly unlikely to be detected by flow cytometry in the abundances reported in cold/temperate environments by Perea-Blázquez et al. (2012), especially at shallow depths where cell size and chlorophyll content are significantly lower than for deeper populations (Partensky et al. 1999). *Synechococcus* sp., however, is known to be highly abundant in temperate regions (Flombaum et al. 2013). "Picoeukaryotes" is a taxonomically and morphologically much broader category than *Prochlorococcus* and *Synechococcus* sp. and is supported by the flow cytometry data showing picoeukaryotes to exhibit significantly greater cell complexity, size, and nucleic acid

content than *Synechococcus* sp. as expected (Figs. B3.5 & B3.6), and therefore represent a diverse food group for sponges.

Some DOC concentrations reported in the present study were considerably higher (< 1_{10}) than reported in other sponge-related studies (e.g. Yahel et al. 2003; de Goeij, 2008; 2013; Mueller et al. 2014). This is not surprising, as most of these earlier reports are from tropical oligotrophic habitats with much lower TOC availability generally. The upper ranges (< 700 µmol C L^{-1}) reported in a review of 3510 estimates of DOC concentrations in coastal waters worldwide (Barrón & Duarte, 2015) correspond more closely to the present study. The particularly high DOC concentrations recorded in Taranaki have two clear ecological explanations: 1) PMR likely receives significant allochthonous DOC input via the Tongapurutu River, which runs through farmland and densely vegetated areas before terminating immediately adjacent to the reef. Two smaller streams also terminate at the reef directly. 2) The reef exhibits particularly high abundance of macroalgae (specifically turfing red algae rather than larger canopy forming species) relative to other New Zealand infralittoral zones (Chapter 2), where particularly high autochthonous DOC production in the benthic layer would also be expected (Khailov & Burlakova, 1969). Significantly higher DOC concentrations occur within temperate benthic boundary layers with vegetated communities generally, where net DOC production is exported from the benthos to the water column (Egea et al. 2019). This also explains the higher than average DOC values (see Barrón & Duarte, 2015) recorded in this study at other sites, as all samples were taken from inside the benthic boundary layer within abundant macroalgal communities.

4.4.2 Sponge diet preference

My results showed significant retention of multiple food groups by multiple sponge species. This generalist feeding strategy likely facilitates continued sponge feeding and community

dominance throughout fluctuating levels in the relative availability of different food groups, both spatially and seasonally (e.g. Ribes et al. 1999; Topçu et al. 2010). However, sponges demonstrated food-group preferences despite the breadth of diet. All WSC species appeared to preferentially feed on picoeukaryotes and *Synechococcus* sp. over the numerically dominant heterotrophic bacteria, and in doing so, exhibited selection of significantly rarer food types. It is possible that this interpretation is misleading given the relatively large standard error exhibited for multiple species in Figure 4.6, where visualization of 95% confidence intervals would show overlap across the 0 (no selectivity) line. However, I would suggest that this is a symptom of low replication rather an error in ecological interpretation where increased replication would generate smaller standard error bars moving away from 0. Food selectivity been demonstrated in sponges in different environments (e.g. Yahel et al. 2007; Topçu et al. 2010; Mcmurray et al. (2016).Considering this, in combination with the observation of significant differences in the selectivity scores for different food groups for multiple species (Tables 4.2 & 4.3) the remainder of this discussion has been formulated under the interpretation that food selectivity is occurring. *Tedania* sp. was an exception and only showed significant retention of picoeukaryotes, as was *Polymastia* sp., which only showed significant retention of DOC (Tables 4.1 & 4.3). However, this might be explained by the combination of particularly high availability of these food groups in the surrounding seawater, suggesting passive rather than pro-active food acquisition, and high variability in retention among replicates.

The potential food selection capacity exhibited by the remaining species is consistent with observations of sponge feeding behaviour in tropical (Mcmurray et al. 2016), deep-sea (Yahel et al. 2007), Mediterranean (Topçu et al. 2010), and temperate (Perea-blazquez et al. (2012) habitats, despite early suggestions that marine sponge feeding is a non-selective process determined by the relative ambient availability of food groups (Pile et al. 1996). More

specifically, the consistent preference for picoeukaryotes and *Synechococcus* sp. over heterotrophic bacteria also reflects findings from other studies in a wide range of habitats. For example, *Callyspongia* sp. from south-western Australia showed positive selection for *Synechococcus* sp. over LDNA heterotrophic bacteria (Hanson et al. 2009). Similarly, *Xestospongia muta* from Conch Reef in Florida (McMurray et al. 2016) and *Spongia offcinalis* from the French Mediterranean (Topçu et al. 2010) both showed positive selection of *Synechococcus* sp. and picoeukaryotes and selected against heterotrophic bacteria. Given these preferences, the extent to which sponges are capable of switching feeding strategies to adapt to changes in the relative availability of these food groups is, according to foraging theory (Stephens & Krebs, 1986), likely to play a significant role in the ability of sponges to persist at consistently high abundances (see responses by *Xestospongia muta* in McMurray et al. (2016)).

4.4.3 Mechanisms and drivers of food selection

The interspecific consistency in food preference of the sponges observed in this study, as well as across multiple other studies (e.g. Topçu et al. 2010; McMurray et al. 2016) is surprising considering the broad taxonomic range of the sponges and food groups assessed, as well as the broad range of associated environmental conditions and habitats. Numerous other studies have observed interspecific variation in sponge feeding behaviour and have attributed this to differences in multiple physical characteristics (Maldonado et al. 2012), including external morphological traits, aquiferous system complexity (Turon et al. 1997), and choanocyte density (Weisz et al. 2008). However, there is a wide range in these same traits across the species (and classes) assessed in this study, yet no interspecific differences were observed in food preference outside of the POC pool (see below). This suggests that active, food-dependent feeding behaviour rather than passive, mechanistic sponge traits are generating these patterns. This is supported by observations of particle size-independent feeding

behaviour of two temperate hexactinellid sponges (*Rhabdocalyptus dawsoni* and *Aphrocallistes vastus*) by Yahel et al. (2006) who suggested selective filtration involves individual processing, recognition, sorting, and transport of food particles through the syncytial tissue. The positive selection of *Synechococcus* sp. and the negative selection of heterotrophic bacteria, which have similar particle size ranges (Figs. B3.5 & B3.6) observed in this, and numerous other studies, further support this suggestion. However, the discrimination of cells based on cell traits beyond size requires mechanisms that are not well understood. The distinguishing features of picoeukaryotes from other food groups might be more obvious with relatively high morphological and cell surface complexity, but the discrimination between heterotrophic bacteria and *Synechococcus* sp. and *Prochlorococcus* (in tropical sponges as well as between HDNA and LDNA cells within heterotrophic bacteria populations themselves suggests more complex selection mechanisms most likely based on cell surface chemistry. An early study by Wilkinson et al. (1984) suggested biochemical, as opposed to mechanical cues, or fixed mechanical-based filtration processes were responsible for the differentiation of bacterial prey and bacterial symbionts with similar gross morphological traits by four sponges in tropical Australia. A more recent study by Degnan (2015) identified specific genes belonging to a family of receptors capable of recognizing and discriminating between specific microbial ligands which might also be playing a role in this behaviour.

4.4.4 Resource partitioning

In this study, any difference (or lack thereof) in food group preference is considered to be an indication of resource partitioning as opposed to differences in food retention efficiency. Food preference within the POC pool was consistent across all species occurring on the WSC and therefore no resource partitioning was observed. This is despite a relatively wide range of gross morphologies and microhabitat preferences, and even crossing taxonomic classes

(Demospongiae and Calcarea). This is contrary to other observations of resource partitioning within the total POC pool by temperate sponge assemblages in New Zealand (Perea-Blázquez et al. 2012). However, these conclusions were based on differences in the retention efficiency of specific food groups across species, which assumes that the y-intercept (α) between food retention efficiency and availability is zero (McMurray et al. 2016) or that food availability remains constant between replicates and species, which is extremely unlikely in natural temperate environments. Significant variability in the ambient food availability between samples, as well as a positive correlation between the availability and retention efficiency of heterotrophic bacteria, was found making the approach used by Perea-Blázquez et al. (2012) potentially misleading. When this issue was not accounted for, the current study found significant interspecific differences between the retention efficiency of specific food groups. This would suggest resource partitioning within the POC pool where it did not exist.

4.4.5 DOC retention, resource partitioning and ecological implications

PMR exhibited significantly higher DOC concentrations than on the WSC and harboured the only sponge species to exhibit significant DOC retention (*Polymastia* sp. and *Polymastia penicillus*). Including these DOC-consuming species in tests for inter-specific differences in food preference revealed resource partitioning. These results imply that inter-specific differences in food selectivity (resource partitioning) are being entirely generated by the consumption of DOC by *Polymastia penicillus* and *Polymastia* sp., and that the remaining species feeding exclusively on POC are exhibiting significant niche overlap and no resource partitioning within the POC pool. However, the specific dynamics of this observation depend on which of the following provide the most accurate explanation: 1) Sponges at PMR are exhibiting trophic plasticity, and consistent with foraging theory, are responding to the higher availability of DOC through an active behavioural change to consume DOC at higher retention efficiency; or 2) The observation is coincidental, as *Polymastia* sp. and *Polymastia*

penicillus exhibit DOC retention generally and would show similar feeding behaviour on the WSC with lower ambient DOC concentrations. The second explanation suggests that providing specific DOC-consuming species are present in sponge assemblages, then resource partitioning is still possible. However, the significant positive correlation between ambient DOC concentration and sponge-DOC retention and selectivity (Fig. 4.9 & Table C4.7) suggests that the first explanation is most likely, where ambient DOC on the WSC had not yet reached sufficient concentrations to generate a shift in behaviour towards DOC retention in the other sponges assessed. Low availability of POC might also generate this switch, but POC concentrations at PMR were not significantly different to those at WSC and therefore were considered unlikely to be a predominant driver in this case.

If the ability to initiate DOC feeding as an active response to food availability is widespread, this would suggest resilience of temperate sponges to changing conditions of carbon availability, both spatially and temporally. While considerable variability of food availability was found within this study, assessments of sponge feeding behaviour along distinct food availability gradients *in situ*, or in response to artificial manipulations of relative DOC/POC concentrations *in vitro*, would provide further confirmation of these results and more specific insights into temperate sponge feeding behaviour, trophic plasticity, and subsequent benthic community population dynamics. Assessing feeding behaviour at seasonal and yearly timescales, where distinct patterns in both food availability and sponge metabolism has been undertaken in numerous studies (e.g. Ribes et al. 1999; Topçu et al. 2010; Perea-Blázquez et al. 2011; Koopmans et al. 2015). Appling this seasonal approach to temperate assemblages with the consideration of DOC feeding would also contribute significantly to our holistic understanding of this matter.

Chapter 5

The contribution of sponge assemblages to pelagic-benthic transfer of carbon in the infralittoral and mesophotic zone

Abstract

The quantification of carbon sequestered by sponge assemblages is of considerable importance to our understanding of the ecological dynamics of benthic habitats. In this chapter I determined the pumping volumes of five particularly common sponge species occurring on the Wellington South Coast *in situ* using SCUBA. I assessed potential correlations between multiple sponge biometrics (mass / number of oscula / size of oscula / total oscula area / pumping velocity) and pumping volume, to determine the most accurate and efficient way to standardize and extrapolate pumping volumes to entire sponge assemblages. I found total oscula area (OSA) to be the best predictor of sponge pumping volume, and that the ratio of total oscula area to sponge size (~ 6%) increased allometrically with sponge size, without any inter-specific variation. I used a range of potential OSA-specific pumping volume estimates in combination with a range of POC retention efficiency estimates of different microbial groups determined in Chapter 4 to generate a potential range of total carbon mass transferred to the benthos by sponges. I then extrapolated this information to assemblage scales at the Poor Knights Marine Reserve and in Doubtful Sound Fiordland using sponge abundance and distribution information from the infralittoral and mesophotic zones of these regions reported in Chapter 2. This study confirms the efficacy of applying OSA-specific pumping volumes to population scales, and demonstrates the significant contribution that sponges make to the transfer of carbon (> 100% of available carbon in the benthic boundary layer *per* hour) to the benthos through the infralittoral and mesophotic zones of New Zealand reefs. This large proportion of available carbon transferred from the water column to the benthos by heterotrophic sponges is likely to have numerous ecological implications. This includes the alteration of water column chemistry and regulating the availability of marine microbial communities which are fundamental to other

important ecological processes, such as primary production, and the microbial loop. Furthermore, the extent of this carbon transfer enables the production of sponge assemblage biomass itself, and therefore, is a fundamental component of all the other ecological functions that sponges perform.

5.1 Introduction

Coastal benthic communities perform important functional roles within marine food webs by regulating water column chemistry and recycling carbon *via* suspension feeding on plankton, detritus, and other organic matter (Gili & Coma, 1998). Suspension feeding activity connects pelagic and benthic environments by drawing carbon and other nutrients from the water column to the benthos, contributing to the production and maintenance of some of the most biodiverse ecosystems in the marine environment (Rossi et al. 2017). Of the numerous benthic suspension feeding groups (e.g. bryozoans, ascidians, cnidarians, polychaetes, bivalves), sponges are often one of the most abundant and extensively distributed globally (Van Soest et al. 2012; Bell et al. 2020). Furthermore, sponges pump particularly high volumes of water (> 35 ml min^{-1} cm^{-3} sponge (Weisz et al. 2008)), and can retain particulate organic carbon (POC) at very high retention efficiencies (up to 99%) (Pile et al. 1997; Coma et al. 2001; McMurray et al. 2018). This suggests that sponges are likely to be particularly important in connecting benthic and pelagic environments *via* their feeding activities compared to other benthic suspension feeders (Gili & Coma, 1998), which has been demonstrated in numerous previous studies (Maldonado et al. 2012; de Goeij et al. 2017; Folkers & Rombouts, 2020).

There is also increasing evidence of sponges consuming large quantities of dissolved organic carbon (DOC) in different environments (Yahel et al. 2003; Maldonado et al. 2012, 2016; Pawlik & McMurray, 2018; 2019) and it has been shown to be the primary source of carbon

for sponges in some cases (Mueller et al. 2014; Hoer et al. 2018). This has important ecological implications as DOC represents the largest and most ubiquitous source of organic carbon in the marine environment (Druffel et al. 1992; Hansell & Carlson, 2014), potentially allowing sponges to persist and proliferate in habitats with low POC resource availability or overcome inter and intra-specific competition in densely populated benthic communities (Perea-Blázquez et al. 2013b; Chapter 3). Furthermore, the interaction between DOC and sponges has been shown to involve the conversion of this abundant, but normally inaccessible resource, into sponge detritus and biomass which can be utilized by the wider ecological community in process termed the 'sponge loop' (de Goeij et al. 2013). However, while there is evidence for the consumption of DOC outside of tropical environments (i.e. Bart et al. 2020; Yahel et al. 2007), this is limited, and there is no evidence of sponge-DOC consumption in shallow temperate environments outside of the Mediterranean region (but see Chapter 4).

The quantity of carbon accumulated by heterotrophic sponges directly dictates the abundance of sponge assemblage biomass itself, and therefore determines the foundation on which all of the other ecological functions performed by sponges rely (see Bell et al. 2008), including: micro-habitat provisioning (Wulff, 2006; Taylor et al. 2007; Webster & Taylor, 2012); habitat complexity (see Chapter 2); competition pressure (Bell & Barnes, 2003; Wulff, 2006); the alteration of benthic boundary flow regimes (Culwick et al. 2020); the functioning of the sponge loop (de Goeij et al. 2013; Rix et al. 2016); and changes in carbon availability and composition in the water column (Perea-Blázquez et al. 2012; Valentine et al. 2019). Considering this, the quantification of sponge-carbon sequestration, and the ratio of carbon retention to carbon availability across regional assemblage scales is of considerable importance to the understanding of ecological dynamics of benthic habitats generally. However, few studies have quantified regional-scale sponge contributions to carbon transfer

(e.g. McMurray et al. 2017) and fewer still have considered temperate environments (see Perea-Blázquez et al. 2012). Furthermore, no studies have quantified the total transfer of carbon across sponge assemblages that span from the infralittoral to the mesophotic zone outside of the tropics. Omitting temperate mesophotic ecosystems (TMEs) when quantifying area-specific sponge contributions to carbon sequestration into the benthos is likely to underestimate these processes, as TME communities have been observed to be consistently dominated by sponges (Chapter 2; Bell et al. *in review*).

The quantification of sponge assemblage carbon sequestration at regional scales can be determined by combining multiple factors which have been systemically investigated throughout this thesis. These factors include sponge abundance patterns (Chapter 2), potential food availability (Chapter 3), and sponge diet and food retention efficiency (Chapter 4). However, the volume of water pumped by sponges during feeding activity is also required to quantify the transfer of carbon mediated by sponges (Morganti et al. 2019; 2021) as pumping volume directly dictates the potential quantity of carbon retained.

Determining the pumping volume and carbon removal rates exhibited by individual sponges is not necessarily problematic, as all necessary components are directly measurable and fixed. However, accurately extrapolating these values to assemblage scales can be more difficult, as this requires an appropriate standardized metric that can account for differences in sponge physiological and morphological variables. Studies extrapolating sponge pumping and feeding behaviour to assemblage or regional scales have traditionally standardized pumping rates to volume (e.g. Perea-Blázquez et al. 2012; McMurray et al. 2017). However, this approach assumes increases in pumping volume with mass and volume to scale allometrically, which is not necessarily the case. Morganti et al. (2019) demonstrated volume-specific pumping rate to decrease with sponge volume and with significant variability between specimens, implying that the application of volume-specific pumping

rates to assemblage-scale extrapolations is potentially erroneous. Furthermore, the application of volume-specific pumping rate to assemblage scales requires the conversion of sponge abundance data (most commonly as two-dimensional percentage cover data to sponge volume estimates, unless the assemblage volume was established directly using three-dimensional volume determination techniques (de Goeij et al. 2017). These have not been widely employed, likely due to technological limitations. The conversion from percentage cover data introduces the potential for further errors to be carried through and inflated in assemblage-scale extrapolations. Recently, the relationship between the osculum cross sectional area and sponge pumping volume has been shown in the laboratory (Strehlow et al. 2016; Kumala et al. 2017; Goldstein et al. 2019; Kealy et al. 2019) and *in situ* (Gökalp et al. 2020), which suggests that the total cross sectional area of the sponge oscula (OSA) (average oscula cross section multiplied by the number of oscula) may be a more efficient and accurate predictor of sponge pumping volume (Morganti. et al 2021). This metric is particularly useful when extrapolating to assemblage scales using percentage cover data, as it does not require any conversion factors. However, to apply this metric to assemblage-scale percentage cover data, first requires the allometric relationships (if any, but hypothesized by Goldstein et al. (2019)) between the OSA and the osculum flow rate to be established for each species (Morganti et al. 2021)

Reporting meaningful values of assemblage-scale contributions of sponges to pelagic-benthic carbon transfer requires the application of volume-specific values in distinct environmental regions, providing an ecologically relevant spatial reference. The intrinsic geography of fiord structures and offshore islands represents ideal ecologically and physically definable habitats to provide this reference. Therefore, the sponge assemblage and food availability data previously collected from the Poor Knights Islands and Doubtful Sound in the Fiordland

Marine Area provide ideal candidates for the assessments of assemblage-scale pelagic-benthic carbon transfer by sponges in temperate environments.

The aims of this chapter were to: 1) investigate the relationships between sponge morphological and physiological traits and sponge pumping volume, to establish a standardized metric for pumping volume; 2) extrapolate a standardized metric of sponge pumping volume determined in Aim 1 to assemblage-scale percentage cover data at Doubtful Sound and the Poor Knights Islands; 3) determine total sponge habitat availability and food availability at these same locations; and 4) estimate the total and proportional exchange of POC from the water column to the benthos by sponges through a combination of habitat availability data, sponge distribution data (Chapter 2), food availability and food retention efficiency information (Chapters 3 & 4), and assemblage pumping information calculated in Aim 2.

5.2 Methods

5.2.1 Study Sites

11 sites in Doubtful Sound in the Fiordland Marine Area, and two sites in the Poor Knights Marine Reserve were chosen for this study (Fig. 5.1). Fiordland sites were distributed along a gradient from the most inner areas of Doubtful Sound at Hall Arm, where a deep-water profile (>80 m) was still available, to the most outward reach of Thompson Sound, immediately adjacent to the open ocean, exhibiting a depth profile of > 300 m. These sites cover an environmental gradient with minimal mixing of the water column, low light availability, and high surface tannin concentrations (inner fiord region), to well mixed, deep light penetration, and reduced surface tannin concentration (outer fiord region) due to closer proximity to the open ocean and likely increased flushing. The Poor Knights exhibit a depth profile of > 80 m and are characterized by high light penetration (up to 3x local coastal

regions (Ayling, 1986)), and a particularly abundant and diverse benthic community (Chapter 2). Both locations exhibit almost vertical rocky reef walls down to flat, sedimented, or sandy substrates (Ayling, 1986; Howe et al. 2010).

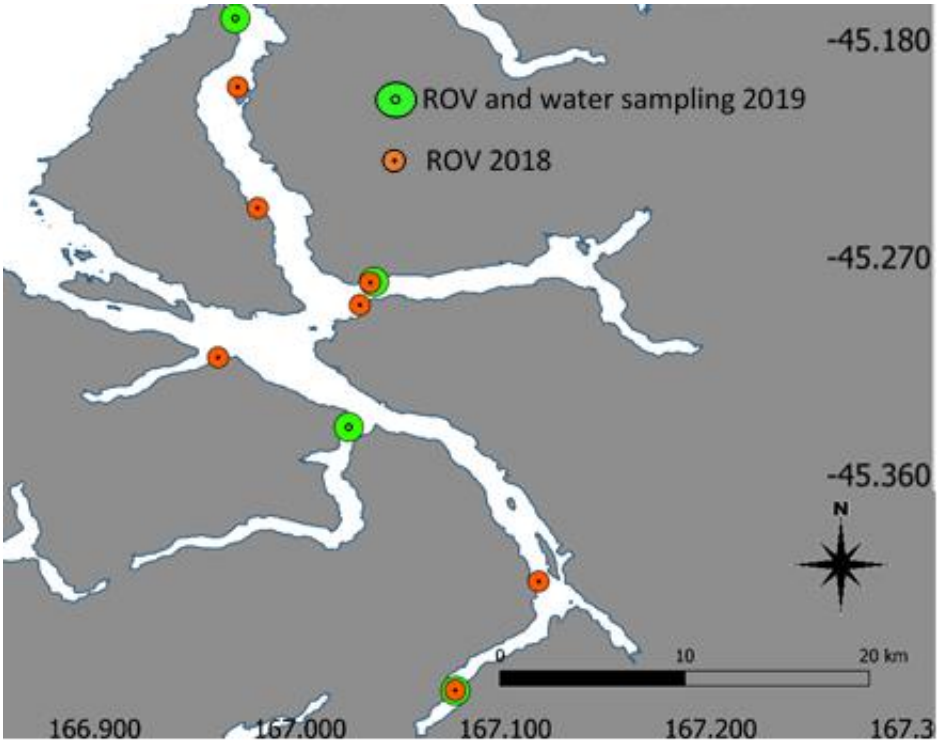

Fig. 5.1 ROV locations in 2018 and ROV and water sample locations at Doubtful Sound in 2019. See Fig. 2.1 for Poor Knights sites.

5.2.2 Habitat assessments

Seawater volume within Doubtful Sound was estimated based on a trapezoid prism volume equation:

$$1/(2)(a + w)dl$$

This shape best represents the geometry of overall fiord bathymetry, as fiord walls are not perfectly vertical resulting in a narrower base width than surface width. a represents the deepest trench width, w is the full fiord arm width on the surface, d is the maximum depth

and l represents fiord arm section length. Due to variability in maximum depth, surface width, and trench width through each fiord arm, volume estimates were taken at every change in depth reported on bathymetric maps produced by the New Zealand Hydrographic Authority and supplied by Land Information New Zealand (LINZ data service 2021) (Fig. 5.2). Surface fiord dimensions were estimated using Google Earth Pro (Google Earth Pro, 2019). Each fiord arm volume was the sum of the multiple trapezoid prism volumes calculated. Total volume of inner, mid, and outer fiord regions was the sum of each fiord arm volume within the categorized regions (Fig. 5.2). The volume of Doubtful Sound was estimated as the sum of the inner, mid, and outer fiord volumes. The Poor Knights are immediately exposed to the open ocean, unlike Doubtful Sound, and lacks any obvious and easily definable geophysical or ecologically based border. The water volume of the Poor Knights was therefore estimated using a standard rectangular prism volume equation $(l * w * d)$ where d as depth was assumed to be vertical. The width of the benthic boundary layer was chosen as a relevant ecological metric to apply as w. This was estimated as a constant of 2 m which was considered the maximum distance from the substrate to represent the maximum benthic layer boundary, where no benthic organisms (including sponges) were observed to extend beyond this distance into the water column from the substrate. l represents the circumference length of each definable island. As with Doubtful Sound volume estimates, the volume of the benthic layer boundary at Poor Knights was the sum of multiple calculated volumes derived from sections according to depth contour changes as displayed on bathymetric maps. Sponge habitat (SH) was estimated using the rectangular prism volume equation and applied to Doubtful Sound and the Poor Knights in the same manner (see assumption 1).

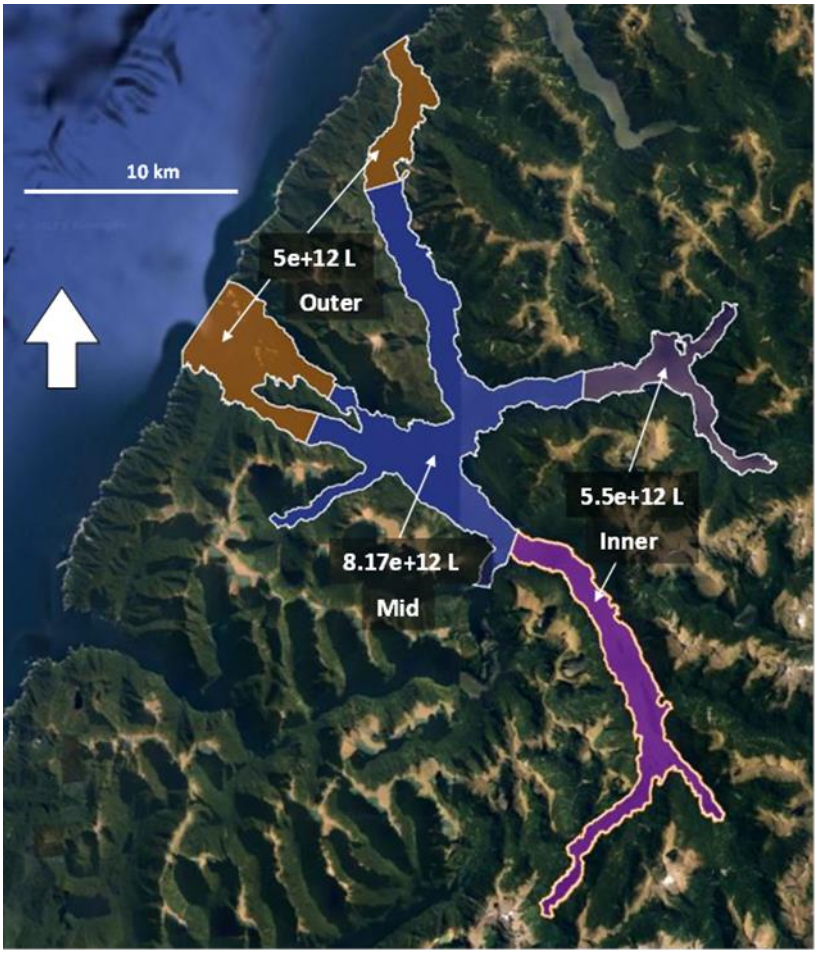

Fig. 5.2 Estimated water volumes of the inner, mid, and outer regions of Doubtful Sound.

5.2.3 Determining sponge abundance

For the full detailed description of the following protocol, see Chapter 2.2. Briefly, the ROV 'SAL', Model DG2 (Deep Trekker Inc.) with an internal and external mounted GoPro 4 silver camera (set at 60 fps at 1080p resolution) and an internal (4k) camera set to linear mode was deployed at each location (Fig. 5.1). The ROV was driven along vertical or near-vertical walls on a horizontal transect for approximately 10 min, producing frame grabs of similar scales. The ROV was then driven upwards for 10 m and another transect completed. This process was repeated at 10 m depth increments until the shallowest transect at 30 m was completed at each site. The maximum depth reached was 120 m at Fiordland and 80 m at the Poor Knights. Sponge assemblages less than 30 m deep were sampled using SCUBA,

whereby the same diver would swim horizontally along a wall at three transect depths of 25, 15, and 0 - 5 m, taking photographs (Nikon D800 with Ikelite Housing and YS50 TTL strobe) approximately every meter and 1 m from the substrate. No significant differences between data derived from ROV and SCUBA images of the same quadrats were found (see Chapter 2 & Fig. A2.1). Videos collected from ROV deployments were analysed using VLC Media Player; 10 frame grabs were extracted from each transect as replicates. The selection of frame grabs was randomized but was largely reliant upon the availability of quality still images. Coral point count (CPC) was used to estimate the percentage cover of sponges (SpC).

Where (SH) is total available sponge habitat, actual sponge cover (SC) (m^2) was calculated as:

$$\frac{SH}{100} * SpC$$

5.2.4 Sponge food (POC) sampling and analysis

For the full detailed description of the following protocol see Chapter 3.2.2. Briefly, water samples from Fiordland sites were collected from the surface (0 – 5 m), and then at 10 m, 30 m, 50 m, 80 m, and 120 m. A limit of 80 m was reached at the Poor Knights. All samples were collected using a 5-L NISKIN bottle (General Oceanics) dispensed into 1.8 ml cryovials, fixed with EM grade 25% glutaraldehyde (Sigma Aldrich, Australia), snap-frozen in liquid nitrogen, and stored at -80°C for subsequent POC analyses using a combination of flow cytometry and scanning electron microscopy.

5.2.5 Flow cytometry

A BD LSRFortessa™ bench-top flow cytometer equipped with six lasers (20 mW 355 nm UV, 50 mW 405 nm Violet, 75 mW 445 nm Blue Violet, 100 mW 488 nm Blue, 150 mW 532 nm Green, and 40 mW 633 nm Red) was used to determine the abundance of different planktonic populations in water samples. The cytometer was calibrated using BD Cytometer Setup and Tracking Beads (Cat No. 641319). Polystyrene beads were used for particle size calibration: 3 μm Rainbow Beads (Spherotech, Cat No. RCP-30-20A) and ApogeeMix that range in size from 110 nm – 1300 nm (Apogee Flow Systems, Cat No. 1493). A 1:40 000 SYBR Green I/sample ratio provided the best compromise between population discrimination and signal saturation and compensation issues (Fig. B3.3). An unstained subsample was run for every sampling depth (*per* location) to provide a gating control for stained samples. The cytometer was set to a flow rate of 40 μm *per* min and run for 300 s for every sample, producing a consistent total analysed volume of 0.2 ml.

Flow cytometry data were analysed using the software package FlowJo V10.8.0. All nucleic-acid positive events (SYBR Green I positive) were discriminated and gated in the first instance using the signal area (A) from side-scattered light (SSC-A, proportional to particle complexity) *vs.* the 515/20 detector off the blue laser (SYBR Green I). The population of nucleic acid positive events was then analysed further to distinguish populations of interest based on distinct fluorescence signatures. Distinct populations exhibiting bright orange fluorescence emission (excited by the Green laser and seen in the 575/25 detector) were considered to be *Synechococcus* sp. Populations emitting bright red fluorescence denoting the presence of chlorophyll *a*, and with dim orange fluorescence were considered as picoeukaryotes (see Chapter 2). The distinct and dense population with minimal fluorescence properties was assumed to be largely heterotrophic bacteria, which lack in chlorophyll. Specific gate locations were drawn separately for each sampled depth at each location but

were kept consistent across replicates and pseudo-replicates (see data analysis). The movement of gates was necessary due to variability and spread of fluorescent signatures across samples according to variations in depth and time of day. However, populations of interest remained distinguishable across samples and their fluorescent signatures remained within the expected regions for each of their assigned categories.

5.2.6 Particle retention efficiency

Briefly, five specimens of five common sponge species (*Tethya* sp., *Tedania* sp., *Suberites* sp., *Dysidea* sp., and *Clathrina* sp.) where chosen for feeding assessments. These species were assessed on the Wellington south coast (see Chapter 4 for study site details and map) but are common across New Zealand rocky reef environments generally, including Doubtful Sound and the Poor Knights (observations from work in Chapter 2). Individuals with larger oscula (minimum > 1 cm diameter) were prioritised, to increase the accessibility of sampling apparatus and reduce the risk of disturbance and sample contamination *via* apparatus-sponge contact. Sampling was carried out based on a modified technique described by Morganti et al. (2016). Once pumping activity was confirmed, two PEEK tubes (25 µm IDM) (IDEX) connected to a flexible tripod were placed 2 cm from the sponge for the sampling of inhalant water and 2 mm inside the most easily accessible exhalent sponge aperture for the sampling of exhalent water. Syringe needles (OD = 0.69 mm) connected to the distal ends of the PEEK tubes were then inserted into two pre-combusted, evacuated EPA 60 ml glass vials with silicone septa caps, and fitted inside a weighted vial holder allowing for the simultaneous collection of ambient (inhalant) and exhalent water. Needles were checked for sample flow, and the time was noted. Extraction rate was targeted to < 1% of the sponge pumping rate to prevent contamination of the exhalent sample from ambient water. Extraction rates remained < 5% of the average *per* osculum pumping rate of each species. Samples for POC analysis were dispensed into 5 ml cryovials from the EPA vials immediately on the surface, fixed with

EM grade 25% glutaraldehyde (0.1% concentration), snap-frozen in liquid nitrogen, and stored at -80^{o}C until analysis. Sponges were photographed for determination of osculum number and size. Particle retention efficiency (RE) (%) was determined for each species from the equation:

$$\frac{rCell}{ambCell} * 100$$

Where $rCell$ is the number of cells retained by the sponge and $ambCell$ is the number of cells available in ambient water. A more thorough description of the methods for the determination of particle retention efficiency can be found in Chapter 4.

5.2.7 Sponge pumping volume

The pumping rates of *Tethya* sp., *Tedania* sp., *Suberites* sp., *Dysidea* sp., and *Clathrina* sp. were determined from eight replicates *per* species *in situ* based on a modified technique described by Yahel (2019). Different specimens were used for pumping volume estimates than those used for feeding assessments, as fewer replicates were applied to feeding estimates due to practical SCUBA restraints. A transparent tube (1 cm ID, 10 cm length) with mm markings was placed immediately over the exhalent aperture of the sponge. The tube was kept in place using a retort stand to minimize interference from ambient current and to provide a measurement reference for dye-front speed assessments. The tube used was always larger than the exhalent aperture being measured. Fluorescein dye was released at the base of the sponge using a 50 ml syringe to determine pumping activity. After pumping confirmation, the movement of the dye was filmed (Gopro 8 Black; 120 fps, 2.7 K) as it was exhaled from the sponge osculum through the transparent tube. VLC Player was used for frame -by-frame analysis (time between each frame = 0.0083 seconds) to determine the total time taken for the dye-front to be exhaled 1 cm into the water column. The number of frames taken before the

dye reached 2 cm was multiplied by 0.0083 s to determine flow velocity, where plug flow was assumed (Pile et al. 1997). All specimens assessed had multiple oscula with narrow inter-specific size ranges (< ± 0.3 mm) but flow velocity was determined from pseudo-replicates of three oscula *per* specimen. Sponge pumping volume (SPV) (ml min^{-1}) was calculated as:

$$v * \pi(d/2)^2(o)$$

Where, v is the exhalent jet velocity, d is the diameter of the oscula and o is the total number of oscula.

5.2.8 SPV – sponge morphological/physiological traits correlations

To determine sponge mass, sponges were removed from the substrate while ensuring that no tissue was left attached the substrate. Specimens were then dried for 48 h at 70 °C, weighed, and then ashed in a muffle furnace for 8 h at 500 °C to determine ash-free dry weight (ASFDW = dry weight – ashed remains). Intra-specific variations in sponge area (SA), mass, oscula number (O), and total oscula area (OSA) were determined to test correlations in morphological/physiological traits and SPV (see Table 5.1).

5.2.9 Regional-scale carbon flux calculations

I found OSA to be the best predictor of SPV and the most effect way to extrapolate SPV to assemblage-scales based on percentage sponge cover information (see Table 5.1). Using a linear regression, I standardized the OSA pumping volume to 1 cm^2 ($OSApv$) for each species (Tables 5.1, 5.2 & Fig. 5.3). I then calculated the OSApv for all species combined. I applied the SE range of the mean as the estimated range of OSApv for the whole assemblage (five species) (see assumption 2). I chose to apply the OSApv ± SE generated from the combined species regression equation instead of the average *per* species OSApv regression results as this provided a more liberal range of OSApv, and there was considerable overlap in

the confidence intervals for *per* species linear regression relationships (Fig. 5.3). Before applying OSApv to assemblage scales, the ratio of OSA to sponge area was calculated as:

$$\frac{OSA}{SA} * 100$$

Here SA is the total sponge area (cm^2). It is necessary that the OSA/SA ratio does not change significantly according to SA for this approach to be viable, which was confirmed (see results). The OSA/SO ratio was also consistent among species further reducing potential error of this approach (see results, but also see assumption 3).

The following equations were applied sequentially to estimate regional scale carbon fluxes through sponge assemblages in inner, mid, and outer regions of Doubtful Sound and the Poor Knights. The number of cells in 0.2 ml was first extrapolated to determine the cell count *per* m^3 ($5x10^6$) referred to as *ambCell* from here on. The carbon mass for each cell group has been determined previously as: 255 fgC·cell^{-1} for *Synechococcus* sp., 2,590 fgC·cell^{-1} for picoeukaryotes (Buitenhuis et al., 2012), and 20 fgC·cell^{-1} for heterotrophic bacteria (Lee and Fuhrman, 1987). The population carbon mass (pCm) of each cell group *per* m^3 was calculated as:

$$\frac{ambCell * sCm}{1x10^{18}}$$

sCm is the specific carbon mass of each cell group (fgC-cell^{-1}). The pCm of each cell group in each region $(pCmA)$ was calculated as:

$$\bar{x}pCm * volA$$

$\bar{x}pCm$ is the mean pCm across all samples at all depths in the study area. $volA$ is the estimated volume of the study area in m^3. Importantly, the sum of the averages of carbon

availability of each Sound area (inner, mid, outer) was applied to the total carbon availability of Doubtful Sound, rather than a pooled average for the whole region, which produced a different total average. This is because each region average was weighted differently due to different area sizes.

After testing correlations between multiple sponge physiological traits and SPV, OSA was applied to extrapolate individual sponge OSApv values to assemblage scales (see sponge SPV methods above and results). Applying OSApv to assemblage scale pumping extrapolations was also determined as the most accurate and effective approach by Morganti *et al.* (2019). The total OSA pumping volume of the full sponge assemblage in each study area $(tOSApv)$ was calculated as

$$\frac{SC}{100} * (OSA{:}\, SA * OSApv)$$

Where SC is total sponge cover (m^2). The quantity of carbon of each cell group pumped through sponge assemblages across each study area in 24 h (TCP) (assuming constant pumping) was therefore estimated as

$$\sum \bar{x}pCm * tOSApv * 1440$$

This equation was applied twice to estimate a range of carbon fluxes based on the ± SE range of $tOSApv$. The overall carbon mass of POC pumped in each region was calculated as the sum of TCP repeated for each cell group (as value of $\bar{x}Cpm$ is specific to each cell group).

Sponges do not necessarily retain POC with 100% efficiency and exhibit significant variability of retention efficiency and selectivity according to particle type, but without any significant inter-specific variability (see Chapter 4). The lack of significant inter-specific differences observed in POC group selectivity in Chapter 4 allows for average retention

efficiency of each food-group across species to be applied with reasonable accuracy. However, there is significant intra-specific SE range in RE (Chapter 4). Therefore, the range of the average SE of the average RE by each species was applied to the following equation to determine the range of total carbon retention in each region:

$$\frac{TCp}{REse}$$

The average RE of heterotrophic bacteria, picoeukaryotes, and *Synechococcus* sp. across seven sponge species was 58 ± 8, 81 ± 6, and 71 ± 9 respectively.

5.2.10 Assumptions / limitations

1. Sponge habitat was assumed to be consistently vertical, potentially underestimating the total available habitat. However, this should not significantly affect sponge abundance data as they were recorded as percentage cover.

2. Pumping volume values were derived from only five species. The application of average SPV from these five species is likely to represent the most significant potential error in the assemblage-scale carbon flux estimations made. However, I applied a large a range of potential SPV to accommodate for this error, though in doing so, reduced precision.

3. Applying the average OSA: SA ratio (6.33%) across the full assemblage assumes that all sponges in the study sites share the allometric relationship observed in the five species assessed. Chapter 2 showed how the morphological diversity of sponges in these regions is high, and likely to increase with depth. A larger range of species and morphological groups would provide more accurate OSA: SA ratios. However, the morphologies of the five study species are also variable, and they represent a large proportion of the species occurring in shallow areas, increasing my confidence in this approach.

4. Averaging microbial cell counts from 0 to 120 m assumes that cell counts beyond 120 m (which were not quantified) do not significantly change the overall average. Autotrophs are likely to be scarce beyond these depths. However, autotrophs at 120 m already reached very low counts, likely reducing this potential error.

5. Averaging sponge abundance across depth categories could also potentially lead to errors where particularly high abundance at shallow depths skews abundance estimates at deeper depths below 120 m (the limit of sponge abundance data) where sponges might be in extremely low abundance. Again, this potential error might be reduced due to recorded abundances at 120 m becoming particularly low and therefore accurately representative of those beyond 120 m.

5.3 Results

5.3.1 Sponge pumping metrics

Multiple inter-specific differences were found in the relationships between pumping velocity, total sponge pumping volume (SPV), and morphological traits including total sponge mass (TSM), total oscula number (TO), and total oscula area (OSA) (Table 5.1).

Dye-front speed is a core component of the SPV equation. However, it did not correlate with any morphological traits or SPV for any species (Table 5.1). SPV only positively correlated with sponge mass for *Suberites* sp. and *Tedania* sp., while *Tethya* sp., *Dysidea* sp., and *Clathrina* sp. showed no correlation between total sponge mass and SPV (Table 5.1). Sponge mass was therefore disregarded as an appropriate standard metric. The TO is also a key component of the SPV equation, but surprisingly, this only positively correlated with SPV for *Clathrina* sp. and *Suberites* sp. and was therefore also disregarded. OSA positively correlated linearly with SPV for all individual species (Table 5.1 & Fig. 5.3a) and was therefore considered as the most appropriate metric for SPV. When all species were combined, the

equation (y = 301.97x + 115.67) describing a positive linear regression relationship between OSA and TVP ($R^2 = 0.68$, $F_{1,33} = 69.24$, $p < 0.0001$) was used to standardize pumping volume to 1 cm^2 OSA, producing an estimate of 417.64 ml cm^2 OSA^{-1} (Fig. 5.3b & Table 5.2). The standard error of the estimate of the linear regression model was ± 307.39 ml cm^2 OSA^{-1} generating a range from the mean of 110 –724 ml cm^2 OSA^{-1} (Table 5.2) to be employed for pumping estimates of sponge assemblages. This range was broader than the standard error range (± 181.6) from the mean SPV of 495.95 ml cm^2 OSA^{-1} across species (i.e., 314 – 677 ml cm^2 OSA^{-1}) and was therefore preferred (Table 5.2).

OSA (cm^2) and 2D sponge area (cm^2) were significantly positively correlated (Fig. 5.4) for all species combined ($R^2 = 0.87$, $F_{1,28} = 175.36$, $p < 0.0001$) and for all individual species (Table 5.3). The average OSA/sponge size ratio when all species were combined was 6.33%. No correlations where observed between OSA/sponge size ratio and sponge size when all species were combined ($R^2 = 0.03$, $F_{1,28} = 0.81$, $p = 0.37$) or for any individual species (Table 5.3), suggesting that the increase in OSA with sponge size follows allometric scaling laws for all species. Furthermore, there was no significant difference in the OSA/sponge size ratio between species (Pseudo-$F_{3,26} = 2.193$, $p = 0.08$) confirming that the average OSA sponge-size ratio (6.33%) can be appropriately applied to the whole assemblage (but see assumption 3).

5.3.2 Habitat and total food availability

Sponge cover of the estimated available habitat of Doubtful Sound (34.57 Km^2) and the Poor Knights (1.22 Km^2) was 11.76% and 50.54% respectively, translating to 4065957 m^2 and 618268 m^2 of sponge, respectively (Table 5.4). The POC potentially available to sponges in Doubtful Sound was estimated to be an average of 3.497 x 10^{-5} Kg/m^3, which translates to 653479 Kg for the whole region (Table 5.5). The Poor Knights were estimated to have 2.068

x 10^{-5} Kg/m^3 of POC potentially available to sponges for the whole region (Table 5.5), which translates to 46.387 Kg of POC within the benthic layer (2 m from substrate, see methods) across the whole region (Table 5.5). Both the count (cells/m^3) and total mass (Kg/m^3) of cells in Doubtful Sound were significantly different according to the cell group (Count: Pseudo-$F_{2,618}$ = 431.58, p < 0.001; Mass: Pseudo-$F_{2,618}$ = 79.93, p = < 0.001). Heterotrophic bacteria were consistently the most abundant cell group followed by *Synechococcus* sp. (Table 5.5) in Doubtful Sound, but picoeukaryotes consistently represented more total mass (Kg/m^3) of available organic carbon than *Synechococcus* sp. (t = 3.114, p < 0.001) (Table 5.5 & Fig. D5.1). Total mass (Kg/m^3) of heterotrophic bacteria reduced significantly (Pseudo-$F_{2,204}$ = 16.03, p = < 0.001) and incrementally from inner to mid (t = 3.55, p < 0.001) and from mid to outer (t = 2.73, p < 0.01) regions of Doubtful Sound. The specific region of Doubtful Sound also had a significant effect on the total mass (Kg/m^3) of picoeukaryotes (Pseudo-$F_{2,204}$ = 8.218, p = < 0.001) and *Synechococcus* sp. (Pseudo-$F_{2,204}$ = 8.452, p = < 0.001) due to a significant drop in total mass from mid to outer regions for both cell groups (picoeukaryotes; t = 3.96, p < 0.001; *Synechococcus* sp.; t = 3.97, p < 0.001). Significantly different cell counts (cells/m^3) were found between cell types at the Poor Knights (Pseudo-$F_{2,618}$ = 79.93, p = < 0.001) but no difference in total mass (Kg/m^3) was observed between cell types (Pseudo-$F_{2,159}$ = 1.277, p = 0.279) despite significantly different *per* cell carbon content (see methods).

5.3.3 Regional scale pumping rates and carbon transfer

The estimated sponge pumping volume range of 110 – 724 (ml cm^2 OSA^{-1}) combined with conservative estimates of sponge habitat and average sponge abundance revealed large sponge assemblage pumping volumes for both Doubtful Sound (283113– 1863396 m^3/min) and the Poor Knights (43050– 283345 m^3 min^{-1}) (Table 5.4).

Combing the previously calculated pumping rate range (110 – 724 ml cm^2 OSA^{-1}) with estimates of ambient concentrations of POC, and sponge abundance data (% cover) revealed that sponge assemblages are pumping large amounts of carbon in both assessed regions (Table 5.6). An estimated 4.865 – 32.019 Kg C min^{-1} as heterotrophic bacteria, 3.169 – 20.860 Kg C min^{-1} as picoeukaryotes, and 1.313 – 8.641 Kg C min^{-1} as *Synechococcus* sp. cells are pumped through the total sponge population of Doubtful Sound (Table 5.6). This represents 2.06 – 13.56% of the total ambient POC every 24 hours, assuming constant pumping (Table 5.6). Applying known average retention efficiencies of each food group revealed that sponges are transferring an estimated 3482 – 30615 Kg C d^{-1} or a total of 8084 – 66980 Kg C d^{-1} (Table 5.7) equivalent to a conservative estimate of 1.24% or a liberal estimate of 10.25% of the total available POC in Doubtful Sound (Table 5.7) and an estimated 870 – 6124 Kg C d^{-1} which represents 1875 – 13202% of the available POC within the benthic layer (2 m from substrate) of the entirety of The Poor Knights (Table 5.7).

Table 5.1 Linear regression tests between multiple morphological traits and pumping rate equation components to determine the best predictor of overall sponge pumping volume.

Species		**Mass**			**Total no. oscula**			**OSA**			**df**
		R^2	**F**	**p**	**R^2**	**F**	**p**	**R^2**	**F**	**p**	
***Tethya*.sp**	Dye-front speed	0.29	3.80	0.1	0.07	0.42	0.06	0.04	0.25	0.64	1,6
	Pumping volume	0.36	3.35	0.12	0.02	0.13	0.73	**0.85**	**28.91**	**>0.01**	1,6
	Mass	……	……	…	0.29	2.48	0.17	0.38	3.09	0.14	1,6
***Tedania*.sp**	Dye-front speed	0.40	3.3	0.13	0.01	0.06	0.82	0.01	0.06	0.82	1,6
	Pumping volume	**0.86**	**31.03**	**0.01**	**0.66**	**9.72**	**0.03**	**0.67**	**9.72**	**0.03**	1,6
	Mass	……	……	…	0.29	4.27	0.9	0.46	4.27	0.09	1,6
***Suberites*.sp**	Dye-front speed	0.13	0.43	0.56	0.21	0.12	0.44	0.02	0.05	0.83	1,5
	Pumping volume	**0.95**	**58.55**	**0.01**	0.59	4.23	0.13	**0.97**	**87.79**	**>0.01**	1,5
	Mass	……	……	…	0.42	2.20	0.23	**0.87**	**20.82**	**0.02**	1,5
***Dysidea*.sp**	Dye-front speed	0.17	1.26	0.3	0.11	0.75	0.42	0.18	1.34	0.29	1,7
	Pumping volume	0.06	0.36	0.57	0.41	4.21	0.09	**0.92**	**73.75**	**> 0.001**	1,7
	Mass	……	……	……	0.01	0.05	0.83	0.06	0.38	0.56	1,7
***Clathrina*.sp**	Dye-front speed	0.13	0.90	0.38	0.11	0.75	0.42	0.14	0.94	0.37	1,7
	Pumping volume	0.06	0.36	0.57	**0.82**	**27.02**	**0.01**	**0.84**	**30.61**	**> 0.01**	1,7
	Mass	……	……	……	**0.96**	**157.**	**0.01**	**0.97**	**226.38**	**> 0.001**	1,7

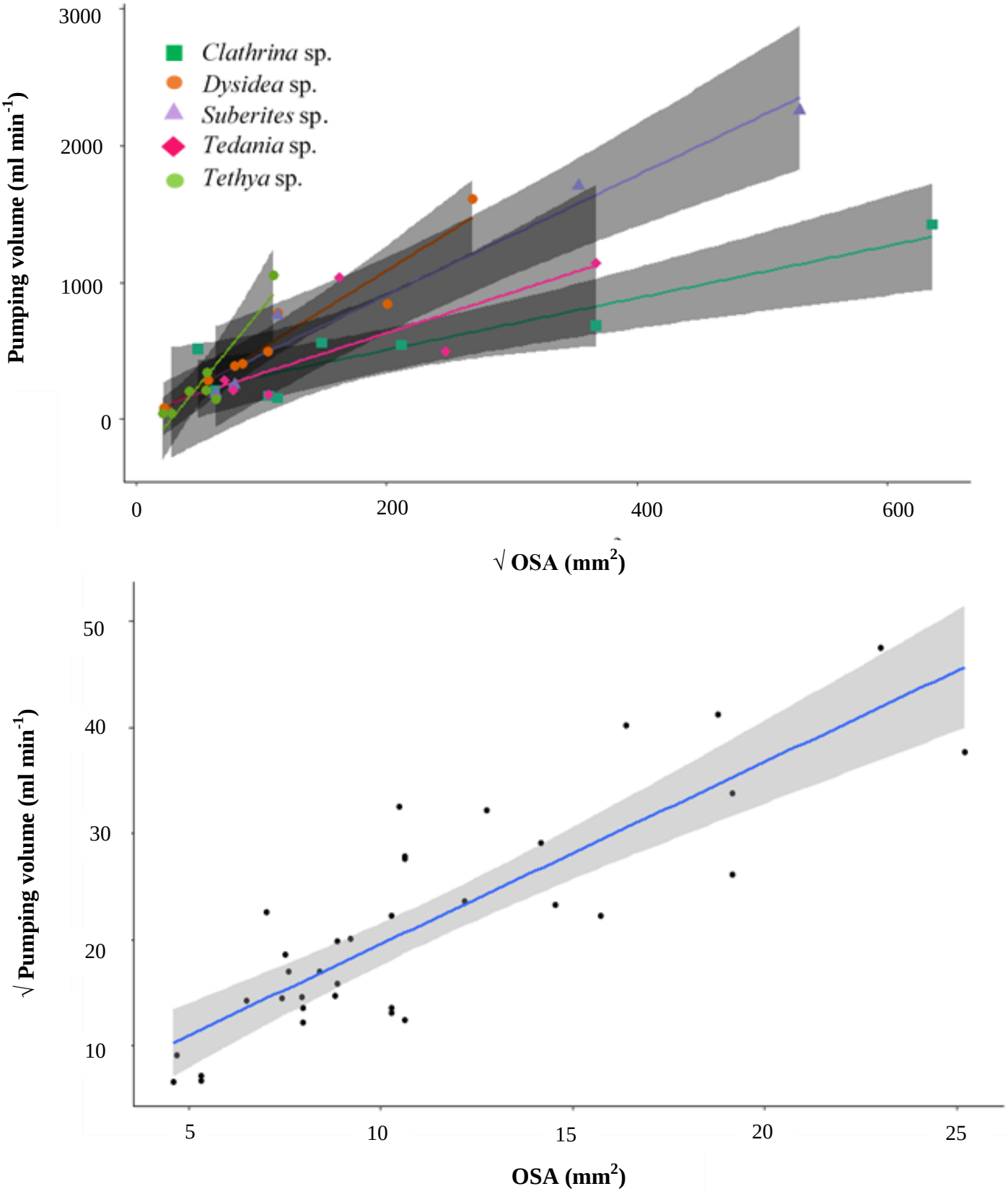

Fig. 5.3 Linear regression relationships (±CI) between the OSA (mm^2) and sponge pumping volumes (ml min^{-1}) of *Dysidea* sp. *Clathrina sp. Suberites* sp. *Tedania* sp. and *Tethya* sp. (A), and all the square-root data of species combined (±CI) (B). See Table 5.1 for R^2 coefficients.

Table 5.2 Average OSA (cm^2), corresponding pumping volume based on predicted y-values from linear regression coefficients of average OSC, and OSC standardized to 1 cm^2 (see Table 5.1 & Fig. 5.3). Error values for OSC pumping volume are the standard error of the estimate in regression formulas. Assemblage range is the assemblage mean ± the standard error of the estimate.

Species	**Average OSA (cm^2)**	**Avg. Full sponge pumping volume (ml/min)**	**Per cm^2 OSC pumping volume (ml/min)**
***Tethya* sp.**	0.539 ± 0.284	267.33	833.67 ± 155.5
***Tedania* sp.**	1.515 ± 0.740	487.99	335.81 ± 276.8
***Suberites* sp.**	2.278 ± 0.921	1030.78	472.74 ± 191.9
***Dysidea* sp.**	1.164 ± 0.450	612.52	519.31 ± 140.5
***Clathrina* sp.**	2.276 ± 0.110	530.63	318.22 ± 180.6
Full assemblage	-	585	417.64 ± 307.39
Assemblage range	-	460-710	110 - 724

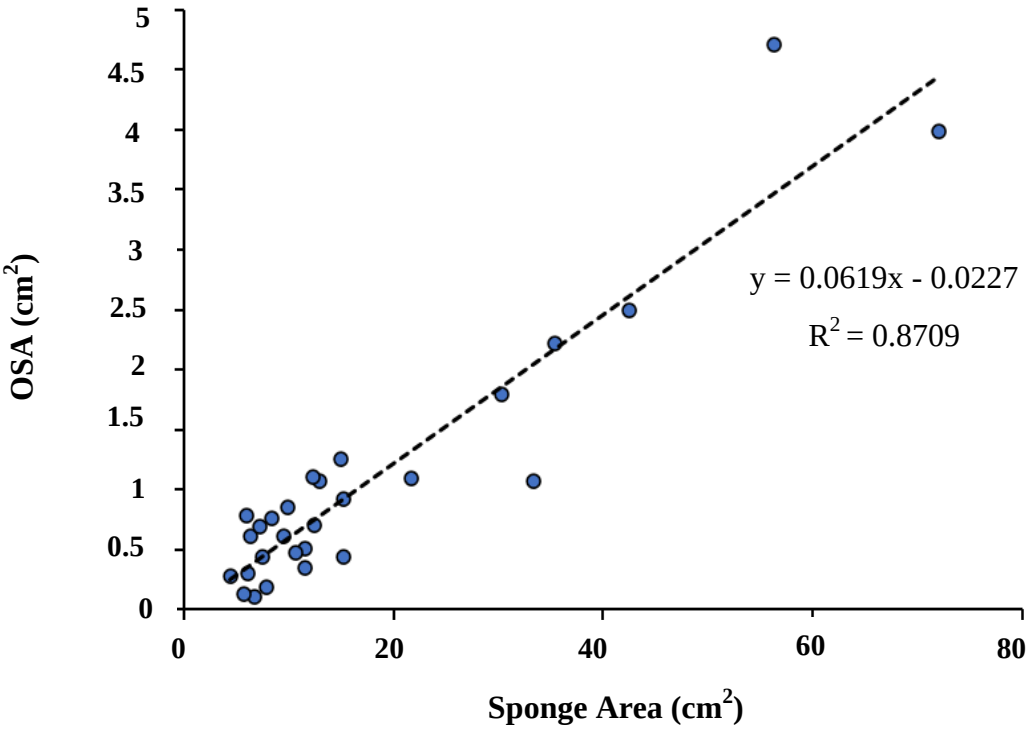

Fig. 5.4 Linear regression relationship between 2D total sponge area (cm^2) and total oscula area (cm^2) of 5 sponge species. See Table 5.1 for R^2 coefficients for individual species.

Table 5.3 Descriptions of morphological traits and allometric scaling relationships between OSC and sponge area (2d cm^2 area).

Species	**Average OSC (cm^2)**	**Sponge 2D size (cm^2)**	**OSC - Sponge ratio (%)**	**OSC / Sponge Size relationship**			**OSC- Sponge ratio / Sponge size relationship**		
				R^2	**F**	**p**	**R^2**	**F**	**p**
***Tethya* sp.**	0.539 ± 0.284	12.43	5.39± 0.88	0.71	$19.96_{1,9}$	< 0.01	0.04	$0.35_{1,9}$	0.57
***Tedania* sp.**	1.515 ± 0.740	8.44	9.27± 1.16	0.72	$10.37_{1,6}$	< 0.05	0.12	$0.39_{1,6}$	0.58
***Dysidea* sp.**	1.164 ± 0.450	21.65	4.36± 0.98	0.99	$1395_{1,6}$	< 0.001	0.31	$1.81_{1,6}$	0.25
***Clathrina* sp.**	2.276 ± 0.110	57.95	4.85± 0.90	0.81	$12.91_{1,7}$	< 0.05	0.11	$0.37_{1,7}$	0.59
Assemblage	-	-	6.33	0.87	$175.36_{1,28}$	< 0.001	0.03	$0.81_{1,28}$	0.37

Table 5.4 Estimated volume of water (m^3), sponge habitat (m^2), sponge cover ± SE, and range of sponge assemblage pumping volume (m^3 min^{-1}) (see methods and Table 5.3) within the inner, mid, outer, and total region of Doubtful Sound and the Poor Knights. Water volume at the Poor Knights is the estimate of the benthic layer (see methods section).

Location	Water volume (m^3)	Sponge habitat (m^2)	Sponge cover (%)	Sponge cover (m^2)	Pumping volume (m^3 min^{-1})
Inner	$5.5048x10^9$	13740298	6.5 ± 1.15	893119	62188 - 409309
Mid	$5.169x10^9$	14395907	12.37 ± 0.70	1780774	123993 – 816115
Outer	$5.002x10^9$	6429858	21.65 ± 1.17	1392064	96930 – 637974
Doubtful	$18.676x10^9$	34566063	11.76 ± 0.58	4065957	283113 - 1863396
Poor Knights	2243164	1223325	50.54 ± 1.83	618268	43050 – 283345

Table 5.5 Estimates of cell counts (individual cells) and equivalent carbon Kg *per* m^3 and *per* region water volume (Table 5.4) of heterotrophic bacteria, picoeukaryotes, *Synechococcus* sp., and all cells combined, at the inner, mid, and outer regions of Doubtful Sound, as well as the entirety of Doubtful Sound and the Poor Knights. Water volume estimates at the Poor Knights include the benthic layer only (see methods).

Location	Units	Heterotrophic bacteria	Picoeukaryotes	*Synechococcus* sp.	All cells
Inner	Cells (m^3)	1.094×10^{12}	5.885×10^{9}	$2.369e \times 10^{10}$	1.123×10^{12}
	Cells (total habitat)	6.022×10^{21}	3.240×10^{19}	1.304×10^{20}	6.185×10^{21}
	C (Kg/m^3)	2.188×10^{-5}	1.524×10^{-5}	6.041×10^{-6}	4.316×10^{-5}
	C (Kg/total habitat)	120436	83905	33254	237594
Mid	Cells (m^3)	9.820×10^{11}	5.707×10^{9}	2.462×10^{10}	1.012×10^{12}
	Cells (total habitat)	8.022×10^{21}	4.662×10^{19}	2.011×10^{20}	8.270×10^{21}
	C (Kg/m^3)	1.964×10^{-5}	1.478×10^{-5}	6.278×10^{-6}	4.070×10^{-5}
	C (Kg/total habitat)	160439	120748	51284	332471
Outer	Cells (m^3)	5.514×10^{11}	1.548×10^{9}	6.423×10^{9}	5.594×10^{11}
	Cells (total habitat)	2.758×10^{21}	7.744×10^{18}	3.213×10^{19}	2.798×10^{21}
	C (Kg/m^3)	1.103×10^{-5}	4.01×10^{-6}	1.638×10^{-6}	1.668×10^{-5}
	C (Kg/total habitat)	55163	20058	8193	83414
Doubtful	Cells (m^3)	8.758×10^{11}	4.380×10^{9}	1.824×10^{10}	8.984×10^{11}
	Cells (total habitat)	1.680×10^{22}	8.676×10^{19}	3.637×10^{19}	1.725×10^{22}
	C (Kg/m^3)	1.752×10^{-5}	1.134×10^{-5}	4.652×10^{-6}	3.352×10^{-5}
	C (Kg/total habitat)	336038	174058	92730	653479
Poor Knights	Cells (m^3)	3.590×10^{11}	2.763×10^{9}	2.487×10^{10}	3.866×10^{11}
	Cells (benthic layer)	8.053×10^{17}	6.198×10^{15}	5.579×10^{16}	8.673×10^{17}
	C (Kg/m^3)	7.180×10^{-6}	7.156×10^{-6}	6.343×10^{-6}	2.068×10^{-5}
	C (Kg/benthic layer)	16.106	16.053	14.227	46.387

Table 5.6 Estimates of carbon (Kg C) in the form of heterotrophic bacteria, picoeukaryotes, and *Synechococcu*s sp., cells as well as all POC groups combined, pumped through full sponge assemblages *per* minute at the inner, mid, and outer regions of Doubtful Sound, as well as the entirety of Doubtful Sound and the Poor Knights. The percentage of the full POC pool being pumped *per* 24 h is also reported. Value ranges are based on the SE range from the mean pumping volume of five species (Table 5.2). The SE range of ambient availability of each POC group occurring in each region is not considered.

Location	**Heterotrophic bacteria pumped (Kg C d^{-1})**	**Picoeukaryotes pumped (Kg C d^{-1})**	***Synechococcus* sp. pumped (Kg C d^{-1})**	**Total pumped (Kg C d^{-1})**
Inner	1959 - 12895	1365 - 8984	541 - 3561	3865 - 25440
% total ambient C	0.825 – 5.427	0.574 – 3.781	0.228 – 1.499	1.627 – 10.707
Mid	3507 - 23081	2639 - 17371	1121 - 7378	7267 - 47829
% total ambient C	1.055 – 6.942	0.794 – 5.225	0.337 – 2.219	2.186 -14.386
Outer	1539 - 10132	560 - 3684	229 - 1505	2328 - 15320
% total ambient C	1.845 – 12.146	0.671 – 4.416	0.274 – 1.804	2.790 - 18.366
Doubtful	7006 - 46107	4563 - 30038	1891 - 12443	13460 - 88059
% total ambient C	1.072 – 7.055	0.698 – 4.597	0.289 – 1.904	2.060 - 13.556
Poor Knights	445 - 2930	444 - 2920	393 - 2588	1282 - 8437
% benthic layer C	960 - 6316	956 - 6295	848 - 5579	2764 -18189

Table 5.7 Estimates of carbon (Kg C) in the form of heterotrophic bacteria, picoeukaryotes, and *Synechococcu*s sp. cells, as well as all POC groups combined, retained by full sponge assemblages *per* 24 h period at the inner, mid, and outer regions of Doubtful Sound, as well as the entirety of Doubtful Sound and the Poor Knights. The percentage of the total carbon retained of the full POC pool *per* 24 h is also reported. Average retention efficiency of heterotrophic bacteria, picoeukaryotes, and *Synechococcus* sp. cells across seven species was 58 ± 8, 81 ± 6, and 71 ± 9 respectively (see Chapter 4). The low and high values range reported are the mean retention efficiency ± SE and mean pumping volume ± SE.

	Heterotrophic bacteria retained (Kg C d^{-1})	**Picoeukaryotes retained (Kg C d^{-1}**	***Synechococcus* sp. retained (Kg C d^{-1})**	**Total retained (Kg C d^{-1})**
Inner	974 - 8562	1024 - 7888	338 - 2859	2335 – 19309
% total ambient C	0.410 – 3.604	0.431 – 3.320	0.142 – 1.203	0.983 – 8.127
Mid	1743 - 15352	1979 - 15251	699 - 5924	4422 – 36501
% total ambient C	0.524 – 4.610	0.595 – 4.587	0.210 – 1.782	1.330 – 10.979
Outer	765 - 6727	420 - 3234	142 - 2108	1327- 1170
% total ambient C	0.917 – 8.065	0.503 – 3.78	0.171 – 1.449	1.591 – 13.391
Doubtful	3482 - 30615	3423 – 26373	1180 – 9992	8084 – 66980
% total ambient C	0.535 - 4.685	0.524 - 4.036	0.181 - 1.529	1.237 – 10.250
Poor Knights	221 - 1945	333 - 2563	316 – 1615	870 - 6124
% total ambient C	477 - 4194	717 - 5527	681 - 3481	1875 - 13202

5.4 Discussion

In Chapter 2 I showed that sponges are consistently the most dominant members of the benthic community through both the infralittoral and mesophotic zones assessed in New

Zealand. In Chapters 3 and 4 I showed how sponge assemblages have very close trophic relationships with the microbial constituents of the particulate organic carbon (POC) pool, retaining carbon and other nutrients from the water column at high efficiencies as has been demonstrated in other studies (e.g. Reiswig, 1975; Ribes et al. 1999; Coma et al. 200l; Perea-Blázquez et al. 2013a). The culmination of these findings suggests that sponge assemblages in New Zealand are performing an important functional role in transferring large amounts of carbon from the water column to the benthos in both shallow and deep water habitats, as has been suggested in other studies from different regions (i.e. Pawlik & McMurray, 2019; Folkers & Rombouts, 2020). Therefore, in this current study I combined the information previously obtained throughout this thesis to quantify sponge carbon retention (as C vol time^{-1}), and extrapolate this to regional assemblage scales using an estimated range of OSA-specific pumping volume (also see Morganti et al. 2021).

5.4.1 Extrapolating to assemblage scale pumping volumes

Extrapolating information derived from individual organisms to entire populations is potentially problematic in ecological contexts generally, as it risks potential errors becoming inflated at scale (Forbes et al. 2008; Ponzi et al. 2019). As such, the first component of this study was to determine the most accurate and efficient extrapolation metric as a pre-requisite for scaling-up SPV and carbon retention values to assemblage scales. Previous studies have frequently employed sponge volume as a standardized metric for such extrapolations (de Goeij et al. 2017). However, Morganti et al. (2019) showed sponge size to be a major determining factor of size-specific pumping rate, suggesting that applying a size-specific metric (SPV, ml min^{-1} cm^{-3} sponge) to assemblage abundance data is likely to generate large errors if the distribution of specific sponge size-classes are not considered (Morganti et al. 2019). The strong positive correlation between OSA and SPV observed for all sponge species in this study (Fig. 5.3) was consistent with the findings of a very recent study by Morganti et

al. (2021). These authors showed OSA to be the best predictor of SPV, and the most appropriate and efficient metric for extrapolating SPV to assemblage scales. OSA, rather than sponge volume, improved the predictive power of pumping rate by 30%. This approach also bypasses the potential error associated with the conversion of sponge percentage cover data (used in this thesis and the most applied method to benthic organism abundance estimates, de Goeij et al. 2017) to sponge volume estimates. However, the efficacy of applying an OSA-specific metric to sponge percentage cover data strongly depends on the ratio of OSA to SA to scale allometrically as hypothesized by Goldstein et al. (2019). The confirmed lack of correlation between OSA: SA ratios and SA found in this study suggests OSA specific pumping volume to be a viable approach and overcomes the necessity to consider sponge size as major determinate of SPV (Morganti et al. 2019). Despite this confirmation, the assumption of allometric scaling of OSA: SA is likely to be the source of the largest potential error of the carbon retention estimates in this study. This is because SPV estimates were determined from only five species, all of which were determined in shallow water (assumption 3), and small changes in OSA: SA ratios translate to significantly different assemblage pumping volumes at scale. This is also the case for feeding retention efficiency estimates, where seven species were used (Chapter 4). While the species chosen appear to represent a significant proportion of the sponge cover in both Doubtful Sound and at the Poor Knights, there are likely to be hundreds of sponge species occurring at these sites (see Chapter 2). Furthermore, some of these species are likely to be found exclusively within the mesophotic zone, such as certain branching (see Chapter 2) or hexactinellid species (e.g. Castello-Branco et al. 2020) with potentially different feeding behaviour and OSA: SA ratios. However, the species chosen represent multiple different morphologies to address this potential problem to the greatest possible extent (*Dysidea* sp. – "Repent"; *Clathrina* sp. –

"Massive"; *Tedania* sp. – "Encrusting"; *Tethya* sp. –"Globular"; *Suberites* sp.; – Massive/Globular).

5.4.2 Assemblage scale carbon retention estimates

This study shows that sponges retain very large quantities of the POC available in different environments even at the lowest end of the estimated ranges (Tables 5.6 & 5.7). For example, the most conservative estimate (using the lowest retention efficiency estimates combined with the lowest pumping rate estimates) of carbon retained by the sponge population across Doubtful Sound was 13460 Kg C d^{-1}. This equates to 14% of the total POC potentially available to the sponge assemblage (as the combination of picoeukaryotes, heterotrophic bacteria and *Synechococcus* sp.) contained within the Sound volume (18.7 Km^3), or 100% retention of available POC every 7.14 days. Considering just the benthic boundary layer at the Poor Knights (extending 2 m from the substrate into the water column) provided a measure of POC immediately available to sponges at a given time. A conservative estimate of 2764% *per* day of this immediately available POC is being retained in the benthos by the sponge assemblages living here, equating to 100% retention of the benthic boundary POC content every 52 minutes. This extent of carbon turnover has important ecological implications, where the members of the benthic community (including sponges) feeding on POC are likely to be subject to high levels of inter-and intra-specific resource competition and bottom up effects (see Chapter 3). However, this will be heavily governed by location-specific hydrographic conditions which may or may not generate sufficient lateral transport, and hence replenishment of resources for the maintenance, growth, and proliferation of the benthic community generally, preventing the formation of a depleted boundary layer above the reef (Genin et al. 2009). Without frequent flushing, a substantial resource deficit is likely to occur over time. This is the most likely explanation for the apparent contradiction found when comparing the food availability / sponge abundance relationship between Fiordland and

the Poor Knights. While the abundance of the "standing crop" of POC was consistently lower at the Poor Knights than Fiordland Site 2 for example (Fig. 3.5). The higher abundance of sponges occurring at Poor Knights is likely to be facilitated by substantial and consistent flushing and subsequent resource replenishment, while mid and inner Fiordland sites are likely to receive much lower flushing and resource replenishment rates, inhibiting the proliferation of the sponge assemblages occurring there. I would therefore suggest the rate of replenishment of POC and other nutrients is therefore an important consideration for future assessments of the role of food availability in determining temperate sponge assemblages. The consideration of lateral water movement, flushing, and nutrient replenishment might also be an important consideration for sponge pumping rates which dictate carbon flux estimates on assemblage scales. The values reported here, assume constant pumping despite some studies showing that environmental factors are likely to affect pumping activity (Riisgård et al. 1993), although, other studies have shown pumping activity to be a function of active behaviour, where sponges can maintain pumping rates under different current conditions (Ludeman et al. 2017).

The observation of heterotrophic bacteria as the most numerically abundant microbial group is consistent with other studies from temperate environments with similar true cell abundance values (Yahel et al. 2007; Perea-Blázquez et al. 2012; Kahn et al. 2015). *Synechococcus* sp. was more numerically abundant than picoeukaryotes, but this was not reflected in estimates of carbon mass availability and retention which are probably a more ecologically relevant metric then cell counts (Kahn et al. 2015). Picoeukaryotes represented significantly more organic carbon available to sponges than *Synechococcus* sp. despite being the least numerically abundant group. This is due to a combination of strong selective preference of picoeukaryotes by the sponges assessed (see Chapter 4) and the significantly greater cell

carbon mass of picoeukaryotes than both heterotrophic bacteria and *Synechococcus* sp. (Lee & Fuhrman, 1987; Buitenhuis et al. 2012).

The water volume-specific carbon retention values demonstrated by the species in this study are within an order of magnitude to those reported for different species in a range of temperate habitats. Yahel et al. (2007) showed that the temperate deep-water Hexactinellid sponges *Aphrocallistes vastus* and *Rhabdocalyptus dawsonito* removed 1.4 ± 0.5 µmol L^{-1} and 1.5 ± 0.7 µmol L^{-1} of bacterial carbon respectively, compared with 0.3 µmol L^{-1} by sponges in the current study. Kahn et al. (2015) showed sponge assemblages in a deep-sea Fjiord in British Columbia exhibited carbon retention values closer to those exhibited in this study (0.016 ± 0.004 mg carbon L^{-1} and 0.033 mg carbon L^{-1}, respectively). The similar carbon retention values relative to carbon availability for different environments in this and other studies, suggests that the observed high turnover of available POC by sponge assemblages is not exclusive to the study regions assessed.

While the current study focused exclusively on the particulate portion of the organic carbon food pool, it is probable that other pathways of energy accumulation are utilized by temperate sponges (Taylor et al. 2007), such as DOC consumption (de Goeij et al. 2013; Rix et al. 2016), and phototrophic (Lemloh et al. 2009) and chemotrophic pathways (Levin et al. 2002). However, the extent to which these sources contribute to overall energy accumulation by sponges (if at all) is likely to be strongly dependent on: sponge species; habitat; environmental conditions; and relative food availability (Vacelet et al. 1995; Taylor et al. 2007). For example, while the metabolization of DOC has potentially significant ecological implications (de Goeij et al. 2013; Rix et al. 2016; Bart et al. 2021), the uptake of DOC in temperate sponges appears to be highly variable with high DOC retention efficiencies reported in some studies (e.g. Bart et al. 2021), and with no evidence of DOC retention in other studies (Yahel et al. 2007). This variability might be a function of relative food

availability, true interspecific differences, or a combination of both (see Chapter 4). DOC is an abundant and ubiquitous resource, and therefore, the utilization of this resource by sponges is likely to be evolutionarily advantageous, especially in habitats where food availability is particularly low, and bottom-up pressure appears to be present. However, due to the inter and intra-specific variability of DOC consumption demonstrated in Chapter 4, and across the literature, the potential contributions of DOC were excluded in this study .This omission of DOC could therefore mean that the total carbon retention values reported here are potentially conservative, especially at the lower range estimates. Considering this, more work needs to be done to assess the consumption of DOC by temperate sponges under different food availability scenarios, and across seasonal changes in multiple relevant ecological factors (temperature, inter-specific pressure, growth etc.) and species.

5.4.3 Broader ecological implications

The strikingly high estimates of carbon flux reported here suggest that sponge assemblages are performing a substantial role in the movement of carbon through coastal ecosystems to an extent that has not been previously understood or appreciated in temperate environments (see Genin et al. (2009) for tropical sponge assemblage carbon flux estimates and Kahn et al. (2015) for specifically deep-water glass sponge assemblages). While net carbon sequestration estimates require the consideration of sponge respiration rates, observations from other studies suggest the majority of carbon intake by sponges is converted into biomass (e.g. Koopmans et al. 2009), enriching benthic communities with organic matter in the form of sponge tissue and detrital waste disposal (Maldonado et al 2012). In addition to this large contribution to the regulation of POC flux through benthic ecosystems, while not quantified here, the role of sponges in regulating the flux of DOC is potentially substantial, and carries its own ecological ramifications in addition to those suggested for POC, most notably, the possibility of a temperate sponge loop. The sponge loop was discovered in the pursuit of

solving the resource deficit observed in tropical sponges (de Goeij et al.2008; 2013; Pawlik & McMurray 2020) but it has now also been indicated in Mediterranean sponge assemblages (Alexander et al. 2014) and observed in deep-sea assemblages (Bart et al. 2021). The critical component of the sponge-loop involves the conversion of DOC to the wider ecological community through detrital (de Goeij et al. 2013) or predatory (McMurray et al. 2018) pathways, or both. A hypothetical temperate sponge loop would play an important ecological role in sponge populations dynamics during seasonal reductions in food availability (Ribes et al. 1999, Perea-Blázquez et al. 2013a) or in the deeper regions of TMEs where food availability in the form of autotrophic microbial communities is substantially lower than shallow regions (see Chapter 3). If only a small number of common sponge species occurring in these environments are assimilating DOC into biomass at a similar extent to those values reported for POC, this is likely having a highly significant impact beyond those specifically associated sponge population dynamics. These broader impacts have been described by the fundamental ecological role of the sponge loop hypothesis, where converted DOC can be utilized by the wider benthic community, potentially altering numerous elements of community dynamics (de Goeij et al. 2013).

Given their consistent dominance throughout temperate reefs into the mesophotic zone (see Chapter 2) in combination with a considerable capacity for carbon flux, I would suggest that sponge assemblages are the primary biotic regulators of carbon into and through coastal rocky-reef benthic ecosystems in New Zealand. My results suggest that through feeding activity, sponges are capable of potentially depleting, and therefore determining, the availability of carbon resources for the wider benthic community through the sequestration of POC (and potentially DOC) from the benthic layer as detrital matter and sponge biomass itself, or lost via respiration activity. Furthermore, sponges have been predicted to be the "winners of climate change" after substantial sponge assemblage proliferation was observed

following the fracture of ice shelves in the Southern Ocean (Dayton et al. 2013). Observations of phase shifts from coral to sponge dominated reefs in tropical environments (Bell et al. 2013) support this suggestion. If this is correct, then sponges may become increasingly important as one of numerous buffers against climate change impacts on marine ecosystems, as carbon concentrations rise and becomes assimilated into sponge tissue. Given their substantial contribution to the fundamental ecological function of resource regulation, I suggest that temperate sponges in mesophotic zones require substantially more attention in the development of effective conservation and management strategies. This is increasingly important as climate change and other anthropogenic stressors continue to increase pressure on these ecologically important, but still poorly understood environments.

Chapter 6
General discussion

6.1 Summary of key findings

The overall aim of this thesis was to address the significant knowledge gap in how marine sponges are distributed through temperate infralittoral and mesophotic zones, and how their feeding behaviour determines sponge population dynamics and broader ecological functions across these habitats. In Chapter 2, using a broad environmental range of marine habitats in New Zealand, I showed how sponges were consistently the most abundant invertebrates (based on percentage cover) within temperate benthic communities, regardless of the location, depth, or wider community composition of the habitats assessed. I also showed how the morphological composition of these sponge assemblages is likely to be contributing to benthic habitat complexity, especially in deeper regions where other habitat provisioners within the benthic community are particularly sparse relative to sponges. In Chapter 3, using a combination of flow cytometry and scanning electron microscopy (SEM), I identified and quantified the microbial constituents of the particulate organic carbon (POC) pool potentially available to sponges across the depth gradients observed in Chapter 2, as well as dissolved organic carbon (DOC). I corrected the previously misidentified cyanobacteria '*Prochlorococcus*' to be picoeukaryotes, a taxonomically broader group of more complex and larger cells. I identified other groups as heterotrophic bacteria and *Synechococcus* sp. which was consistent with earlier studies. I showed how the distribution of these microbial groups varied significantly with depth and location, and that these distributions correlated strongly with the sponge abundance patterns previously observed. These correlations suggest that the distribution of temperate sponges below the infralittoral zone is likely to be driven by the availability of food in the form of microbial particulate organic carbon (POC), but not necessarily by DOC availability, which was highly variable and did not correlate with sponge distributions. In Chapter 4, I confirmed that the microbial POC components previously identified were being retained by the sponge species assessed, but with interspecific

variability in retention efficiency. I showed that these sponges demonstrate food preferences for specific food groups, most notably, picoeukaryotes. However, I concluded that interspecific differences in retention efficiencies of different microbial groups is not necessarily indicative of resource partitioning within the POC pool, contrary to the conclusions of a previous study in New Zealand, which did not include food selectivity metrics. I confirmed the significant retention of DOC by temperate sponges (*Polymastia penicillius* and *Polymastia* sp.) in shallow reefs outside of the Mediterranean for the first time. My results suggest interspecific similarities in food preferences within the POC pool, but potential resource partitioning across POC and DOC food pools, as well as potential trophic plasticity in response to food availability. Observations of high retention efficiency of autotrophic cells and linear increases in food retention with food availability support the hypothesis of food limitation, and bottom-up effects, on temperate sponges, as suggested in Chapter 3. In Chapter 5, I combined all the information systematically collected throughout this thesis to determine the assemblage-scale contributions of sponges to carbon cycling across specific infralittoral and mesophotic habitats in New Zealand. I combined the microbial retention efficiency data of five sponge species collected in Chapter 4, with newly collected pumping volume data from the same species, to extrapolate the pumping and feeding behaviour of shallow-water surrogates to entire sponge assemblages occurring through the full depth profiles of the study locations (5 – 120 m). I found that, consistent with the conclusions of a very recent study, total oscula area was an effective way of extrapolating sponge pumping volumes to full sponge assemblages determined by percentage cover metrics. I demonstrated how temperate sponges are retaining a high proportion of the carbon available in ecologically and geographically distinct regions over short time periods, even at the lowest end of retention efficiency and pumping volume estimate ranges. At the higher end of estimated ranges, 100% of the carbon available in the benthic layer of the Poor Knights

was calculated as being retained approximately every 50 minutes, and that sponges are retaining 100% of the available POC pool in Doubtful Sound approximately every 7 days. These results are conservative due to the omission of potentially significant DOC retention rates by certain species. This large proportion of available carbon transferred from the water column to the benthos by heterotrophic sponges is likely to have substantial ecological implications. These include the alteration of water column chemistry and regulating the availability of microbial communities, which are fundamental to other important ecological processes, such as primary production, and the microbial loop. Furthermore, while numerous ecological (predation, habitat availability, resource competition) and physiological (respiration, gamete production) variables are likely to contribute to the presence and proliferation of sponges, the extent of carbon transfer (as demonstrated in this thesis) fundamentally determines the production of heterotrophic sponge assemblage biomass itself, and is therefore the central component of all the other ecological functions sponges perform (see section 6.4).

6.2 Temperate mesophotic ecosystems and sponges

In Chapter 2 I addressed a substantial knowledge gap in the composition and distribution of temperate benthic communities through infralittoral and mesophotic zones (down to 120 m). In a review of descriptions of benthic TME communities globally, Bell et al. (*in review*) found only 7 other studies that employed percentage cover metrics to quantitatively describe benthic community changes from shallow to TME habitats. These studies all report a shared characteristic of TME benthic communities; that sponges are consistently the most abundant benthic organism occurring in these habitats (Bell et al. *in review*), as demonstrated in this thesis. Despite the scarcity of available information, the consistency of this observation suggests that the domination of sponges on rocky reef TME habitats could be a global phenomenon. While considerably more research effort is required to confirm the universality

of this pattern, if this suggestion is correct, then the contribution of marine sponges to marine ecological dynamics on a global scale is likely to be substantial, and currently greatly underestimated.

Aside from providing substantial potential habitat for functionally important benthic invertebrates (including sponges), TMEs are of significant value, both ecologically (e.g. James et al. 2017) and economically (de Oliveira-Soares et al. 2020) in other ways. For example, it has been suggested that mesophotic ecosystems in more thoroughly studied tropical environments act as refugia for shallower water species facing threats from stressors imposed in shallow water environments, in a phenomenon known as the deep reef refuge/refugia" hypothesis (DRRH) (Glynn, 1996; Bongaerts et al. 2010; Bongaerts et al. 2019). These threats to shallow water ecosystems include natural phenomena, such as storm surges (Harmelin-Vivien, 1994) and heat-wave events (e.g. Leggat et al. 2019). However, they also include numerous immediate anthropogenic threats such as unsustainable fishing practices (Saila et al. 1993) acute pollution events (van Dam et al. 2011) or direct habitat destruction (Eddy et al. 2021), as well a long-term global-scale threats, such as oceanic warming and acidification (De'ath et al. 2012; Hughes et al. 2017). While the DRRH has been primarily associated with MCEs (Bongaerts et al. 2010; Bongaerts et al. 2019), it is likely that TMEs provide a similar role for shallow temperate reefs. Long term, and large-scale anthropogenic threats such as oceanic warming and acidification are also likely to impact TMEs themselves (Rocha et al. 2018; Bell et al. *in review*). However, temperate sponges have demonstrated relatively strong resistance to warming (Riisgård et al. 1993) and acidification levels (Bates et al. 2018) within IPCC projections. This suggests that temperate sponges may become increasingly dominant and more important provisioners of habitat complexity for TME species, as well as shallower species conforming to the DDFH under future IPCC scenarios. The concept of resilient sponge species benefiting from increased

warming and acidification due to reduced spatial competition with less adaptable species has been posited by Bell et al. (2013; 2018), although this has only been examined in specific tropical habitats, where spatially competitive, reef building corals are particularly vulnerable to both ocean warming (e.g. Hoegh-Guldberg et al. 2017) and ocean acidification (e.g. Hoegh-Guldberg et al. 2007), which have amplified negative synergistic effects (Prada et al. 2017). Further investigation is required to determine the responses of sponges to climate change scenarios in temperate environments, and how this might manifest in the functions they perform on large scales across both infralittoral and mesophotic habitats. Given the likely significant rocky reef habitat TMEs represent globally, and the apparent domination of sponges in these habitats universally (Bell et al. 2020; Bell et al. *in review*), I suggest temperate sponges, and the functional roles they perform in TMEs should be of high research and management priority moving forward.

6.3 Sponge feeding: sponge population dynamics

Despite some early investigations on the feeding behaviour of temperate species (e.g. Reiswig, 1975; Riisgård et al. 1993; Pile et al. 1996; Ribes et al. 1999), most of the available information of sponge diet, feeding behaviour, and subsequent population dynamics, is from tropical habitats, with several longstanding studies (e.g. Reiswig, 1973; 1974) as well as multiple more recent studies (e.g. Wooster et al. 2019). While this research bias is reflected across the full spectrum of sponge-related studies generally, the more recent bias might be partly due to the observation of sponge-DOC consumption and recycling via the sponge loop (de Goeij et al. 2013), which was originally assumed to be exclusive to tropical sponges exhibiting high microbial abundance (HMA) (Maldonado et al. 2012). However, it is now clear that DOC consumption and subsequent contributions to the sponge loop are also apparent in sponges outside of the tropics, including deep-sea habitats (Bart et al. 2020). Despite this recognition, Chapter 4 represents the only study to my knowledge that has

confirmed significant DOC retention by sponge species outside of the Mediterranean in a true temperate environment, where other studies have demonstrated no uptake or significant net DOC production (e.g. Ribes et al. 1999). However, the DOC consumption observed in *P. penicillus* and *Polymastia* sp. in Chapter 4 requires further investigation, as this coincided with very high ambient DOC concentrations. It is therefore unclear if this is a generic response by temperate sponges to high DOC availability, or if this observation was coincidental, and this species commonly exhibits significant DOC retention in a wide-range of ambient DOC concentration scenarios. The answer to this question is ecologically important as it determines how this novel observation of temperate sponge-DOC retention can be interpreted in a broader ecological context of sponge population dynamics and carbon cycling. If the DOC consumption observed is a generic sponge response to high DOC availability, then this provides an essential piece of information regarding the mechanisms that determine sponge distributions, and their vulnerability to bottom-up effects as investigated in Chapter 3 (see Lesser & Slattery, 2013; Pawlik et al. 2018). However, this would depend on the threshold of the DOC concentration required for sponges to make the 'switch' to DOC feeding. It is also likely to depend heavily on the source and composition of the DOC itself (Rix et al. 2017). DOC is frequently defined throughout the literature (including this thesis) at a crude operational level (all carbon that passes through a GF/F filter), but this is an extremely broad category within which multiple sources and forms of carbon are likely to be represented, and with varying degrees of lability (Nelson et al. 2014). Specific sources and composition of DOC would therefore be a useful consideration of sponge-DOC retention studies generally (see Rix et al. 2017). Alternatively, if the feeding strategy exhibited by *P. penicillus* and *Polymastia* sp. is species-specific, this would be more indicative of resource partitioning across DOC and POC food pools within temperate sponge assemblages, as suggested and discussed in Chapter 4. One study from New Zealand (Perea-

Blázquez et al. 2013b) has suggested resource partitioning is occurring in shallow sponge assemblages within the POC food pool. However, this conclusion was derived from the observation of interspecific differences in retention efficiency of POC groups, which I suggest is a misinterpretation as it this does not account for the relative weighting of resource availability. True selectivity indices can be applied to overcome this issue as was done in Chapter 4, where no partitioning within the POC food pool was observed, suggesting species-specific consumption of DOC to be particularly important in facilitating abundant multi-species sponge assemblages. Confirming the observations of DOC feeding made in Chapter 4 as either a sponge-generic response to DOC availability, or as species-specific feeding behaviour, would also contribute significantly to the on-going and contentious debate surrounding bottom-up effects, and the potential of food limitation in sponges (see Trussell et al. 2006; Lesser & Slattery, 2013; review by Pawlik et al. 2015; comment by Slattery & Lesser (2015); reply by Pawlik et al. 2015; and debate reviews by Pawlik, 2018; Scott & Pawlik, 2019). However, again, this debate has been focused exclusively on tropical environments.

6.4 Sponge feeding: wider ecological implications

Numerous physiological variables contribute to the flux of sponge assemblage biomass including; respiration (Thomassen & Riisgård, 1995; Koopmans et al. 2010), pumping energy expenditure (Leys et al. 1995; Riisgård & Larsen, 1995), and the production of mucus (Biggerstaff et al. 2017), detritus (Alexander et al. 2014), and gametes. Other ecological variables also contribute to this process including predation (Pawlik, 1998), resource competition (Loh & Pawlik, 2014), and abiotic stressors (e.g. wave impact (Monteiro & Muricy, 2004)). However, the production of sponge biomass is most fundamentally dictated by the extent of carbon they retain from the water column, and therefore determines the extent of all the other ecological functions sponges perform (see Bell et al. 2008) including;

micro-habitat provisioning (Wulff, 2006; Taylor et al. 2007; Webster & Taylor, 2012), habitat complexity (Chapter 2), competition pressure (Bell & Barnes, 2003; Wulff, 2006), the alteration of benthic boundary flow regimes (Culwick et al. 2020), the functioning of the sponge loop (de Goeij et al. 2013; Rix et al. 2016) and changes in carbon availability and composition in the water column (Perea-Blázquez et al. 2012; Valentine et al. 2019). However, the relative importance of these functions is likely to change through infralittoral and mesophotic zones as the abundance of other organisms with varying degrees of functional overlap (e.g. the provisioning of habit by macroalgae, Graham et al. 2016) decreases with depth.

Marine microbes regulate fundamental ecological processes at the base of the food web, such as primary production (Flombaum et al. 2013) and the microbial loop (Azam et al. 1983). It would therefore be expected that the substantial pelagic-benthos transfer of microbial community constituents via sponge feeding (as demonstrated in Chapter 5) has important ecological ramifications. However, this also includes consequences for heterotrophic sponge assemblages themselves, where a negative trophic feedback-loop is likely to occur if the microbial community becomes sufficiently reduced by sponge feeding, as according to fundamental predator-prey interaction theory (e.g. Krebs et al. 1995). While I did not consider the potential of ambient food depletion in the Chesson's-Manly alpha food selectivity equations of individual sponges used in Chapter 3, food-depletion and predator-prey theory might help explain what appears to be a discrepancy between the suggestion of food limitation (proposed in Chapter 3), and the microbial and sponge abundance patterns observed in Chapters 2 and 3. For example, the abundance of microbial community components within the inner region of Doubtful Sound was not significantly lower than that of mid and outer regions, and was significantly higher than these other regions at certain depths. This appears to contradict the suggestion of food limitation (assessed as depth-based

as opposed to location-based sponge-food correlations) as the sponge assemblage was significantly more depauperate in the inner region compared to mid and outer regions. Alternatively, the Poor Knights had lower microbial community abundances than all Fiordland regions despite exhibiting an extremely abundant and diverse sponge assemblage. I suggest that this apparent discrepancy can be explained by a combination of classical predator-prey theory, and the consideration of the specific character of the environments assessed. Given the high carbon retention rates exhibited by the sponge assemblage at the Poor Knights, it is likely that the abundance of the surrounding microbial community is being measurably depleted, but the immediate proximity of the Poor Knights to the open ocean allows this process to be sustained at a high level, overcoming the negative feedback loop described in predator-prey theory, and explaining the lack of any apparent food limitation effects occurring here. However, predator-prey feedback loops are much more likely to be observable at inner Fiordland sites where higher food availability is a consequence of reduced pressure from sponge feeding, but cannot facilitate sustained increases in sponge abundance over time (as would occur in a traditional predator-prey theory model) due to the likely drastic reduction in microbial proliferation as a consequence of low light availability (and primary productivity potential), and restricted flushing from the open ocean. I would therefore also suggest that while food limitation appears to an important driver of temperate sponge distributions, the specific environmental context is an essential consideration, where food availability alone is not a viable proxy for sponge abundance distributions.

The ramifications of DOC retention for sponge population dynamics has been briefly discussed (section 6.3) but this might have wider ecological implications; for example, the potential of a temperate sponge loop. Originally, the sponge loop was discovered in the pursuit of solving the resource deficit observed in tropical sponges (de Goeij et al.2008; 2013; Pawlik & McMurray 2020) but it has now also been indicated in Mediterranean sponge

assemblages (Alexander et al. 2014) and observed in deep-sea sponge (Bart et al. 2021) assemblages. The confirmation of the sponge loop requires three components. The first step is to establish that sponges are retaining DOC (as determined in Chapter 4), the second step is to track and confirm the assimilation of DOC into the form of detritus or sponge biomass itself (Rix et al. 2016; Bart et al. 2020; Maier et al. 2020). The third step requires the observation of this material being passed onto to the wider benthic community through detrital (de Goeij et al. 2013) or predatory (McMurray et al. 2018) pathways, or both. Given the substantially lower predation pressure on temperate sponges compared to in the tropics (Wulff, 2006), it is likely that a hypothetical temperate sponge loop would manifest through a detrital pathway, as shown in tropical sponges by Rix et al. (2018). The sponge loop is considered a critical component in maintaining the efficiency of nutrient assimilation and release in environments of low resource availability such as tropical and deep-sea habitats. However, a hypothetical temperate sponge loop is also likely to play an important ecological role especially during seasonal reductions in food availability (Ribes et al. 1999, Perea-Blázquez et al. 2013a) or in the deeper regions of TMEs where food availability in the form of autotrophic microbial communities is significantly reduced (see Chapter 3).

6.5 Limitations and future directions

The restriction of direct observations of sponge feeding and pumping behaviour to shallow-water specimens (as deep-water surrogates) represents the most significant limitation throughout this thesis. *In situ* work below 30 m was not possible due to first person access constraints, including decompression limits imposed by SCUBA, and technological constraints, including limiting remote operated vehicle (ROV) operations to video data collection and sponge tissue sampling only. While assessments of shallow water sponges provide a useful proxy for deep-water sponge behaviour, it is possible that sponges of the same species under similar food availability scenarios may exhibit different feeding

behaviour in the mesophotic zone. This could be another explanation for the DOC retention observed only in sponges in Parininihi marine reserve, as the general characterization of this habitat has been suggested to be more representative of a mesophotic environment (Battershill & Page, 1996). Although, only certain features of the benthic community composition data reported in this thesis support this suggestion (see Chapter 2). A solution to these limitations would be the *in situ* application of advanced Class III ROV technologies to sponge feeding assessments in TMEs, as demonstrated in other studies (e.g. Yahel et al. 2007), or rebreather technology for first-person assessments (Sieber et al. 2010). Class III ROV technologies are capable of the intricate sampling techniques used in feeding assessments (e.g. Yahel et al. 2007), but these machines require extensive deployment infrastructure and multiple professional operators and technicians making this approach often prohibitively expensive. However, Class I ROVs are rapidly increasing in sophistication and popularity, subsequently reducing costs, and generating market pressure to improve their accessibility and range of applications (Tillin et al. 2018). As such, future studies on relatively small budgets may well be able to undertake sophisticated *in situ* protocols using new generation Class I models.

A significant limiting factor of quantifying marine community composition and structure generally, is the high taxonomic resolution and quantity of data easily derived from ROV video footage. This limitation is imposed by the quality of the footage itself, but also by the processing time required to extract appropriate still images and subsequently quantify the abundance of benthic groups manually. New technological advances in ROVs and internal camera systems are likely to help solve this problem at front end with the introduction of relatively cheap integrated 5K cameras, as well as stereoscopic 360° cameras, potentially producing 3-dimensional volume and biomass estimates with high accuracy. On the backend, continued advances in machine learning and artificial intelligence (AI) (Shinde et al. 2018)

are likely to substantially reduce the time required to process video footage manually into numerical data. I envisage this processing time can be potentially reduced to zero without any significant advances in current technologies, where benthic community abundance and composition information can be translated into useable, numerical data frames by automated underwater vehicle (AUV)-AI integrated systems in real-time. These technologies are already in use in different contexts, including real-time facial recognition in beef and pork farming tracking systems (Neethirajan, 2020) as well as in heavily human populated urban areas worldwide (Zhang et al. 2021). The integration and application of these technologies into marine ecological science endeavours worldwide would provide enormous contributions to our understanding of mesophotic and deep-sea benthic habitats and the ecological communities they support globally.

References

Alexander, B.E., Liebrand, K., Osinga, R., van der Geest, H.G., Admiraal, W., Cleutjens, J.P., & de Goeij, J.M. (2014). Cell turnover and detritus production in marine sponges from tropical and temperate benthic ecosystems. *PLoS One*, *9*(10), e109486.

Austen, M.C., Lambshead, P.J.D., Hutchings, P.A., Boucher, G., Snelgrove, P.V.R., Heip, C., & Smith, C. (2002). Biodiversity links above and below the marine sediment-water interface that may influence community stability. *Biodiversity Conservation*, 11(1), 113-136.

Azam, F., Fenchel, T., Field J., Gray, J., Meyer-Reil, L., & Thingstad, F. (1983). The Ecological Role of Water-Column Microbes in the Sea. *Marine Ecology Progress Series*, *10*, 257-263.

Baker, E.K. & Harris, P.T. (Eds.). (2016). Mesophotic coral ecosystems: A lifeboat for coral reefs? United Nations Environment Programme and GRID-Arendal.

Balmford, A. & Gaston, K.J. (1999). Why biodiversity surveys are good value. *Nature* 398(6724), 204-205.

Barrón, C. & Duarte, C.M. (2015). Dissolved organic carbon pools and export from the coastal ocean. *Global Biogeochemical Cycles*, *29*(10), 1725-1738

Bart, M.C., de Kluijver, A., Hoetjes, S., Absalah, S., Mueller, B., Kenchington, E., & de Goeij, J. M. (2020). Differential processing of dissolved and particulate organic matter by deep-sea sponges and their microbial symbionts. *Scientific Reports*, 10(1), 1-13.

Bart, M.C., Hudspith, M., Rapp, H.T., Verdonschot, P.F., & de Goeij, J.M. (2021). A deep-sea sponge loop? Sponges transfer dissolved and particulate organic carbon and nitrogen to associated fauna. *Frontiers in Marine Science*, 8, 229.

Bart, M.C., Mueller, B., Rombouts, T., van de Ven, C., Tompkins, G.J., Osinga, R., & de Goeij, J.M. (2021). Dissolved organic carbon (DOC) is essential to balance the metabolic demands of four dominant North-Atlantic deep-sea sponges. *Limnology and Oceanography*, *66*(3), 925-938.

Bates, T.E.M. & Bell, J.J. (2018). Responses of two temperate sponge species to ocean acidification. *New Zealand Journal of Marine and Freshwater Research* , 52(2), 247-263

Battershill, C.N. & Page, M.J. (1996). Preliminary Survey of Pariokariwa Reef North Taranaki. Report prepared by the National Institute of Water and Atmospheric Research.

Beazley, L.I., Kenchington, E.L., Murillo, F.J., & Sacau, M.D.M. (2013). Deep-sea sponge grounds enhance diversity and abundance of epibenthic megafauna in the Northwest Atlantic. *ICES Marine Science,* 70(7), 1471-1490.

Bell, J.J. (2002). The sponge community in a semi-submerged temperate sea cave: Density, diversity and richness. *Marine Ecology*, 23(4), 297-311.

Bell, J.J. (2007). The ecology of sponges in Lough Hyne Marine Nature Reserve (south-west Ireland): Past, present and future perspectives. *Journal of the Marine Biological Association of the United Kingdom,* 87, 1655-1668.

Bell, J.J. (2008). The functional roles of marine sponges. *Estuarine, Coastal and Shelf Science,* 79(3), 341-353.

Bell, J.J. & Barnes, D.K.A. (2000). The influences of bathymetry and flow regime upon the morphology of sublittoral sponge communities *Journal of the Marine Biological Association of the United Kingdom,* 80(4), 707-718.

Bell, J.J. & Barnes, D.K.A. (2001). Sponge morphological diversity: A qualitative predictor

of species diversity? *Aquatic Conservation: Marine Freshwater Ecosystems* 11(2): 109-121.

Bell, J.J. & Barnes, D.K.A. (2003). The importance of competitor identity, morphology and ranking methodology to outcomes in interference competition between sponges. *Marine Biology* 143(3): 415-426.

Bell, J.J., Jompa, J., Haris, A., Werorilangi, S., Shaffer, M., & Mortimer, C. (2019). Domination of mesophotic ecosystems in the Wakatobi Marine National Park (Indonesia) by sponges, soft corals and other non-hard coral species *Journal of the Marine Biological Association of the United Kingdom* 99(4): 771-775.

Bell, J.J., Bennett, H.M., Rovellini, A., & Webster, N.S. (2018). Sponges to Be Winners under Near-Future Climate Scenarios. *BioScience*, 68(12).

Bell, J.J., Davy, S.K., Jones, T., Taylor, M.W., & Webster, N.S. (2013). Could some coral reefs become sponge reefs as our climate changes? *Global Change Biology*, 19(9), 2613-2624.

Bell, J. J., McGrath, E., Biggerstaff, A., Bates, T., Bennett, H., Marlow, J., & Shaffer, M. (2015). Sediment impacts on marine sponges. *Marine Pollution Bulletin*, *94*(1-2), 5-13.

Bell, J.J., McGrath, E., Kandler, N.M., Marlow, J., Beepat, S.S., Bachtiar, R., Shaffer, M.R., Mortimer, C., Micaroni, V., Mobilia, V., Rovellini, A., Harris, B., Farnham, E., Strano, F., & Carballo, J.L. (2020). Interocean patterns in shallow water sponge assemblage structure and function. *Biological Reviews*, 95(6), 1720-1758.

Bergquist, P.R. (2001). Porifera (Sponges). e *LS*.

Berman, J. & Bell, J.J. (2016). Short-term temporal variability in a temperate sponge assemblage. *Marine Biology*, 163(3), 1-9.

Berman, J., & Bell, J.J. (2010). Spatial variability of sponge assemblages on the Wellington South Coast, New Zealand. *The Open Marine Biology Journal*, 4(1).

Bianchelli, S., Pusceddu, A., Canese, S., Greco, S., & Danovaro, R. (2013). High meiofaunal and nematodes diversity around mesophotic coral oases in the Mediterranean Sea. *PLoS One*, 8(6), e66553.

Biggerstaff, A., Smith, D.J., Jompa, J., & Bell, J.J. (2017). Metabolic responses of a phototrophic sponge to sedimentation supports transitions to sponge-dominated reefs. *Scientific Reports*, *7*(1), 1-11.

Bo, M., Bertolino, M., Bavestrello, G., Canese, S., Giusti, M., Angiolillo, M., & Taviani, M. (2012). Role of deep sponge grounds in the Mediterranean Sea: A case study in southern Italy. *Hydrobiologia*, 687(1), 163-177.

Bo, M., Bertolino, M., Borghini, M., Castellano, M., Covazzi Harriague, A., Di Camillo, C. G., & Bavestrello, G. (2011). Characteristics of the mesophotic megabenthic assemblages of the Vercelli seamount (North Tyrrhenian Sea). *PLoS One*, 6(2), e16357.

Boavida, J., Assis, J., Reed, J., Serrão, E.A., & Gonçalves, J.M.S. (2016). Comparison of small remotely operated vehicles and diver-operated video of circalittoral benthos. *Hydrobiologia* 766(1): 247-260.

Bolam, S.G., Fernandes, T.F., & Huxham, A.M. (2002). Diversity, Biomass, and Ecosystem Processes in the Marine Benthos. *Ecological Monographs*, 72(4), 599-615. doi: 10.2307/3100059.

Bongaerts, P., Ridgway, T., Sampayo, E.M., & Hoegh-Guldberg, O. (2010). Assessing the 'deep reef refugia hypothesis: focus on Caribbean reefs. *Coral Reefs*, 29(2), 309-327.

Bongaerts, P., & Smith, T. B. (2019). Beyond the "Deep Reef Refuge" hypothesis: a

conceptual framework to characterize persistence at depth. *Mesophotic coral ecosystems*, 881-895.

Breitburg, D.L. (1984). Residual effects of grazing: inhibition of competitor recruitment by encrusting coralline algae. *Ecology*, 65(4), 1136-1143.

Brunner, E., Ehrlich, H., Schupp, P., Hedrich, R., Hunoldt, S., Kammer, M., & Born, R. (2009). Chitin-based scaffolds are an integral part of the skeleton of the marine demosponge Ianthella basta. *Journal of Structural Biology*, 168(3), 539-547.

Brylinsky, M. (1977). Release of dissolved organic matter by some marine macrophytes. *Marine Biology*, 39(3), 213-220.

Buitenhuis, E.T., Li, W.K., Vaulot, D., Lomas, M.W., Landry, M.R., Partensky, F., & McManus, G. B. (2012). Picophytoplankton biomass distribution in the global ocean. *Earth System Science Data*, 4(1), 37-46.

Cárdenas, C.A., Davy, S.K., & Bell, J.J. (2012). Correlations between algal abundance, environmental variables and sponge distribution patterns on southern hemisphere temperate rocky reefs. *Aquatic Biology*, 16(3), 229-239.

Cárdenas, C.A, Davy, S.K, & Bell, J.J. (2016). Influence of canopy-forming algae on temperate sponge assemblages. *Journal of the Marine Biological Association of the United Kingdom*, 96(2), 351-362

Castello-Branco, C., Collins, A.G., & Hajdu, E. (2020). A collection of hexactinellids (Porifera) from the deep South Atlantic and North Pacific: new genus, new species and new records. *PeerJ*, 8, e9431.

Cattaneo-Vietti, R., Chiantore, M., Misic, C., Povero, P., & Fabiano, M. (1999). The role of pelagic-benthic coupling in structuring littoral benthic communities at Terra Nova Bay

(Ross Sea) and in the Straits of Magellan. *Scientia Marina*, 63(1), 113-121.

Cerrano, C., Bastari, A., Calcinai, B., Di Camillo, C., Pica, D., Puce, S., Torsani, F., & Valisano, L. (2019) Temperate mesophotic ecosystems: gaps and perspectives of an emerging conservation challenge for the Mediterranean Sea. *The European Zoological Journal,* 86(1): 370-388.

Cerrano, C., Danovaro, R., Gambi, C., Pusceddu, A., Riva, A., & Schiaparelli, S. (2010). Gold coral (*Savalia savaglia*) and gorgonian forests enhance benthic biodiversity and ecosystem functioning in the mesophotic zone. *Biodiversity and Conservation*, 19(1), 153-167.

Chadwick, N.E., & Morrow, K.M. (2011). Competition Among Sessile Organisms on Coral Reefs. In: Dubinsky Z, Stambler N (Eds.) *Coral Reefs: An Ecosystem in Transition*. Springer, Dordrecht.

Chesson, J. (1983). The estimation and analysis of preference and its relationship to foraging models. *Ecology*, 64(5), 1297-1304.

Chimienti, G., Bo, M., & Mastrototaro, F. (2018). Know the distribution to assess the changes: Mediterranean cold-water coral bioconstructions. Rendiconti Lincei. *Scienze Fisiche e Naturali*, 29(3), 583-588.

Chimienti, G., Mastrototaro, F., & D'Onghia, G. (2019). Mesophotic and deep-sea vulnerable coral habitats of the Mediterranean Sea: overview and conservation perspectives. In: *Advances in the Studies of the Benthic Zone* (20). IntechOpen.

Choat, J.H., & Schiel, D.R. (1982). Patterns of distribution and abundance of large brown algae and invertebrate herbivores in subtidal regions of northern New Zealand. *Journal of Experimental Marine Biology and Ecology*, 60(2-3), 129-162.

Coma, R., Ribes, M., Gili, J.M., & Hughes, R.N. (2001). The ultimate opportunists: consumers of seston. *Marine Ecology Progress Series*, 219, 305-308.

Costello, M.J., Coll, M., Danovaro, R., Halpin, P., Ojaveer, H., & Miloslavich, P. (2010). A census of marine biodiversity knowledge, resources, and future challenges. *PLoS One*, 5(8).

Covich, A.P., Austen, M.C., Bärlocher, F., Chauvet, E., Cardinale, B.J., Biles, C.L., & Moss, B. (2004). The role of biodiversity in the functioning of freshwater and marine benthic ecosystems. *BioScience*, 54(8), 767-775.

Crossland, C.J. (1987). In situ release of mucus and DOC-lipid from the corals *Acropora variabilis* and *Stylophora pistillata* in different light regimes. *Coral Reefs*, 6(1), 35-42.

Culwick, T., Phillips, J., Goodwin, C., Rayfield, E. J., & Hendry, K.R. (2020). Sponge density and distribution constrained by fluid forcing in the deep sea. *Frontiers in Marine Science*, 7, 395.

Danovaro, R., Snelgrove, P.V.R., & Tyler, P. (2014). Challenging the paradigms of deep-sea ecology. *Trends in Ecology and Evolution*, 29: 465-475.

de Bakker, D.M., Van Duyl, F.C., Bak, R.P., Nugues, M.M., Nieuwland, G., & Meesters, E.H. (2017). 40 Years of benthic community change on the Caribbean reefs of Curaçao and Bonaire: the rise of slimy cyanobacterial mats. *Coral Reefs*, *36*(2), 355-367.

de Goeij, J.M., Lesser, M.P., & Pawlik, J.R. (2017). Nutrient fluxes and ecological functions of coral reef sponges in a changing ocean.*Climate change, ocean acidification and sponges*, 373-410.

de Goeij, J.M., Van Den Berg, H., Van Oostveen, M.M., Epping, E.H.G., & Van Duyl, F.C. (2008). Major bulk dissolved organic carbon (DOC) removal by encrusting coral reef

cavity sponges. *Marine Ecology Progress Series*, 357, 139-151.

de Goeij, J.M., Van Oevelen, D., Vermeij, M.J., Osinga, R., Middelburg, J.J., de Goeij, A.F., & Admiraal, W. (2013). Surviving in a marine desert: the sponge loop retains resources within coral reefs. *Science*, 342(6154), 108-110.

De Oliveira Soares, M., de Araújo, J.T., Ferreira, S.M.C., Santos, B.A., Boavida, J.R.H., Costantini, F., & Rossi, S. (2020). Why do mesophotic coral ecosystems have to be protected? *Science of the Total Environment*, 726, 138456.

de Voogd, N.J., Becking, L.E., Hoeksema, B.W., & van Soest, R.W.M. (2004). Sponge interactions with spatial competitors in the Spermonde Archipelago. *Bolletino di Museo e Istituto di Biologia dell'Universita di Genova*. 68, 253-261.

De'ath, G., Fabricius, K.E., Sweatman, H., & Puotinen, M. (2012). The 27-year decline of coral cover on the Great Barrier Reef and its causes. *Proceedings of the National Academy of Sciences*, 109(44), 17995-17999.

Degnan, S.M. (2015). The surprisingly complex immune gene repertoire of a simple sponge, exemplified by the NLR genes: a capacity for specificity? *Developmental & Comparative Immunology*, 48(2), 269-274.

Di Camillo, C.G., Boero, F., Gravili, C., Previati, M., Torsani, F., & Cerrano, C. (2013). Distribution, ecology and morphology of *Lytocarpia myriophyllum* (Cnidaria: Hydrozoa), a Mediterranean Sea habitat former to protect. *Biodiversity and Conservation*, 22(3), 773-787.

Diaz, M.C. & Rützler, K. (2001). Sponges: an essential component of Caribbean coral reefs. *Bulletin of Marine Science*, 69(2), 535-546.

Diaz, M.C. & Ward, B.B. (1997). Sponge-mediated nitrification in tropical benthic

communities. *Marine Ecology Progress Series*, 156, 97-107.

Downey, R.V., Griffiths, H.J., Linse, K., & Janussen, D. (2012). Diversity and distribution patterns in high Southern latitude sponges. *PLoS One,* 7(7).

Druffel, E.R., Williams, P.M., Bauer, J.E., & Ertel, J.R. (1992). Cycling of dissolved and particulate organic matter in the open ocean. *Journal of Geophysical Research: Oceans*, 97(C10), 15639-15659.

Duckworth, A.R. (2015). Substrate type affects the abundance and size of a coral-reef sponge between depths. *Marine and Freshwater Research*, 67(2), 246-255.

Duckworth, A.R. & Battershill, C.N. (2001). Population dynamics and chemical ecology of New Zealand Demospongiae Latrunculia sp. nov. and Polymastia croceus (Poecilosclerida: Latrunculiidae: Polymastiidae). *New Zealand Journal of Marine and Freshwater Research*, 35(5), 935-949.

Easson, C.G., Slattery, M., Baker, D.M., & Gochfeld, D.J. (2014). Complex ecological associations: competition and facilitation in a sponge-algal interaction. *Marine Ecology Progress Series,* 507, 153-167.

Egea, L.G., Barron, C., Jiménez-Ramos, R., Hernandez, I., Vergara, J.J., Pérez-Lloréns, J. L., & Brun, F.G. (2019). Coupling carbon metabolism and dissolved organic carbon fluxes in benthic and pelagic coastal communities. *Estuarine, Coastal and Shelf Science*, 227, 106336.

Enrichetti, F., Bavestrello, G., Betti, F., Coppari, M., Toma, M., Pronzato, R., & Bo, M. (2020). Keratose-dominated sponge grounds from temperate mesophotic ecosystems (NW Mediterranean Sea). *Marine Ecology*, 41(6), e12620.

Enrichetti, F., Bo, M., Morri, C., Montefalcone, M., Toma, M., Bavestrello, G., & Bianchi,

C.N. (2019). Assessing the environmental status of temperate mesophotic reefs: A new, integrated methodological approach. *Ecological Indicators*, 102, 218-229.

Evans, G.T. & Parslow, J.S. (1985). A model of annual plankton cycles. *Biological Oceanography*, 3(3), 327-347.

Falkowski, P.G., Barber, R.T., & Smetacek, V. (1998). Biogeochemical controls and feedbacks on ocean primary production. *Science*, 281(5374), 200-206.

Ferrari, R., Marzinelli, E.M., Ayroza, C.R., Jordan, A., Figueira, W.F., Byrne, M., & Steinberg, P.D. (2018). Large-scale assessment of benthic communities across multiple marine protected areas using an autonomous underwater vehicle. *PLoS One* 13(3)

Flombaum, P., Gallegos, J.L., Gordillo, R.A., Rincón, J., Zabala, L.L., Jiao, N., & Martiny, A.C. (2013). Present and future global distributions of the marine Cyanobacteria Prochlorococcus and Synechococcus. *Proceedings of the National Academy of Sciences*, 110(24), 9824-9829.

Folkers, M. & Rombouts, T. (2020). Sponges Revealed: A Synthesis of Their Overlooked Ecological Functions Within Aquatic Ecosystems. In: Jungblut S, Liebich V, Bode-Dalby (Eds) *YOUMARES 9 - The Oceans: Our Research, Our Future*. Springer, Cham: (181-193).

Forbes, V.E., Calow, P., & Sibly, R.M. (2008). The extrapolation problem and how population modeling can help. *Environmental Toxicology and Chemistry: An International Journal*, 27(10), 1987-1994.

Freese, J.L. & Wing, B.L. (2003). Juvenile red rockfish, Sebastes sp., associations with sponges in the Gulf of Alaska. *Marine Fisheries Review*, 65(3), 38-42.

Fromont, J. & Garson, M. (1999). Sponge bleaching on the West and East coasts of Australia.

Coral Reefs, 18(4), 340.

Gantt, S.E., McMurray, S.E., Stubler, A.D., Finelli, C.M., Pawlik, J.R., & Erwin, P.M. (2019). Testing the relationship between microbiome composition and flux of carbon and nutrients in Caribbean coral reef sponges. *Microbiome*, 7(1), 1-13.

Genin, A.S.G., Monismith, M.A., Reidenbach, G. Yahel, & J.R. Koseff. (2009). Intense benthic grazing of phytoplankton in a coral reef. Limnology and Oceanography, 54, 938–951.

George, A.M., Brodie, J., Daniell, J., Capper, A., & Jonker, M. (2018). Can sponge morphologies act as environmental proxies to biophysical factors in the Great Barrier Reef, Australia? *Ecological Indicators*, 93, 1152-1162.

Gherardi M., Giangrande, A., & Corriero, G. (2001). Epibiontic and endobiontic polychaetes of Geodia cydonium (Porifera, Demospongiae) from the Mediterranean Sea. *Hydrobiologia* 443(1), 87-101.

Gili, J.M. & Coma, R. (1998). Benthic suspension feeders: Their paramount role in littoral marine food webs. *Trends in Ecology and Evolution*, 13(8), 316-321.

Glynn, P.W. (1996). Coral reef bleaching: facts, hypotheses and implications. *Global Change Biology*, 2(6), 495-509.

Gökalp, M., Kuehnhold, H., de Goeij, J.M., & Osinga, R. (2020). Depth and turbidity affect *in situ* pumping activity of the Mediterranean sponge *Chondrosia reniformis* (Nardo, 1847). *BioRxiv*, 2020.03.30.009290

Goodwin, E., & Cornelisen, C.D. (2012). Near-surface water temperatures in Doubtful Sound and response to natural and anthropogenic drivers. *New Zealand Journal of Marine and Freshwater Research*, *46*(3), 411-429.

Goldstein, J., Riisgård, H.U., & Larsen, P.S. (2019). Exhalant jet speed of single-osculum explants of the demosponge Halichondria panicea and basic properties of the sponge-pump. *Journal of Experimental Marine Biology and Ecology*, 511, 82-90.

Graham, N.A.J., & Nash, K.L. (2013). The importance of structural complexity in coral reef ecosystems. *Coral Reefs*, 32(2): 315-326.

Graham, M.H., Fox, M.D., & Hamilton, S.L. (2016). Macrophyte productivity and the provisioning of energy and habitat to nearshore systems. *Marine macrophytes as foundation species*, 133-152.

Haas, A.F., Nelson, C.E., Wegley-Kelly, L., Carlson, C.A., Rohwer, F., Leichter, J.J., & Smith, J.E. (2011). Effects of coral reef benthic primary producers on dissolved organic carbon and microbial activity. *PloS One*, 6(11), e27973.

Hadas, E., Ilan, M., & Shpigel, M. (2008). Oxygen consumption by a coral reef sponge. *Journal of Experimental Biology*, 211(13), 2185-2190.

Hadas, E., Shpigel, M., & Ilan, M. (2009). Particulate organic matter as a food source for a coral reef sponge. *Journal of Experimental Biology*, 212(22), 3643-3650.

Hansell, D.A., Carlson, C.A. (Eds.). (2014). Biogeochemistry of marine dissolved organic matter. Elsevier Science USA (Academic Press), San Diego.

Hanson, C.E., McLaughlin, M.J., Hyndes, G.A., & Strzelecki, J. (2009). Selective uptake of prokaryotic picoplankton by a marine sponge (Callyspongia sp.) within an oligotrophic coastal system. *Estuarine, Coastal and Shelf Science*, 84(2), 289-297.

Harmelin-Vivien, M.L. (1994). The effects of storms and cyclones on coral reefs: a review. *Journal of Coastal Research*, 211-231.

Harmelin, J.G., Boury-Esnault, N., & Vacelet, J. (1994). A bryozoan-sponge symbiosis: the

association between *Smittina cervicornis* and *Halisarca cf. dujardini* in the Mediterranean. *Biology and Palaeobiology of Bryozoans*, 69-74.

Hartman, W.D. (1964). Taxonomy of Calcareous Sponges: A Revision of the Classification of the Calcareous Sponges. *Science*, 144(3619), 711-712.

Hatcher, B.G. (1990). Coral reef primary productivity. A hierarchy of pattern and process. *Trends in Ecology & Evolution*, 5(5), 149-155.

Hawkes, N., Korabik, M., Beazley, L., Rapp, H. T., Xavier, J.R., & Kenchington, E. (2019). Glass sponge grounds on the Scotian Shelf and their associated biodiversity. *Marine Ecology Progress Series*, 614, 91-109.

Henkel, T.P. & Pawlik, J.R. (2005). Habitat use by sponge-dwelling brittlestars. *Marine Biology* 146(2), 301-313.

Heyns, E.R., Bernard, A.T.F., Richoux, N.B., & Götz, A. (2016). Depth-related distribution patterns of subtidal macrobenthos in a well-established marine protected area. *Marine Biology*, 163(2), 39.

Hill, M.S., Lopez, N.A., & Young, K.A. (2005). Anti-predator defenses in western North Atlantic sponges with evidence of enhanced defense through interactions between spicules and chemicals. *Marine Ecology Progress Series*, 291, 93-102.

Hinderstein, L.M., Marr, J.C.A., Martinez, F.A., Dowgiallo, M.J., Puglise, K.A., Pyle, R.L., Zawada, D.G., & Appeldoorn, R. (2010). Theme section on "Mesophotic coral ecosystems: characterization, ecology, and management. *Coral Reefs*, (29)2, 247-251.

Hoegh-Guldberg, O., Mumby, P.J., Hooten, A.J., Steneck, R.S., Greenfield, P., Gomez, E., & Hatziolos, M.E. (2007). Coral Reefs under rapid climate change and ocean acidification. *Science*, 318(5857), 1737-1742.

Hoegh-Guldberg, O., Poloczanska, E.S., Skirving, W., & Dove, S. (2017). Coral reef ecosystems under climate change and ocean acidification. *Frontiers in Marine Science*, 4, 158.

Hoer, D.R., Gibson, P.J., Tommerdahl, J.P., Lindquist, N.L., & Martens, C.S. (2018). Consumption of dissolved organic carbon by Caribbean reef sponges. *Limnology and Oceanography*, 63(1), 337-351.

Hogg, M.M., Tendal, O.S., Conway, K.W., Pomponi, S.A., van Soest, R.W.M., Gutt, J., Krautter, M., & Roberts, J.M. (2010). Deep-Sea Sponge Grounds: Reservoirs of Biodiversity. UNEP-WCMC Biodiversity Series (32). UNEP-WCMC, Cambridge, UK.

Howe, J.A., Austin, W.E.N., Forwick, M., Paetzel, M., Harland, R., & Cage, A.G. (2010) Fjord systems and archives: A review. *Geololgical Society Special Publication*, 344: 5-15

Hooper, J.N. & van Soest, R.W & Willenz, P. (2002). Systema Porifera. a guide to the classification of sponges. In: Hooper, J.N. & van Soest, R.W (Eds.). *Systema Porifera*, Springer, Boston, MA.

Hughes, T.P., Barnes, M.L., Bellwood, D.R., Cinner, J.E., Cumming, G.S., Jackson, J.B., & Scheffer, M. (2017). Coral Reefs in the Anthropocene. *Nature*, 546(7656), 82-90.

Hunting, E.R., Franken, O., Knopperts, F., Kraak, M.H., Vargas, R., Röling, W.F., & Van Der Geest, H. G. (2013). Substrate as a driver of sponge distributions in mangrove ecosystems. *Marine Ecology Progress Series*, 486, 133-141.

Idan T., Shefer S., Feldstein T., Yahel R., Huchon D., & Ilan, M. (2018) Shedding light on an East-Mediterranean mesophotic sponge ground community and the regional sponge fauna Mediterranean. *Journal of Marine Science*, 19(1), 84-106.

James, L.C., Marzloff, M.P., Barrett, N., Friedman, A., & Johnson, C.R. (2017). Changes in deep reef benthic community composition across a latitudinal and environmental gradient in temperate Eastern Australia. *Marine Ecology Progress Series*, 565, 35-52.

Jørgensen, C.B. (1955). Quantitative aspects of filter feeding in invertebrates. *Biological Reviews*, 30(4), 391-453.

Kahn, A.S., Ruhl, H.A., & Smith, K.L. (2012). Temporal changes in deep-sea sponge populations are correlated to changes in surface climate and food supply. *Deep Sea Research I*, 70, 36-41.

Kahn, A S., Yahel, G., Chu, J.W., Tunnicliffe, V., & Leys, S.P. (2015). Benthic grazing and carbon sequestration by deep-water glass sponge reefs. *Limnology and Oceanography*, 60(1), 78-88.

Kahng, S.E., Garcia-Sais, J.R., Spalding, H.L., Brokovich, E., Wagner, D., Weil, E., & Toonen, R.J. (2010). Community ecology of mesophotic coral reef ecosystems. *Coral Reefs*, 29(2), 255-275.

Kahng, S.E., Copus, J.M., & Wagner, D. (2014). Recent advances in the ecology of mesophotic coral ecosystems (MCEs). *Current Opinion in Environmental Sustainability*, 7, 72-81.

Kealy, R.A., Busk, T., Goldstein, J., Larsen, P.S., & Riisgård, H.U. (2019). Hydrodynamic characteristics of aquiferous modules in the demosponge Halichondria panicea. *Marine Biology Research*, 15, 531-540.

Keesing, J.K., Usher, K.M., & Fromont, J. (2012). First record of photosynthetic cyanobacterial symbionts from mesophotic temperate sponges. *Marine and freshwater research*, 63(5), 403-408.

Kelly, M. & Rowden, A.A. (2019). New sponge species from hydrothermal vent and cold seep sites off New Zealand. *Zootaxa*, 4576(3): 401-438

Kelly, M. & Sim-Smith, C. (2009). A literature review on the Poor Knights Islands Marine Reserve. *Report prepared by the National Institute of Water & Atmospheric Research Ltd for Department of Conservation*, Northland Conservancy 122.

Khailov, K.M. & Burlakova, Z.P. (1969). Release of dissolved organic matter by marine seaweeds and distribution of their total organic production to inshore communities. *Limnology and Oceanography*, 14(4), 521-527.

Klitgaard, A.B. (1995). The fauna associated with outer shelf and upper slope sponges (Porifera, Demospongiae) at the Faroe Islands, northeastern Atlantic. *Sarsia*, 80(1), 1-22.

Klitgaard, A.B. & Tendal, O.S. (2004). Distribution and species composition of mass occurrences of large-sized sponges in the northeast Atlantic. *Progress in Oceanography*, 61(1), 57-98.

Knudby, A., Kenchington, E., & Murillo, F.J. (2013). Modeling the distribution of Geodia sponges and sponge grounds in the Northwest Atlantic. *PloS One*, 8(12), e82306.

Konar, B. & Iken, K. (2005). Competitive dominance among sessile marine organisms in a high Arctic boulder community. *Polar Biology*, 29(1), 61-64.

Koopmans, M., Martens, D., & Wijffels, R.H. (2010). Growth efficiency and carbon balance for the sponge Haliclona oculata. *Marine biotechnology*, 12(3), 340–349.

Koopmans, M., van Rijswijk, P., Boschker, H.T., Marco, H., Martens, D., & Wijffels, R.H. (2015). Seasonal variation of fatty acids and stable carbon isotopes in sponges as indicators for nutrition: biomarkers in sponges identified. *Marine Biotechnology*, 17(1),

43-54.

Krause-Jensen, D., Middelboe, A.L., Carstensen, J., & Dahl, K. (2007). Spatial patterns of macroalgal abundance in relation to eutrophication. *Marine Biology*, 152(1), 25-36.

Krebs, C.J., Boutin, S., Boonstra, R., Sinclair, A.R.E., Smith, J. N. M., Dale, M.R., & Turkington, R. (1995). Impact of food and predation on the snowshoe hare cycle. *Science*, 269(5227), 1112-1115.

Kristensen, E. (1984). Effect of natural concentrations on nutrient exchange between a polychaete burrow in estuarine sediment and the overlying water. *Journal of Experimental Marine Biology and Ecology*, 75(2), 171-190

Kristensen, E. & Blackburn, T.H. (1987). The fate of organic carbon and nitrogen in experimental marine sediment systems: Influence of bioturbation and anoxia. *Journal of Marine Research*, 45(1), 231-257.

Kumala, L., Riisgård, H.U., & Canfield, D.E. (2017). Osculum dynamics and filtration activity in small single-osculum explants of the demosponge Halichondria panicea. *Marine Ecological Progress Series*, 572, 117-128.

Kutti, T., Bannister, R.J., & Fosså, J.H. (2013). Community structure and ecological function of deep-water sponge grounds in the Traenadypet MPA—Northern Norwegian continental shelf. *Continental Shelf Research*, 69, 21-30.

Lam, K., Shin, P.K.S., Bradbeer. R., Randall, D., Ku, K.K.K., Hodgson, P., & Cheung, S.G. (2006). A comparison of video and point intercept transect methods for monitoring subtropical coral communities. *Journal of Experimental Marine Biology and Ecology*, 333(1), 115-128.

Eddy, T.D., Lam, V.W., Reygondeau, G., Cisneros-Montemayor, A.M., Greer, K.,

Palomares, M.L.D., & Cheung, W.W. (2021). Global decline in capacity of coral reefs to provide ecosystem services. *One Earth*, *4*(9), 1278-1285.

Lee, C., Wakeham, S. & Arnosti, C. (2004). Particulate organic matter in the sea: the composition conundrum. AMBIO: *A Journal of the Human Environment*, 33(8), 565-575.

Lee, S. & Fuhrman, J.A. (1987). Relationships between biovolume and biomass of naturally derived marine bacterioplankton. *Applied and Environmental Microbiology*, 53(6), 1298-1303.

Leggat, W.P., Camp, E.F., Suggett, D.J., Heron, S.F., Fordyce, A.J., Gardner, S., & Ainsworth, T.D. (2019). Rapid coral decay is associated with marine heatwave mortality events on reefs. *Current Biology*, 29(16), 2723-2730.

Lemloh, M.L., Fromont, J., Brümmer, F., & Usher, K.M. (2009). Diversity and abundance of photosynthetic sponges in temperate Western Australia. *BMC Ecology*, 9(1), 1-13.

Lesser, M.P. (2006). Benthic-pelagic coupling on coral reefs: feeding and growth of Caribbean sponges. *Journal of Experimental Marine Biology and Ecology*, 328(2), 277-288.

Lesser, M.P. & Slattery, M. (2013). Ecology of Caribbean sponges: Are top-down or bottom-up processes more important? *PloS One* 8(11), 1-9.

Lesser, M.P. & Slattery, M. (2019). Sponge density increases with depth throughout the Caribbean: Reply. *Ecosphere*, 10(4).

Lesser, M.P., Slattery, M., & Leichter, J.J. (2009). Ecology of mesophotic coral reefs. *Journal of Experimental Marine Biology and Ecology*, 375, 1-8.

Lesser, M.P., Slattery, M., & Mobley, C.D. (2018). Biodiversity and functional ecology of

mesophotic coral reefs. *Annual Review of Ecology, Evolution, and Systematics* 49, 49-71.

Levin, L.A. & Michener, R.H. (2002). Isotopic evidence for chemosynthesis-based nutrition of macrobenthos: The lightness of being at Pacific methane seeps. *Limnology and Oceanography*, 47(5), 1336-1345.

Loh, T.L. & Pawlik, J.R. (2014). Chemical defenses and resource trade-offs structure sponge communities on Caribbean coral reefs. *Proceedings of the National Academy of Sciences*, 111(11), 4151-4156.

López-Victoria, M., Zea, S., & Weil, E. (2006). Competition for space between encrusting excavating Caribbean sponges and other coral reef organisms. *Marine Ecology Progress Series*, 312, 113-121.

Ludeman, D.A., Reidenbach, M.A., & Leys, S.P. (2017). The energetic cost of filtration by demosponges and their behavioural response to ambient currents. *Journal of Experimental Biology*, *220*(6), 995-1007.

Maier, S.R., Kutti, T., Bannister, R.J., Fang, J.K.H., van Breugel, P., van Rijswijk, P., & Van Oevelen, D. (2020). Recycling pathways in cold-water coral reefs: Use of dissolved organic matter and bacteria by key suspension feeding taxa. *Scientific Reports*, 10(1), 1-13.

Maldonado, M., Aguilar, R., Bannister, R., Bell, J., Conway, K., Dayton, P.K., Díaz, C., Gutt, J., Kelly, M., Kenchington, E.L. and Leys, S.P., (2017). Sponge grounds as key marine habitats: a synthetic review of types, structure, functional roles and conservation concerns. In: Rossi S, Bramanti L, Gori A, Orejas Saco del Valle C (Eds.). Springer, Cham. *Marine Animal Forests*. 2015, 1-39.

Maldonado, M., Ribes, M., & van Duyl, F.C. (2012). Nutrient fluxes through sponges: biology, budgets, and ecological implications. *Advances in Marine Biology*, 62, 113-182.

Maldonado, M., Zhang, X., Cao, X., Xue, L., Cao, H., & Zhang, W. (2010). Selective feeding by sponges on pathogenic microbes: a reassessment of potential for abatement of microbial pollution. *Marine Ecology Progress Series*, *403*, 75-89.

Marie, D., Brussaard, C.P., Thyrhaug, R., Bratbak, G., & Vaulot, D. (1999). Enumeration of marine viruses in culture and natural samples by flow cytometry. *Applied and Environmental Microbiology*, 65(1), 45-52.

Marie, D., Partensky, F., Jacquet, S., & Vaulot, D. (1997). Enumeration and cell cycle analysis of natural populations of marine picoplankton by flow cytometry using the nucleic acid stain SYBR Green I. *Applied and Environmental Microbiology*, 63(1), 186-193.

Maschette, D., Fromont, J., Platell, M.E., Coulson, P.G., Tweedley, J.R., & Potter, I.C. (2020). Characteristics and implications of spongivory in the Knifejaw Oplegnathus woodwardi (Waite) in temperate mesophotic waters. *Journal of Sea Research*, 157, 101847.

McClintock, J.B., Amsler, C.D., Baker, B.J., & Van Soest, R.W. (2005). Ecology of Antarctic marine sponges: an overview. *Integrative and Comparative Biology*, l 45(2), 359-368.

Mcgrath, E.C., Woods, L., Jompa, J., Haris, A., & Bell, J.J. (2018). Growth and longevity in giant barrel sponges: Redwoods of the reef or Pines in the Indo-Pacific? *Scientific Reports*, 8, 15317.

McMurray, S.E., Finelli, C.M., & Pawlik, J.R. (2015). Population dynamics of giant barrel sponges on Florida coral reefs. *Journal of Experimental Marine Biology and Ecology*, 473, 73-80.

McMurray, S.E., Johnson, Z.I., Hunt, D.E., Pawlik, J.R., & Finelli, C.M. (2016). Selective feeding by the giant barrel sponge enhances foraging efficiency. *Limnology and Oceanography*, 61(4), 1271-1286.

McMurray, S.E., Pawlik, J.R., & Finelli, C.M. (2017). Demography alters carbon flux for a dominant benthic suspension feeder, the giant barrel sponge, on Conch Reef, Florida Keys. *Functional Ecology*, 31(11), 2188-2198.

McMurray, S.E., Stubler, A.D., Erwin, P.M., Finelli, C. M., & Pawlik, J.R. (2018). A test of the sponge-loop hypothesis for emergent Caribbean reef sponges. *Marine Ecology Progress Series*, 588, 1-14.

Mentges, A., Feenders, C., Deutsch, C., Blasius, B., & Dittmar, T. (2019). Long-term stability of marine dissolved organic carbon emerges from a neutral network of compounds and microbes. *Scientific Reports*, 9(1), 1-13.

Meylan, A. (1988). Spongivory in hawksbill turtles: a diet of glass. *Science*, 239(4838), 393-395.

Miller, R.J., Hocevar, J., Stone, R.P., & Fedorov, D.V. (2012). Structure-Forming Corals and Sponges and Their Use as Fish Habitat in Bering Sea Submarine Canyons. *PloS One* 7(3), e33885.

Ministry for the Environment (2014). Fiordland (Te Moana o Atawhenua) *Marine Management Act* (2005).

Monteiro, L. C., & Muricy, G. (2004). Patterns of sponge distribution in Cagarras

Archipelago, Rio de Janeiro, Brazil. *Journal of the Marine Biological Association of the United Kingdom*, *84*(4), 681-687.

Morganti, T., Yahel., G., Ribes, M., & Coma, R. (2016). VacuSIP, an improved InEx method for in situ measurement of particulate and dissolved compounds processed by active suspension feeders. *JoVE (Journal of Visualized Experiments)*, (114), e54221.

Morganti, T.M., Ribes, M., Moskovich, R., Weisz, J.B., Yahel, G., & Coma, R. (2021). In situ Pumping Rate of 20 Marine Demosponges Is a Function of Osculum Area. *Frontiers in Marine Science*, *8*, 583188.

Morganti, T.M., Ribes, M., Yahel, G., & Coma, R. (2019). Size is the major determinant of pumping rates in marine sponges. *Frontiers in physiology*, *10*, 1474.

Mostajir B., Amblard C., Buffan-Dubau E., De Wit R., Lensi R., Sime-Ngando T. (2015) Microbial Food Webs in Aquatic and Terrestrial Ecosystems. In: Bertrand, J.C., Caumette P., Lebaron P., Matheron R., Normand P., Sime-Ngando T. (Eds.). *Environmental Microbiology: Fundamentals and Applications.* Springer, Dordrecht

Mueller, B., de Goeij, J.M., Vermeij, M.J.A., Mulders, Y., Van Der Ent, E., Ribes, M., & Van Duyl, F.C. (2014). Natural diet of coral-excavating sponges consists mainly of dissolved organic carbon (DOC). *PloS One*, 9(2).

Müller, W.E. (2003). The origin of metazoan complexity: Porifera as integrated animals. *Integrative and Comparative Biology*, 43(1), 3-10.

Murillo, F.J., Muñoz, P.D., Cristobo, J., Ríos, P., González, C., Kenchington, E., & Serrano, A. (2012). Deep-sea sponge grounds of the Flemish Cap, Flemish Pass and the Grand Banks of Newfoundland (Northwest Atlantic Ocean): distribution and species

composition. *Marine Biology Research*, 8(9), 842-854.

Muscente, A.D., Michel, F.M., Dale, J.G., & Xiao, S. (2015). Assessing the veracity of Precambrian 'sponge'fossils using in situ nanoscale analytical techniques. *Precambrian Research*, 263, 142-156.

Naumann, M.S., Haas, A., Struck, U., Mayr, C., el-Zibdah, M., & Wild, C. (2010). Organic matter release by dominant hermatypic corals of the Northern Red Sea. *Coral Reefs*, 29(3), 649-659.

Neethirajan, S. (2020). The role of sensors, big data and machine learning in modern animal farming. *Sensing and Bio-Sensing Research*, (29), 100367.

Nelson, W.A. (2009). Calcified macroalgae-critical to coastal ecosystems and vulnerable to change: a review. *Marine Freshwater Research*, 60(8). 787-801.

Nelson, C.E., & Wear, E. K. (2014). Microbial diversity and the lability of dissolved organic carbon. *Proceedings of the National Academy of Sciences*, 111(20), 7166-7167.

Norström, A.V., Nyström, M., Lokrantz, J., & Folke, C. (2009). Alternative states on coral reefs: beyond coral-macroalgal phase shifts. *Marine Ecology Progress Series*, 376, 295-306.

Palumbi, S.R. (1986). How body plans limit acclimation: responses of a demosponge to wave force. *Ecology*, 67(1), 208-214.

Parker, G.H. (1914). On the strength and the volume of the water currents produced by sponges. *Journal of Experimental Zoology*, 16(3), 443-446.

Partensky, F., Blanchot, J., & Vaulot, D. (1999). Differential distribution and ecology of Prochlorococcus and Synechococcus in oceanic waters: a review. *Bulletin de l'institut océanographique de Monaco, (spécial 19),* 457-475.

Partensky, F., Hess, W.R., & Vaulot, D. (1999). Prochlorococcus, a marine photosynthetic prokaryote of global significance. *Microbiology and Molecular Biology Reviews*, 63(1), 106-127.

Pawlik, J.R. (1998). Coral reef sponges: Do predatory fishes affect their distribution? *Limnology and Oceanography*, 43(6), 1396-1399.

Pawlik, J.R., & McMurray, S.E. (2020). The emerging ecological and biogeochemical importance of sponges on coral reefs. *Annual Review of Marine Science*, 12, 315-337.

Pawlik, J.R., Chanas, B., Toonen, R.J., & Fenical, W. (1995). Defenses of Caribbean sponges against predatory reef fish. I. Chemical deterrency. *Marine Ecology Progress Series*, 127, 183-194.

Pawlik, J.R., Loh, T.L., & McMurray, S.E. (2018). A review of bottom-up vs. top-down control of sponges on Caribbean fore-reefs: what's old, what's new, and future directions. *PeerJ*, 6, e4343.

Pawlik, J. R., Loh, T. L., McMurray, S. E., & Finelli, C. M. (2013). Sponge communities on Caribbean coral reefs are structured by factors that are top-down, not bottom-up. *PloS One*, 8(5), e62573.

Pawlik, J.R., McMurray, S.E., Erwin, P., & Zea, S. (2015). A review of evidence for food limitation of sponges on Caribbean reefs. *Marine Ecology Progress Series*, 519, 265-283.

Pawlik, J.R., McMurray, S.E., Erwin, P., & Zea, S. (2015). No evidence for food limitation of Caribbean reef sponges: reply to Slattery & Lesser (2015). *Marine Ecology Progress Series*, 527, 281-284.

Perea-Blázquez, A., Price, K., Davy, S.K., & Bell, J.J. (2010). Diet composition of two

temperate calcareous sponges: Leucosolenia echinata and Leucetta sp. from the Wellington South Coast, New Zealand. *The Open Marine Biology Journal*, 4(1).

Perea-Blázquez A., Davy S.K., Bell J.J. (2011). Nutrient utilisation by shallow water temperate sponges in New Zealand. In: Maldonado M., Turon X., Becerro M., Jesús Uriz M. (Eds.). *Ancient Animals, New Challenges. Developments in Hydrobiology*, (219). Springer, Dordrecht.

Perea-Blázquez, A., Davy, S.K, Bell, J.J. (2012). Estimates of particulate organic carbon flowing from the pelagic environment to the benthos through sponge assemblages. *PloS One* 7(1), e29569.

Perea-Blázquez, A., Davy, S.K., Magana-Rodríguez, B., & Bell, J.J. (2013a). Temporal variation in food utilisation by three species of temperate demosponge. *Marine Ecology Progress Series*, 485, 91-103.

Perea-Blázquez, A., Davy, S.K., & Bell, J.J. (2013b). Low functional redundancy in sponges as a result of differential picoplankton use. *Biological Bulletin*, 224(1), 29-34.

Pile, A.J., Patterson, M.R. & Witman, J.D. (1996). In situ grazing on plankton <10 μm by the boreal sponge Mycale lingua, *Marine Ecology Progress Series*, 141(1-3), 95-102.

Pile, A.J., Patterson, M.R., Savarese, M., Chernykh, V.I., & Fialkov, V.A. (1997). Trophic effects of sponge feeding within Lake Baikal's littoral zone. 2. Sponge abundance, diet, feeding efficiency, and carbon flux. *Limnology and Oceanography*, 42(1), 178-184.

Ponzi, E., Keller, L.F., & Muff, S. (2019). The simulation extrapolation technique meets ecology and evolution: A general and intuitive method to account for measurement error. *Methods in Ecology and Evolution*, 10(10), 1734-1748.

Poore, G.C.B. & Wilson, G. (1993). Marine species richness - Reply. *Nature*, 361(6413),

598.

Prada, F., Caroselli, E., Mengoli, S., Brizi, L., Fantazzini, P., Capaccioni, B., & Goffredo, S. (2017). Ocean warming and acidification synergistically increase coral mortality. *Scientific Reports*, 7(1), 1-10.

Preciado, I., & Maldonado, M. (2005). Reassessing the spatial relationship between sponges and macroalgae in sublittoral rocky bottoms: a descriptive approach. *Helgoland Marine Research*, 59(2), 141-150.

Randall, J. E., & Hartman, W. D. (1968). Sponge-feeding fishes of the West Indies. *Marine Biology*, *1*(3), 216-225.

Raymond, P.A., & Spencer, R.G. (2015). Riverine DOM. In: D.A. Hansell, C.A. Carlson (Eds.). *Biogeochemistry of marine dissolved organic matter* (509-533). Academic Press, Elsevier, Amsterdam.

Reiswig, H.M. (1973). Population Dynamics of Three Jamaican Demospongiae. *University of Miami - Rosentiel School of marine Atmospheric Science*, 23(2), 191-226.

Reiswig, H.M. (1974). Water transport, respiration and energetics of three tropical marine sponges. *Journal of Experimental Marine Biology and Ecology*, 14(3), 231-249.

Reiswig, H.M. (1975). Bacteria as food for temperate-water marine sponges. *Canadian Journal of Zoology*, 53(5), 582-589.

Reiswig, H.M. (1981). Partial Carbon and Energy Budgets of the Bacteriosponge *Verohgia fistularis* (Porifera: Demospongiae) in Barbados. *Marine Ecology*, 2(4), 273-293.

Ribeiro, S.M., Omena, E.P., & Muricy, G. (2003). Macrofauna associated to Mycale microsigmatosa (Porifera, Demospongiae) in rio de Janeiro state, SE Brazil. *Estuarine, Coastal and Shelf Science*, 57(5-6), 951-959.

Ribes, M., Coma, R., & Gili, J.M. (1999). Natural diet and grazing rate of the temperate sponge Dysidea avara (Demospongiae, Dendroceratida) throughout an annual cycle. *Marine Ecology Progress Series*, 176, 179-190.

Ribes, M., Jiménez, E., Yahel, G., López-Sendino, P., Díez, B., Massana, R., & Coma, R. (2012). Functional convergence of microbes associated with temperate marine sponges. *Environmental Microbiology*, 14(5), 1224-1239.

Riedi, M.A. & Smith, A.M. (2015). Tube growth and calcification of two reef-building ecosystem engineers in southern New Zealand: Galeolaria hystrix and Spirobranchus cariniferus (Polychaeta: Serpulidae). *Marine Geology*, 367, 212-219

Riisgård, H.U., Thomassen, S., Jakobsen, H., Weeks, J.M., & Larsen, P.S. (1993). Suspension feeding in marine sponges *Halichondria panicea* and *Haliclona urceolus*: effects of temperature on filtration rate and energy cost of pumping. *Marine Ecology Progress Series*, 177-188.

Riisgaard, H.U. & Larsen, P.S. (1995). Filter-feeding in marine macro-invertebrates: pump characteristics, modelling and energy cost. *Biological Reviews*, *70*(1), 67-106.

Rivero Calle, S. (2010). Ecological aspects of sponges in mesophotic coral ecosystems. PhD thesis, *University of Puerto Rico,* Mayaguez, Puerto Rico.

Rix, L., de Goeij, J.M., Mueller, C.E., Struck, U., Middelburg, J.J., Van Duyl, F C., & Van Oevelen, D. (2016). Coral mucus fuels the sponge loop in warm-and cold-water coral reef ecosystems. *Scientific Reports*, 6(1), 1-11.

Rix, L., de Goeij, J.M., van Oevelen, D., Struck, U., Al-Horani, F.A., Wild, C., & Naumann, M.S. (2017). Differential recycling of coral and algal dissolved organic matter via the sponge loop. *Functional Ecology*, 31(3), 778-789.

Roberts, D.E., Cummins, S.P., Davis, A.R., & Chapman, M.G. (2006). Structure and dynamics of sponge-dominated assemblages on exposed and sheltered temperate reefs. *Marine Ecology Progress Series*, 321, 19-30.

Rocha, L.A., Pinheiro, H.T., Shepherd, B., Papastamatiou, Y.P., Luiz, O.J., Pyle, R.L., & Bongaerts, P. (2018). Mesophotic coral ecosystems are threatened and ecologically distinct from shallow water reefs. *Science,* 361(6399), 281-284.

Rossi, S., Bramanti, L., Gori, A., & Orejas, C. (Eds.). (2017). *Marine animal forests: the ecology of benthic biodiversity hotspots* (1-28). Cham: Springer International Publishing.

Russ, G.R. (1982) Overgrowth in a marine epifaumal community: Competitive hierarchies and competitive networks. *Oecologia,* 53(1), 12-19.

Rützler, K. (1970). Spatial competition among porifera: Solution by epizoism. *Oecologia,* 5(2), 85-95.

Rützler, K. (2002). Impact of crustose clionid sponges on Caribbean reef corals. *Acta Geologica Hispanica*, 61-72.

Ryer. C.H., Stoner, A.W., & Titgen, R.H. (2004). Behavioural mechanisms underlying the refuge value of benthic habitat structure for two flatfishes with differing anti-predator strategies. *Marine Ecology Progress Series*, 268, 231-243.

Saffo, M.B. (1992). Invertebrates in endosymbiotic associations. *American Zoologist*, 32(4), 557-565.

Saila, S.B., Kocic, V.L., & McManus, J.W. (1993). Modelling the effects of destructive fishing practices on tropical coral reefs. *Marine Ecology Progress Series*, 51-60.

Saller, U. (1988). Oogenesis and larval development of Ephydatia fluviatilis (Porifera,

Spongillidae). *Zoomorphology*, 108(1), 23-28.

Scheffers, S.R., Van Soest, R.W., Nieuwland, G., & Bak, R.P. (2010). Coral reef framework cavities: Is functional similarity reflected in composition of the cryptic macrofaunal community? *Atoll Research Bulletin,* (583).

Schlacher, T.A., Schlacher-Hoenlinger, M.A., Williams, A., Althaus, F., Hooper, J.N.A., & Kloser, R. (2007). Richness and distribution of sponge megabenthos in continental margin canyons off southeastern Australia. *Marine Ecology Progress Series*, 340, 73-88.

Schmidt, T.M. (Ed.). (2019). *Encyclopedia of Microbiology*. Academic Press.

Schönberg, C.H.L. (2016). Happy relationships between marine sponges and sediments-a review and some observations from Australia. *Journal of the Marine Biological Association of the United Kingdom*, 96(2), 493-514.

Schönberg, C.H., Fang, J.K., Carreiro-Silva, M., Tribollet, A., & Wisshak, M. (2017). Bioerosion: the other ocean acidification problem. *ICES Journal of Marine Science*, 74(4), 895-925.

Scott, A.R., Battista, T.A., Blum, J.E., Noren, L.N., & Pawlik, J.R. (2019). Patterns of benthic cover with depth on Caribbean mesophotic reefs. *Coral Reefs*, 38(5), 961-972

Scott, A.R. & Pawlik, J.R. (2019). A review of the sponge increase hypothesis for Caribbean mesophotic reefs. *Marine Biodiversity*, 49(3), 1073-1083.

Shinde, P.P., & Shah, S. (2018). A review of machine learning and deep learning applications. *Fourth international conference on computing communication control and automation (ICCUBEA),* (1-6).

Sieber, A. & Pyle, R. (2010). A review of the use of closed-circuit rebreathers for scientific diving. *Underwater Technology*, 29(2), 73-78.

Slattery, M. & Lesser, M.P. (2015). Trophic ecology of sponges from shallow to mesophotic depths (3 to 150 m): Comment on Pawlik et al. (2015). *Marine Ecology Progress Series* 527(1), 275-279.

Snelgrove, P.V.R. (1999). Getting to the Bottom of Marine Biodiversity: Sedimentary Habitats Ocean bottoms are the most widespread habitat on Earth and support high biodiversity and key ecosystem services. *BioScience*, 49(2), 129-138.

Stephens, D.W. & Krebs, J.R. (1986). Foraging Theory. *Princeton University Press, NJ*.

Strehlow, B.W., Jorgensen, D., Webster, N.S., Pineda, M.C., & Duckworth, A. (2016). Using a thermistor flowmeter with attached video camera for monitoring sponge excurrent speed and oscular behaviour. *PeerJ* 4, e2761.

Taylor, M.W., Radax, R., Steger, D., & Wagner, M. (2007). Sponge-associated microorganisms: evolution, ecology, and biotechnological potential. *Microbiology and Molecular Biology Review*s, 71(2), 295-347.

Thomassen, S. & Riisgård, H.U. (1995). Growth and energetics of the sponge Halichondria panacea. *Marine Ecology Progress Series*, 128(1-3), 239-246.

Thornton, D.C. (2014). Dissolved organic matter (DOM) release by phytoplankton in the contemporary and future ocean. *European Journal of Phycology*, 49(1), 20-46.

Tillin, H., Luff A., Graham, G., Wadsworth, T., Shirley, M., Dando, P., Baldock, L., van Rein, H. (2018). Remotely Operated Vehicles for use in marine benthic monitoring. *Marine Monitoring Platform Guidelines*, JNCC, Peterborough.

Topçu, N.E., Pérez, T., Grégori, G., & Harmelin-Vivien, M. (2010). In situ investigation of Spongia officinalis (Demospongiae) particle feeding: coupling flow cytometry and stable isotope analysis. *Journal of Experimental Marine Biology and Ecology*, 389(1-2),

61-69.

Trussell, G.C., Lesser, M.P., Patterson, M.R., & Genovese, S.J. (2006). Depth-specific differences in growth of the reef sponge Callyspongia vaginalis: role of bottom-up effects. *Marine Ecology Progress Series,* 323, 149-158.

Turner, J.A., Babcock, R.C., Hovey, R., & Kendrick, G.A. (2017). Deep thinking: a systematic review of mesophotic coral ecosystems. *ICES Journal of Marine Science*, 74(9), 2309-2320.

Turner, J.A. (2019). Key Questions for Research and Conservation of Mesophotic Coral Ecosystems and Temperate Mesophotic Ecosystems. In: Loya Y, Puglise K, Bridge T (Eds.). *Mesophotic Coral Ecosystems. Coral Reefs of the W*orld, (12). Springer, Cham.

Turner, E.C. (2021). Possible poriferan body fossils in early Neoproterozoic microbial reefs. *Nature*, 596(7870), 87-91.

Turon, X., Galera, J., & Uriz, M.J. (1997). Clearance rates and aquiferous systems in two sponges with contrasting life-history strategies. *Journal of Experimental Zoology*, 278(1), 22-36.

Tuya, F., Boyra, A., Sanchez-Jerez, P., Barbera, C., & Haroun, R.J. (2004). Relationships between rocky-reef fish assemblages, the sea urchin Diadema antillarum and macroalgae throughout the Canarian Archipelago. *Marine Ecology Progress Series,* 278 157-169.

Vacelet, J., & Boury-Esnault, N. (1995). Carnivorous sponges, *Nature*, 373(6512), 333-335.

van Dam, J.W., Negri, A.P., Uthicke, S., & Mueller, J.F. (2011). Chemical pollution on coral reefs: exposure and ecological effects. In: Sánchez-Bayo, F., van den Brink, P.J., & Mann, R.M. *Ecological Impacts of Toxic Chemicals, 9,* (187-211). Bentham Science Publishers Ltd.

Van Jaarsveld, A.S., Freitag, S., Chown, S.L., Muller, C., Koch, S., Hull, H., & Scholtz, C.H. (1998). Biodiversity assessment and conservation strategies. *Science*, 279(5359), 2106-2108.

Van Soest, R.W., Boury-Esnault, N., Vacelet, J., Dohrmann, M., Erpenbeck, D., de Voogd, N.J., Santodomingo, N., Vanhoorne, B., Kelly, M. & Hooper, J.N. (2012). Global diversity of sponges (Porifera). *PloS One*, 7(4), e35105.

Villamizar, E., Diaz, M.C., Rützler, K., & de Nobrega, R. (2013). Biodiversity, ecological structure, and change in the sponge community of different geomorphological zones of the barrier fore-reef at Carrie Bow Cay, Belize. *Marine Ecology*, 35(4), 425-435.

Vives-Rego, J., Lebaron, P., & Caron, N. (2000). Current and future applications of £ ow cytometry in aquatic microbiology. *FEMS Microbiology Reviews*, 24(2000), 429-448.

Vogel, S. (1974). Current-induced flow through the sponge, Halichondria. *The Biological Bulletin*, 147(2), 443-456.

Watanabe, K., Yoshida, G., Hori, M., Umezawa, Y., Moki, H., & Kuwae, T. (2020). Macroalgal metabolism and lateral carbon flows can create significant carbon sinks. *Biogeoscience*s, 17(9), 2425-2440.

Webster, N.S. & Taylor, M.W. (2012). Marine sponges and their microbial symbionts: love and other relationships. *Environmental Microbiology*, 14(2), 335-346.

Weisz, J.B., Lindquist, N., & Martens, C.S. (2008). Do associated microbial abundances impact marine demosponge pumping rates and tissue densities? *Oecologia*, 155, 367-376.

Whitman, W.B., Coleman, D.C., & Wiebe, W.J. (1998). Prokaryotes: the unseen majority. *Proceedings of the National Academy of Sciences*, 95(12), 6578-6583.

Wilkinson, C.R. (1987). Interocean differences in size and nutrition of coral reef sponge populations. *Science*, 236(4809), 1654-1657.

Wilkinson, C.R. & Cheshire, A.C. (1990). Comparisons of sponge populations across the Barrier Reefs of Australia and Belize: evidence for higher productivity in the Caribbean. *Marine Ecology Progress Series*, 67(3), 285-294.

Wilkinson, C.R., Garrone, R., & Vacelet, J. (1984). Marine sponges discriminate between food bacteria and bacterial symbionts: electron microscope radioautography and in situ evidence. *Proceedings of the Royal society of London. Series B. Biological sciences*, 220(1221), 519-528.

Wooster, M.K., McMurray, S.E., Pawlik, J.R., Morán, X.A.G, & Berumen, M.L. (2019). Feeding and respiration by giant barrel sponges across a gradient of food abundance in the Red Sea. *Limnology and Oceanography*, 64(4), 1790-1801.

Worden, A.Z., Nolan, J.K., & Palenik, B. (2004). Assessing the dynamics and ecology of marine picophytoplankton: the importance of the eukaryotic component. *Limnology and Oceanography*, 49(1), 168-179.

Wulff, J.L. (1994). Sponge feeding by Caribbean angelfishes, trunkfishes, and filefishes. In: van Soest; Van Kempmen, & Braekman (Eds.). *Sponges in time and space*, 265-271. Balkema, Rotterdam.

Wulff, J.L. (2006). Ecological interactions of marine sponges. *Canadian Journal of Zoology*, 84(2), 146-166.

Yahel, G., Eerkes-Medrano, D.I., & Leys, S.P. (2006). Size independent selective filtration of ultraplankton by hexactinellid glass sponges. *Aquatic Microbial Ecology*, 45(2), 181-194.

Yahel, G., Marie, D., & Genin, A. (2005). InEx - a direct in situ method to measure filtration rates, nutrition and metabolism of active suspension feeders. *Limnology and Oceanography*, 3, 46-58.

Yahel, G., Sharp, J.H., Marie, D., Häse, C., & Genin, A. (2003). In situ feeding and element removal in the symbiont-bearing sponge *Theonella swinhoei*: Bulk DOC is the major source for carbon. *Limnology and Oceanography*, 48(1), 141-149.

Yahel, G., Whitney, F., Reiswig, H.M., Eerkes-Medrano, D.I., & Leys, S.P. (2007). In situ feeding and metabolism of glass sponges (Hexactinellida, Porifera) studied in a deep temperate fjord with a remotely operated submersible. *Limnology and oceanography*, 52(1), 428-440.

Zhang, X.G. & Pratt, B.R. (1994). New and extraordinary Early Cambrian sponge spicule assemblage from China. *Geology*, 22(1), 43-46.

Zhang, H., Huang, X., Huang, L., Bao, F., Xiong, S., Wang, K., & Zhang, D. (2018). Microeukaryotic biogeography in the typical subtropical coastal waters with multiple environmental gradients. *Science of the Total Environment*, *635*, 618-628.

Zhang, Z., Zhao, L., & Yang, T. (2021). Research on the Application of Artificial Intelligence in Image Recognition Technology. *In Journal of Physics: Conference Series*, 1992(3), 032118.

Appendices

Appendix A

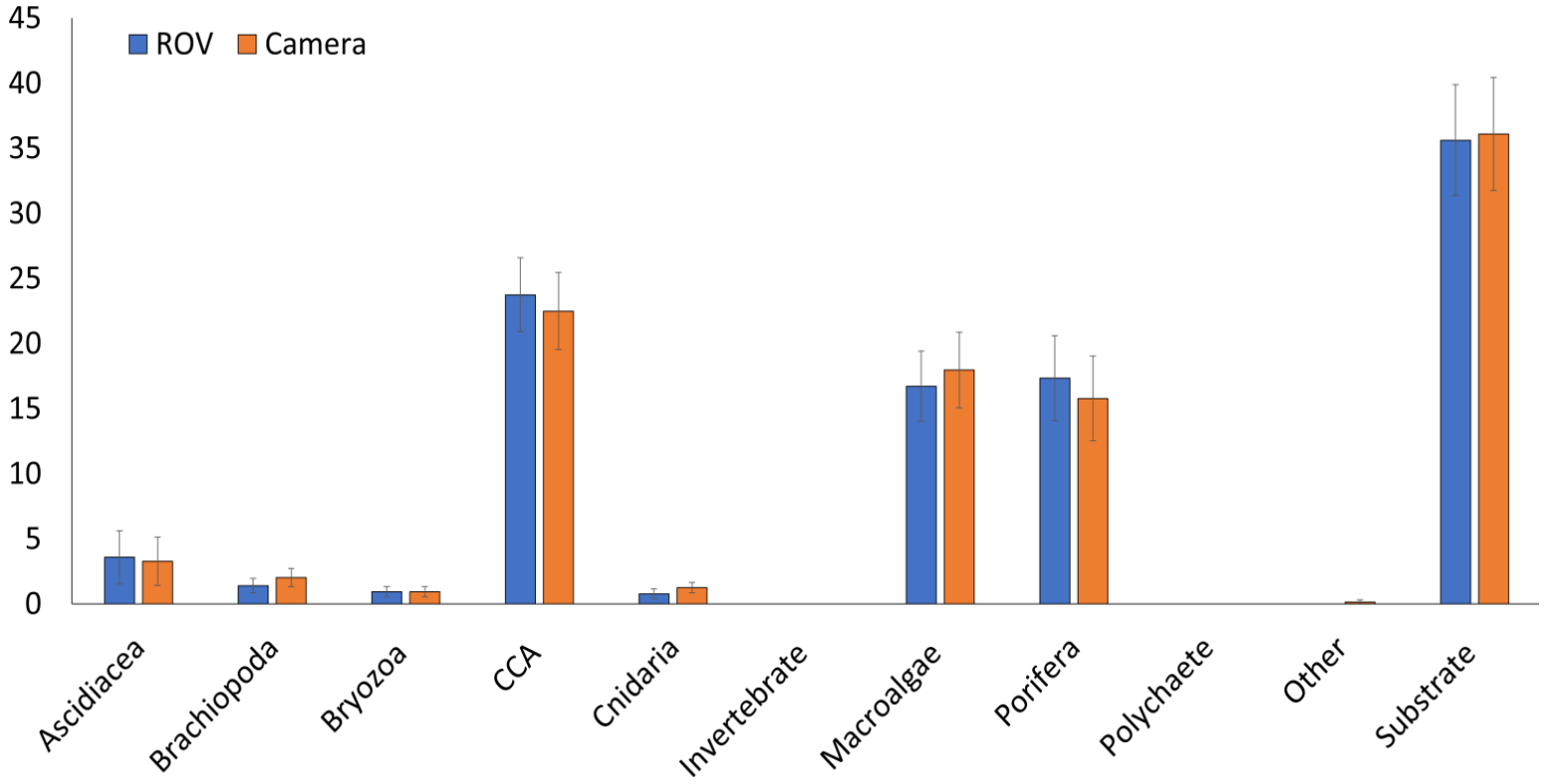

Fig. A2.1 Comparison of benthic community abundance data collected from ROV video stills and photographs from Nikon D800 of 16 quadrats. CPC points were randomised explaining the small, non-significant differences between the two techniques.

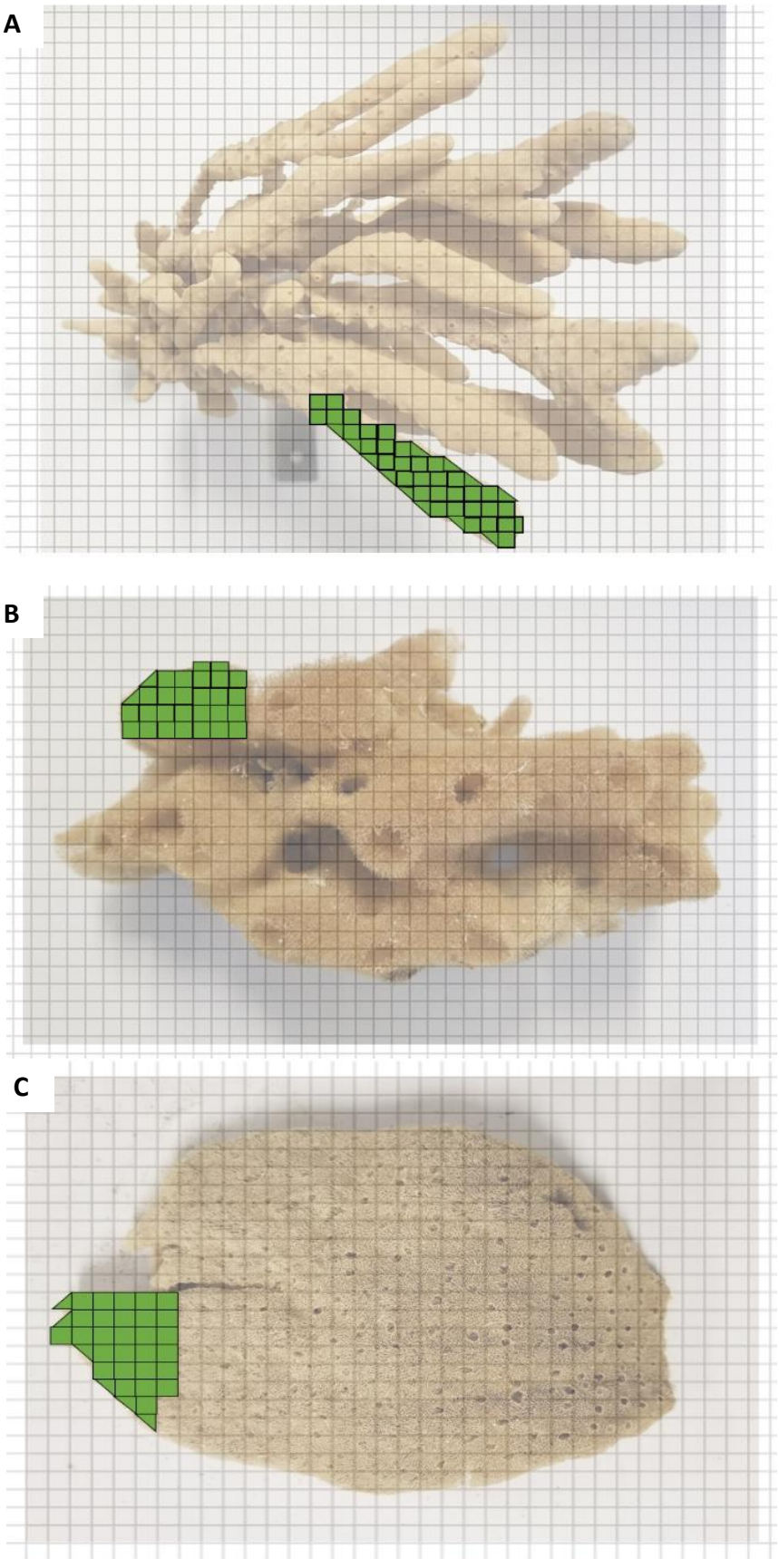

Fig. A2.2 Image to demonstrate the calculation of image cover (number of squares) /surface area (true surface area) ratios of high (A), medium (B), and low (C) complexity morphologies.

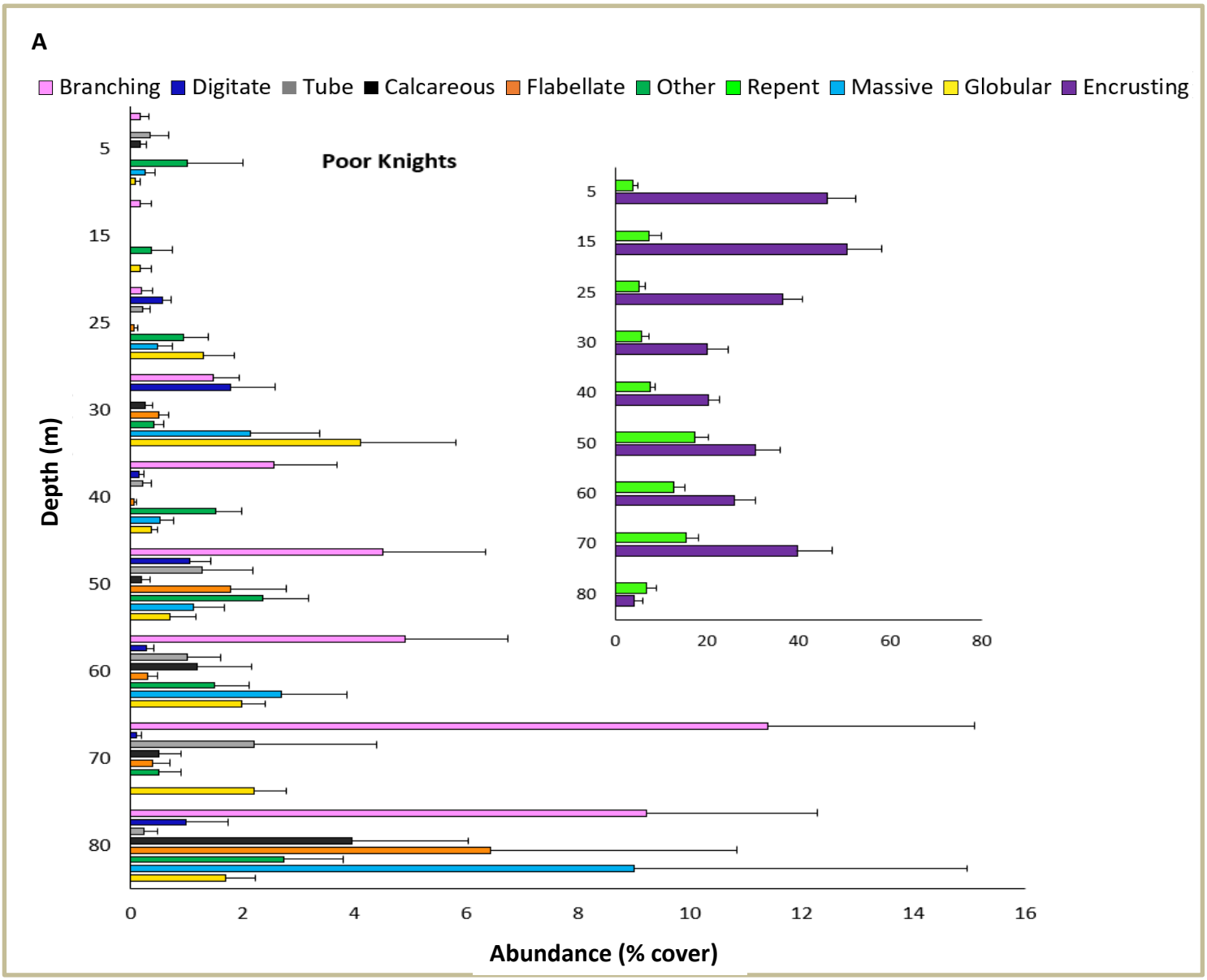
A
Branching
Digitate
Tube
Calcareous
Flabellate
Other
Repent
Massive
Globular
Encrusting
Poor Knights
Depth (m)
5
15
25
30
40
50
60
70
80
0
2
4
6
8
10
12
14
16
Abundance (% cover)
0
20
40
60
80

B

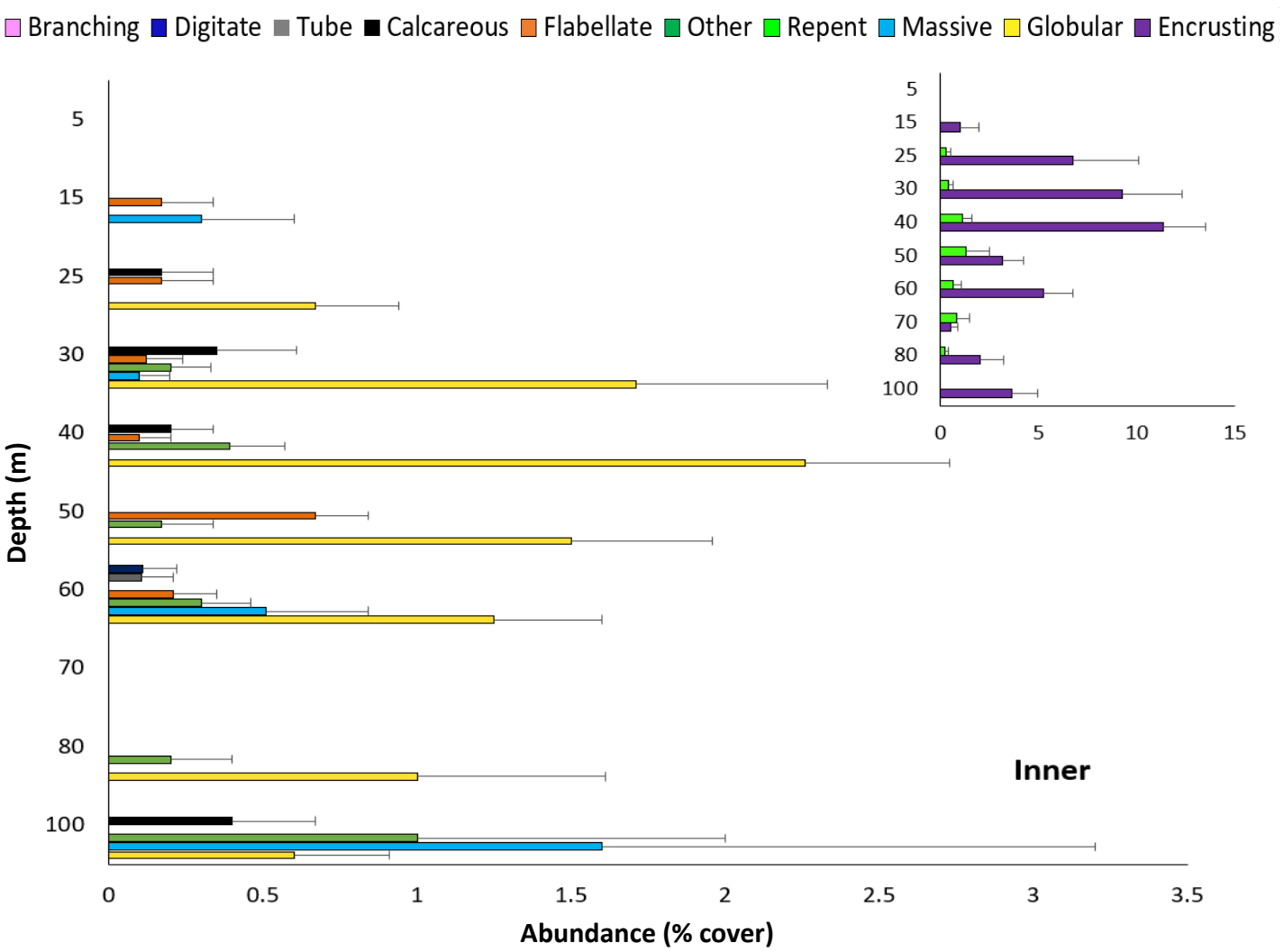
Branching
Digitate
Tube
Calcareous
Flabellate
Other
Repent
Massive
Globular
Encrusting
Depth (m)
5
15
25
30
40
50
60
70
80
100
0
0.5
1
1.5
2
2.5
3
3.5
Abundance (% cover)
Inner
0
5
10
15

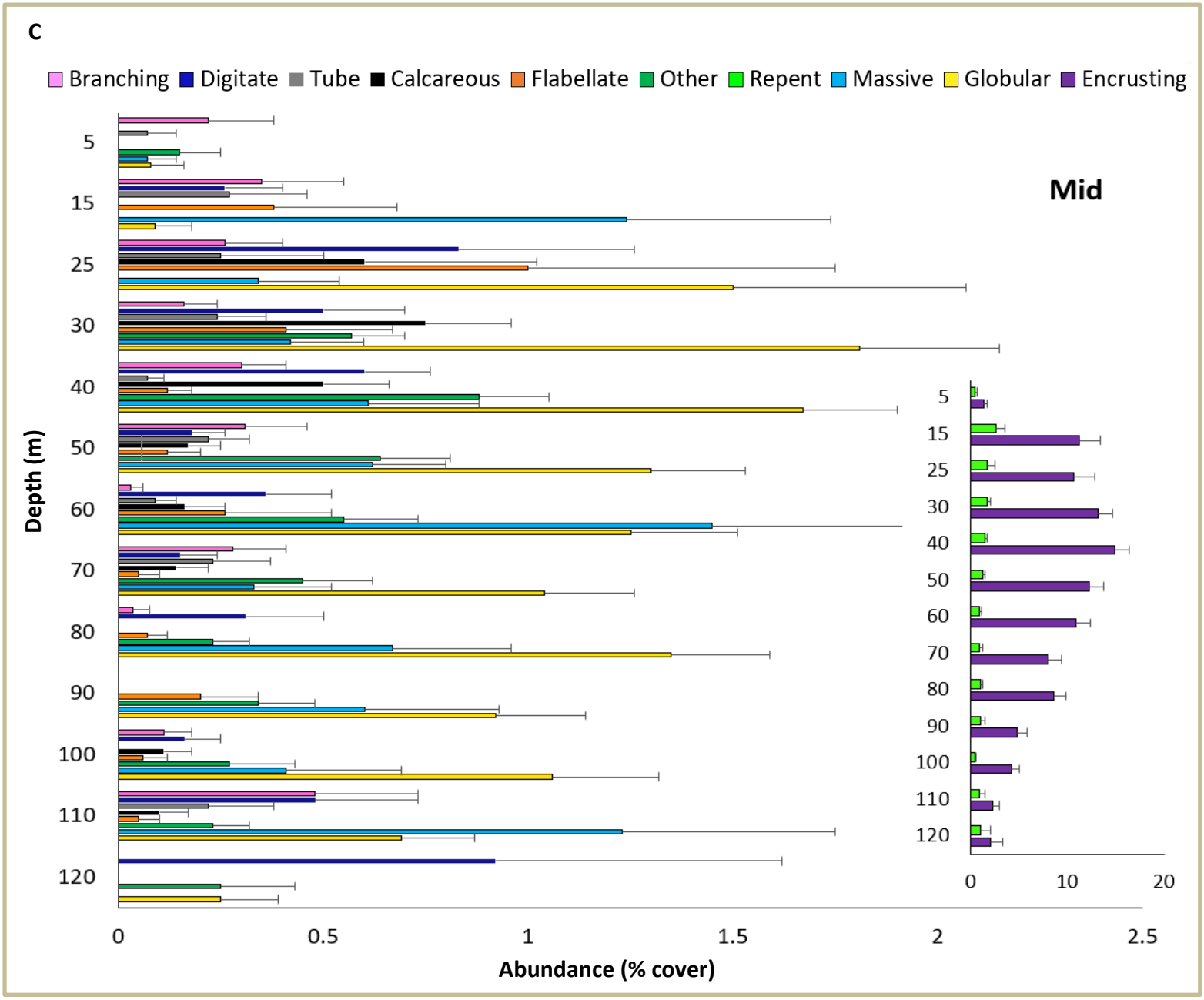
C
Branching
Digitate
Tube
Calcareous
Flabellate
Other
Repent
Massive
Globular
Encrusting
Mid
Depth (m)
5
15
25
30
40
50
60
70
80
90
100
110
120
0
0.5
1
1.5
2
2.5
Abundance (% cover)
0
10
20

D

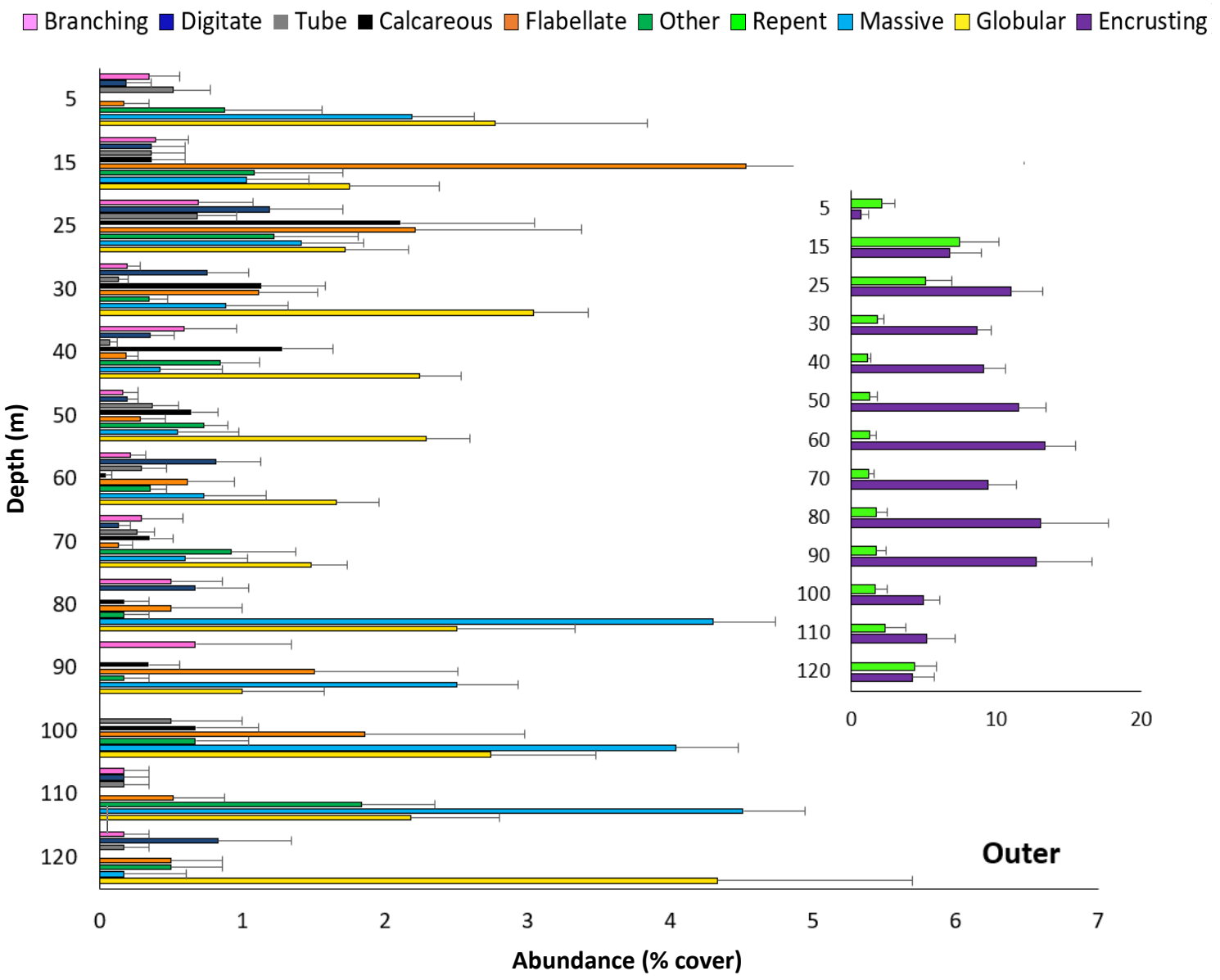

E

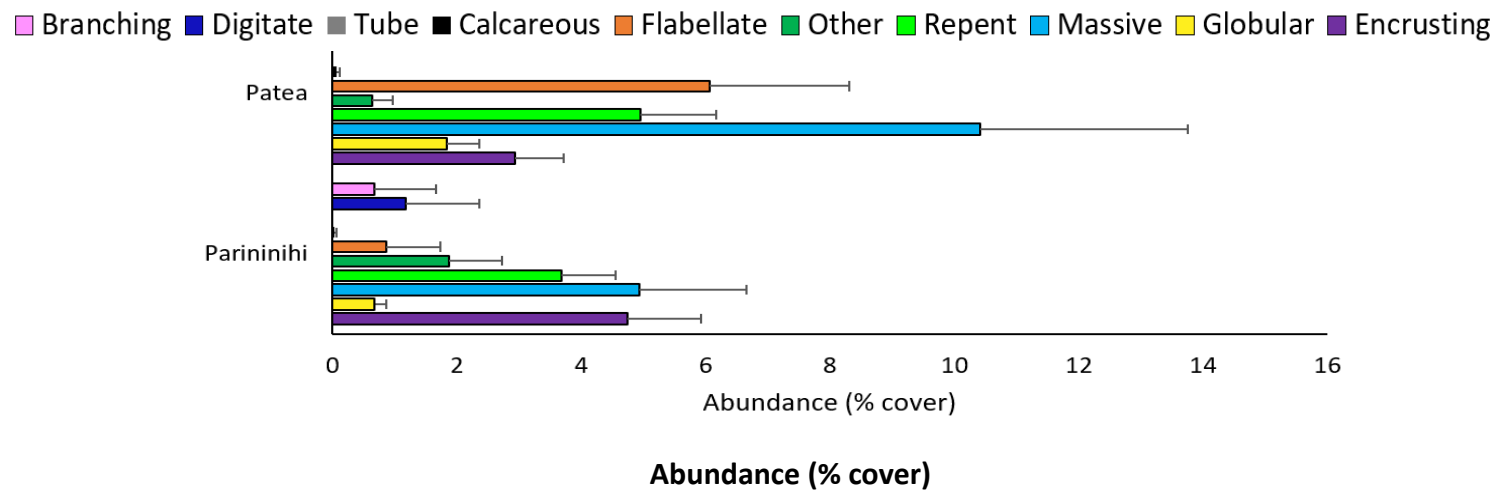

Abundance (% cover)

Fig. A2.3 Abundance (% coverage) of sponge morphological types across 10 m depth increments at Poor Knights (A), inner (B), mid (C), and outer Fiordland (D), Patea, and Parininihi marine reserve (E). Repent and Encrusting forms have been separated to maintain easier visualization of less abundant groups.

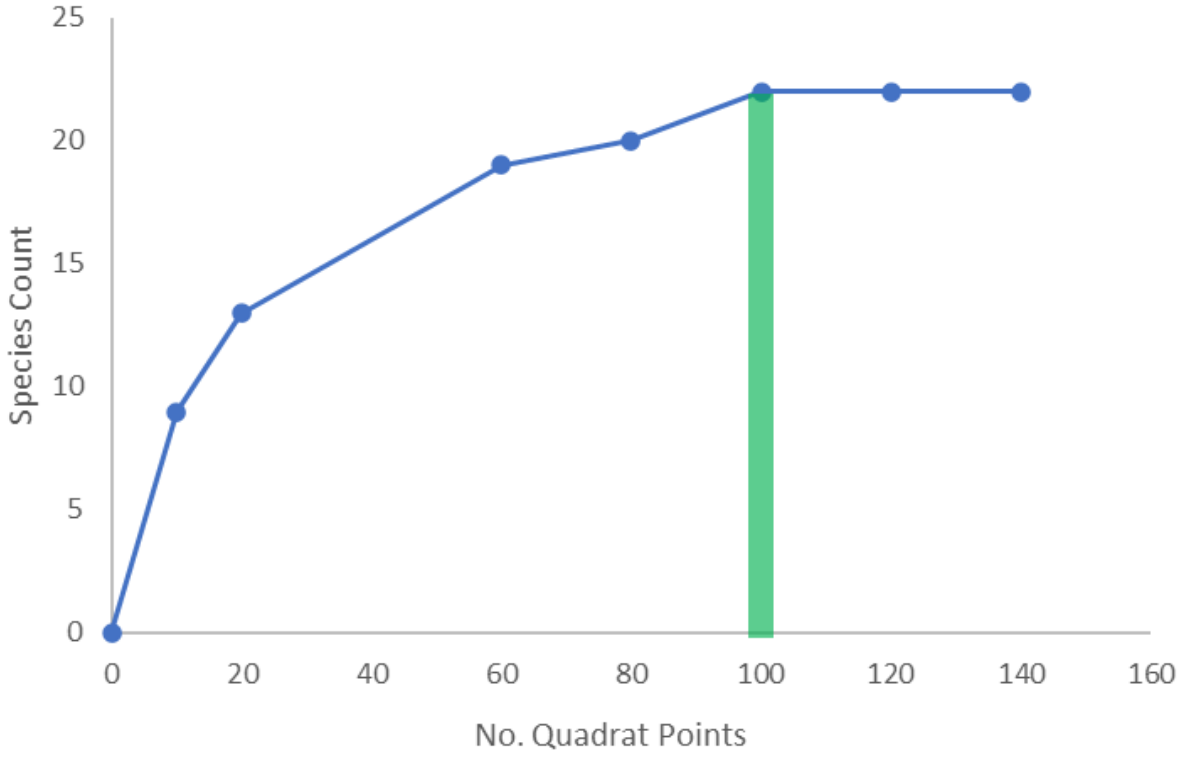

Fig. A2.4 Species accumulation curve showing the number of points assigned to randomised frame-grabs to determine the optimal number of points to be assigned to quadrats in CPC analyses

Table A2.1. All transects undertaken using ROV and SCUBA at all locations.

YEAR	LOCATION	SOUND/SITE	SITE /DISTANCE FROM OPEN SEA (KM)	COORDINATES	TRANSECT DEPTHS (M)	ROV/ SCUBA
2018	**Fiordland**	Breaksea	Mid / 10.2	45° 33.401 S 166° 53.649 E	40 50 70 80	ROV
			Mid / 10.2	45° 31.835 S 166° 52.770 E	30 40 50 60	ROV
			Mid / 11.6	45° 31.352 S 166° 55.457 E	30 40 50 60 70 80 90 100 110	ROV
			Mid / 8.1	45° 34.134 S 166° 46.133 E	N/A	Abort
			Mid / 10.2	45° 31.320 S 166° 55.594 E	N/A	Abort
			Mid / 10.4	45° 31.726 S 166° 53.766 E	40 50 70	ROV
			Outer / 2.1	45° 36.146 S 166° 42.577 E	40 50	ROV
			Outer / 3.6	45° 37.573 S 166° 43.017 E	30	ROV
			Outer / 3.7	45° 37.575 S 166° 43.017 E	40	ROV
			Outer / 4	45° 38.120 S 166° 52.183 E	N/A	Abort
			Outer /1.9	45° 35.985 S 166° 42.809 E	80	ROV
			Outer / 2	45° 34.926 S 166° 42.824 E	30 40 50 60 70	ROV
			Inner / >20	45° 33.503 S 166° 57.472 E	N/A	Abort
		Dusky	Inner / 16.9	45° 44.861 S 166° 50.981 E	30	ROV
			Inner / 18	45° 43.439 S 166° 51.822 E	40 60 80 100	ROV
			Inner / 17.8	45° 43.439 S 166° 51.820 E	N/A	Abort
			Mid / 10	45° 44.928 S 166° 40.936 E	30 40	ROV
			Mid / 10.2	45° 44.930 S 166° 40.935 E	50 60	ROV
			Outer / 5.1	45° 47.366 S 166° 34.360 E	30 40 50	ROV
			Outer/ 6.8	45° 45.418 S 166° 36.417 E	40 50 60 70	ROV
			Mid / 12.5	45° 42.899 S 166° 43.207 E	40 50 60 70 80	ROV
		Doubtfull	Outer / 5.8	45° 19.291 S 166° 57.610 E	60 70	ROV
			Outer / 6.8	45° 14.910 S 166° 58.770 E	60	ROV
			Outer / 3.3	45° 11.363 S 166° 58.185 E	60	ROV
			Mid / 8.1	45° 17.752 S 167° 01.757 E	60	ROV
			Mid / 8.6	45° 17.093 S 167° 02.058 E	30 40 50 60 70	ROV
			Mid / 8.5	45° 17.093 S 167° 02.056 E	80 90 100 110	ROV
			Mid / 7.8	45° 17.750 S 167° 02.055 E	N/A	Abort
	Poor Knights	Northern Arch	N/A 0.1	35°26'53.9"S 174°43'52.3"E	5 15 25	SCUBA
					30 40 50 60 70 80	ROV
	Poor Knights	Motu Kapiti	N/A 0.1	35°28'10.6"S 174°43'55.2"E	30 40 50 60 70 80	ROV
	Parininihi		N/A 0.1	38°52'10.2"S 174°30'59.4"E	25	Both
			N/A 0.1	38°53'07.1"S 174°30'44.6"E	25	Both
			N/A 0.1	38°51'34.9"S 174°29'48.8"E	25	Both
			N/A 0.1	38°53'04.6"S 174°30'40.0"E	25	Both
	Patea		N/A 0.1	39°49'37.9"S 174°23'53.2"E	25	ROV
			N/A 0.1	39°49'50.5"S 174°24'54.4"E	25	ROV
			N/A 0.1	39°50'06.0"S 174°23'48.8"E	25	ROV
2019	**Fiordland**	Hall Arm	Inner / 20.2	45°29'03.6"S 167°04'33.0"E	5 15 25	SCUBA
					30 40 50 60 70	ROV
		Crooked Arm	Mid / 9.9	45°21'19.9"S 167°01'26.0"E	5 15 25	SCUBA
					30 40 50 60 70 80 90 100 110 120	ROV
		Bradshaw	Mid / 9.2	45°17'04.1"S 167°02'10.2"E	5 15 25	SCUBA
					30 40 50 60 70 80 90 100 110 120	ROV
		Thompson	Outer / 0.8	45°09'20.9"S 166°58'07.0"E	5 15 25	SCUBA
					30 40 50 60 70 80 90 100 110 120	ROV
	Poor Knights	Northern Arch	N/A 0.1	35°26'53.9"S 174°43'52.3"E	5 15 25	SCUBA
					30 40 50 60 70 80	ROV
	Poor Knights	Motu Kapiti	N/A 0.1	35°28'10.6"S 174°43'55.2"E	30 40 50 60 70 80	ROV
	Parininihi		N/A 0.1		25	Both

Table A2.2. Comparison of sponge morphology complexities based on surface area to 2-dimensional image-cover-area ratios.

MORPHOLOGY	COMPLEXITY RANK	COMPLEXITY SCORE
ENCRUSTING	Low	1
GLOBULAR	Low	2
REPENT	Low	2
MASSIVE	Medium	3
FLABELLATE	Medium	3
OTHER	Medium	3
CALCAREOUS	Medium	3
TUBE	High	4
DIGITATE	High	4
BRANCHING	High	5

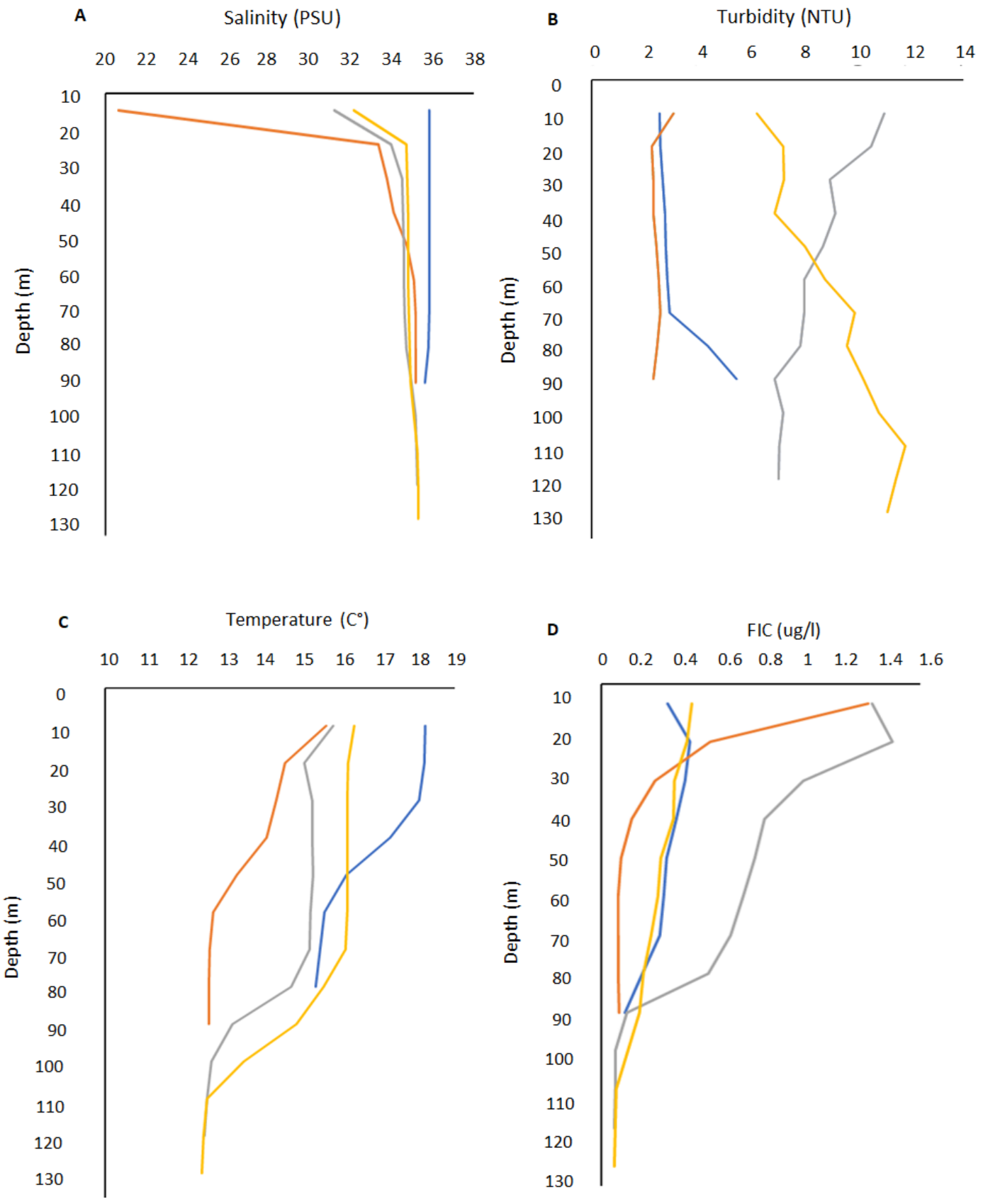

Fig. A2.5 Depth changes in salinity (A), turbidity(B), temperature (C), FlC (fluorescence as chlorophyll *a*) (D) from CTD deployments at the Poor Knights (blue), inner Fiordland (orange), mid Fiordland (grey), outer Fiordland (yellow).

Table A2.3 *Post-hoc* pairwise t-tests comparing differences in benthic community composition at 10 m intervals from 5 to 80 m at the Poor Knights.

Groups	t	P(perm)	perms
5m, 15m	1.3896	0.126	999
5m, 25m	2.3445	0.001	999
5m, 30m	2.6718	0.001	999
5m, 40m	3.6309	0.001	997
5m, 50m	2.939	0.001	998
5m, 60m	3.0494	0.001	998
5m, 70m	2.9478	0.001	999
5m, 80m	2.7835	0.001	999
15m, 25m	1.7338	0.031	999
15m, 30m	2.486	0.001	998
15m, 40m	3.4678	0.001	999
15m, 50m	2.5302	0.001	999
15m, 60m	2.4508	0.002	996
15m, 70m	2.5681	0.001	998
15m, 80m	2.549	0.001	957
25m, 30m	1.9821	0.011	998
25m, 40m	2.7086	0.001	999
25m, 50m	2.4887	0.001	998
25m, 60m	2.0049	0.003	999
25m, 70m	2.7474	0.001	999
25m, 80m	2.4892	0.002	997
30m, 40m	3.8472	0.001	998
30m, 50m	3.7815	0.001	998
30m, 60m	3.0548	0.001	999
30m, 70m	3.7979	0.001	999
30m, 80m	3.49	0.001	999
40m, 50m	2.3416	0.001	998
40m, 60m	2.127	0.002	998
40m, 70m	3.2773	0.001	999
40m, 80m	3.0569	0.001	998
50m, 60m	1.0767	0.368	999
50m, 70m	1.3474	0.13	999
50m, 80m	1.7764	0.02	997
60m, 70m	1.6404	0.03	999
60m, 80m	1.6889	0.022	999
70m, 80m	2.3384	0.001	975

Table A2.4 SIMPER results to compare differences in benthic community composition across 10 m intervals from 5-80 m at the Poor Knights.

Group 5m

Average similarity: 66.46

Species	Av.Abund	Av.Sim	Sim/SD	Contrib%	Cum.%
PORIFERA	6.99	28.54	2.24	42.93	42.93
BRYOZOAN	2.50	9.07	2.66	13.65	56.59
CND	3.25	8.86	1.19	13.33	69.92
MACROALGAE	3.02	8.81	1.56	13.26	83.18
CCA	1.72	5.00	1.04	7.53	90.71

Group 15m

Average similarity: 68.24

Species	Av.Abund	Av.Sim	Sim/SD	Contrib%	Cum.%
PORIFERA	7.57	34.73	3.17	50.88	50.88
CCA	2.99	11.26	2.74	16.50	67.38
BRYOZOAN	2.81	10.56	1.89	15.48	82.86
CND	1.93	5.40	1.06	7.91	90.77

Group 25m

Average similarity: 65.49

Species	Av.Abund	Av.Sim	Sim/SD	Contrib%	Cum.%
PORIFERA	6.67	29.70	3.89	45.35	45.35
BRYOZOAN	4.76	17.30	1.44	26.42	71.77
CCA	2.19	4.96	0.91	7.57	79.34
MACROALGAE	2.16	4.65	0.83	7.10	86.44
ASCIDIAN	1.57	3.63	0.81	5.54	91.98

Group 30m

Average similarity: 67.92

Species	Av.Abund	Av.Sim	Sim/SD	Contrib%	Cum.%
PORIFERA	5.80	21.19	2.86	31.19	31.19
MACROALGAE	3.26	10.42	2.37	15.34	46.53
BRYOZOAN	3.29	10.30	1.66	15.17	61.70
CCA	3.07	9.26	1.80	13.64	75.33
ASCIDIAN	2.19	7.11	2.17	10.48	85.81
OTHER	1.68	5.20	1.47	7.65	93.46

Group 40m

Average similarity: 76.61

Species	Av.Abund	Av.Sim	Sim/SD	Contrib%	Cum.%
PORIFERA	6.37	27.14	6.19	35.42	35.42
BRYOZOAN	4.64	17.40	2.21	22.71	58.13
CND	4.14	15.88	2.72	20.73	78.86
ASCIDIAN	2.68	8.84	1.88	11.54	90.40

Group 50m

Average similarity: 70.98

Species	Av.Abund	Av.Sim	Sim/SD	Contrib%	Cum.%
PORIFERA	7.76	37.83	4.63	53.29	53.29
BRYOZOAN	3.49	12.24	1.67	17.24	70.53
CND	2.94	9.50	1.14	13.38	83.91
ASCIDIAN	1.75	5.85	1.24	8.25	92.16

Group 60m

Average similarity: 69.42

Species	Av.Abund	Av.Sim	Sim/SD	Contrib%	Cum.%
PORIFERA	7.15	33.52	4.56	48.28	48.28
BRYOZOAN	3.67	14.14	2.46	20.37	68.65
CND	2.36	7.41	1.09	10.68	79.33
OTHER	1.63	5.36	1.18	7.72	87.04
ASCIDIAN	1.84	5.22	0.99	7.52	94.56

Group 70m

Average similarity: 78.18

Species	Av.Abund	Av.Sim	Sim/SD	Contrib%	Cum.%
PORIFERA	8.45	43.76	5.74	55.97	55.97
CND	2.73	11.08	3.03	14.18	70.15
BRYOZOAN	2.84	9.89	1.76	12.65	82.80
CCA	1.00	5.53	10.56	7.07	89.87
OTHER	1.07	3.80	1.24	4.86	94.73

Group 80m

Average similarity: 70.61

Species	Av.Abund	Av.Sim	Sim/SD	Contrib%	Cum.%
PORIFERA	6.74	41.24	3.74	58.41	58.41
BRYOZOAN	3.20	14.93	2.90	21.15	79.56
CND	3.13	7.46	0.76	10.56	90.12

Table A.25 *Post-hoc* pairwise t-tests comparing differences in benthic community composition at 10 m intervals from 5 to 100 m at inner Fiordland.

Groups	t	P(perm)	perms
30m, 100m	3.4772	0.001	999
30m, 40m	1.4542	0.103	999
30m, 60m	2.7797	0.001	998
30m, 80m	4.0027	0.001	998
30m, 5m	4.6724	0.001	999
30m, 15m	3.2289	0.001	998
30m, 25m	1.6819	0.061	998
30m, 50m	3.5159	0.001	999
30m, 70m	3.7836	0.001	999
100m, 40m	2.7804	0.002	999
100m, 60m	1.8452	0.016	998
100m, 80m	1.1256	0.296	988
100m, 5m	3.2731	0.001	993
100m, 15m	6.1302	0.001	995
100m, 25m	4.4936	0.001	989
100m, 50m	0.97782	0.484	986
100m, 70m	1.3016	0.163	990
40m, 60m	1.9358	0.018	999
40m, 80m	3.5178	0.001	999
40m, 5m	4.9185	0.001	996
40m, 15m	4.429	0.001	999
40m, 25m	2.8742	0.001	999
40m, 50m	2.6675	0.001	998
40m, 70m	3.5648	0.001	997
60m, 80m	2.5246	0.003	999
60m, 5m	4.618	0.001	998
60m, 15m	5.7346	0.001	999
60m, 25m	4.1716	0.001	998
60m, 50m	1.4802	0.082	999
60m, 70m	2.6926	0.001	999
80m, 5m	3.531	0.001	990
80m, 15m	6.7789	0.001	993
80m, 25m	5.0714	0.001	988
80m, 50m	1.6364	0.054	993
80m, 70m	1.1921	0.235	990
5m, 15m	5.7954	0.001	991
5m, 25m	4.7275	0.001	995
5m, 50m	3.8785	0.001	994
5m, 70m	2.8249	0.001	995
15m, 25m	2.5082	0.001	994
15m, 50m	7.2695	0.001	991
15m, 70m	5.6102	0.001	991
25m, 50m	5.0146	0.001	994
25m, 70m	4.4902	0.001	992
50m, 70m	1.853	0.013	994

Table A2.6 *Post-hoc* pairwise t-tests comparing differences in benthic community composition at 10 m intervals from 5 to 120 m at mid Fiordland.

Groups	t	P(perm)	perms
100m,110m	0.75583	0.683	998
100m,120m	1.5129	0.056	999
100m, 15m	6.5371	0.001	998
100m, 25m	5.3589	0.001	999
100m, 30m	5.7998	0.001	999
100m, 40m	5.3204	0.001	998
100m, 5m	8.3185	0.001	999
100m, 50m	3.8251	0.001	998
100m, 60m	2.6147	0.001	998
100m, 80m	1.6335	0.024	999
100m, 90m	0.91337	0.56	998
100m, 70m	1.7016	0.019	999
110m,120m	1.0404	0.378	999
110m, 15m	6.0008	0.001	999
110m, 25m	4.9249	0.001	997
110m, 30m	5.736	0.001	997
110m, 40m	5.4241	0.001	999
110m, 5m	7.6184	0.001	999
110m, 50m	3.8837	0.001	999
110m, 60m	2.6734	0.001	997
110m, 80m	1.8883	0.008	997
110m, 90m	1.2069	0.198	997
110m, 70m	2.1955	0.001	996
120m, 15m	5.9127	0.001	999
120m, 25m	4.9367	0.001	999
120m, 30m	5.0333	0.001	998
120m, 40m	4.8745	0.001	997
120m, 5m	6.5154	0.001	999
120m, 50m	3.7218	0.001	999
120m, 60m	2.728	0.001	999
120m, 80m	2.2079	0.001	999
120m, 90m	1.4228	0.09	998
120m, 70m	2.6611	0.001	999
15m, 25m	2.4453	0.001	999
15m, 30m	3.1412	0.001	998
15m, 40m	3.8506	0.001	998
15m, 5m	3.986	0.001	999
15m, 50m	3.7223	0.001	999
15m, 60m	4.6236	0.001	998
15m, 80m	5.8657	0.001	999
15m, 90m	6.3544	0.001	999
15m, 70m	6.1959	0.001	997
25m, 30m	1.849	0.009	999
25m, 40m	2.1014	0.002	997
25m, 5m	5.1113	0.001	999
25m, 50m	2.3577	0.001	999
25m, 60m	3.3275	0.001	998
25m, 80m	4.8137	0.001	999
25m, 90m	5.2855	0.001	999
25m, 70m	4.9236	0.001	999
30m, 40m	1.7502	0.018	999

30m, 5m			
30m, 50m	2.5364	0.002	999
30m, 60m	3.862	0.001	999
30m, 80m	5.6648	0.001	999
30m, 90m	5.7651	0.001	999
30m, 70m	5.1729	0.001	998
40m, 5m	6.4513	0.001	999
40m, 50m	1.8703	0.007	999
40m, 60m	3.0236	0.001	998
40m, 80m	4.9617	0.001	998
40m, 90m	5.2146	0.001	999
40m, 70m	4.4775	0.001	998
5m, 50m	6.3874	0.001	998
5m, 60m	7.1402	0.001	999
5m, 80m	7.9405	0.001	999
5m, 90m	7.8056	0.001	998
5m, 70m	8.2951	0.001	998
50m, 60m	1.8598	0.005	998
50m, 80m	3.6034	0.001	999
50m, 90m	3.8791	0.001	999
50m, 70m	3.1631	0.001	999
60m, 80m	2.2486	0.002	999
60m, 90m	2.7126	0.001	999
60m, 70m	2.3708	0.001	997
80m, 90m	1.401	0.091	999
80m, 70m	1.3792	0.103	998
90m, 70m	1.814	0.003	998

Table A2.7 *Post-hoc* pairwise t-tests comparing difference in benthic community composition at 10 m intervals from 5 to 120 m at outer Fiordland.

30m, 15m	3.817	0.001	998
30m, 25m	1.8357	0.005	999
30m, 5m	5.109	0.001	998
30m, 80m	2.1712	0.001	999
30m, 90m	2.4455	0.001	999
60m, 70m	1.3026	0.129	999
60m, 100m	0.51793	0.906	999
60m, 110m	0.91301	0.525	999
60m, 120m	1.0839	0.316	999
60m, 15m	4.2884	0.001	998
60m, 25m	2.8959	0.001	999
60m, 5m	4.878	0.001	998
60m, 80m	0.98311	0.452	998
60m, 90m	1.5279	0.055	999
70m, 100m	0.94943	0.505	998
70m, 110m	0.99925	0.449	997
70m, 120m	1.3895	0.093	999
70m, 15m	4.7067	0.001	999
70m, 25m	3.4254	0.001	998
70m, 5m	5.0585	0.001	999
70m, 80m	1.3289	0.132	998
70m, 90m	1.43	0.077	997
100m, 110m	0.73873	0.691	991
100m, 120m	0.85829	0.638	992
100m, 15m	4.3563	0.001	993
100m, 25m	2.9043	0.001	990
100m, 5m	4.9339	0.001	996
100m, 80m	0.47811	0.892	991
100m, 90m	1.0129	0.364	993
110m, 120m	0.411	0.918	990
110m, 15m	5.8927	0.001	993
110m, 25m	4.0755	0.001	993
110m, 5m	6.5322	0.001	989
110m, 80m	0.79663	0.697	991
110m, 90m	1.2459	0.195	989
120m, 15m	5.7534	0.001	992
120m, 25m	4.2702	0.001	994
120m, 5m	6.265	0.001	995
120m, 80m	1.0341	0.387	995
120m, 90m	1.3999	0.113	994
15m, 25m	2.323	0.001	990
15m, 5m	3.2768	0.001	996
15m, 80m	5.1016	0.001	987
15m, 90m	4.9989	0.001	992
25m, 5m	4.3448	0.001	990
25m, 80m	3.3869	0.001	993
25m, 90m	3.3596	0.001	997
5m, 80m	5.8209	0.002	995
5m, 90m	5.4808	0.001	991
80m, 90m	0.54028	0.894	993

Groups	t	P(perm)	perms
40m, 50m	1.3198	0.118	999
40m, 30m	2.117	0.001	999
40m, 60m	1.8322	0.008	996
40m, 70m	2.1027	0.002	999
40m, 100m	1.2059	0.192	998
40m, 110m	1.5709	0.038	999
40m, 120m	1.9704	0.004	999
40m, 15m	3.9774	0.001	999
40m, 25m	2.6145	0.001	999
40m, 5m	4.8125	0.001	999
40m, 80m	1.48	0.052	999
40m, 90m	1.6284	0.023	999
50m, 30m	1.2816	0.138	996
50m, 60m	1.9296	0.003	999
50m, 70m	2.2567	0.001	999
50m, 100m	1.3962	0.103	998
50m, 110m	1.8241	0.008	998
50m, 120m	2.1796	0.001	998
50m, 15m	3.5529	0.001	999
50m, 25m	2.0474	0.002	998
50m, 5m	4.581	0.001	998
50m, 80m	1.7403	0.009	999
50m, 90m	2.04	0.007	998
30m, 60m	2.5311	0.001	998
30m, 70m	3.316	0.001	999
30m, 100m	1.9128	0.001	999
30m, 110m	2.4698	0.001	998
30m, 120m	2.8494	0.001	999

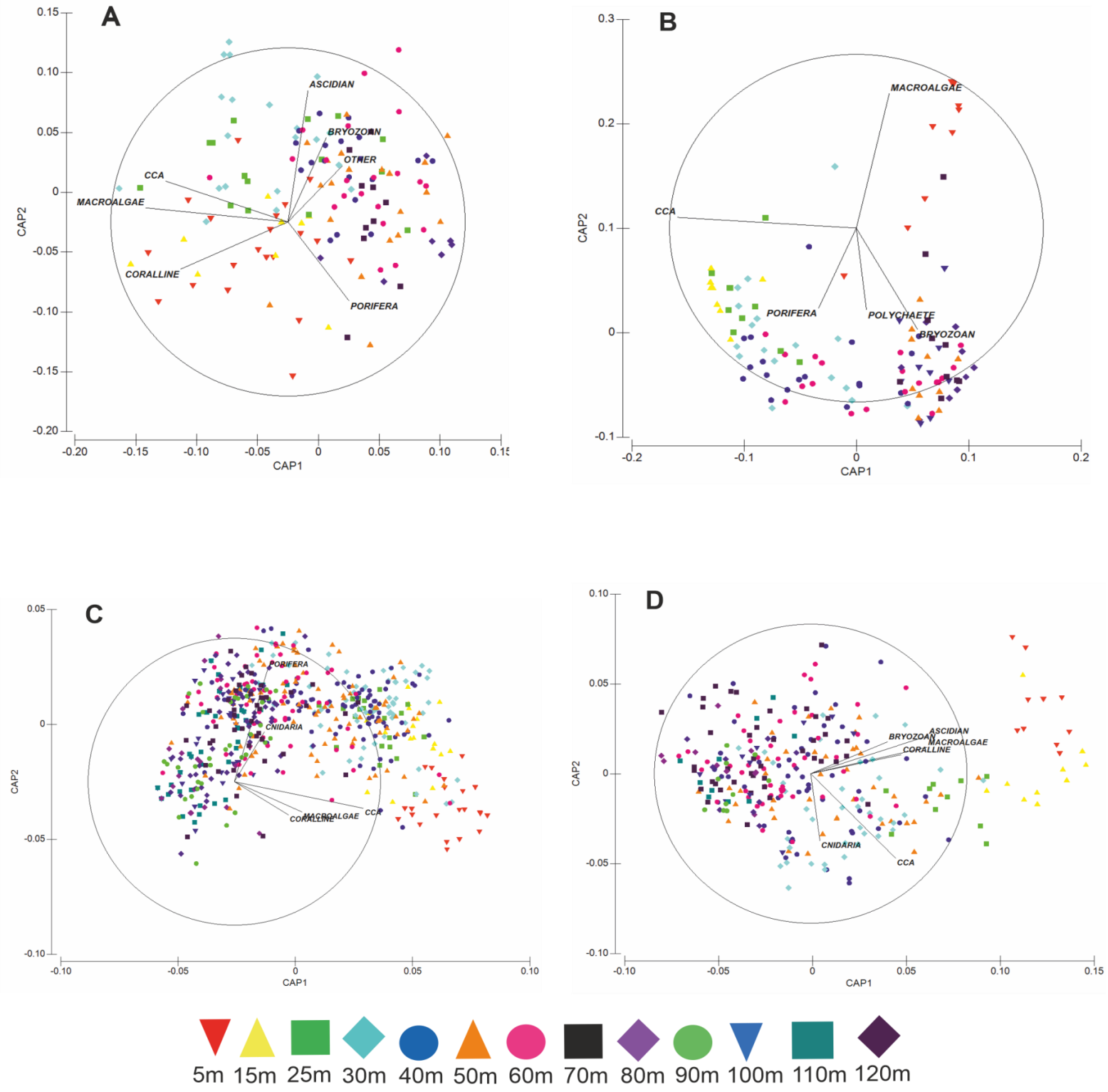

Fig. A2.6 Canonical analysis of principle components for benthic community composition structured by depth (m) at Poor Knights (A), inner Fiordland (B), mid Fiordland (C) and outer Fiordland (D). Pearson's correlation vectors (r > 0.4) represent the abundance of individual benthic groups.

Table A2.8 SIMPER results to compare differences in benthic community composition across 10 m intervals from 5-120 m at outer Fiordland

Group 40m

Average similarity: 56.08

Species	Av.Abund	Av.Sim	Sim/SD	Contrib%	Cum.%
PORIFERA	3.84	25.56	2.85	45.58	45.58
BRYOZOAN	2.06	12.84	2.19	22.90	68.47
CNIDARIA	1.92	8.36	0.91	14.91	83.39
POLYCHAETE	1.32	5.27	0.76	9.40	92.79

Group 50m

Average similarity: 55.66

Species	Av.Abund	Av.Sim	Sim/SD	Contrib%	Cum.%
PORIFERA	4.08	22.90	3.27	41.13	41.13
BRYOZOAN	2.47	13.11	2.34	23.55	64.69
POLYCHAETE	2.13	7.40	0.93	13.29	77.98
CNIDARIA	1.77	6.36	0.77	11.43	89.41
CCA	1.49	2.92	0.42	5.25	94.65

Group 30m

Average similarity: 61.55

Species	Av.Abund	Av.Sim	Sim/SD	Contrib%	Cum.%
PORIFERA	4.26	24.97	4.66	40.56	40.56
BRYOZOAN	2.00	9.40	2.62	15.27	55.83
POLYCHAETE	2.00	8.45	1.31	13.72	69.55
CNIDARIA	2.03	7.35	1.06	11.94	81.50
CCA	1.74	6.35	0.84	10.32	91.82

Group 60m

Average similarity: 56.87

Species	Av.Abund	Av.Sim	Sim/SD	Contrib%	Cum.%
PORIFERA	4.16	28.88	2.74	50.78	50.78
BRYOZOAN	1.75	12.27	2.51	21.58	72.36
POLYCHAETE	2.02	9.71	1.06	17.08	89.44
CNIDARIA	0.98	2.84	0.49	5.00	94.44

Group 70m

Average similarity: 57.19

Species	Av.Abund	Av.Sim	Sim/SD	Contrib%	Cum.%
PORIFERA	3.56	23.57	2.50	41.22	41.22
BRYOZOAN	1.98	14.47	2.25	25.31	66.53
POLYCHAETE	2.16	11.91	1.25	20.83	87.36
CNIDARIA	1.41	5.24	0.68	9.17	96.53

Group 100m

Average similarity: 61.27

Species	Av.Abund	Av.Sim	Sim/SD	Contrib%	Cum.%
PORIFERA	4.11	33.93	2.81	55.38	55.38
BRYOZOAN	1.66	12.03	2.83	19.63	75.01
POLYCHAETE	2.27	9.26	1.13	15.12	90.13

Group 110m

Average similarity: 69.70

Species	Av.Abund	Av.Sim	Sim/SD	Contrib%	Cum.%
PORIFERA	4.09	37.39	5.55	53.64	53.64
POLYCHAETE	2.04	15.11	1.74	21.67	75.31
BRYOZOAN	1.69	13.59	2.29	19.50	94.82

Group 120m

Average similarity: 66.81

Species	Av.Abund	Av.Sim	Sim/SD	Contrib%	Cum.%

PORIFERA	3.92	41.21	5.39	61.68	61.68
BRYOZOAN	1.47	14.29	3.37	21.39	83.07
POLYCHAETE	1.76	10.30	0.82	15.41	98.49

Group 15m

Average similarity: 74.48

Species	Av.Abund	Av.Sim	Sim/SD	Contrib%	Cum.%
PORIFERA	4.96	19.60	8.02	26.32	26.32
MACROALGAE	4.37	15.43	3.95	20.72	47.04
BRYOZOAN	4.16	13.90	4.10	18.67	65.71
ASCIDIAN	2.85	10.11	4.75	13.58	79.29
CCA	2.69	8.18	1.81	10.99	90.28

Group 25m

Average similarity: 70.02

Species	Av.Abund	Av.Sim	Sim/SD	Contrib%	Cum.%
PORIFERA	5.19	21.57	5.72	30.80	30.80
ASCIDIAN	2.82	10.53	5.11	15.04	45.84
CCA	2.59	9.67	2.32	13.80	59.65
BRYOZOAN	2.74	9.25	2.42	13.21	72.85
CNIDARIA	2.23	8.36	3.12	11.94	84.79
MACROALGAE	1.58	4.27	1.13	6.10	90.89

Group 5m

Average similarity: 76.78

Species	Av.Abund	Av.Sim	Sim/SD	Contrib%	Cum.%
MACROALGAE	7.64	33.53	6.85	43.67	43.67
ASCIDIAN	2.93	12.09	6.36	15.74	59.41
PORIFERA	3.08	10.94	2.84	14.25	73.66
BRYOZOAN	2.57	9.37	7.06	12.20	85.85
CORALLINE	2.00	5.96	1.72	7.76	93.62

Group 80m

Average similarity: 65.06

Species	Av.Abund	Av.Sim	Sim/SD	Contrib%	Cum.%
PORIFERA	4.78	36.40	4.19	55.95	55.95
POLYCHAETE	2.11	11.10	1.22	17.06	73.01
BRYOZOAN	1.38	9.93	4.77	15.26	88.28
CNIDARIA	1.85	6.68	0.83	10.26	98.54

Group 90m

Average similarity: 61.42

Species	Av.Abund	Av.Sim	Sim/SD	Contrib%	Cum.%
PORIFERA	4.22	27.78	2.98	45.23	45.23
CNIDARIA	2.48	12.30	1.01	20.03	65.26
POLYCHAETE	2.21	10.84	1.08	17.64	82.90
BRYOZOAN	1.06	10.28	3.34	16.73	99.63

Table A2.9 SIMPER results to compare differences in benthic community composition across 10 m intervals from 5-100 m at inner Fiordland. Dummy variable added in Av.Abundance.

Group 30m

Average similarity: 58.45

Species	Av.Abund	Av.Sim	Sim/SD	Contrib%	Cum.%
CCA	5.07	26.47	1.52	45.29	45.29
PORIFERA	3.14	15.42	2.05	26.39	71.68
BRYOZOAN	1.64	9.46	2.71	16.19	87.87
POLYCHAETE	1.38	4.79	0.79	8.20	96.07

Group 100m

Average similarity: 56.51

Species	Av.Abund	Av.Sim	Sim/SD	Contrib%	Cum.%
PORIFERA	2.46	25.61	2.06	45.32	45.32
BRYOZOAN	2.04	23.38	3.25	41.37	86.70
POLYCHAETE	1.07	6.68	0.69	11.83	98.53

Group 40m

Average similarity: 59.16

Species	Av.Abund	Av.Sim	Sim/SD	Contrib%	Cum.%
PORIFERA	3.86	22.97	2.54	38.84	38.84
CCA	4.19	12.56	0.85	21.23	60.07
BRYOZOAN	2.02	11.73	3.17	19.83	79.90
POLYCHAETE	1.46	7.94	0.95	13.42	93.31

Group 60m

Average similarity: 58.86

Species	Av.Abund	Av.Sim	Sim/SD	Contrib%	Cum.%
PORIFERA	2.78	19.43	2.85	33.01	33.01

BRYOZOAN	2.11	17.53	1.93	29.79	62.80
POLYCHAETE	2.20	15.31	1.59	26.02	88.82
CCA	1.71	4.30	0.48	7.30	96.12

Group 80m

Average similarity: 60.58

Species	Av.Abund	Av.Sim	Sim/SD	Contrib%	Cum.%
BRYOZOAN	2.68	36.41	2.19	60.11	60.11
PORIFERA	1.74	18.92	2.86	31.24	91.34

Group 5m

Average similarity: 55.68

Species	Av.Abund	Av.Sim	Sim/SD	Contrib%	Cum.%
MACROALGAE	3.19	23.26	1.00	41.78	41.78
PORIFERA	1.00	13.56	5.73	24.35	66.13
BRYOZOAN	1.00	13.56	5.73	24.35	90.48

Group 15m

Average similarity: 86.29

Species	Av.Abund	Av.Sim	Sim/SD	Contrib%	Cum.%
CCA	9.44	70.31	8.74	81.48	81.48
PORIFERA	1.40	8.00	4.85	9.28	90.76

Group 25m

Average similarity: 69.38

Species	Av.Abund	Av.Sim	Sim/SD	Contrib%	Cum.%
CCA	6.80	46.52	3.13	67.05	67.05
PORIFERA	2.53	11.29	2.22	16.28	83.33
BRYOZOAN	1.24	7.97	5.97	11.49	94.81

Group 50m

Average similarity: 61.80

Species	Av.Abund	Av.Sim	Sim/SD	Contrib%	Cum.%
PORIFERA	2.46	24.04	3.28	38.90	38.90
BRYOZOAN	2.04	21.10	2.36	34.14	73.04
POLYCHAETE	1.67	12.01	1.19	19.44	92.47

Group 70m

Average similarity: 51.35

Species	Av.Abund	Av.Sim	Sim/SD	Contrib%	Cum.%
BRYOZOAN	2.49	26.00	2.32	50.63	50.63
PORIFERA	1.36	18.77	4.65	36.55	87.18
POLYCHAETE	0.72	3.31	0.38	6.45	93.64

Table A2.10 SIMPER results to compare differences in benthic community composition across 10 m intervals from 5-120 m at mid Fiordland.

Group 100m

Average similarity: 61.19

Species	Av.Abund	Av.Sim	Sim/SD	Contrib%	Cum.%
POR	2.60	22.18	2.52	36.25	36.25
POLY	2.68	18.69	1.63	30.54	66.79
BRYO	2.04	16.34	2.22	26.70	93.49

Group 110m

Average similarity: 56.06

Species	Av.Abund	Av.Sim	Sim/SD	Contrib%	Cum.%
POR	2.46	20.41	2.57	36.40	36.40
BRYO	1.77	16.52	2.12	29.47	65.87
POLY	2.44	14.91	1.17	26.60	92.47

Group 120m

Average similarity: 53.72

Species	Av.Abund	Av.Sim	Sim/SD	Contrib%	Cum.%
POR	1.99	20.38	1.84	37.94	37.94
BRYO	1.87	19.32	2.51	35.96	73.90
POLY	2.16	13.45	0.99	25.04	98.94

Group 15m

Average similarity: 66.96

Species	Av.Abund	Av.Sim	Sim/SD	Contrib%	Cum.%
CCA0	4.33	15.48	2.83	23.12	23.12
POR	3.92	14.45	3.38	21.59	44.70
ASC	3.30	11.75	2.12	17.54	62.25
CND	2.10	7.77	3.65	11.61	73.85
BRYO	2.20	7.41	2.51	11.06	84.92
ALG	1.47	4.56	1.15	6.81	91.73

Group 25m

Average similarity: 68.37

Species	Av.Abund	Av.Sim	Sim/SD	Contrib%	Cum.%
CCA0	4.52	20.39	2.42	29.82	29.82
POR	3.97	17.83	2.74	26.08	55.90
BRYO	2.10	9.18	3.04	13.43	69.33
CND	1.75	7.34	1.69	10.74	80.06
ASC	1.77	6.65	1.38	9.73	89.80
POLY	1.56	5.91	1.08	8.65	98.45

Group 30m

Average similarity: 57.14

Species	Av.Abund	Av.Sim	Sim/SD	Contrib%	Cum.%
POR	4.29	20.93	2.83	36.63	36.63

CCA0	3.44	14.00	1.10	24.51	61.14
BRYO	1.87	7.82	2.60	13.69	74.83
POLY	1.91	6.12	0.93	10.72	85.55
CND	1.79	4.96	0.81	8.69	94.24

Group 40m

Average similarity: 60.55

Species	Av.Abund	Av.Sim	Sim/SD	Contrib%	Cum.%
POR	4.44	23.70	3.58	39.15	39.15
CCA0	3.09	11.26	0.94	18.60	57.75
BRYO	2.13	10.48	2.59	17.31	75.06
POLY	2.21	8.76	1.16	14.46	89.53
CND	1.31	3.85	0.73	6.36	95.88

Group 5m

Average similarity: 62.39

Species	Av.Abund	Av.Sim	Sim/SD	Contrib%	Cum.%
CCA0	5.74	24.92	3.89	39.95	39.95
COR	3.60	9.40	0.75	15.07	55.01
ALG	2.69	8.60	1.41	13.78	68.80
BRYO	2.73	8.18	1.64	13.11	81.90
POR	1.68	6.47	2.88	10.37	92.28

Group 50m

Average similarity: 54.75

Species	Av.Abund	Av.Sim	Sim/SD	Contrib%	Cum.%
POR	3.88	20.79	2.40	37.97	37.97
BRYO	2.06	10.81	2.48	19.75	57.71
POLY	1.97	8.84	1.02	16.15	73.87
CND	1.83	6.46	0.88	11.80	85.67
CCA0	1.85	5.00	0.53	9.13	94.80

Group 60m

Average similarity: 55.60

Species	Av.Abund	Av.Sim	Sim/SD	Contrib%	Cum.%
POR	3.81	26.31	2.22	47.32	47.32
BRYO	1.87	12.62	2.73	22.70	70.02
POLY	2.10	9.94	1.04	17.88	87.90
CND	1.04	2.73	0.43	4.91	92.81

Group 80m

Average similarity: 58.02

Species	Av.Abund	Av.Sim	Sim/SD	Contrib%	Cum.%
POR	3.30	22.93	2.42	39.53	39.53
BRYO	2.54	18.21	2.38	31.39	70.91
POLY	2.63	12.85	0.92	22.15	93.07

Group 90m

Average similarity: 60.36

Species	Av.Abund	Av.Sim	Sim/SD	Contrib%	Cum.%
POR	2.68	21.01	2.87	34.80	34.80
BRYO	2.30	20.38	2.74	33.76	68.56
POLY	2.46	15.96	1.30	26.44	95.00

Group 70m

Average similarity: 62.29

Species	Av.Abund	Av.Sim	Sim/SD	Contrib%	Cum.%
POR	3.30	20.88	2.83	33.52	33.52
POLY	3.11	19.66	2.61	31.57	65.09
BRYO	2.59	16.47	2.16	26.44	91.52

Table A2.11 Single factor PERMANOVA results for change in sponge assemblage morphological composition with depth at Poor Knights

PERMANOVA table of results

Source	df	SS	MS	Pseudo-F	P(perm)	Unique perms
De	8	30697	3837.1	5.6504	0.001	9893
Res	133	90320	679.1			
Total	141		1.2102E5			

Table A2.12 Single factor PERMANOVA results for change in sponge assemblage morphological composition at inner Fiordland

PERMANOVA table of results

Source	df	SS	MS	Pseudo-F	P(perm)	Unique perms
De	9	40633	4514.8	4.5296	0.001	9912
Res	116	1.1562E5	996.73			
Total	125	1.5625E5				

Table A2.13 Single factor PERMANOVA results for change in sponge assemblage morphological composition at mid Fiordland

PERMANOVA table of results

Source	df	SS	MS	Pseudo-F	P(perm)	Unique perms
De	12	99695	8307.9	6.9921	0.001	9882
Res	577	6.8559E5	1188.2			
Total	589	7.8528E5				

Table A2.14 Single factor PERMANOVA results for change in sponge assemblage morphological composition at outer Fiordland

PERMANOVA table of results

Source	df	SS	MS	Pseudo-F	P(perm)	Unique perms
De	12	48806	4067.2	3.3687	0.001	9854
Res	293	3.5375E5	1207.3			
Total	305	4.0256E5				

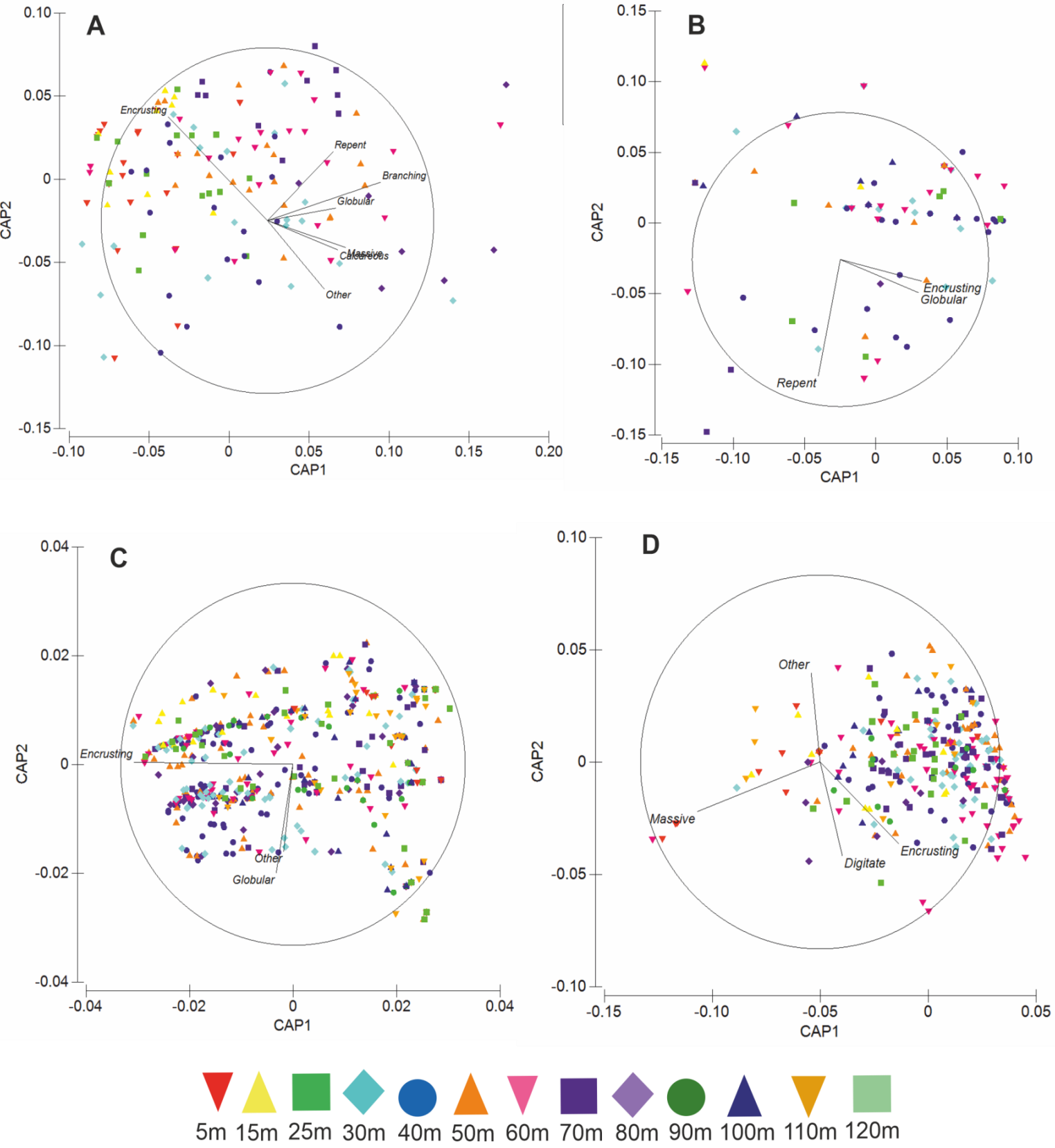

Fig. A2.7 Canonical analysis of principle components for sponge assemblage morphological composition structured by depth (m) at Poor Knights (A), inner Fiordland (B), mid Fiordland (C) and outer Fiordland (D). Pearson's correlation vectors (r>0.4) represent the abundance of the different morphological groups.

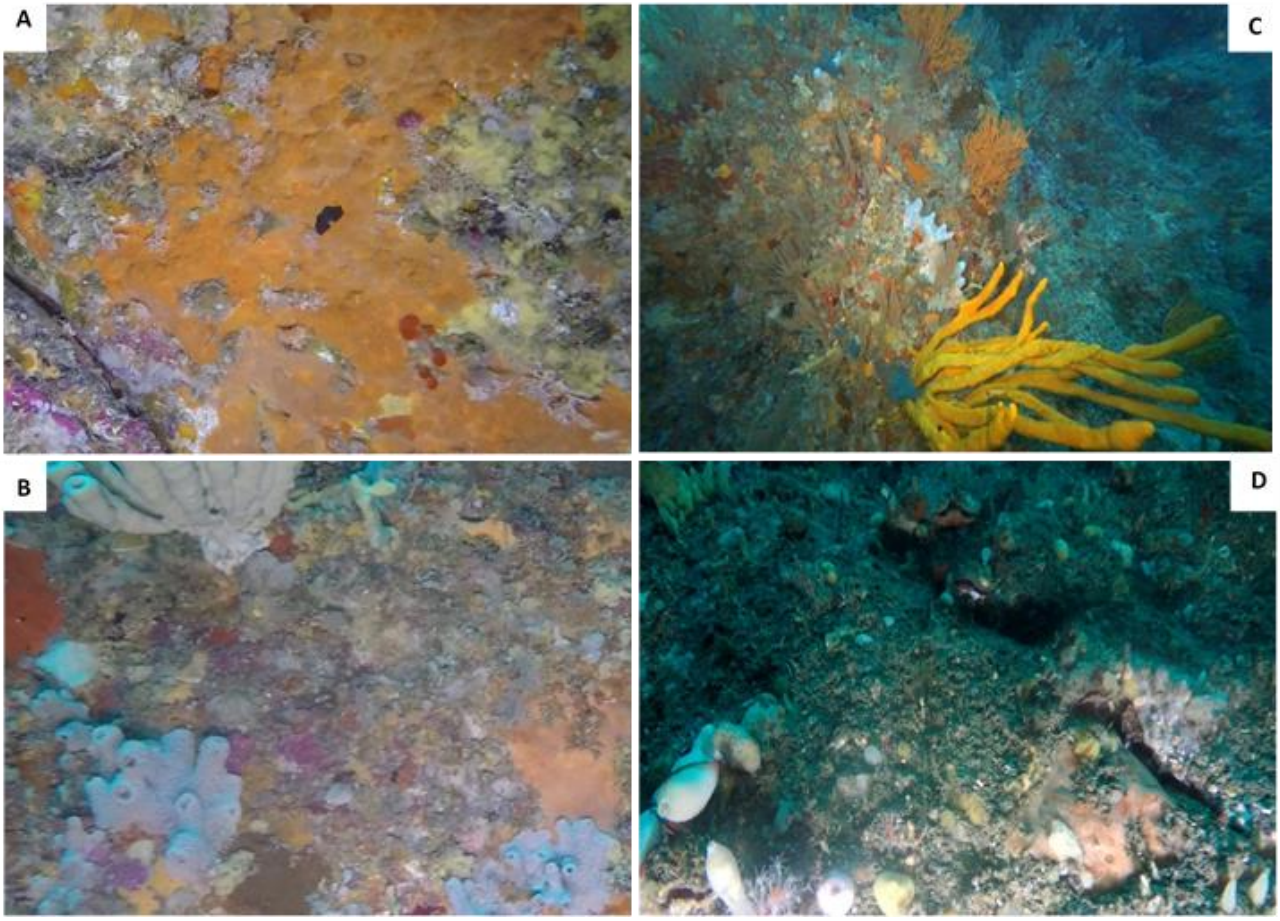

Fig. A2.8 Quadrats with high abundance of low (A), medium and high sponge complexity (B) at Poor knights from 40 m and 60 m respectively. Images C and D show wide angle perspectives of high overall abundance of a range of low, medium, and high complexity forms at 70 m at Poor knights and 40 m at outer Fiordland respectively.

Appendix B

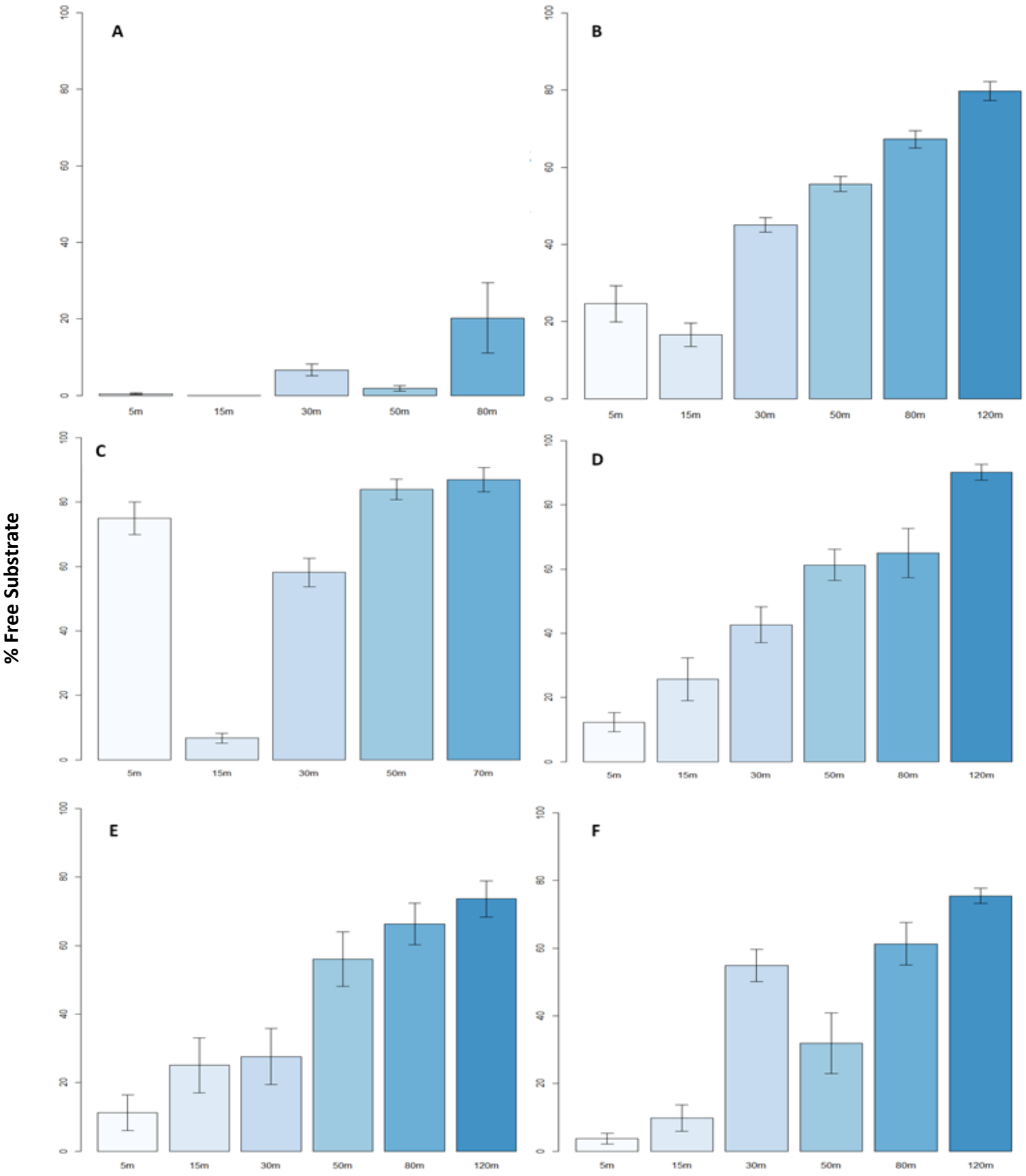
A
B
C
D
E
F
% Free Substrate
Depth
0
20
40
60
80
100
5m
15m
30m
50m
70m
80m
120m

Fig. B3.1 Distribution of free substrate through multiple depth categories, at the Poor Knights (A), all Fiordland sites combined (B), Site 1 (C), Site 2 (D), Site 3 (E), and Site 4 (F).

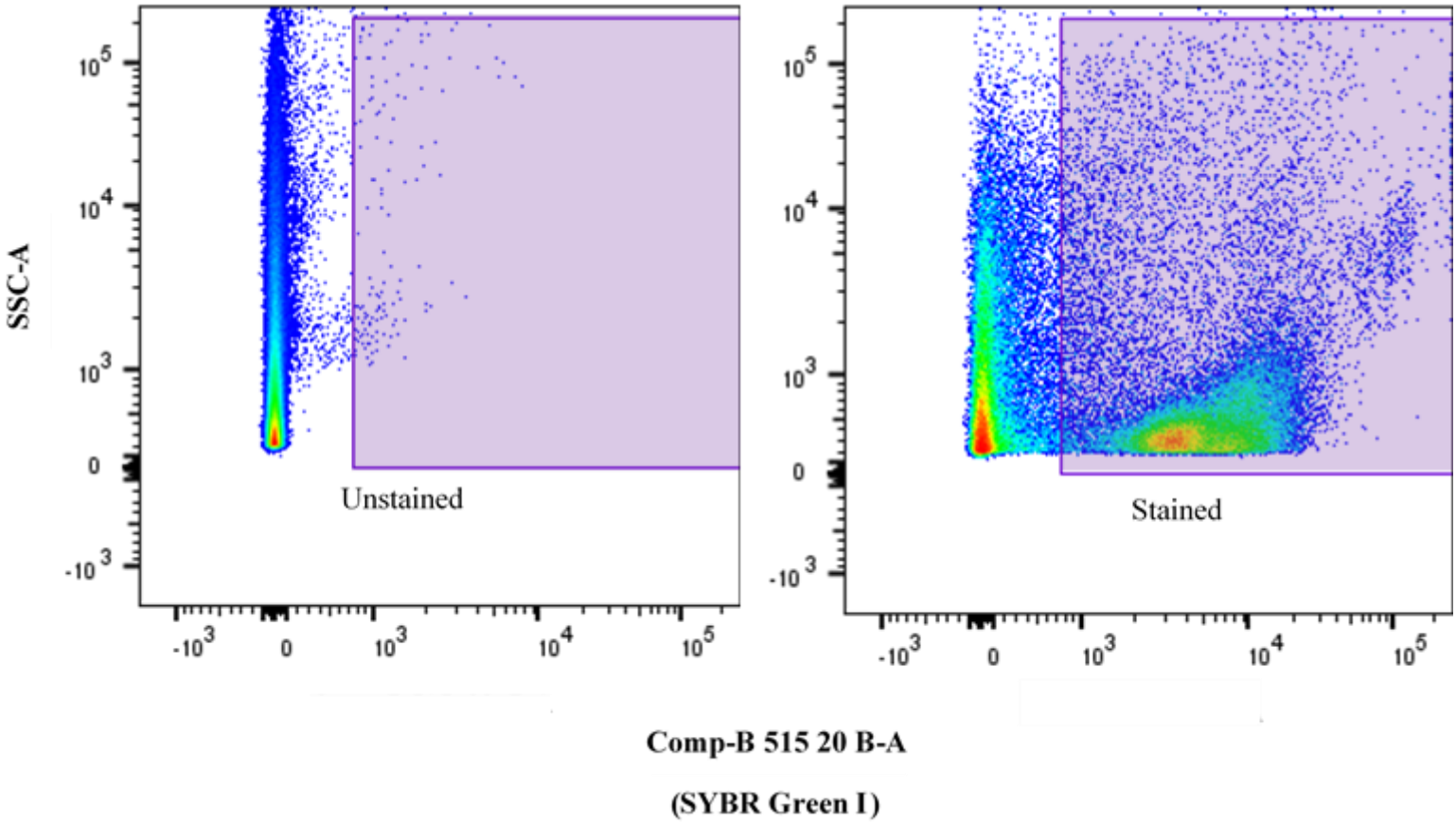

Fig. B3.2 Pseudocolor dotplot showing the gating technique used to discriminate nucleic-acid positive events from non-biological events. The 'nucleic-acid positive events' gate was placed on an unstained (A) sample (no SYBR Green I stain) , where less than 0.1% of events fell into the gate. The gate was then transposed onto the same stained sample (B) revealing the 'nucleic-acid positive events' population of interest.

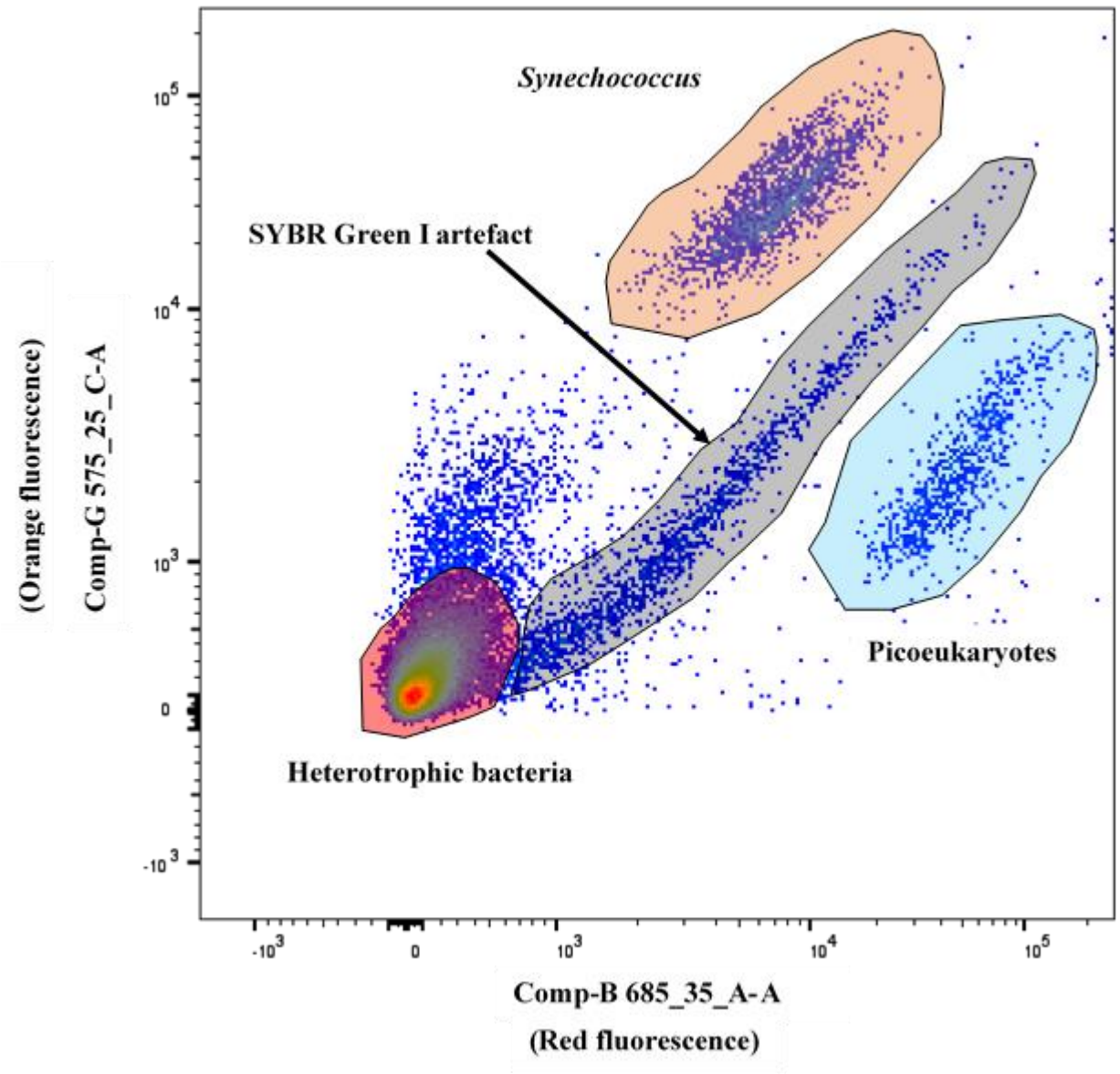

Fig. B3.3 Example of typical pseudocolor dotplot, pre-gated on nucleic-acid positive events, showing 3 major food group gates. Central highlighted line shows SYBR Green I dye bleeding across detectors to be removed in subsequent analyses.

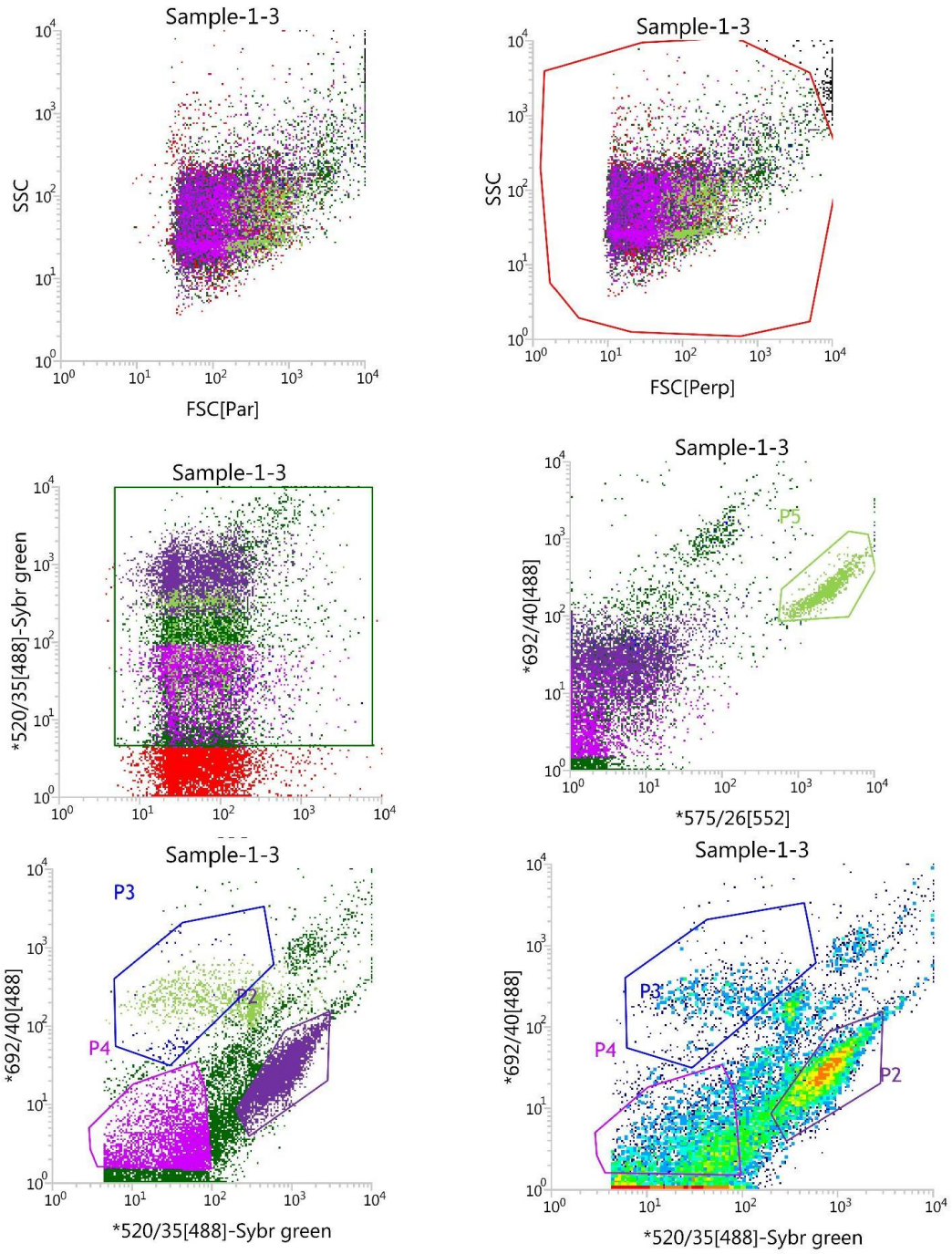

Statistics: *Sample-1-3*

Populations	Events	% Total	% Parent	*520/35... Mean	*692/40... Mean
All Events	20,000	100.00%	####	316	82
0.5um bead...	0	0.00%	0.00%	####	####
BOI	19,753	98.76%	98.76%	291	58
P1	14,297	71.48%	72.38%	401	80
P2	4,092	20.46%	28.62%	786	29
P3	681	3.40%	4.76%	79	277
P4	3,101	15.50%	21.69%	40	4
P5	1,105	5.52%	7.73%	259	232

Fig. B3.4 Sorting plots from BD Facs small particle software for microbial population discrimination and particle sorting for SEM imaging

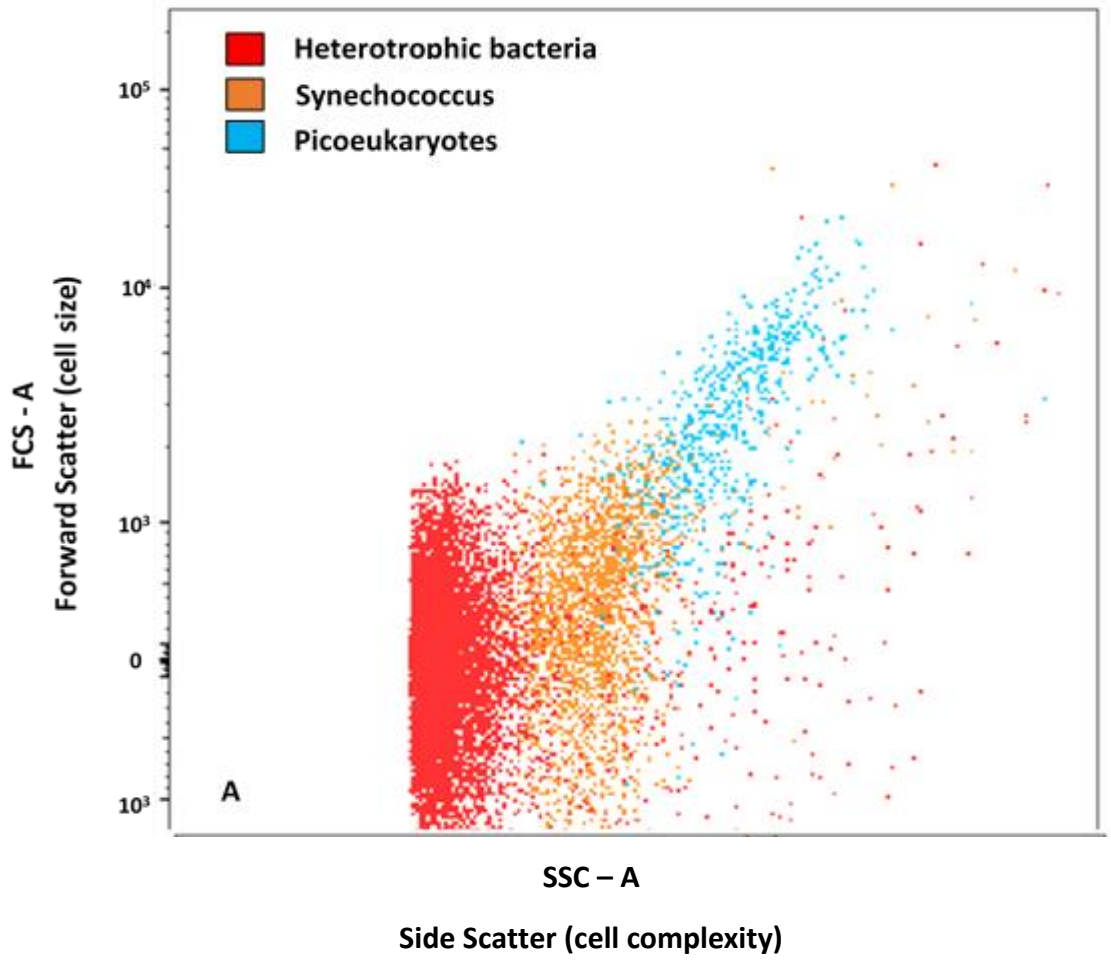

Fig. B3.5 Example of isolated populations of three main food groups from an inhalant water sample for *Tethya* sp. Cytogram shows clear distinctions in populations according to relative cell complexity and cell size (A)

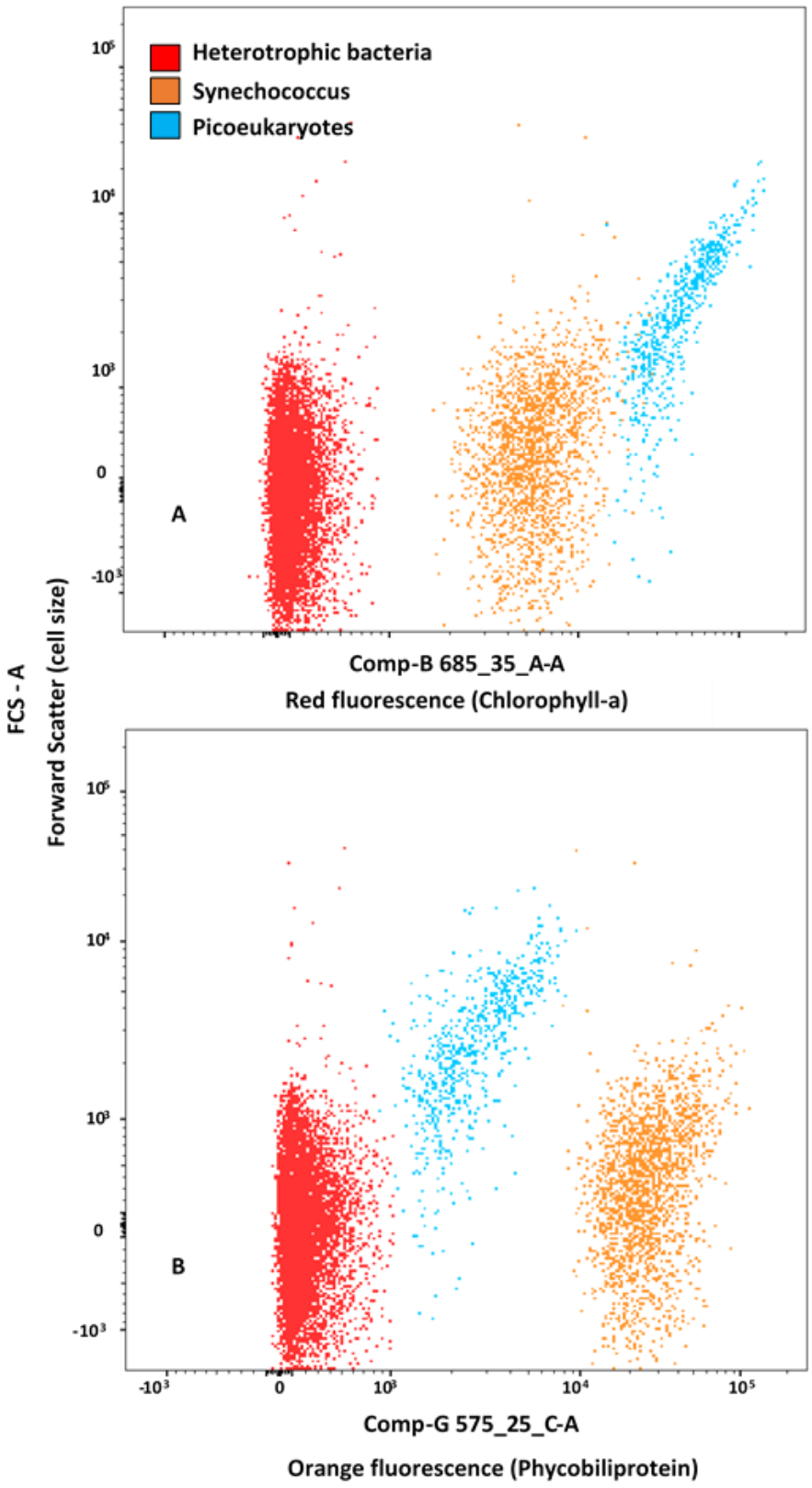

Fig. B3.6 Example of isolated populations of three main food groups from an inhalant water sample for *Tethya* sp. Cytogram shows clear distinctions in populations according to relative cell complexity and cell chlorophyll-a content (A) and cell size and phycobiliprotein content (B). Figure corresponds to the same populations discriminated by fluorescent properties in Fig. B3.5

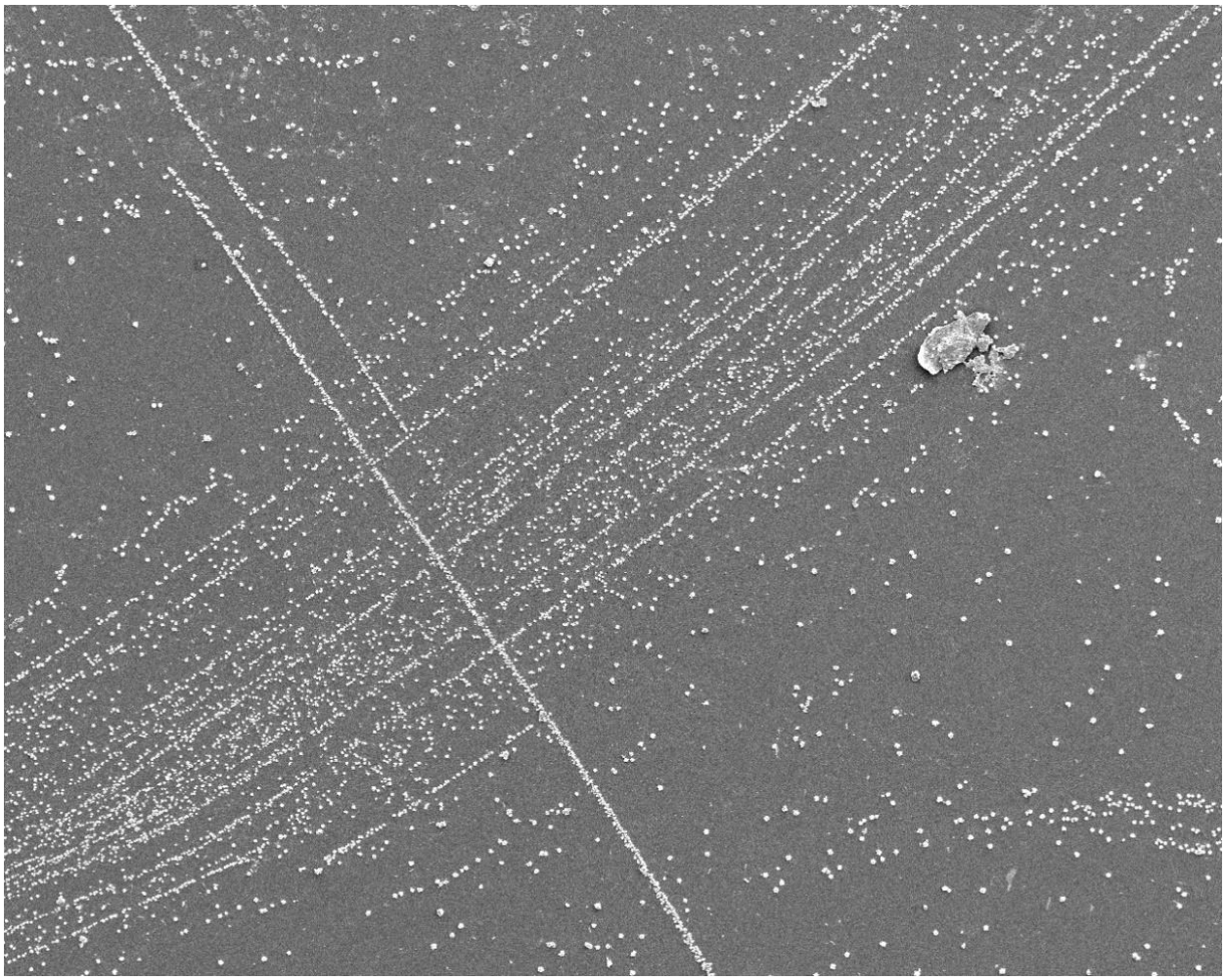

Fig. B3.7 Organized distribution of unknown artefacts generated during SEM preparation protocol.

Table B3.1 PERMANOVA table of results of pairwise differences in the abundance of total nucleic acid events and three microbial groups between 5 depth categories at the Poor Knights.

Depth	Nucleic-acid + events		Heterotrophic bacteria		Picoeukaryotes		*Synechococcus* sp.	
	t	P(perm)	t	P(perm)	t	P(perm)	t	P(perm)
0m, 10m	3.3269	0.001	3.6379	0.0002	3.4406	0.0042	1.0799	0.3136
0m, 30m	4.3386	0.002	4.4216	0.0004	10.108	0.0002	2.4821	0.0192
0m, 50m	2.6842	0.023	4.3861	0.0007	25.524	0.0001	3.8282	0.0025
0m, 80m	8.1626	0.001	10.966	0.0001	21.41	0.0002	23.232	0.0001
10m, 30m	1.282	0.209	1.029	0.3146	5.4694	0.0001	0.9966	0.3325
10m, 50m	2.758	0.003	2.7811	0.0028	8.2499	0.0001	0.31389	0.7668
10m, 80m	0.47509	0.652	0.42428	0.7	2.7933	0.0111	9.4188	0.0001
30m, 50m	3.2295	0.003	3.0189	0.0063	2.2765	0.0331	0.86783	0.4002
30m, 80m	1.0802	0.291	2.1323	0.0455	3.7905	0.0015	9.8255	0.0001
50m, 80m	6.2576	0.001	8.4823	0.0002	13.509	0.0001	18.22	0.0001

Table B3.2 PERMANOVA table of results of pairwise differences in the abundance of total nucleic acid events and three microbial groups between 5 depth categories at Fiordland Site 1.

Depth	**Nucleic-acid + events**		**Heterotrophic bacteria**		**Picoeukaryotes**		***Synechococcus* sp.**	
	t	P(perm)	t	P(perm)	t	P(perm)	t	P(perm)
80m, 50m	2.4533	0.028	2.4777	0.0203	4.2771	0.0019	3.036	0.0083
80m, 30m	1.8412	0.077	1.5913	0.1305	15.999	0.0002	13.677	0.0001
80m, 10m	8.7755	0.001	7.2637	0.0001	70.365	0.0001	68.806	0.0001
80m, 0m	4.1888	0.002	3.7814	0.0027	27.815	0.0001	47.914	0.0001
50m, 30m	5.1286	0.001	4.7214	0.0001	12.272	0.0002	11.67	0.0002
50m, 10m	27.179	0.001	23.985	0.0002	60.453	0.0001	57.095	0.0001
50m, 0m	11.219	0.001	11.303	0.0001	23.192	0.0001	36.35	0.0001
30m, 10m	6.7427	0.002	5.305	0.0003	34.402	0.0001	19.501	0.0001
30m, 0m	2.0916	0.039	1.8583	0.0795	8.574	0.0002	5.7844	0.0002
10m, 0m	6.9508	0.001	5.9446	0.0001	25.581	0.0002	30.969	0.0001

Table B3.3 PERMANOVA table of results of pairwise differences in the abundance of total nucleic acid events and 3 microbial groups between 5 depth categories at Fiordland Site 2.

Depth	Nucleic-acid + events		Heterotrophic bacteria		Picoeukaryotes		*Synechococcus* sp.	
	t	P(perm)	t	P(perm)	t	P(perm)	t	P(perm)
120m, 80m	1.2384	0.251	1.5087	0.1602	14.648	0.0001	8.2243	0.0001
120m, 50m	7.2466	0.001	6.8434	0.0004	15.839	0.0001	14.835	0.0002
120m, 30m	8.9883	0.001	8.0129	0.0001	20.84	0.0001	23.828	0.0002
120m, 10m	1.7158	0.154	1.2176	0.2513	6.9484	0.0002	15.143	0.0003
120m, 0m	12.353	0.001	10.766	0.0001	41.297	0.0002	21.322	0.0002
80m, 50m	2.3068	0.032	1.6736	0.1133	3.1148	0.0061	4.5864	0.0008
80m, 30m	2.6582	0.016	1.899	0.0767	5.4091	0.0004	8.0458	0.0001
80m, 10m	0.18474	0.876	0.59125	0.5752	1.5531	0.1403	0.32932	0.7607
80m, 0m	4.2008	0.003	3.2118	0.0088	30.154	0.0001	11.595	0.0001
50m, 30m	0.62374	0.542	0.51525	0.621	1.054	0.3006	2.9046	0.0079
50m, 10m	2.4343	0.027	3.4412	0.006	0.3504	0.7587	6.555	0.0001
50m, 0m	4.0214	0.001	3.9591	0.0004	22.782	0.0001	8.0556	0.0005
30m, 10m	2.8701	0.011	3.8886	0.0019	0.001	0.9934	17.857	0.0002
30m, 0m	4.0695	0.004	4.1023	0.0012	29.199	0.0002	7.1091	0.0002
10m, 0m	4.69	0.002	5.8171	0.0003	8.3224	0.0001	15.264	0.0001

Table B3.4 PERMANOVA table of results of pairwise differences in the abundance of total nucleic acid events and 3 microbial groups between 5 depth categories at Fiordland Site 3.

Depth	Nucleic-acid + events		Heterotrophic bacteria		Picoeukaryotes		*Synechococcus* sp.	
	t	P(perm)	t	P(perm)	t	P(perm)	t	P(perm)
120m, 80m	9.1774	0.001	10.497	0.0002	8.858	0.0003	11.379	0.0003
120m, 50m	7.7817	0.001	7.7247	0.0004	14.393	0.0001	22.85	0.0001
120m, 30m	4.9619	0.001	4.5373	0.0001	33.251	0.0002	22.214	0.0001
120m, 10m	2.6253	0.022	4.4295	0.0009	41.679	0.0002	26.866	0.0002
120m, 0m	23.247	0.002	27.292	0.0001	36.279	0.0003	56.818	0.0001
80m, 50m	2.9631	0.013	4.5217	0.0009	3.6799	0.0029	2.8334	0.0125
80m, 30m	1.4541	0.166	1.9209	0.0709	1.5595	0.1428	2.9587	0.0081
80m, 10m	12.622	0.001	14.979	0.0001	0.1106	0.8938	3.114	0.0049
80m, 0m	14.464	0.001	15.802	0.0001	17.907	0.0001	16.236	0.0001
50m, 30m	0.42739	0.709	0.71973	0.4902	7.2074	0.0001	0.28131	0.7693
50m, 10m	12.266	0.001	13.706	0.0001	12.107	0.0001	0.53019	0.5926
50m, 0m	18.783	0.001	22.281	0.0003	29.69	0.0001	34.854	0.0001
30m, 10m	6.7944	0.001	6.7577	0.0001	11.829	0.0001	0.21422	0.8307
30m, 0m	12.514	0.001	12.984	0.0002	28.594	0.0001	34.921	0.0002
10m, 0m	27.212	0.001	32.491	0.0001	27.038	0.0001	37.532	0.0001

Table B3.5 PERMANOVA table of results of pairwise differences in the abundance of total nucleic acid events and 3 microbial groups between 5 depth categories at Fiordland Site 4.

Depth	Nucleic-acid + events		Heterotrophic bacteria		Picoeukaryotes		*Synechococcus* sp.	
	t	P(perm)	t	P(perm)	t	P(perm)	t	P(perm)
0m, 10m	4.3801	0.001	4.9851	0.0004	10.673	0.0001	5.2339	0.0002
0m, 30m	6.2344	0.001	7.0905	0.0001	16.427	0.0001	7.3098	0.0001
0m, 50m	7.3757	0.001	8.2637	0.0001	14.872	0.0003	8.096	0.0003
0m, 80m	6.5501	0.001	7.3553	0.0002	15.864	0.0001	7.6438	0.0001
0m, 120m	6.7067	0.001	7.5956	0.0001	17.653	0.0001	9.8447	0.0001
10m, 30m	1.3554	0.221	1.6893	0.1113	15.242	0.0002	1.9937	0.0676
10m, 50m	3.1906	0.006	3.5925	0.0045	9.488	0.0001	3.352	0.0059
10m, 80m	2.8553	0.011	3.2359	0.0073	12.687	0.0002	2.9383	0.0117
10m, 120m	2	0.063	2.4005	0.0318	18.64	0.0001	5.9463	0.0001
30m, 50m	4.046	0.002	4.3601	0.0004	3.0634	0.003	2.7362	0.0144
30m, 80m	2.5517	0.027	2.7392	0.0145	1.5743	0.1442	1.9209	0.0701
30m, 120m	2.6849	0.017	2.7905	0.0136	11.913	0.0001	10.263	0.0001
50m, 80m	0.59269	0.547	0.79466	0.4316	1.7589	0.1002	0.008	0.9304
50m, 120m	2.9874	0.014	3.1594	0.0031	7.0558	0.0002	4.1737	0.0004
80m, 120m	2.0144	0.06	2.17	0.0441	7.5722	0.0001	3.0375	0.0071

Table B3.6 Linear regression relationships between sponge abundance and the abundance of DNA positive events, heterotrophic bacteria, picoeukaryotes, and *Synechococcus* sp. (cells *per* ml) and DOC concentration at individual Fiordland sites.

Location	**Nucleic-acid events**			**Heterotrophic bacteria**			**Picoeukaryotes**			***Synechococcus* sp.**			**DOC**		
	R^2	F	P	R^2	F	P	R^2	F	P	R^2	F	P	R^2	F	P
Site 1	0.08	0.27	0.64	0.07	0.23	0.66	0.13	0.44	0.56	0.08	0.29	0.63	0.74	8.50	0.06
Site 2	0.06	0.25	0.64	0.08	0.36	0.58	0.08	0.36	0.58	0.003	0.00	0.99	0.01	0.04	0.85
Site 3	0.52	4.42	0.10	0.52	4.40	0.10	0.44	3.13	0.15	0.43	3.02	0.16	0.02	0.09	0.78
Site 4	0.4	2.69	0.18	0.4	2.91	0.16	0.21	1.09	0.36	0.25	1.37	0.31			
						Excluding 0 – 10 m									
Site 1	0.05	0.11	0.77	0.04	0.09	0.79	0.15	0.34	0.62	0.08	0.19	0.71	0.85	11.31	0.08
Site 2	0.92	32.66	0.01*	0.92	35.93	0.01*	0.76	9.69	0.05*	0.98	156.17	0.01*	0.67	6.11	0.09
Site 3	0.13	0.43	0.56	0.12	0.42	0.56	0.01	0.04	0.85	0.00	0.01	0.92	0.01	0.04	0.85
Site 4	0.29	1.25	0.34	0.36	1.66	0.29	0.21	0.79	0.44	0.00	0.00	0.99			

Appendix C

Table C4.1 PERMANOVA table of results showing post-hoc pairwise t tests of species differences in cell retention efficiency (% of cells retained from ambient cell concentrations) of three POC groups, total POC and DOC

Species pairs	**Picoeukaryotes**		***Synechococcus* sp.**		**Heterotrophic bac.**	
	t	**p**	**t**	**p**	**T**	**p**
Tethya- Tedania	2.0738	0.113	1.7558	0.15	1.2571	0.186
Tethya- Suberites	1.9543	0.109	0.82319	0.443	2.3849E-2	0.984
Tethya- Polymastia p.	1.2609	0.276	1.4437	0.12	1.5526	0.071
Tethya- Polymastia sp.	2.3715	0.03*****	1.8933	0.031*****	2.2537	0.018*****
Tethya- Dysidea	1.4088	0.07	1.5263	0.087	1.708	0.031*****
Tethya- Clathrina	0.85244	0.618	1.0664	0.321	3.3107	0.014*****
Tedania- Suberites	0.9611	0.385	1.7485	0.151	1.2592	0.181
Tedania- Polymastia p.	0.94637	0.469	1.5859	0.271	0.96567	0.461
Tedania- Polymastia sp.	2.1839	0.091	8.9186E-2	0.812	0.65542	0.546
Tedania- Dysidea	0.29566	0.83	1.6953	0.148	0.54041	0.587
Tedania- Clathrina	0.22117	0.845	1.6462	0.251	0.97106	0.441
Suberites- Polymastia p.	1.0981	0.437	1.3653	0.203	1.5715	0.053*****
Suberites- Polymastia sp.	2.2755	0.056	1.8852	0.038*****	2.2566	0.024*****
Suberites- Dysidea	0.83053	0.673	1.3141	0.232	1.7096	0.027*****
Suberites- Clathrina	0.27595	0.999	0.97352	0.498	3.4083	0.015*****

Polymastia sp.-Polymastia p.	1.3875	0.249	1.7057	0.101	1.8572	0.095
Polymastia p.- Dysidea	0.83061	0.715	0.8006	0.646	1.4862	0.292
Polymastia p.- Clathrina	0.98292	0.54	0.41957	0.544*****	0.28137	0.844
Polymastia sp.- Dysidea	2.1064	0.085	1.8265	0.056	0.41808	0.696
Polymastia sp.- Clathrina	2.1987	0.074	1.7726	0.08	1.864	0.051*****
Dysidea- Clathrina	0.40487	0.485	0.33821	0.882	1.4965	0.438

Species pairs	**POC**		**DOC**	
	t	**p**	**t**	**p**
Tethya- Tedania	0.56068	0.698	1.6551	0.116
Tethya- Suberites	0.5422	0.689	9.4667E-2	0.85
Tethya- Polymastia p.	2.1602	0.037*****	1.1209	0.05*****
Tethya- Polymastia sp.	1.6416	0.138	2.0739	0.036*****
Tethya- Dysidea	1.9133	0.077	1.7217	0.029*****
Tethya- Clathrina	1.9263	0.062	2.4697	0.016*****
Tedania- Suberites	2.7559E-2	0.949	1.6614	0.081
Tedania- Polymastia p.	2.0126	0.049*****	0.60099	0.802
Tedania- Polymastia sp.	1.7026	0.13	0.59759	0.571
Tedania- Dysidea	1.8695	0.092	7.1969E-2	0.713

Tedania- Clathrina	1.8759	0.092	1.314	0.428
Suberites- Polymastia p.	1.9789	0.052*****	1.1305	0.05*****
Suberites- Polymastia sp.	1.6703	0.169	2.0879	0.025*****
Suberites- Dysidea	1.8357	0.109	1.7288	0.029*****
Suberites- Clathrina	1.8427	0.08	2.5242	0.015*****
Polymastia sp.- Polymastia p.	0.91383	0.37	0.71552	0.536
Polymastia p.- Dysidea	1.3619	0.184	0.62567	0.561
Polymastia p.- Clathrina	0.60887	0.549	0.77809	0.539
Polymastia sp.- Dysidea	0.33205	0.841	0.54874	0.716
Polymastia sp.- Clathrina	0.43201	0.703	1.2096	0.187
Dysidea- Clathrina	0.31818	0.743	1.3272	0.407

Table C4.2 PERMANOVA table of results showing post-hoc pairwise t tests of all species differences in Chesson's index scores for POC groups and DOC included in formulae for Polymastia species.

Groups	**t**	**P(perm)**
Tethya - Suberites	8.9318E-2	0.9504
Tethya - Tedania	1.4763	0.0897
Tethya - Penicillus	3.0778	0.0029
Tethya - Polymastia	1.767	0.0782

Tethya - Dysidea	0.77712	0.7
Tethya - Clathrina	0.63833	0.5594
Suberites - Tedania	1.4798	0.084
Suberites - Penicillus	3.1298	0.0028
Suberites - Polymastia	1.7721	0.0755
Suberites - Dysidea	0.79959	0.7021
Suberites - Clathrina	0.68026	0.5262
Tedania - Penicillus	1.8559	0.0045
Tedania - Polymastia	0.6011	0.6936
Tedania - Dysidea	1.2947	0.3144
Tedania - Clathrina	1.4062	0.2079
Penicillus - Polymastia	1.7675	0.0339
Penicillus - Dysidea	1.6739	0.0878
Penicillus - Clathrina	2.179	0.0359
Polymastia - Dysidea	1.5293	0.1077
Polymastia - Clathrina	1.6591	0.0811
Dysidea - Clathrina	0.38437	0.9925

Table C4.3 PERMANOVA table of results showing post,hoc pairwise t tests of all species differences in Chesson's index scores for POC groups only.

Species Pair	t	P(perm)
Tethya - Suberites	8.9318E-2	0.951
Tethya - Tedania	1.4763	0.0898
Tethya - Penicillus	0.14153	0.898
Tethya - Polymastia	1.9108	0.017
Tethya - Dysidea	0.77712	0.7195
Tethya - Clathrina	0.63833	0.5496
Suberites - Tedania	1.4798	0.0801
Suberites - Penicillus	0.22139	0.8401
Suberites - Polymastia	1.9142	0.0144
Suberites - Dysidea	0.79959	0.7054
Suberites - Clathrina	0.68026	0.5265
Tedania - Penicillus	1.4686	0.0935
Tedania - Polymastia	0.53962	0.6748
Tedania - Dysidea	1.2947	0.3245
Tedania - Clathrina	1.4062	0.2034
Penicillus - Polymastia	1.9035	0.0182

Penicillus - Dysidea	0.72769	0.747
Penicillus - Clathrina	0.5482	0.5985
Polymastia - Dysidea	1.7246	0.051
Polymastia - Clathrina	1.8401	0.0436
Dysidea - Clathrina	0.38437	0.9917

Table C4.4 PERMANOVA table of results showing post,hoc pairwise t tests of all species differences in Chesson's index scores with DOC feeding Polymastia species excluded.

Groups	t	P(perm)
Tethya - Suberites	8.9318E-2	0.951
Tethya - Tedania	1.4763	0.0825
Tethya - Dysidea	0.77712	0.7149
Tethya - Clathrina	0.63833	0.5582
Suberites - Tedania	1.4798	0.0802
Suberites - Dysidea	0.79959	0.7015
Suberites - Clathrina	0.68026	0.5194
Tedania - Dysidea	1.2947	0.3102
Tedania - Clathrina	1.4062	0.2053
Dysidea - Clathrina	0.38437	0.9925

Table C4.5 PERMANOVA table of results showing post,hoc pairwise t tests of species differences in cell retention (number of cells retained by sponge) of three POC groups, total POC and DOC.

Species pairs	**Picoeukaryotes**		***Synechococcus* sp.**		**Heterotrophic bac.**	
	t	**p**	**t**	**p**	**t**	**P**
Tethya - Tedania	1.1004	0.335	1.1971	0.116	0.97046	0.751
Tethya - Suberites	0.83406	0.438	0.72599	0.458	3.4766	0.009*****
Tethya - Polymastia p.	1.2387	0.19	0.61566	0.61	0.12827	0.943
Tethya - Polymastia sp.	2.6112	0.027*****	1.628	0.234	1.2627	0.041*****
Tethya - Dysidea	4.2449	0.01*****	3.2136	0.023*****	1.645	0.13
Tethya - Clathrina	2.2128	0.07	5.6696	0.011*****	1.6918	0.125
Tedania - Suberites	1.3069	0.148	0.96824	0.48	1.0687	0.095
Tedania - Polymastia p.	1.4288	0.185	1.2348	0.066	0.96696	0.752
Tedania - Polymastia sp.	0.47783	0.659	0.55129	1	0.35958	0.469
Tedania - Dysidea	0.38873	0.807	0.9457	0.543	0.6549	0.332
Tedania - Clathrina	0.68135	0.626	0.96599	0.509	0.95133	0.946
Suberites - Polymastia p.	0.11345	0.893	0.89869	0.371	3.4949	0.016*****
Suberites - Polymastia sp.	2.5254	0.049*****	1.4614	0.365	1.4554	0.01*****
Suberites - Dysidea	2.3715	0.05*****	0.7765	0.484	1.7332	0.01*****
Suberites - Clathrina	1.6134	0.191	0.83238	0.403	7.4055	0.006*****
Polymastia p. - Polymastia sp.	2.8615	0.022*****	1.6497	0.161	1.2541	0.05*****
Polymastia p. - Dysidea	3.1311	0.028*****	3.8151	0.021*****	1.6409	0.139

Polymastia p. - Clathrina	2.1715	0.068	7.9581	0.01*	1.4565	0.18
Polymastia C - Dysidea	1.1861	0.283	1.4743	0.452	0.57592	1
Polymastia sp. - Clathrina	1.807	0.128	1.4921	0.453	1.1907	0.096
Dysidea - Clathrina	1.4892	0.175	0.11464	0.935	1.6152	0.376

Species pairs	POC		DOC	
	t	P	t	P
Tethya - Tedania	1.5938	0.349	1.1882	0.263
Tethya - Suberites	3.4288	0.005*	0.91953	0.428
Tethya - Polymastia p.	1.1167	0.299	2.9877	0.011*
Tethya - Polymastia sp.	1.6368	0.198	2.7477	0.021*
Tethya - Dysidea	1.6356	0.188	1.5065	0.174
Tethya - Clathrina	1.5193	0.186	1	
Tedania - Suberites	1.6639	0.07	.6711	0.111
Tedania - Polymastia p.	1.6164	0.346	0.33117	0.564
Tedania - Polymastia sp.	6.5122E-2	0.799	2.8562	0.006*
Tedania - Dysidea	6.6152E-2	0.66	2.7501	0.007*
Tedania - Clathrina	1.5593	0.445	2.1684	0.009*
Suberites - Polymastia p.	2.9164	0.038*	2.2312	0.015*
Suberites - Polymastia sp.	1.7197	0.027*	2.15	0.007*
Suberites - Dysidea	1.719	0.012*	2.0709	0.017*
Suberites - Clathrina	4.6501	0.011*	1.6234	0.183
Polymastia p. - Polymastia sp.	1.6636	0.157	1.6699	0.158
Polymastia p. - Dysidea	1.6626	0.031*	0.42113	0.71
Polymastia p. - Clathrina	2.678	0.009*	6.0707	0.007*
Polymastia sp. Dysidea	5.1195E-3	1	2.7894	0.023*
Polymastia sp. - Clathrina	1.5945	0.323	3.8664	0.01*
Dysidea - Clathrina	1.5931	0.389	2.1254	0.065

Table C4.6 Relationships between specific food group availability and retention efficiency of 7 sponge species combined.

Ambient food group – retention efficiency relationship	**R^2**	**F-statistic**	**p-value**	**Df**
Ambient POC – POC retention efficiency	0.14	5.23	>0.03*	1,33
Ambient *Synechococcus* – *Synechococcus* retention efficiency	0.04	1.28	0.267	1,33
Ambient picoeukaryotes – picoeukaryote retention efficiency	0.03	0.139	0.711	1,33
Ambient heterotrophic bacteria – heterotrophic bacteria retention efficiency	0.09	3.42	0.073	1,33
Ambient DOC – DOC efficiency	0.05	1.40	0.215	1,33

Table C4.7. Relationships between specific food group availability and food selectivity of 7 sponge species combined.

Ambient food group – selectivity relationship	**R^2**	**F-statistic**	**p-value**	**Df**
Ambient *Synechococcus* – *Synechococcus* selectivity	0.07	2.48	0.125	1,33
Ambient *Synechococcus* – *Synechococcus* selectivity *Outliers removed*	0.16	6.26	0.017	1,33
Ambient picoeukaryotes – picoeukaryote selectivity	0.07	0.22	0.642	1,33
Ambient heterotrophic bacteria – heterotrophic bacteria selectivity	0.04	1.38	0.249	1,33
Ambient DOC – DOC retention selectivity	0.21	8.64	>0.01*	1,33

Table C4.8. Linear regression model results of ambient POC availability to POC retention (left) and retention efficiency (right) relationships across all species and for each individual species. Cell count (cells/ml) data was log-transformed, and percentage data was square root transformed to meet assumptions of distribution normality.

	Ambient POC – POC retention count			Ambient POC – POC retention efficiency		
Species	**R^2**	**F-statistic**	**p-value**	**R^2**	**F-statistic**	**p-value**
All Species	0.50	33.63	>0.001*	0.14	5.23	> 0.03*
Tethya sp.	0.99	20498	> 0.001*	0.89	28.04	> 0.01*
Tedania sp.	0.61	0.612	0.491	0.01	0.04	0.848
Suberites sp.	0.98	87.68	> 0.001*	0.58	4.162	0.134
Polymastia Penicillus	0.00	0.00	0.976	0.24	0.94	0.183
Polymastia sp.	0.27	1.09	0.374	0.08	0.248	0.653
Dysidea sp.	0.41	5.219	0.107	0.55	3.733	0.149
Clathrina sp.	0.12	0.7298	0.4557	0.06	0.1999	0.6851

Table S10. Linear regression model results of ambient picoeukaryote availability to picoeukaryote retention (left) and retention efficiency (right) relationships across all species and for each individual species. Cell count (cells/ml) data was log-transformed, and percentage data was square root transformed to meet assumptions of distribution normality.

	Ambient picoeukaryote count – picoeukaryote retention count			Ambient picoeukaryote count – picoeukaryotes retention efficiency		
Species	**R^2**	**F-statistic**	**p-value**	**R^2**	**F-statistic**	**p-value**
All Species	0.60	50.20	> 0.001**	0.001	0.05	0.830
Tethya sp.	0.96	86.47	> 0.01**	0.65	5.49	0.101
Tedania sp.	0.55	3.68	0.151	0.38	1.88	0.265
Suberites sp.	0.99	3374	> 0.001**	0.01	0.04	0.859
Polymastia Penicillus	0.43	2.261	0.229	0.00	0.00	0.961
Polymastia sp.	0.04	0.128	0.7447	0.01	0.03	0.867
Dysidea sp.	0.72	206 .4	> 0.01**	0.01	0.03	0.870
Clathrina sp.	0.95	62.18	> 0.01**	- 0.93	39.73	> 0.01**

Table S11. Linear regression model results of ambient *Synechococcus* sp. availability to *Synechococcus* sp. retention (left) and retention efficiency (right) relationships across all species and for each individual species. Cell count (cells/ml) data was log-transformed, and percentage data was square root transformed to meet assumptions of distribution normality.

	Ambient Synechoccocus – Synechoccocus retention count			**Ambient Synechoccocus – Synechoccocus retention efficiency**		
Species	**R^2**	**F-statistic**	**p-value**	**R^2**	**F-statistic**	**p-value**
All Species	0.46	27.91	> 0.001*	0.037	1.275	0.267
Tethya sp.	0.99	826.8	> 0.001*	0.66	5.901	0.0935
Tedania sp.	0.27	1.1	0.371	0.33	1.483	0.310
Suberites sp.	0.99	3112	> 0.001*	- 0.86	18	>0.05*
Polymastia Penicillus	0.04	0.113	0.76	- 0.83	14.82	> 0.05*
Polymastia sp.	0.56	3.73	0.149	0.50	3.02	0.181
Dysidea sp.	0.94	48.54	> 0.01*	0.31	1.34	0.331
Clathrina sp.	0.41	2.076	0.2453	- 0.95	57.66	> 0.01*

Table S12. Linear regression model results of ambient heterotrophic bacteria availability to heterotrophic bacteria retention (left) and retention efficiency (right) relationships across all species and for each individual species. Cell count (cells/ml) data was log-transformed, and percentage data was square root transformed to meet assumptions of distribution normality.

	Ambient heterotrophic bacteria – heterotrophic bacteria retention count			**Ambient heterotrophic bacteria – heterotrophic bacteria retention efficiency**		
Species	**R^2**	**F-statistic**	**p-value**	**R^2**	**F-statistic**	**p-value**
All Species	0.49	31.88	>0.001**	0.20	8.1	>0.01**
Tethya sp.	0.99	924.8	> 0.001**	0.98	130.3	> 0.01**
Tedania sp.	0.11	0.3837	0.5795	0.12	0.39	0.58
Suberites sp.	0.95	57.82	> 0.01**	0.44	2.37	0.222
Polymastia Penicillus	0.00	0.006	0.940	0.00	0.01	0.936
Polymastia sp.	0.03	0.123	0.749	0.28	1.17	0.359
Dysidea sp.	0.54	3.467	0.160	0.53	3.34	0.165
Clathrina sp.	0.01	0.018	0.903	0.46	2.53	0.210

Table S13. Linear regression model results of ambient DOC availability to DOC retention (left) and retention efficiency (right) relationships across all species and for each individual species. DOC concentration data was log-transformed, and percentage data was square root transformed to meet assumptions of distribution normality.

	Ambient DOC – DOC retention			**Ambient DOC – DOC retention efficiency**		
Species	**R^2**	**F-statistic**	**p-value**	**R^2**	**F-statistic**	**p-value**
All Species	0.47	29.09	>0.001*	0.05	1.599	0.215
Tethya sp.	0..06	0.1893	0.6929	0.15	0.5842	0.5003
Tedania sp.	- 0.95	54.37	> 0.01*	- 0.92	33.43	> 0.01*
Suberites sp.	0.04	0.0379	0.8581	0.05	0.15	0.721
Polymastia Penicillus	0.56	3.859	0.144	0.28	1.17	0.359
Polymastia sp.	0.04	0.133	0.740	0.01	0.02	0.890
Dysidea sp.	0.51	3.136	0.1747	0.00	0.01	0.931
Clathrina sp.	0.98	149.2	> 0.01*	0.92	32.45	> 0.01*

Table S15. Linear regression model results of ambient DOC availability to POC retention (left) and retention efficiency (right) relationships across all species and for each individual species. Cell count (cells/ml) and DOC concentration data was log-transformed, and percent data was square root transformed to meet assumptions of distribution normality.

	Ambient DOC –POC retention count			**Ambient DOC – POC retention Efficiency**		
Species	**R^2**	F-statistic	p-value	**R^2**	F-statistic	p-value
All Species	0.01	0.26	0.614	0.23	0.893	0.415
Tethya sp.	0.42	2.171	0.237	0.21	0.775	0.4435
Tedania sp.	0.16	0.56	0.508	0.16	0.5688	0.5055
Suberites sp.	0.73	8.178	0.0646*	0.60	4.43	0.126
Polymastia Penicillus	0.20	0.773	0.444	0.25	0.989	0.393
Polymastia sp.	0.07	0.225	0.668	0.05	0.168	0.710
Dysidea sp.	0.01	0.02	0.884	0.01	0.02	0.894
Clathrina sp.	0.30	1.289	0.339	0.18	0.658	0.477

Table S14. Linear regression model results of ambient POC availability to DOC retention (left) , retention efficiency (middle), and POC retention efficiency to DOC retention efficiency (right) relationships across all species and for each individual species. Cell count (cells/ml) data was log-transformed, and percent data was square root transformed to meet assumptions of distribution normality.

	Ambient POC – DOC retention count			**Ambient POC – DOC retention efficiency**			**POC retention efficiency – DOC retention efficiency**		
Species	R2	F-statistic	p-value	R2	F-statistic	p-value	R2	F-statistic	p-value
All Species	0.00	0.04	0.835	0.00	0.110	0.743	0.00	0.00	0.99
Tethya sp.	0.13	0.466	0.5438	0.07	0.233	0.662	0.43	2.26	0.230
Tedania sp.	0.24	0.9574	0.4	0.08	0.274	0.637	0.26	1.07	0.377
Suberites sp.	0.03	0.091	0.783	0.13	0.451	0.55	0.34	1.53	0.304
Polymastia Penicillus	0.00	0.002	0.964	0.01	0.04	0.860	0.08	0.26	0.645
Polymastia sp.	0.14	0.49	0.420	0.14	0.478	0.539	0.06	0.21	0.680
Dysidea sp.	0.67	6.184	0.09	0.78	12.85	> 0.05*	0.59	4.23	0.132
Clathrina sp.	0.05	0.151	0.724	0.03	0.104	0.768	0.18	0.66	0.475

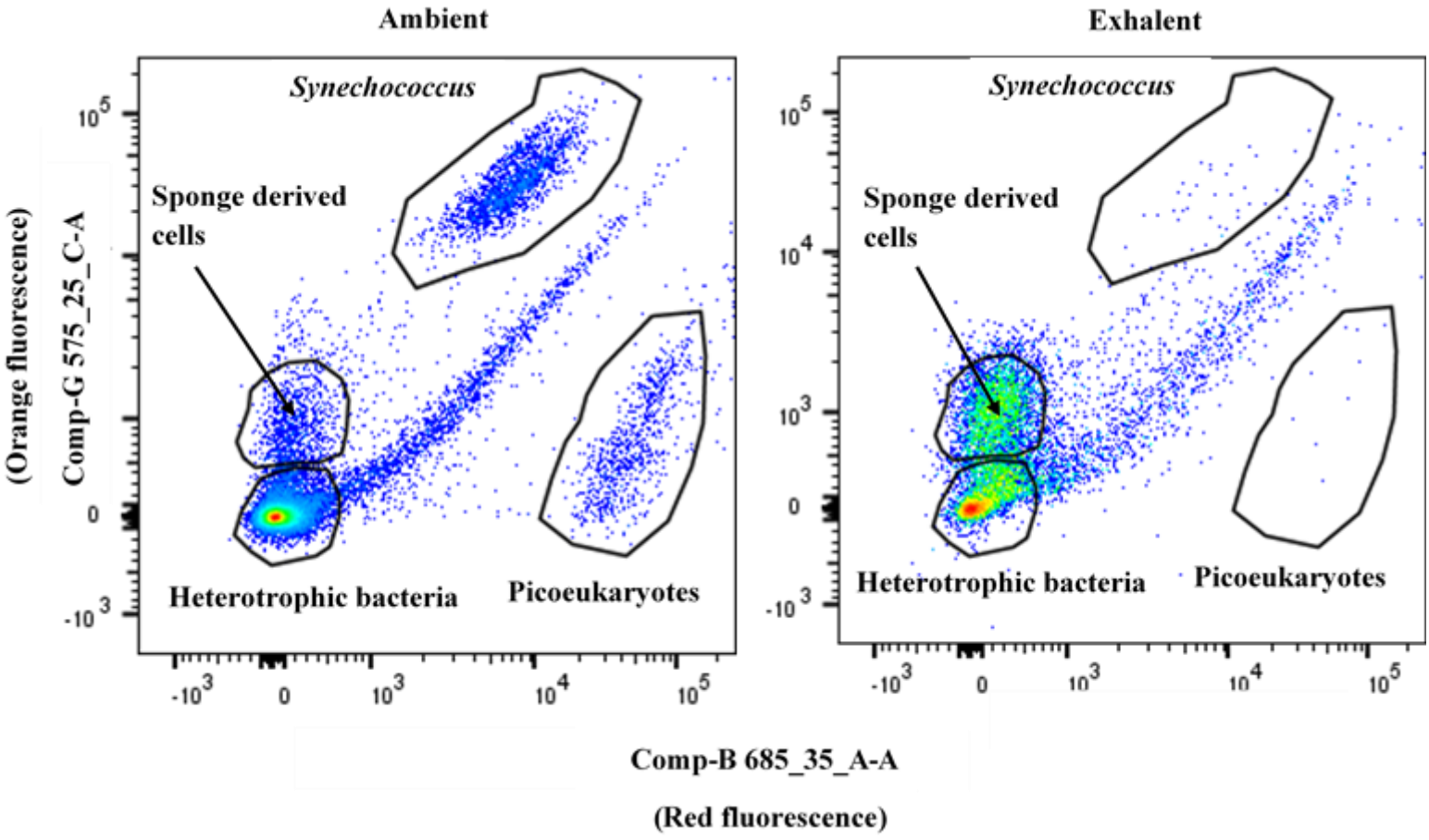

Fig. C4.1 Gated populations overlayed to show an example of sponge exudates emmitted in *Tethya* sp. exhalent water. Note increase in 'sponge cell' (ambient = 923 cells < exhalent = 3598 cells) population and significant decreases in other populations in exhalent water.

Appendix D

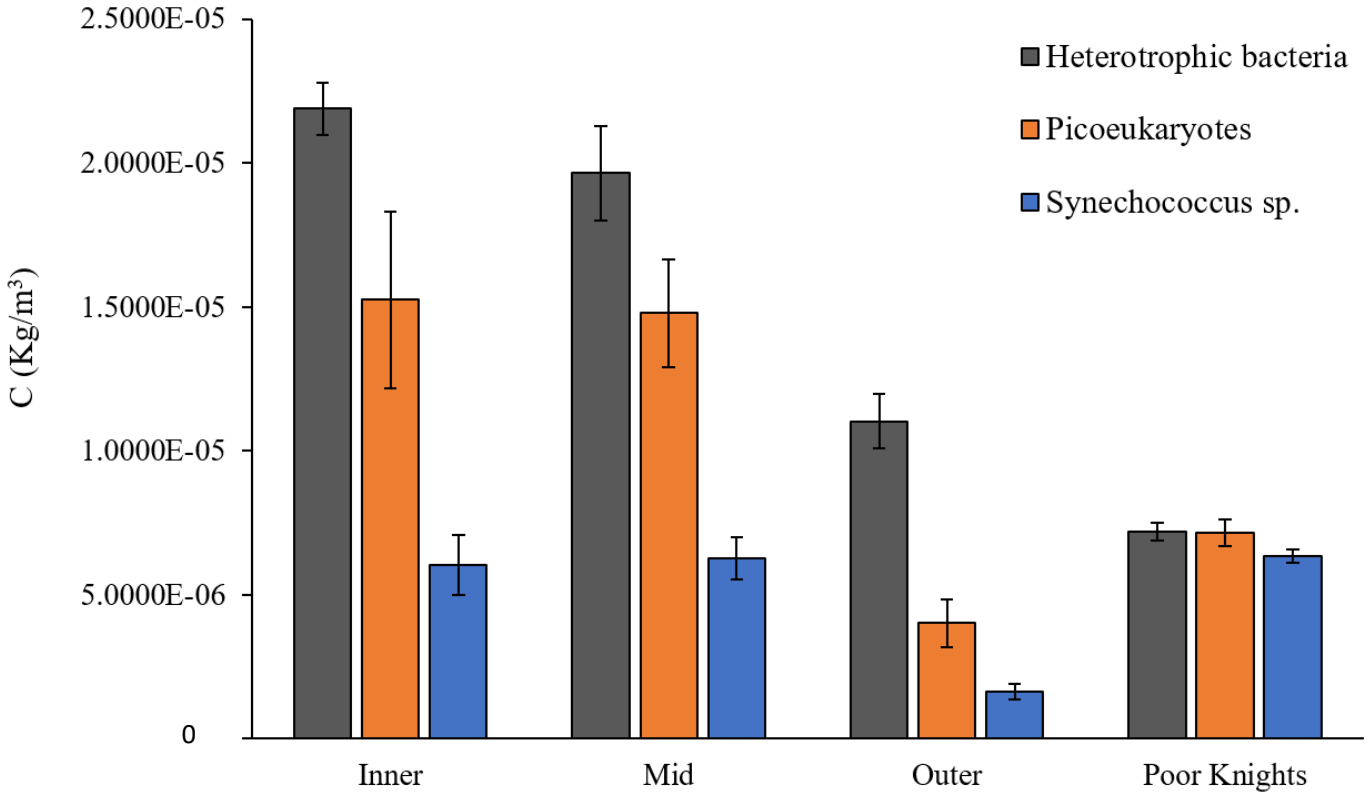

Fig. D5.1 Carbon weight (Kg/m^3) of heterotrophic bacteria, picoeukaryotes and *Synechococcus* sp. at inner mid and outer regions of Doubtful Sound and the Poor Knights. Error bars are mean ± SE. This figure is a visual representation of Table 5.7 for easier visualization of the data.